

LEVEL II



AFWAL-TR-80-3023

AD A 096759

ADVANCED FIBER REINFORCED THERMOPLASTIC STRUCTURES

April 1980

Technical Report AFWAL-TR-80-3023
Final Report for Period August 1976 - August 1979

Approved For Public Release, Distribution Unlimited

Flight Dynamics Laboratory
Air Force Wright Aeronautical Laboratories
Air Force Systems Command
Wright-Patterson Air Force Base, Ohio 45424



DTIC FILE COPY

Boeing Aerospace Company
Military Airplane Development
P.O. Box 3999
Seattle, Washington 98124

THIS DOCUMENT IS BEST COPY
THE COPY FURNISHED TO DDC 3-11-1981
SIGNIFICANT NUMBER OF PAGES WHICH DO NOT
REPRODUCE LEGIBLY.

440 258

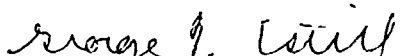
81 3 24 056


NOTICE

When Government drawings, specifications, or any other data used for any purpose other than in connection with a definitely related Government procurement operation, the United States Government thereby incurs no responsibility nor any obligation whatsoever; and the fact that the government may have formulated, furnished, or in any way supplied the said drawings, specifications, or other data, is not to be regarded by implication or otherwise as in any manner licensing the holder or any other person or corporation, or conveying any rights or permission to manufacture, use, or sell any patented invention that may in any way be related thereto.

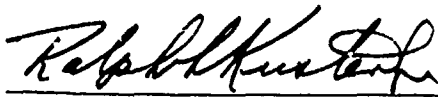
This report has been reviewed by the Office of Public Affairs (ASD/PA) and is releaseable to the National Technical Information Service (NTIS). At NTIS, it will be available to the general public, including foreign nations.

This technical report has been reviewed and is approved for publication.


George T. Estill
Project Engineer
Structural Concepts Evaluation Gp


Floyd G. Hemmig, Captain, USAF
Actg Chf, Structural Concepts Br
Structures & Dynamics Division

FOR THE COMMANDER


RALPH L. KUSTER, Jr., Colonel, USAF
Chief, Structures & Dynamics Division

"If your address has changed, if you wish to be removed from our mailing list, or if the addressee is no longer employed by your organization please notify AFWAL/FIBCB, W-PAFB, OH 45433 to help us maintain a current mailing list".

Copies of this report should not be returned unless return is required by security considerations, contractual obligations, or notice on a specific document.

DISCLAIMER NOTICE

**THIS DOCUMENT IS BEST QUALITY
PRACTICABLE. THE COPY FURNISHED
TO DTIC CONTAINED A SIGNIFICANT
NUMBER OF PAGES WHICH DO NOT
REPRODUCE LEGIBLY.**

SECURITY CLASSIFICATION OF THIS PAGE (When Data Entered)

REPORT DOCUMENTATION PAGE		READ INSTRUCTIONS BEFORE COMPLETING FORM	
1. REPORT NUMBER AFWAL-TR-80-3023	2. GOVT ACCESSION NO. AD-A096759	3. RECIPIENT'S CATALOG NUMBER	
4. TITLE (and Subtitle) ADVANCED FIBER REINFORCED THERMOPLASTIC STRUCTURES		5. TYPE OF REPORT & PERIOD COVERED FINAL REPORT 1.413 76-1 AUG. 1976 - AUG. 1979	
6. PERFORMING ORG. REPORT NUMBER		8. CONTRACT OR GRANT NUMBER(s) F33615-76-C-3048	
7. AUTHOR(s) J. T./Hoggatt S./Oken E. E./House		10. PROGRAM ELEMENT, PROJECT, TASK AREA & WORK UNIT NUMBERS Program Element 62201F Project 2401 Task 240103 Work Unit 24010318	
9. PERFORMING ORGANIZATION NAME AND ADDRESS Boeing Aerospace Company Box 3707 Seattle, WA 98124		12. REPORT DATE April 1980	
11. CONTROLLING OFFICE NAME AND ADDRESS Air Force Wright Aeronautical Laboratories (AFSC) Wright-Patterson AFB, OH 45433		13. NUMBER OF PAGES 255	
14. MONITORING AGENCY NAME & ADDRESS (if different from Controlling Office)		15. SECURITY CLASS (of this report) Unclassified	
16. DISTRIBUTION STATEMENT (of this Report) Approved for public release; distribution unlimited.		15a. DECLASSIFICATION/DOWNGRADING SCHEDULE	
17. DISTRIBUTION STATEMENT (of the abstract entered in Block 20, if different from Report)			
18. SUPPLEMENTARY NOTES			
19. KEY WORDS (Continue on reverse side if necessary and identify by block number) Composites, Thermoplastic, Polysulfone, Graphite, Elevator			
20. ABSTRACT (Continue on reverse side if necessary and identify by block number) The objective of the program was to demonstrate the performance and cost savings of graphite/polysulfone. This objective was attained through a thirteen task program which culminated in the design, fabrication and test of a full scale elevator torque box. The P-1700 polysulfone resin was selected and used with A-S unidirectional graphite fibers (Hercules 3004/A-S/P1700 prepreg) and with T-300 woven graphite fibers (Hexcel T-3004/23x24, 811 Satin Prepreg). Tooling concepts, consolidation and post forming processes, and field repair procedures were developed. The graphite/thermoplastic elevator had a 27% weight (OVER)			

DD FORM 1 JAN 73 1473 EDITION OF 1 NOV 65 IS OBSOLETE

UNCLASSIFIED

SECURITY CLASSIFICATION OF THIS PAGE (When Data Entered)

410758

UNCLASSIFIED

SECURITY CLASSIFICATION OF THIS PAGE(When Data Entered)

savings as compared to the aluminum elevator, and a cost saving of 20%, by the tenth elevator shipset. A limited study of a Union Carbide proprietary thermoplastic, known as PKXA, which has much improved solvent resistance as compared to P-1700 polysulfone, was conducted. This limited study showed that PKXA appeared to be a viable substitute for P-1700 polysulfone. It is recommended that a further study of PKXA be made in order to further optimize the manufacturing procedures for it.

UNCLASSIFIED

SECURITY CLASSIFICATION OF THIS PAGE(When Data Entered)

Foreword

This report summarizes the work performed by the Boeing Aerospace Company (BAC) under the Air Force Contract F33615-76-C-3048 during the period of August 1, 1976 through August 1, 1979.

This program was sponsored by the Materials Laboratory and the Flight Dynamics Directorate, Air Force Wright Aeronautical Laboratories (AFSC), Wright-Patterson AF Base, Ohio. The program monitors were G. Estill, AFFDL, Capt. F. T. Bannink, AFFDL and H. S. Reinert, AFML.

This contract was performed and managed by Engineering Technology personnel at BAC. Mr. J. T. Hoggatt and D. B. Arnold were the program managers and Mr. S. Oken the technical leader. The principal contributors during the course of the program were K. Hernley, design; A. L. Dobyns, stress; E. E. House and S. G. Hill, materials and processes; D. L. Muretta and D. A. Anderson, manufacturing research; and J. D. Swenson, testing.

Accession For	
NTIS	1981
Availability Codes	
Avail and/or	
Dist	Special
A	23

TABLE OF CONTENTS

	PAGE
SECTION 1.0	1
1.1 INTRODUCTION	1
1.2 SUMMARY	1
Section 2.0 RESIN AND FIBER SELECTION/EVALUATION	5
SECTION 3.0 CONCEPTUAL DESIGN/CONCEPT EVALUATION	11
3.1 INTRODUCTION	11
3.1.1 COST PROCEDURE	11
3.2 YC-14 FUSELAGE BODY SECTION 43	17
3.3 LARGE TRANSPORT A/C FUSELAGE PANEL	17
3.4 FIREBEE DRONE SECTION COMPONENTS	24
3.5 YC-14 STIFFENED LAMINATE WING BOX	24
3.6 YC-14 HONEYCOMB WING BOX	34
3.7 YC-14 HORIZONTAL STABILIZER	34
3.8 COMPASS COPE HORIZONTAL STABILIZER	38
3.9 CONCLUSIONS	45
SECTION 4.0 MANUFACTURING DEVELOPMENT	47
4.1 CONSOLIDATION	47
4.1.1 PRESS CONSOLIDATION	47
4.1.2 AUTOCLAVE CONSOLIDATION	50
4.1.3 PULTRUSION COMPACTION	50
4.1.4 ROLL FORMING COMPACTION	52
4.2 POST FORMING	52
4.2.1 PRESS MATCH DIE POST FORMING	54
4.2.2 AUTOCLAVE POST FORMING	54
4.2.3 VACUUM FORMING	57
4.3 BONDING/JOINING METHODS	57
4.3.1 FUSION BONDING	57
4.3.2 ADHESIVE BONDING	66
4.3.3 MECHANICAL FASTENING	66
4.4 CHOPPED FIBER MOLDING	70
4.4.1 INJECTION MOLDING	70
4.4.2 CLOSE DIE MOLDING	70
SECTION 5.0 FIELD MAINTENANCE/REPAIR METHODS	89
SECTION 6.0 SUBCOMPONENT EVALUATION	99
6.1 IN-PLANE SHEAR TESTS	99
6.2 JOINT TESTS	105
6.2.1 BONDED JOINTS	106
6.2.2 MECHANICAL ATTACHMENT JOINTS	114
6.3 SHEAR PANEL BUCKLING TESTS	119
6.4 COMPRESSION PANEL BUCKLING TESTS	134
6.5 FRACTURE PANEL TESTS	146
6.6 LOAD INTRODUCTION TESTS	146

TABLE OF CONTENTS (Cont'd.)

	PAGE
SECTION 7.0 YC-14 ELEVATOR FULL-SCALE DESIGN AND FABRICATION	161
7.1 DESIGN REQUIREMENTS AND CRITERIA	161
7.2 PRELIMINARY DESIGN	169
7.2.1 "Z" STIFFENED PANEL CONCEPT	169
7.2.2 CORRUGATED STIFFENED PANEL CONCEPTS	173
7.2.3 HONEYCOMB STIFFENED COVER PANEL CONCEPT	173
7.2.4 PRELIMINARY DESIGN STUDY RESULTS	178
7.3 DETAIL DESIGN AND ANALYSIS	182
7.3.1 DESIGN	183
7.3.2 ANALYSIS	183
 SECTION 8.0 FULL-SCALE ELEVATOR TOOLING AND FABRICATION	 201
8.1 ELEVATOR DETAIL FABRICATION	201
8.2 SUBASSEMBLY FABRICATION	201
8.3 ELEVATOR ASSEMBLY TOOLING AND FABRICATION	206
 SECTION 9.0 DEMONSTRATION ARTICLE TESTING	 219
 SECTION 10.0 COST AND PAYOFF ANALYSIS	 247
 SECTION 11.0 PKXA EVALUATION	 253

LIST OF ILLUSTRATIONS

<u>Figure</u>	<u>Title</u>	<u>Page</u>
1	Effect of Temperature on Flexure Strength - Graphite/Polysulfone Composites	6
2	Effect of Temperature on Flexure Modulus	7
3	Effect of Temperature on Interlaminar Shear	7
4	Effect of Temperature on Tensile Strength	8
5	Effect of Temperature on Tensile Modulus	8
6	Part Fabrication Time	14
7	Assembly Time	15
8	Tooling Time	16
9	YC-14 Fuselage Structure Centerline Diagram	18
10	Fuselage Section 43 - Details	19
11	Typical Graphite Reinforced Polysulfone Body Structure (Unpressurized)	21
12	Firebee Drone Profile and Selected Gr/Ps Components	25
13	Prototype Gr/Ps Component Design Concept Details	26
14	Skin Installation - Centerbody Section	27

LIST OF ILLUSTRATIONS (Cont'd.)

<u>Figure</u>	<u>Title</u>	<u>Page</u>
15	Delivered GRTP Components for the Firebee Drone Center Body Section	29
16	YC-14 Wing Structure Diagram	31
17	YC-14 Stiffened Laminate Wing Concept	32
18	Stiffened Laminate Stringer Configurations	33
19	YC-14 Honeycomb Wing Concept	35
20	YC-14 Horizontal Stabilizer Centerline Diagram	39
21	Typical Spar/Rib Attachment	40
22	Compass Cope Materials Systems	42
23	Compass Cope - Horizontal Stabilizer Composite Design	43
24	Compass Cope Horizontal Stabilizer Details	44
25	Press Consolidated Unidirectional Laminate	49
26	Press Consolidated 181 Style Graphite Fabric Laminate	49
27	Thermoplastic Pultrusion Facility	51
28	Graphite Thermoplastic Pultruded Sections	53
29	Press Match-Die Molded Post Formed Channel	55
30	Press Molded Shapes - Silicone Plug Mold	55

LIST OF ILLUSTRATIONS (Cont'd.)

<u>Figure</u>	<u>Title</u>	<u>Page</u>
31	Shear Web Molded From $(0^0, 90^0)_S$ Graphite Tape Composite	56
32	Shear Web Molded From Graphite Fabric	56
33	Vacuum Formed Shear Web $(0^0, 90^0)_S$ Sheet Stock	58
34	Vacuum Formed Shear Web Graphite Fabric	58
35	Chemithon Thermoforming Machine	59
36	Vacuum Forming Chamber-Schematic	60
37	Graphite Thermoplastic Vacuum Forming - Part Removal	61
38	Polysulfone Adhesive Films with Self Contained Heating Wires and Screen	63
39	Fusion Joint - Resistant Heating Wires	63
40	Fusion Joint - Close Up	64
41	Fusion Joint - Resistant Heating Screen	64
42	Electromagnetic Bonding	65
43	Punched Hole - 1/4 Diameter (50X)	68
44	Drilled/Reamed Hole - 1/4 Diameter (50X)	69

LIST OF ILLUSTRATIONS (Cont'd.)

<u>Figure</u>	<u>Title</u>	<u>Page</u>
45	YC-14 Elevator Molded Link Fitting	73
46	Molded Fitting - Preformed Fabric Pan	75
47	Molded Fitting - Pan Compaction Tool and Caul Plates	75
48	Molded Fitting - Compacted Pan Prior to Trim	76
49	Molded Fitting - Chopped Graphite Fiber Molded Truss	78
50	Molded Fitting - Truss Compaction Tool	79
51	Molded Fittings - Fabric Truss	79
52	Molded Fitting - Detail Parts and Fusion Assembly Tool	80
53	Molded Fitting - Fusion Tool with Details Installed	80
54	Molded Fitting - Details and Pans in Tool	81
55	Molded Fittings - Fusion Assembly Tool Ready for Press	81
56	Molded Fitting - Graphite/Polysulfone	82

LIST OF ILLUSTRATIONS (Cont'd.)

<u>Figure</u>	<u>Title</u>	<u>Page</u>
57	Molded Fitting - Test Set-Up Without Side Plate	83
58	Molded Fitting - Test Set-Up	83
59	Molded Fitting - Test Load Conditions	84
60	Molded Fitting - Pull-Out Test	86
61	Fabric Truss Molded Fitting Failure	87
62	Chopped Fiber Truss Molded Fitting Failure	87
63	Fusion Bond Damage Repair	90
64	Fusion Bond Repair - Vacuum Bag and Heat Source	91
65	Fusion Bond Repair Cross Section	92
66	Adhesive Bond Repair	94
67	Repair Panel-Failed Specimens	96
68	In-Plane Shear	101
69	Rail Shear Static Test Set-Up	102
70	Failed Rail Shear Specimens	103
71	Failed Rail Shear Specimens - Doublers Bonded in Attachment Areas	104
72	Failed Rail Shear Specimen-Rails Bonded In-Place	105

LIST OF ILLUSTRATIONS (Cont'd.)

<u>Figure</u>	<u>Title</u>	<u>Page</u>
73	Rail Shear Fatigue Data	107
74	Rail Shear Failed Specimens	108
75	Lap Shear Specimen	109
76	Fusion Bonded Joint	112
77	Fusion Bond Lap Shear Fatigue (Fabric at ± 45)	115
78	Fusion Bond - Rail Shear Specimen	116
79	Mechanical Attachment Joint Test Data	117
80	Failed Mechanical Attachment Specimens	118
81	Mechanical Attachment Fatigue Specimen Failures	121
82	Shear Beam Element	122
83	Chord Details - Beam Element	124
84	Beam Element Details	125
85	Beam Element Assembly	126
86	Beam Element - Test Setup	127
87	Shear Beam Overall Test Set-Up	128

LIST OF ILLUSTRATIONS (Cont'd.)

<u>Figure</u>	<u>Title</u>	<u>Page</u>
102	Compression Panel Lateral Displacement Profile- Zero and 100% Ultimate Load	145
103	Compression Panel Fatigue	147
104	Slotted Panel Test Specimen	148
105	Fracture Panel Failure and Control Panels	150
106	<u>+45</u> Graphite/Epoxy Center Notched Panel Fracture Response	151
107	Load Introduction Test Element	153
108	Static Test No. 1 Setup	155
109	Static Test No. 2 and Fatigue Test Setup	156
110	Load Introduction Box - Test Setup	157
111	Load Introduction Box - Test Set-Up, Front View	158
112	Load Introduction Box - Test Set-Up. Side View	158
113	Static Test No. 3, Side Load Test Setup	159
114	YC-14 Outboard Elevator GJ Comparisons	165

LIST OF ILLUSTRATIONS (Cont'd.)

<u>Figure</u>	<u>Title</u>	<u>Page</u>
88	Shear Panel Instrumentation	129
89	Shear Beam Test Schematic - Moire' Displacement	130
90	Shear Panel Moire' Fringe Zero Load	131
91	Shear Panel Moire' Fringe 50% Ultimate Load	132
92	Shear Panel Moire' Fringe 100% Ultimate Load	133
93	Shear Panel Schematic - Latera' Displacement Line	135
94	"T" Stifferer Panel Displacement Profile Zero and 100% Shear Load	136
95	Shear Buckling - Theory vs Test	137
96	Shear Buckling Fatigue Test	138
97	Compression Buckling - Panel Element	140
98	Compression Panel Instrumentation	141
99	Compression Panel Test Set-Up	142
100	Compression Panel Test - Back Side	143
101	Compression Panel Moire' Fringe - 100% Ultimate Load	144

LIST OF ILLUSTRATIONS (Cont'd.)

<u>Figure</u>	<u>Title</u>	<u>Page</u>
115	YC-14 Outboard Elevator EI Comparisons	166
116	Fatigue of Intermediate Strength Graphite/Epoxy	168
117	YC-14 Elevator Schematic	170
118	YC-14 Elevator Gr/Ps Z Stiffened Cover Concept	171
119	YC-14 Elevator Graphite/Polysulfone Corrugated Stiffened Cover Concept	175
120	Graphite/Epoxy Elevator Test Component	177
121	Honeycomb Stiffened Design Concept	179
122	Elevator Splice Locations	184
123	YC-14 Elevator Fairings	185
124	GRTP Outboard Elevator YC-14 (Sh 1)	187
125	GRTP Outboard Elevator YC-14 (Sh 2)	189
126	GRTP Outboard Elevator YC-14 (Sh 3)	191
127	GRTP Outboard Elevator YC-14 (Sh 4)	193
128	GRTP Outboard Elevator YC-14 (Sh 5)	195
129	GRTP Outboard Elevator YC-14 (Sh 6)	197

LIST OF ILLUSTRATIONS (Cont'd.)

<u>Figure</u>	<u>Title</u>	<u>Page</u>
130	Differential Thermal Growth	199
131	YC-14 GR/PS Elevator SAMECS Plot	200
132	Thermoplastic Elevator Assembly Sequence	202
133	Stiffener Match Die Tooling and Details	203
134	Matched Die Rib Tooling and Completed Rib	204
135	YC-14 Elevator Subassemblies	205
136	YC-14 Elevator Spar Web Assemblies	205
137	Details Located in Fusion Assembly Tool	207
138	Details in Fusion Tool with Chord Pressure Bars in Place	208
139	Fusion Tool, Loaded, Bagged and Ready for Fusion Cycle	209
140	Completed Side Panel Fusion Assembly-90 Inch Length	210
141	YC-14 Elevator Large Section Assembly Fixture - Front View	211

LIST OF ILLUSTRATIONS (Cont'd.)

<u>Figure</u>	<u>Title</u>	<u>Page</u>
142	YC-14 Elevator Large Section Assembly Fixture - Side View	211
143	YC-14 Elevator Middle and Small Section Assembly Fixture	212
144	Details Placed in Assembly Fixture	212
145	YC-14 Elevator Spar Web and Chord Installation	213
146	YC-14 Elevator Section Assembly	213
147a	Elevator Assembly - No Covers	215
147b	YC-14 Elevator No. 2	216
148	YC-14 Elevator - Typical Visu-Lok Blind Fastener Installation	217
149	Strain Gage Locations	220
150	Strain Gage Locations	221
151	Loading Points and Deflection Indicator Locations	222
152	Elevator Test Set-Up	223
153	GR/TP YC-14 Elevator Box Test - Test Article and Fixtures	224
154	GR/TP YC-14 Elevator Box Test - Test Article and Fixtures	225

LIST OF ILLUSTRATIONS (Cont'd.)

<u>Figure</u>	<u>Title</u>	<u>Page</u>
155	GR/TP Elevator Box Test - Test Article and Fixtures	226
156	GR/TP YC-14 Elevator Box Test - Instrumentation and Control	227
157	Test - Loading Schedule, Graphite Thermoplastic YC-14 Elevator Box Test	228
158	Test - Loading Schedule, Graphite Thermoplastic YC-14 Elevator Box Test	229
159	Test - Loading Schedule, Graphite Thermoplastic YC-14 Elevator Box Test	230
160	Test - Loading Schedule, Graphite Thermoplastic YC-14 Elevator Box Test	231
161	Test - Loading Schedule, Graphite Thermoplastic YC-14 Elevator Box Test	232
162	Upper Cover Failure - Test 1.9 - Elevator Box #1	234
163	Front Spar Failure - Test 1.9 - Elevator Box #1	235
164	Front Spar Failure - Test 1.9 - Elevator Box #1	236
165	Front Spar Failure - Test 2.3 - Elevator Box #2	237
166	Front Spar Failure - Test 2.3 - Elevator Box #2	238
167	Front Spar Repair - Elevator Box #2	239

LIST OF ILLUSTRATIONS (Cont'd.)

<u>Figure</u>	<u>Title</u>	<u>Page</u>
168	Lower Cover/Rear Spar Bond Failure - Test 2.4 Elevator Box #2	240
169	Lower Cover Failure - Test 2.4 - Elevator Box #2	241
170	Load Point and EDI Locations GR/PKXA YC-14 Elevator Box #3	243
171	GR/PKXA YC-14 Elevator Box #3 - Test Article in Fixtures	244
172	GR/PKXA YC-14 Elevator Box #3 - Test Article in Fixtures	245
173	Chemical Formulas of PKXA and P-1700 Polysulfone	254
174	PKXA-P-1700 Rail Shear Fatigue Data Comparison	258

LIST OF TABLES

<u>Table</u>	<u>Title</u>	<u>Page</u>
1	Thermoplastic Prepregs	6
2	Graphite Fabric/PI700 Average Test Data	9
3	PI700/A-S Tape Laminate Properties	9
4	Properties of Polyphenylene Sulfide Graphite Fiber Reinforced Molding Compound	10
5	Conceptual Design and Evaluation Components	12
6	Cost Factors and Assumptions	12
7	Fabrication Costs for Advanced Composite Designs YC-14 Fuselage Body Section 43	20
8	Fabrication Cost for Advanced Composite Designs Large Transport A/C Fuselage Panel	23
9	Fabrication Costs for Advanced Composite Designs Firebee Drone Body Component	30
10	Wing Box Weight Summary-Stiffened Laminate Design	35
11	Fabrication Costs for Advanced Composite Designs YC-14 Stiffened Laminate Wing Box	35
12	Wing Box Weight Summary - Honeycomb Concept	37
13	Fabrication Costs for Advanced Composite Design - YC-14 Honeycomb Wing Box	37

LIST OF TABLES

<u>Table</u>	<u>Title</u>	<u>Page</u>
14	YC-14 Advanced Composite Horizontal Stabilizer Cost Estimate	41
15	Compass Cope Advanced Composite Horizontal Stabilizer Cost Estimate	46
16	Compass Cope Horizontal Stabilizer Cost Estimate - Glass/Epoxy and Graphite/Polysulfone	46
17	Task IV - Manufacturing Development	48
18	Processing Time for Consolidation	48
19	Adhesive Lap Shear Strengths	67
20	Bonding Methods - Typical Values	67
21	Attachment Studies - Hole Fabrication Evaluation	68
22	Attachment Studies - Reamed Hole Evaluation	69
23	Injection Molding Material Flexural Properties - Ryton PPS (Phillips)	71
24	Repair Panel Static Tests	95
25	Repair Panel Fatigue Tests	95
26	Subcomponent Tests	100

LIST OF TABLES

<u>Table</u>	<u>Title</u>	<u>Page</u>
27	Rail Shear Static Tests - <u>+45</u> Graphite Fabric/ P1700	100
28	Adhesive Lap Shear Strengths	111
29	Lap Shear Strength (psi) (4 plies <u>+45</u> Fabric)	113
30	Mechanical Attachment Fatigue Data	120
31	Fracture Panel Tests	149
32	Cost Summary - Graphite Polysulfone YC-14 Elevator	181
33	Areas of Cost Savings	248
34	Processing Time for Post Forming	250
35	Element Cost Savings with GR/TP	250
36	PKXA Static Rail Shear Test Results	254
37	PKXA Mechanical Attachment, Lap Shear Test Results	256
38	PKXA Fusion Bond, Lap Shear Test Results	256
39	PKXA Fracture Panel, Tension Test Results	257
40	PKXA Rail Shear Fatigue Results	257
41	PKXA Polysulfone Static Element Test Data Comparison	258

SECTION 1.0

1.1 INTRODUCTION

This program was performed to demonstrate the improved performance and cost savings made available by the use of Advanced Fiber Reinforced Thermoplastics (AFRTP) in aircraft structures. To demonstrate these improvements, full size aircraft components were fabricated and tested. The YC-14 left-hand outboard elevator was selected as the component to be used in this evaluation. This part has a span of 19 ft and a maximum chord of 18 in. The studies showed that a graphite/thermoplastic elevator offers a 27 percent weight savings and 20 percent cost savings over the presently used aluminum elevator by the tenth elevator shipset. In this program we:

- o Evaluated and refined manufacturing techniques for use with AFRTP's.
- o Demonstrated the potential of AFRTP's to reduce the fabrication and assembly costs of aircraft structures.
- o Demonstrated the structural integrity and durability of AFRTP components.
- o Developed repair procedures and logistics for maintaining composite structures.
- o Laid the groundwork for the production and flight service test of an AFRTP component.

1.2 SUMMARY

To attain the objectives of this program the 13 tasks described below were performed.

Task I--Resin and Fiber Selection/Evaluation

P-1700 polysulfone was selected as the thermoplastic matrix material to be used in this program. Graphite fibers in both tape and fabric form were tested to obtain mechanical and environmental properties. Molding components incorporating short graphite fibers were investigated for use as hinge fitting material.

Task II--Conceptual Design/Concept Evaluation

Seven major aircraft and missile components were selected for GRTP application studies. Cost and weight savings were identified for each of the designs and compared to equivalent graphite/epoxy and aluminum designs.

Task III--Preliminary Design

Three preliminary GRTP designs of the outboard YC-14 elevator were prepared. One of the designs, a stiffener stabilized panel concept, was selected for further study and evaluation.

Task IV--Manufacturing Development

Manufacturing Development investigations were performed in the areas of laminate consolidation, post-forming methods, bonding and joining methods, chopped fiber and fabric molding, assembly methods, and quality assurance techniques.

Task V--Field Maintenance/Repair Methods

Maintenance and repair included inspection, routine cleaning and restoration, major refurbishment and repair.

Task VI--Subcomponent Tooling

The tooling concepts established in Task IV, Manufacturing Development, were used to fabricate the elements and subcomponents in Task VII.

Task VII--Subcomponent Manufacture and Testing

Elements and subcomponents representative of the selected design were fabricated and tested.

Task VIII--Final Design

A final design of the selected concept (Task III) was prepared. The design drawings were sufficiently detailed to supply all manufacturing information required to fabricate the elevator component.

Task IX--Demonstration Article Tooling

The major tools required to fabricate three elevators were designed and fabricated.

Task X--Demonstration Article Fabrication

Three full-scale GRTP YC-14 elevators were fabricated. Processes governing all aspects of manufacturing were developed.

Task XI--Demonstration Article Testing

Two elevators were tested. The first elevator was tested initially to determine torsional and bending stiffnesses. It was then proof-tested and then cyclic loaded for four lifetimes. The part was then loaded to destruction to determine residual strength. The second was tested to determine torsional and flexural stiffness, and then it was loaded to failure.

Task XII--Cost and Payoff Analysis

A detailed cost analysis was made to determine the cost of the GRTP elevator for a 300-aircraft production run. This analysis was developed from cost tracing data obtained during the course of the program. These costs were compared to production costs of the existing aluminum design.

Task XIII--Graphite/PKXA Thermoplastic Structural Element Evaluation

A comparison was made between the structural integrity of PKXA graphite reinforced thermoplastic (GRTP) and P-1700 GRTP. Critical YC-14 elements made of PKXA GRTP were fabricated and tested. The results from these tests were compared to equivalent data obtained from polysulfone GRTP composites. Fabrication cost comparisons determined that PKXA parts would be produced at the same costs as polysulfone composite parts.

2.0 RESIN AND FIBER SELECTION/EVALUATION

Several samples of developmental thermoplastic prepregs (Table 1) were obtained and evaluated for the purpose of obtaining a satisfactory commercial prepreg for use on this program. The materials finally selected were Hercules' 3004 (A-S/P-1700) unidirectional tape and Hexcel's 23 x 24 eight Harness satin fabric/P-1700 prepreg. Laminates of these materials were fabricated and tested. Figure 1 shows the effect of temperature on their flexural strength and Figure 2 on flexural modulus. Figure 3 shows the effect of temperature on interlaminar shear, and Figures 4 and 5 show the effect of temperature on their tensile strength and tensile modulus. Additional property data for the fabric material is shown in Table 2 and for tape in Table 3.

The graphite fabric prepreg was selected as the primary reinforcing material because it simplified lay-up, was easier to handle and was a more reproducible and uniform prepreg.

Two molding compounds were selected for manufacturing studies. These materials were Fiberite's RTP 1387 polyphenylene sulfide/graphite and RTP 907 polysulfone/glass molding compounds. The vendor designated properties of the PPS material are shown in Table 4.

Table 1.. Thermoplastic Prepregs

- 1) HERCULES 3004A-S 3" WIDE TAPE
- 2) DUPONT A-S/P-1700 POLYSULFONE 6" WIDE TAPE
- 3) HEXCEL/T300 181 GRAPHITE FABRIC/P-1700
- 4) FIBERITE/T300 181 GRAPHITE FABRIC/P-1700
- 5) U.S. POLYMERIC T-300/P-1700 POLYSULFONE 12" WIDE TAPE

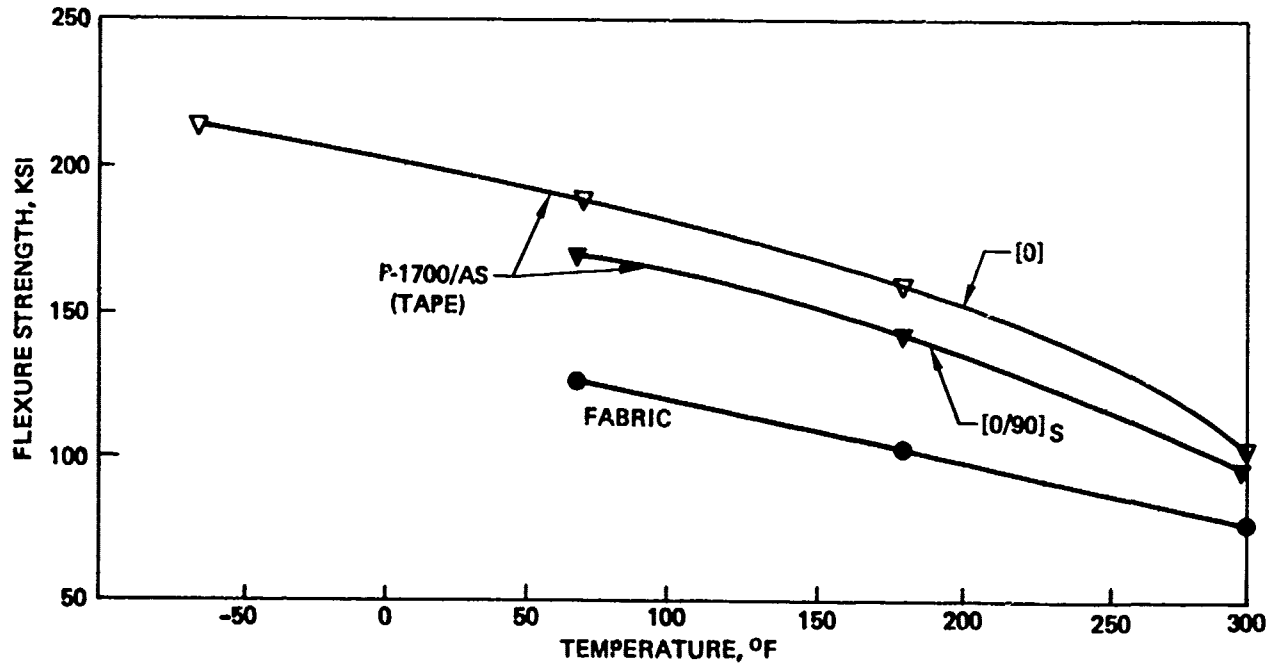


Figure 1. Effect of Temperature on Flexure Strength – Graphite/polysulfone Composites

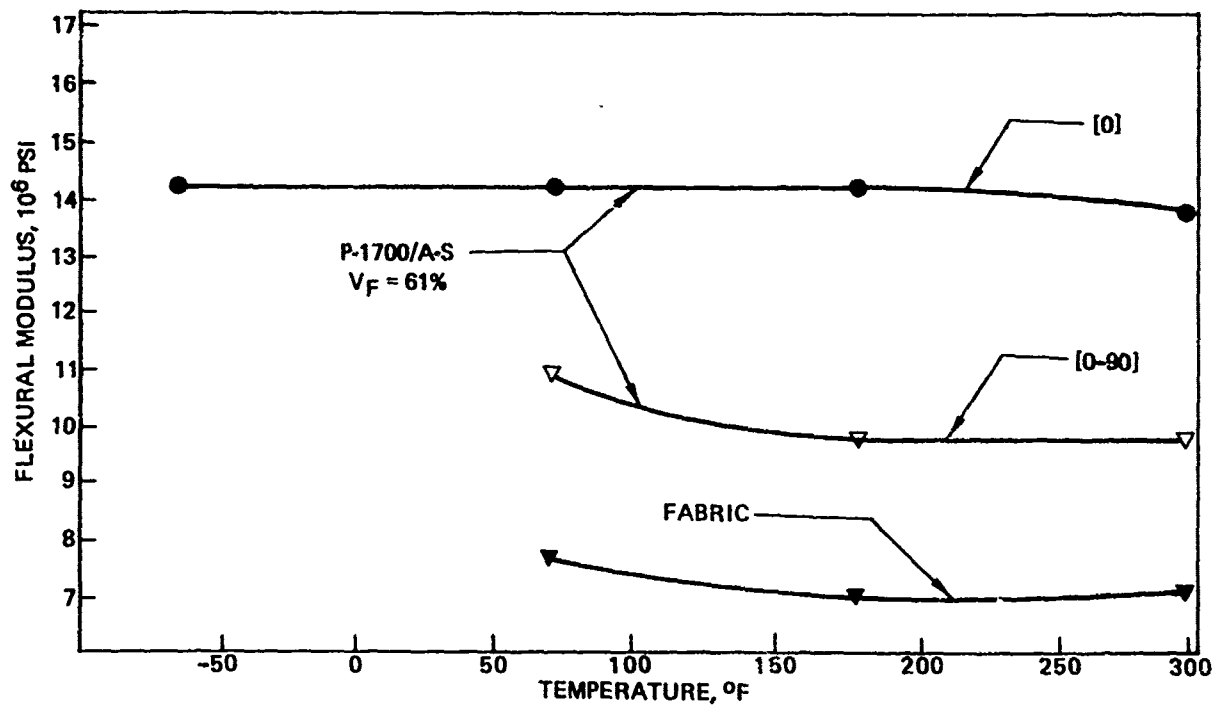


Figure 2. Effect of Temperature on Flexure Modulus

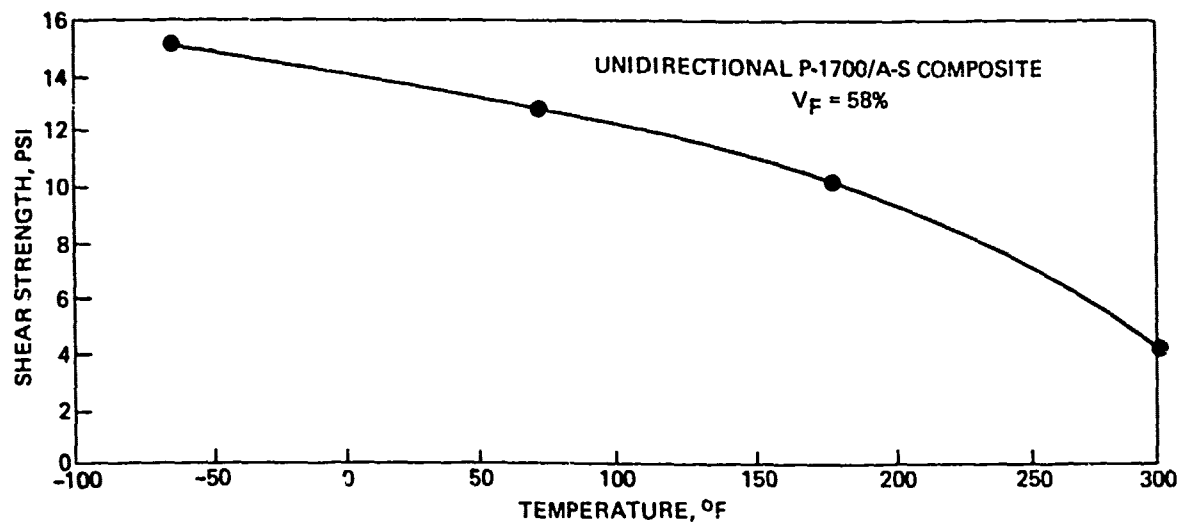


Figure 3. Effect of Temperature on Interlaminar Shear

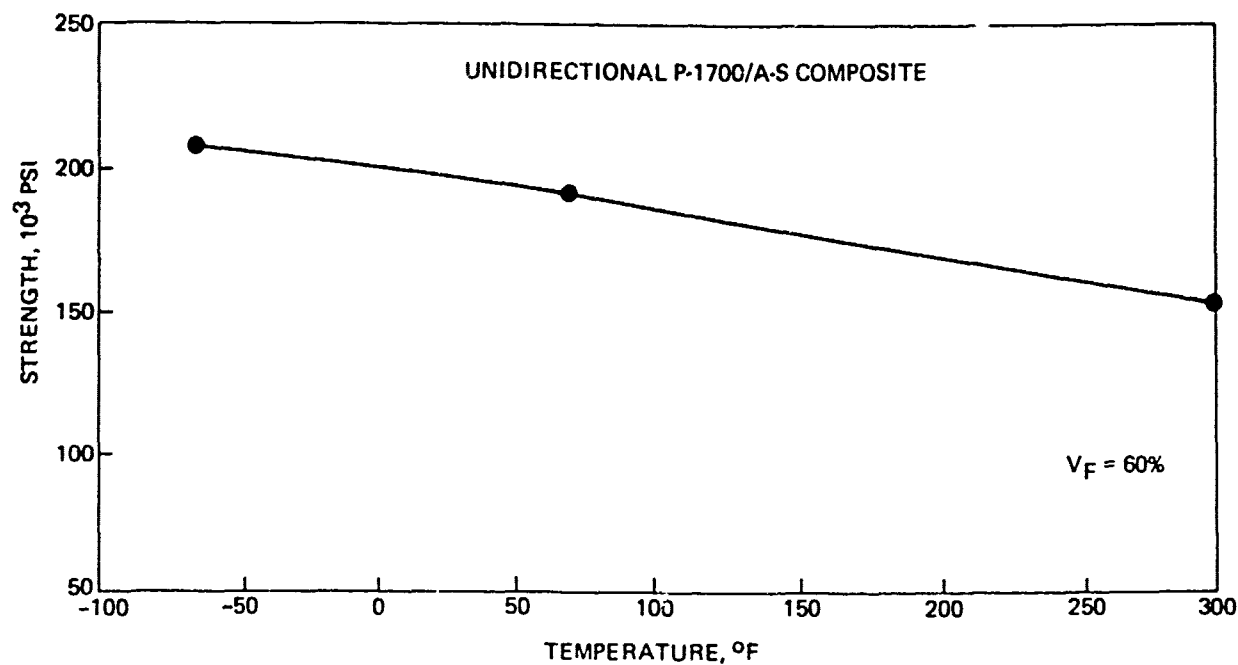


Figure 4. Effect of Temperature on Tensile Strength

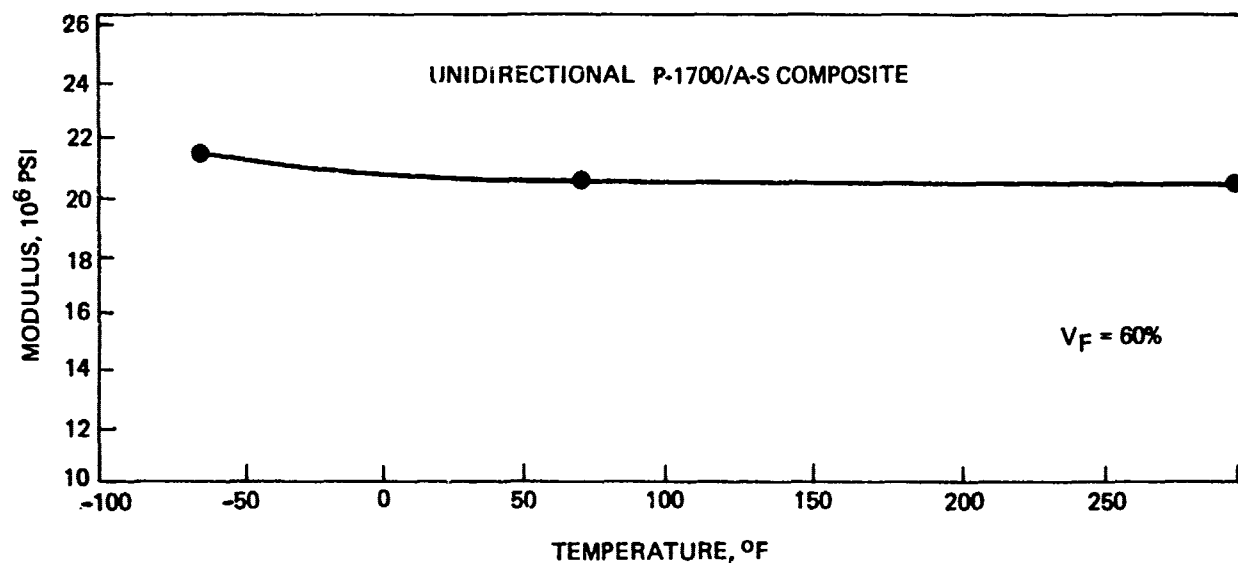


Figure 5. Effect of Temperature on Tensile Modulus

Table 2. Graphite Fabric/P1700 Average Test Data

TEST DIRECTION (DEGREES)	TEST TEMP.	COMPRESSION		FLEXURE		ILS PSI X 10 ³	TENSILE	
		ULT STRESS PSI X 10 ³	MODULUS PSI X 10 ⁶	ULT STRESS PSI X 10 ³	MODULUS PSI X 10 ⁶		ULT STRESS PSI X 10 ³	MODULUS PSI X 10 ⁶
0	RT	56.0	9.2	128.3	7.7	6.5	77.1	10.2
0	180°F			114.8	7.1		-	-
0	300°F	36.2	10.6	88	7.2	3.5	61.4	10.4
90	RT			96.7	7.7	-	-	-
90	180°F			80.0	7.7	-	-	-
90	300°F			66.4	6.7	-	-	-
181 STYLE GRAPHITE FABRIC (HMF)/P1700 RESIN LAMINATE.								

Table 3. P1700/A-S Tape Laminate Properties

COMPRESSION STRENGTH/MODULUS – TAPE LAMINATES					
LAMINATE	TEST DIR.	TEST	+70°F	+180°F	300°F
0° LAMINATE	0°	STR.	151,300	102,600	86,200
		E	15.6	16.1	13.1
0° LAMINATE	90	STR.	20,500	15,800	10,500
		E	1.07	1.03	0.97
±45 LAMINATE	0°	STR.	21,000	16,200	12,600
		E	2.17	2.04	1.48
FLEXURE PROPERTIES – TAPE LAMINATES					
[0 - 90]	0°	STR.	168,000	141,000	113,600
		E	11.3	10.3	10.0
[±45°]	0°	STR.	40,000	33,800	24,800
		E	2.0	1.74	1.85

Table 4. Properties of Polyphenylene Sulfide Graphite Fiber Reinforced Molding Compound

COMPOUND PROPERTIES		AVERAGE VALUES			
Color		Black			
Injection Pressure, PSI		15-20000			
Injection Cylinder Temp., °F.		575-650			
Mold Temp., °F.		100-350			
PROPERTIES OF INJECTION MOLDED SPECIMENS					
PERMANENCE	BASE RESIN	RTP 1383	RTP 1385	RTP 1387	ASTM TEST METHOD
Carbon Graphite Fiber, %	0	20	30	40	
Specific Gravity	1.3	1.38	1.42	1.46	D-792
Molding Shrinkage, in/in, 1/8" Section	0.010	0.0015	0.001	0.0005	D-955
1/4" Section	0.009	0.002	0.001	0.0005	
Water Absorption, %, 24 hrs. @ 23° C.	0.02	0.02	0.02	0.02	D-570
MECHANICAL					
Impact Strength, IZOD, Notched 1/4"	0.4	0.8	1.2	1.2	D-256
Unnotched 1/4"	1.8	3.0	4.0	4.0	
Tensile Strength, PSI	9500	22000	25000	26500	D-638
Tensile Elongation, %	1.6	0.75	0.5	0.5	D-638
Tensile Modulus, PSI X 10 ⁴	0.63	2.5	3.7	4.5	D-638
Flexural Strength, PSI	14000	27000	31000	34000	D-790
Flexural Modulus, PSI X 10 ⁴	0.55	2.1	2.5	3.5	D-790
Compressive Strength, PSI	16000	24000	26000	27000	D-695
Hardness, Rockwell R	120	122	123	123	D-785
ELECTRICAL					
Dielectric Strength, VPM, S/T	380	NA*	NA*	NA*	D-149
Dielectric Constant, 1 MC, Dry	3.1	NA	NA	NA	D-150
Dissipation Factor, 1 MC, Dry	0.0009	NA	NA	NA	D-150
Arc Resistance, Seconds	20	NA	NA	NA	D-495
Volume Resistivity, Ohm CM	10 ¹⁴	75	40	30	D-257
THERMAL					
Deflection Temp., °F., @ 264 PSI:	275	500	500	500	D-648
@ 66 PSI	300	500+	500+	500+	
Flammability	SE	SE	SE	SE	D-635
Flammability, UL Sub. 94, 1/8"	VEO	VEO	VEO	VEO	
Coefficient of Linear Thermal Expansion, in/in/°F. X 10 ⁻⁵	2.7	1.1	0.89	0.78	D-696
Thermal Conductivity, BTU/Hr./Ft ² /°F./in.	2.0	2.1	2.5	3.3	C-177

DATA SOURCE: FIBERITE CORPORATION

3.0 CONCEPTUAL DESIGN/CONCEPT EVALUATION

3.1 INTRODUCTION

Concept design and evaluations were performed to determine the cost trends between graphite structural components fabricated using epoxy resin systems and those using thermoplastic resin systems. These studies also showed structural weight savings provided by the advanced composite materials systems.

Several components as shown in Table 5, from the YC-14, a large transport aircraft, the Firebee missile, and Compass Cope drone were selected for study. All of them had been previously designed with fiberglass or aluminum alloys. New designs were developed using graphite/epoxy and graphite/thermoplastic construction. The resin systems were considered to have a maximum use temperature of 275°F. The graphite-epoxy and graphite-polysulfone designs for each component were basically the same with slight variations made to accommodate the unique characteristics of each material. The weight therefore of each component using the two advanced composite systems was the same. However, the costs of fabricating the components with the two advanced composite materials systems were quite different since different modes of construction were used. A summary of the cost factors and assumptions used in the cost studies is shown in Table 6.

3.1.1 COST PROCEDURE

Cost procedures were used that were based on cost histories from actual component fabrication. They were initially established for graphite-epoxy composite parts but with some modifications were also used for AF RTP composites. The resulting method has proven to be accurate for preliminary cost estimates.

To obtain fabrication time for producing detail parts the number of plies or precompacted laminates and the areas for each part were determined. These two values were multiplied to obtain the square foot-ply. This value times the

Table 5. Conceptual Design and Evaluation Components

STUDY COMPONENTS	APPLICATION
BODY	YC-14 LARGE TRANSPORT BQM-34E FIREBEE DRONE
WING (YC-14)	STIFFENED LAMINATE HONEYCOMB
HORIZONTAL STABILIZER	YC-14 COMPASS COPE

Table 6. Cost Factors and Assumptions

MATERIAL COSTS:

GRAPHITE/EPOXY	\$25/lb
GRAPHITE/POLYSULFONE (PRE-COMPACTED)	\$25/lb
S-GLASS/EPOXY OR S-GLASS/POLYSULFONE	\$12/lb
ADHESIVE	\$ 1/ft ²
HONEYCOMB CORE	\$ 0.03/in ³

LABOR COSTS

\$30/hr

LOSS FACTORS

PARTS SCRAPPAGE FACTOR – 5% FOR Gr/E – 1% FOR Gr/Ps
MATERIAL LOSS (INCLUDES RESIN, SOLVENT AND STORAGE
LOSSES AND CUTTING SCRAPPAGE BUT NOT OVERAGE
MATERIAL) – 30% FOR Gr/E – 15% FOR Gr/Ps

LABOR FACTORS

MANUFACTURING ENGINEERING	0.35 x Production hr.
QUALITY CONTROL	0.15 x Production hr.
TOOL MAINTENANCE	0.15 x Production hr.
TOOL DESIGN	0.30 x Tool Fab hr.

LEARNING FACTORS

85% LEARNING CURVE FOR BOTH THERMOSET AND
THERMOPLASTIC SYSTEMS
10 UNITS = 7.116 x Unit 1
100 UNITS = 43.754 x Unit 1

factor (mhr/sq ft-ply) provided the manhours required per part and, when all were added together, gave the total parts manhour cost. The curves used to select the above factor are shown in Figure 6. The figure relates mhr/sq ft-ply to the area of the part. Four curves were used to indicate complexity. These curves were developed from actual fabrication experience and are intended to establish the costs of the first production unit.

Assembly time was obtained by multiplying the total area of the parts by a factor mhr/ft² as shown in Figure 7. Three curves are shown which indicate complexity of the component. These curves were also based on cost data obtained from actual assembly of composite components.

To obtain the total production cost the manhours for each part were added and the total multiplied by a parts scrappage factor. The assembly cost was then added to obtain the production hours. The manufacturing engineering, quality control, and tool maintenance manhours were obtained by factoring these production hours. This total was the value used as the recurring production cost.

The material costs were obtained by adding the cost of the composite to the cost of other materials used such as honeycomb and adhesive. The net composite weight was obtained by adding the sq ft-ply values obtained for each part and multiplying by the proper factor (lb/sq ft-ply). A material loss factor and a part scrappage factor were added to obtain the total composite weight required. A cost per pound value was then used to get the composite cost. Honeycomb cost was determined by finding the cubic inches of core requirement and using a cost per cubic inch factor. The adhesive cost was determined from the area and the cost per unit area.

The tooling costs were obtained using Figure 8 which indicated the relationship of tool area to cost per unit area. Four levels of complexity are indicated. These curves were based on actual tool fabrication data and indicated the shop hours required to fabricate the tool. The design hours required for tooling were obtained by factoring the fabrication hours. The sum of the tool design and fabrication hours gave the total nonrecurring tooling hours.

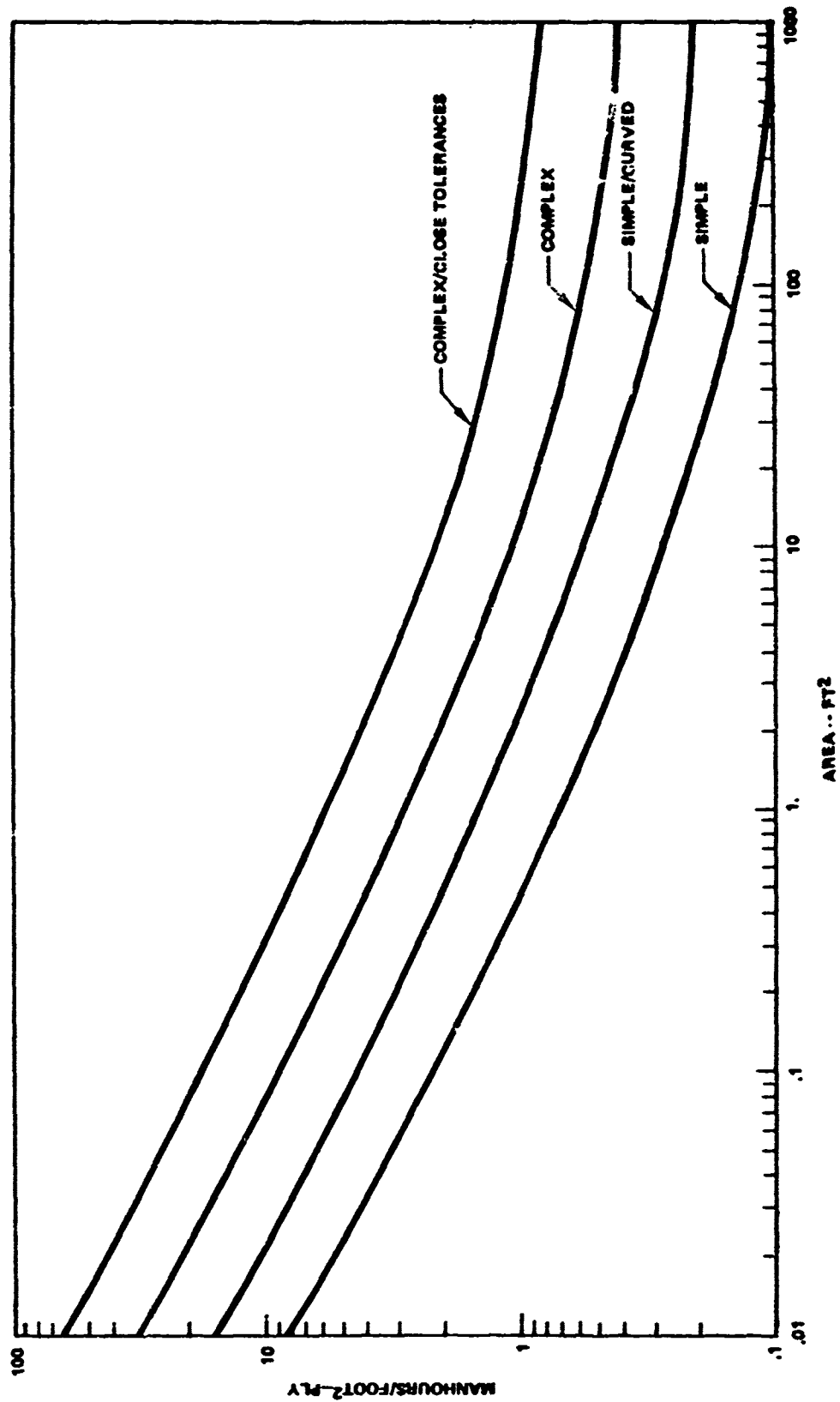


Figure 6. Part Fabrication Time

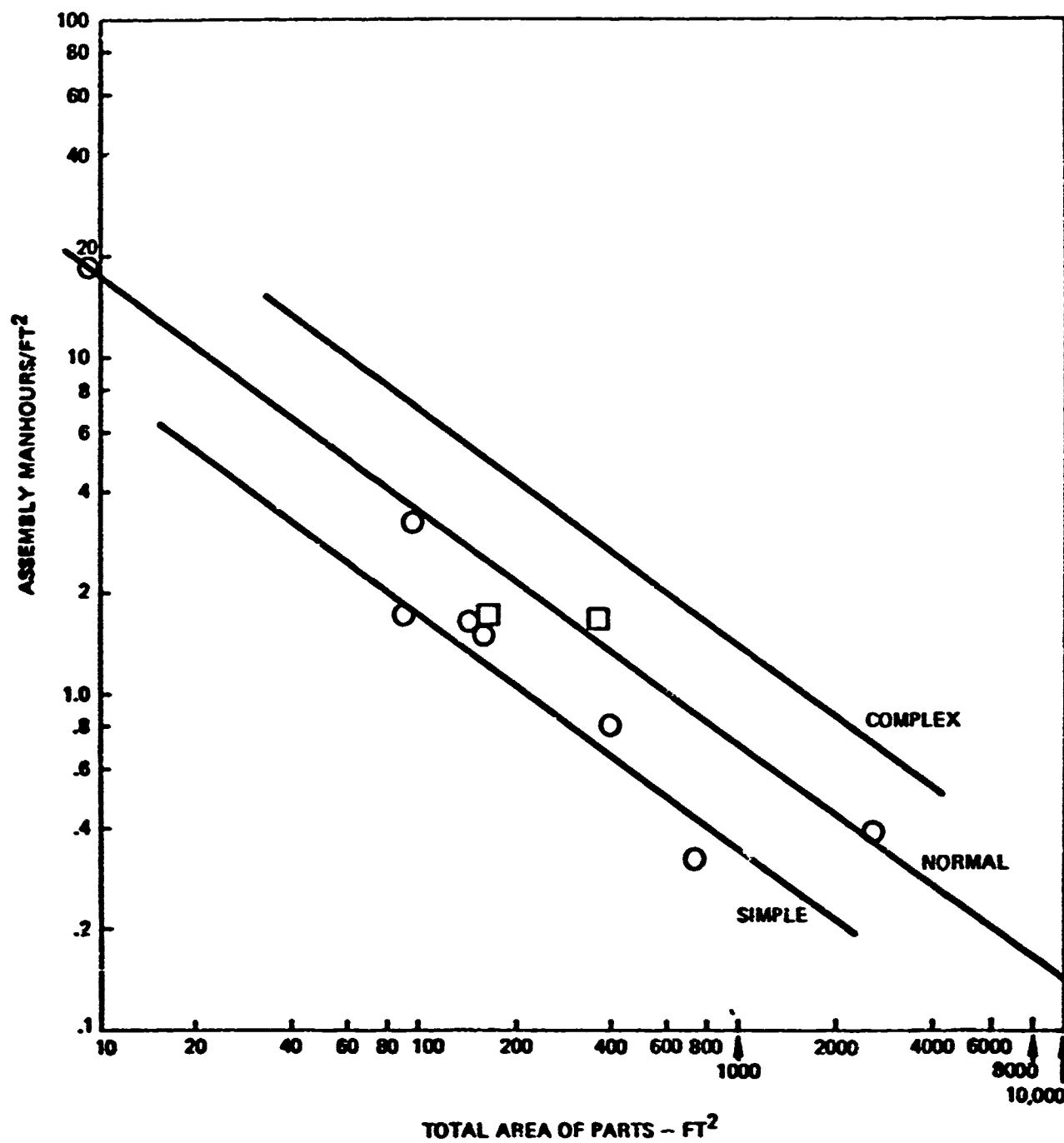


Figure 7. Assembly Time

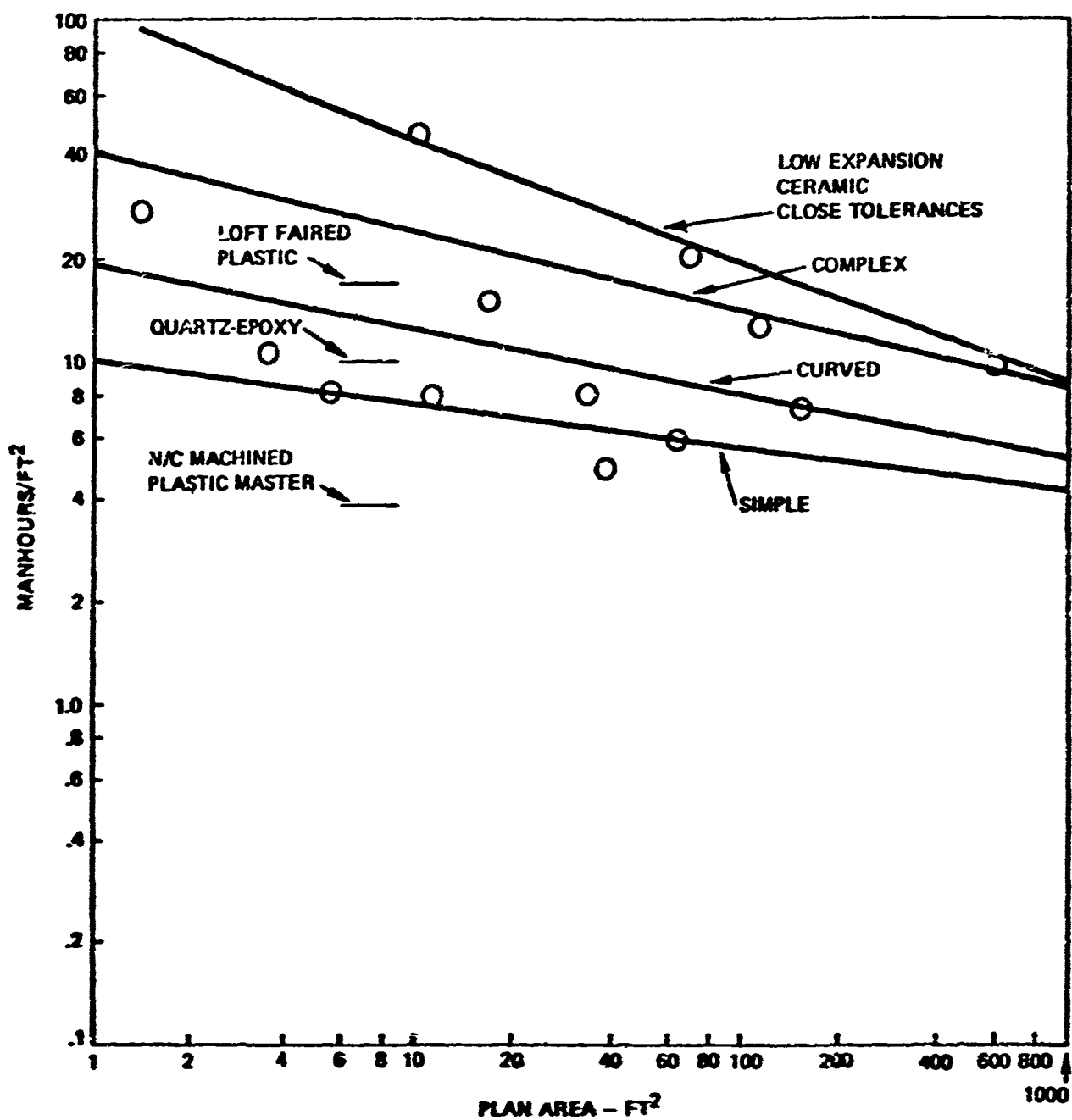


Figure 8. Tooling Time

3.2 YC-14 FUSELAGE BODY SECTION 43

A YC-14 fuselage advanced composite design was developed which uses a honeycomb sandwich shell as the primary load carrying structure. The honeycomb construction incorporated HRH honeycomb and graphite-epoxy or graphite-polysulfone skins. The design utilized large bonded assemblies and a minimum number of frames and bulkheads to reduce the total number of parts. Major assemblies were assembled using mechanical fasteners. Figure 9 shows the structural centerline drawing of this design.

Body section 43 was selected as a representative YC-14 fuselage component for the weight and cost study. Figure 10 shows the details of this section. A detailed weight and cost estimate of the section between Stations 300 and 440 was made and then scaled to obtain the Section 43 estimated weights and costs. Both advanced composite designs were approximately 20 percent lighter than the equivalent aluminum design. The cost estimates comparing graphite-epoxy and the graphite-polysulfone designs are shown in Table 7. As shown, the cost of the graphite-polysulfone design is significantly less by the tenth part and its cost effectiveness continues to improve as production quantities increase.

3.3 LARGE TRANSPORT A/C FUSELAGE PANEL

A typical sidebody panel for a large transport A/C was studied to compare the costs between a graphite-epoxy design and a graphite-polysulfone design. The all-aluminum design had conventional hat stringer stiffened skin and zee section frames. The advanced composite design described in Figure 11 has a graphite laminate skin stiffened by graphite "T" stringers, three composite rings, and two aluminum frames. Graphite pultrusions reinforced the outstanding legs of the stringers. The ring stiffeners are made of HRP core with graphite laminate face skins. Graphite laminate shear clips attach the aluminum frames to the skin.

Both advanced composite designs were approximately 16 percent lighter than the equivalent aluminum design. The cost estimates comparing graphite-epoxy and graphite-polysulfone designs are shown in Table 8. As shown, the graphite-polysulfone components were more cost effective than the graphite-epoxy components after only a few of the assemblies were produced.

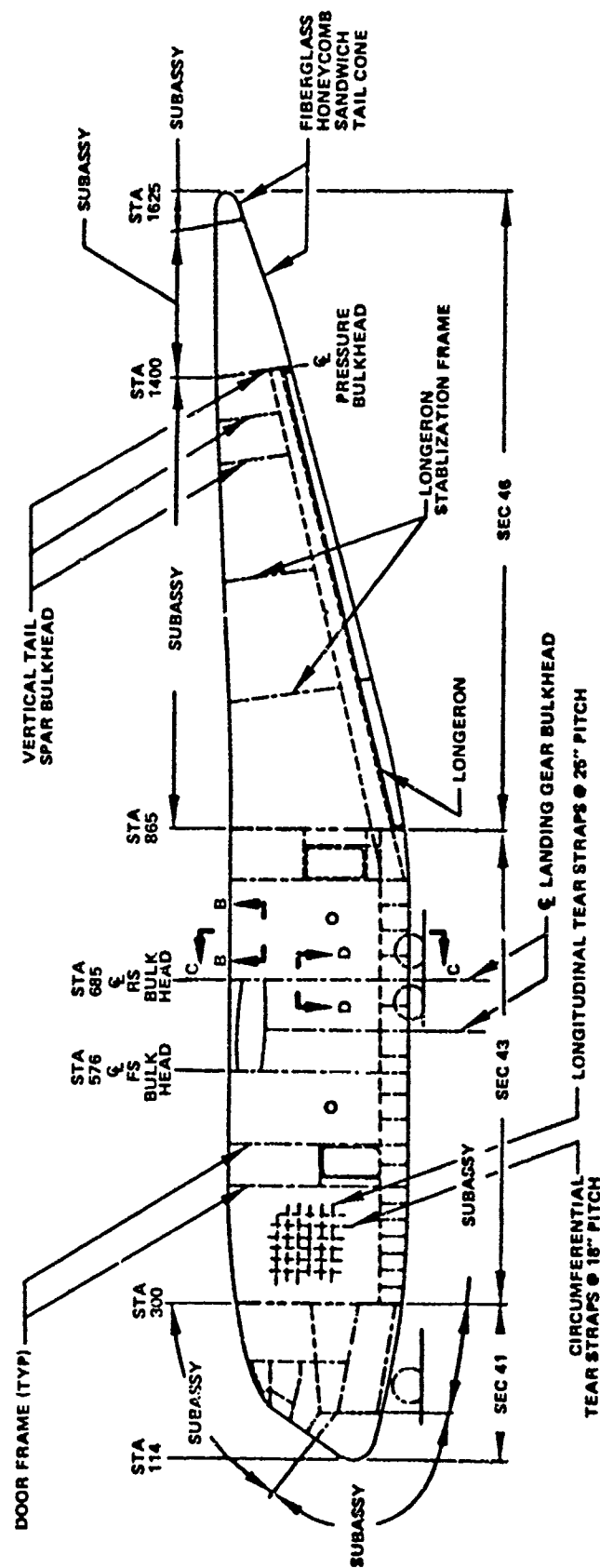
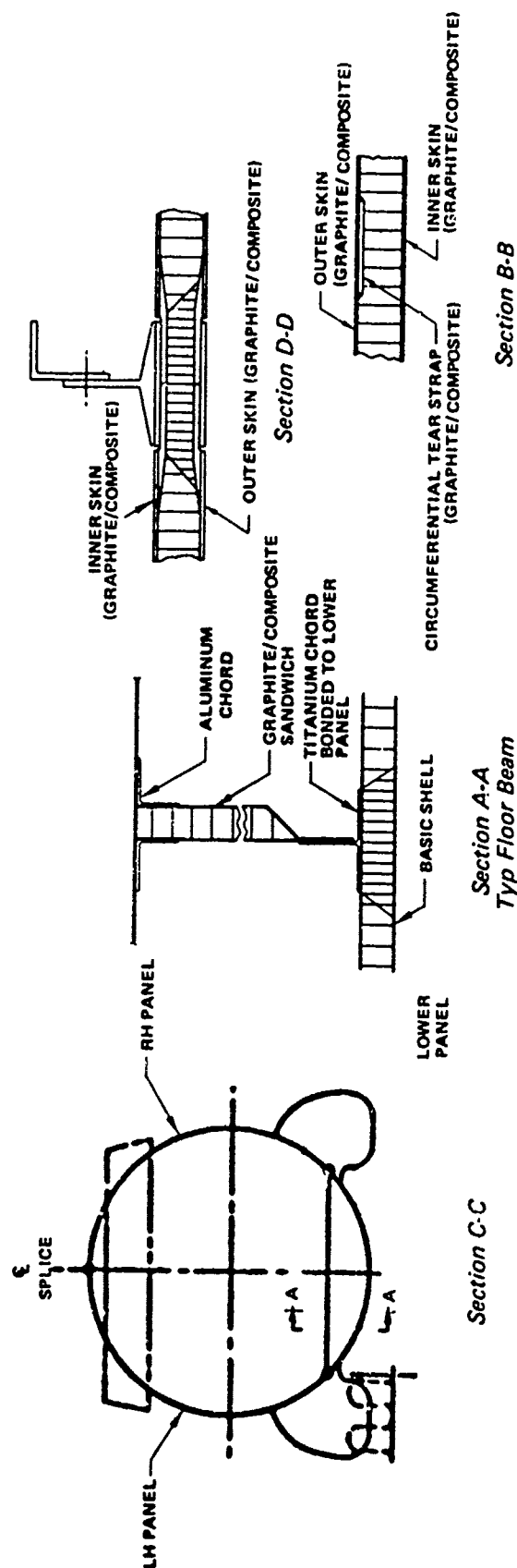
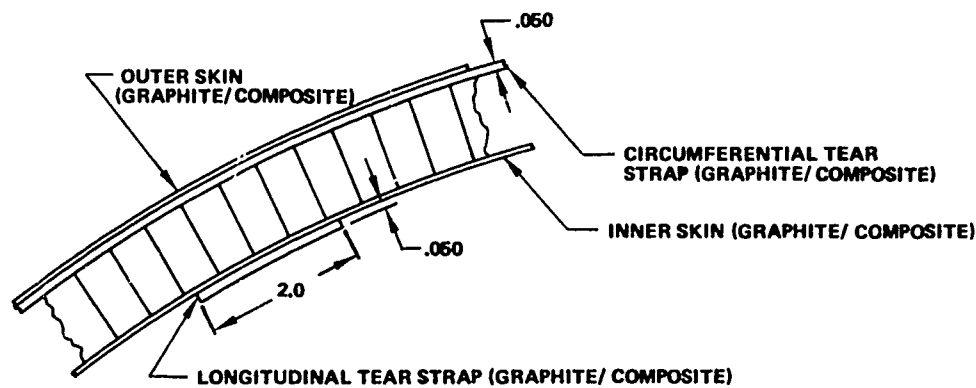
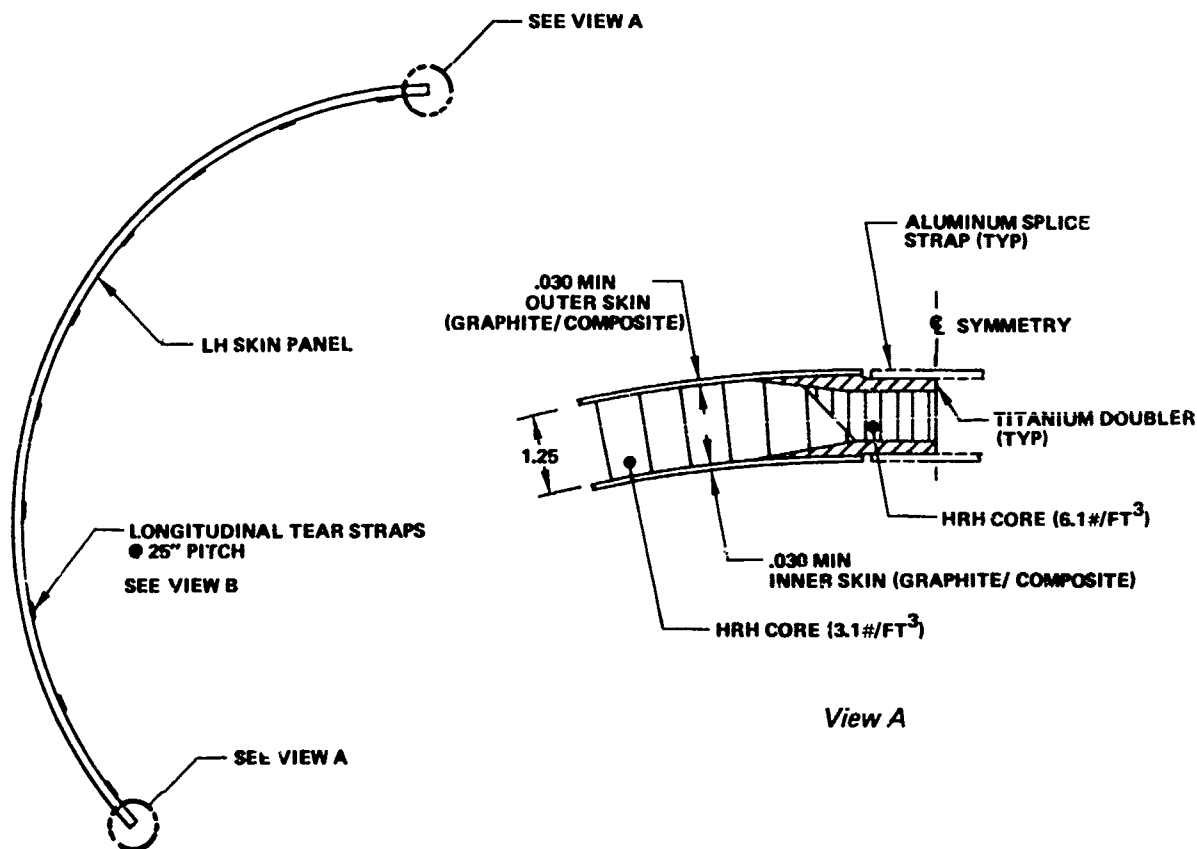


Figure 9. YC-14 Fuselage Structure Centerline Diagram



View B

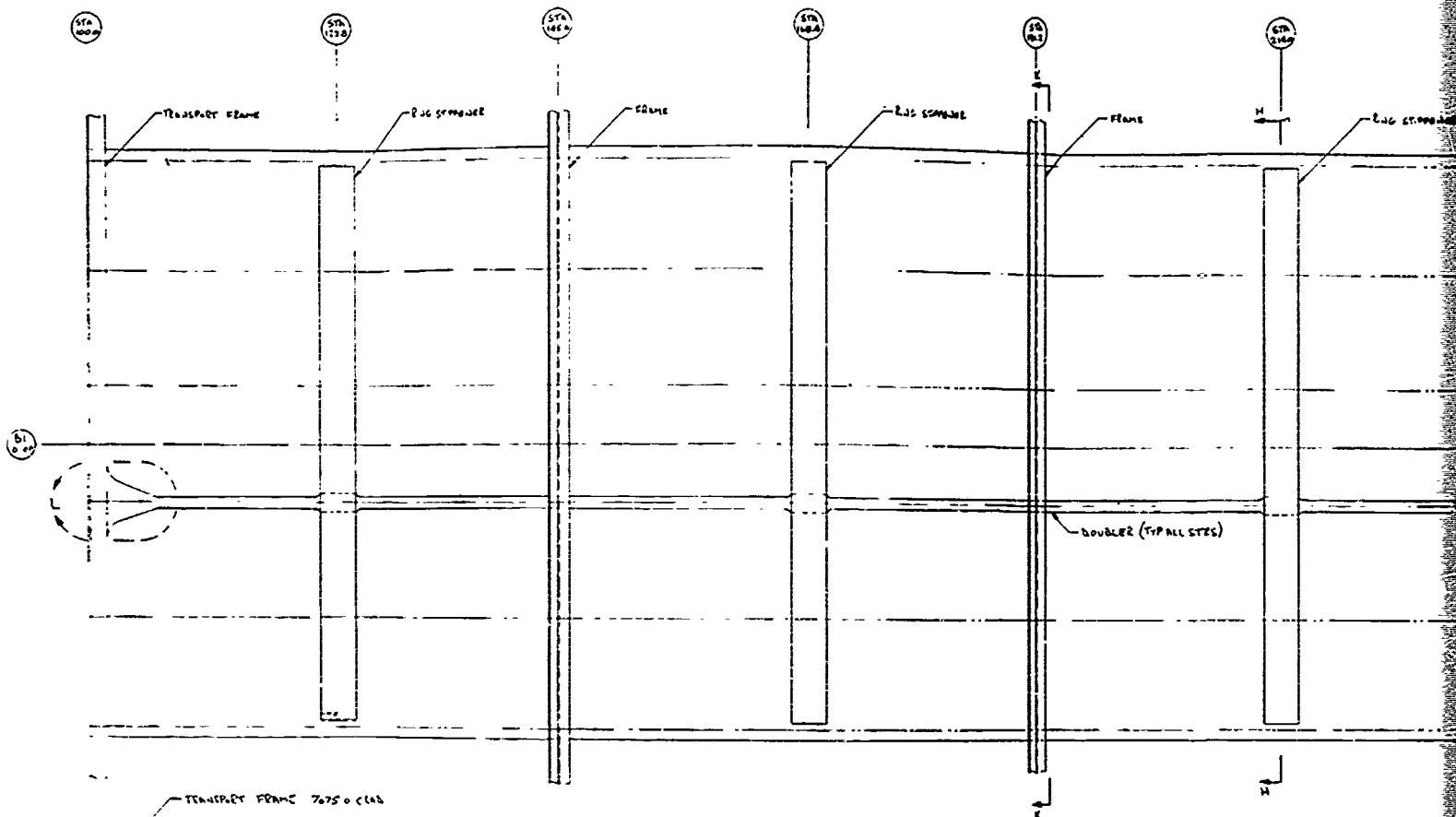


View A

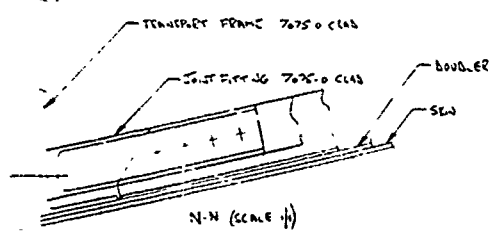
Figure 10. Fuselage Section 43 – Details

Table 7. Fabrication Costs for Advanced Composite Designs YC-14 Fuselage Body Section 43

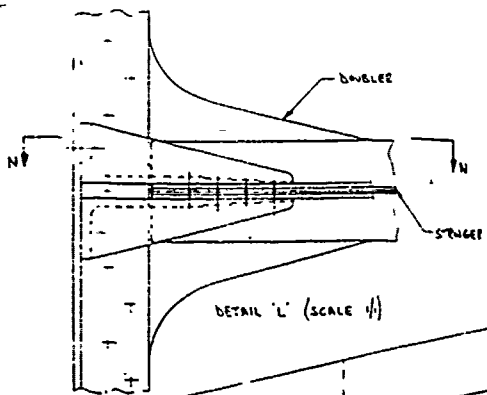
ADVANCED COMPOSITE MATERIAL	NO. OF UNITS	PRODUCTION HRS.	MATERIAL DOLLARS	TOOLING HRS.	TOTAL COST DOLLARS
GRAPHITE/EPOXY	1	14,877	83,418	23,904	1,705,848
	10	105,865	830,418	23,904	1,705,848
	100	650,928	8,304,180	23,904	28,000,000
GRAPHITE/POLYSULFONE	1	6,066	71,242	39,884	1,449,742
	10	43,166	712,420	39,884	3,203,910
	100	265,412	7,124,200	39,884	16,283,072



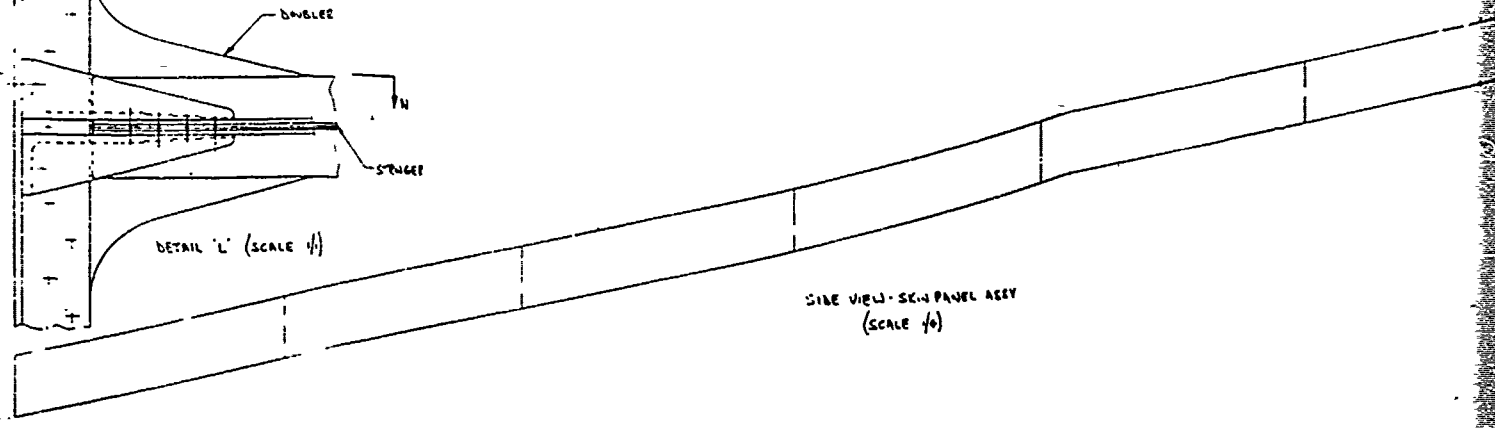
PLAN VIEW - SKIN PANEL ASSY
(SCALE 1/4)



N-N (SCALE 1/4)



DETAIL 'M' (SCALE 1/4)



SIDE VIEW - SKIN PANEL ASSY
(SCALE 1/4)

WL 1000
WL 1000

Table 8. Fabrication Cost for Advanced Composite Designs Large Transport A/C Fuselage Panel

ADVANCED COMPOSITE MATERIAL	NO. OF UNITS	PRODUCTION HRS.	MATERIAL DOLLARS	TOOLING HRS.	TOTAL COST DOLLARS
GRAPHITE/EPOXY	1	1,425	7,452	1,310	84,502
	10	10,140	24,520	1,310	386,020
	100	62,349	245,200	1,310	2,154,970
GRAPHITE/POLYSULFONE	1	961	2,099	2,184	96,449
	10	6,838	20,990	2,184	291,650
	100	42,048	209,900	2,184	1,536,860

3.4 FIREBEE DRONE CENTERBODY SECTION COMPONENTS

The XBQM-34E supersonic Firebee drone graphite-thermoplastic panel and door component designs were developed, fabricated, and delivered to NADC for ground testing under NADC Contract NG2269-74-C-0368, "Development of a Low Cost Graphite Reinforced Composite Primary Structural Component." The location of the components on the drone are shown in Figure 12 and their design details are shown in Figures 13 and 14. Figure 15 is a photograph of the actual delivered hardware.

Element and subcomponent tests confirmed the practicality and structural performance of the design concept. Weight saving for the retrofitted graphite-thermoplastic components was 5 percent.

Estimates were made of the costs for producing these components using graphite-epoxy and graphite-polysulfone. Table 9 shows a comparison of these two cost estimates. As shown, the graphite-polysulfone components are more cost effective than the graphite-epoxy components after the first few production parts.

3.5 YC-14 STIFFENED LAMINATE WING BOX

A multi-rib skin stringer wing box design was developed for the YC-14 as shown in Figure 16. The box was designed to be fabricated as a single component from tip to tip. It consisted of upper and lower stringer stiffened graphite laminate skins, a front and rear spar, and 66 ribs. The spars were a graphite laminate construction and the ribs HRH honeycomb core with graphite laminate face skins. The spars and ribs are detailed in Figure 17. The skin stringer consisted of an HRH honeycomb core filler and graphite pultrusions overwrapped with $\pm 45^\circ$ graphite laminate plies. The honeycomb is used to maintain a constant stringer cross section as the pultrusions are tapered along the length of the wing box. The upper skin panel stringers incorporate four pultrusions, the lower skin panel stringers two pultrusions. Details of the stringers are shown in Figure 18. The wing box design was sized to have the same bending and torsional stiffness as the YC-14 aluminum box. The surface panels were limited to $\epsilon_{\max} = 0.0044$ in./in. at ultimate load.

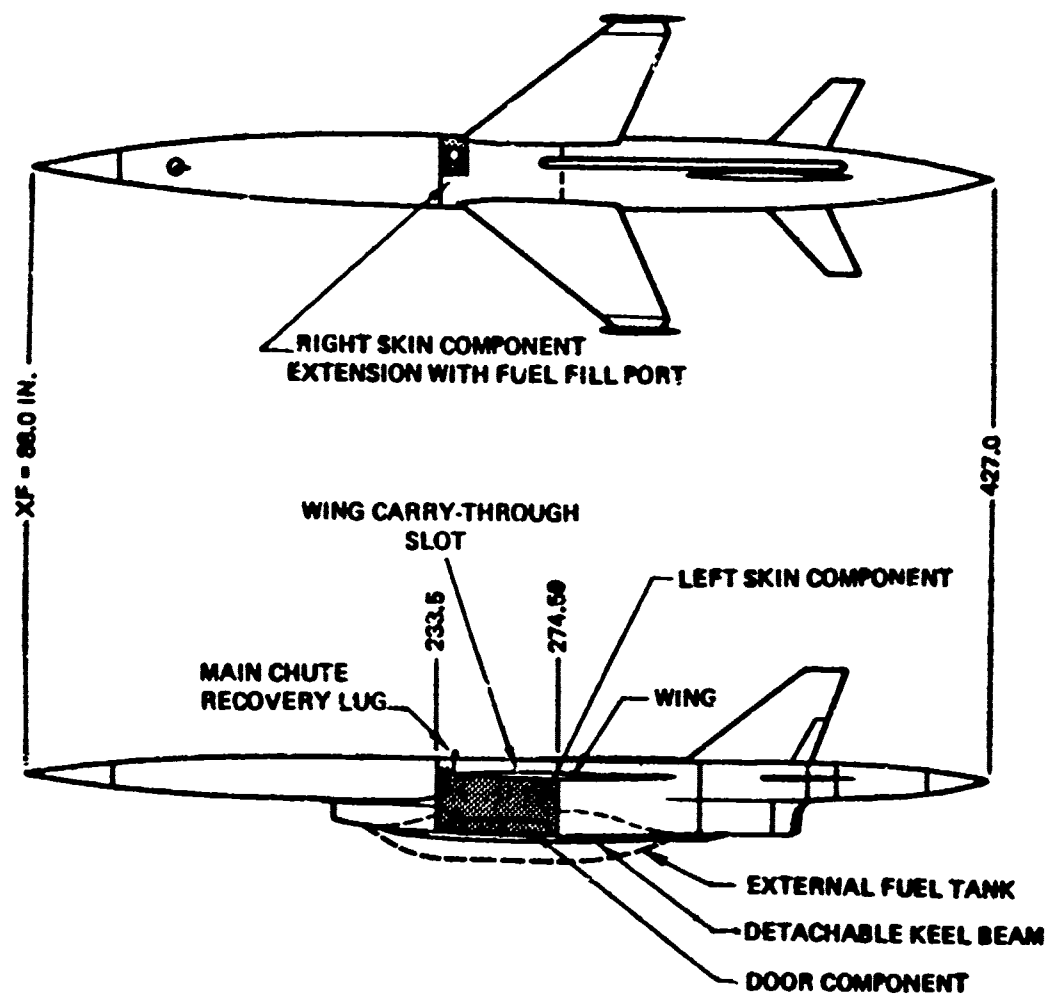


Figure 12. Firebee Drone Profile and Selected Gr/Ps Components

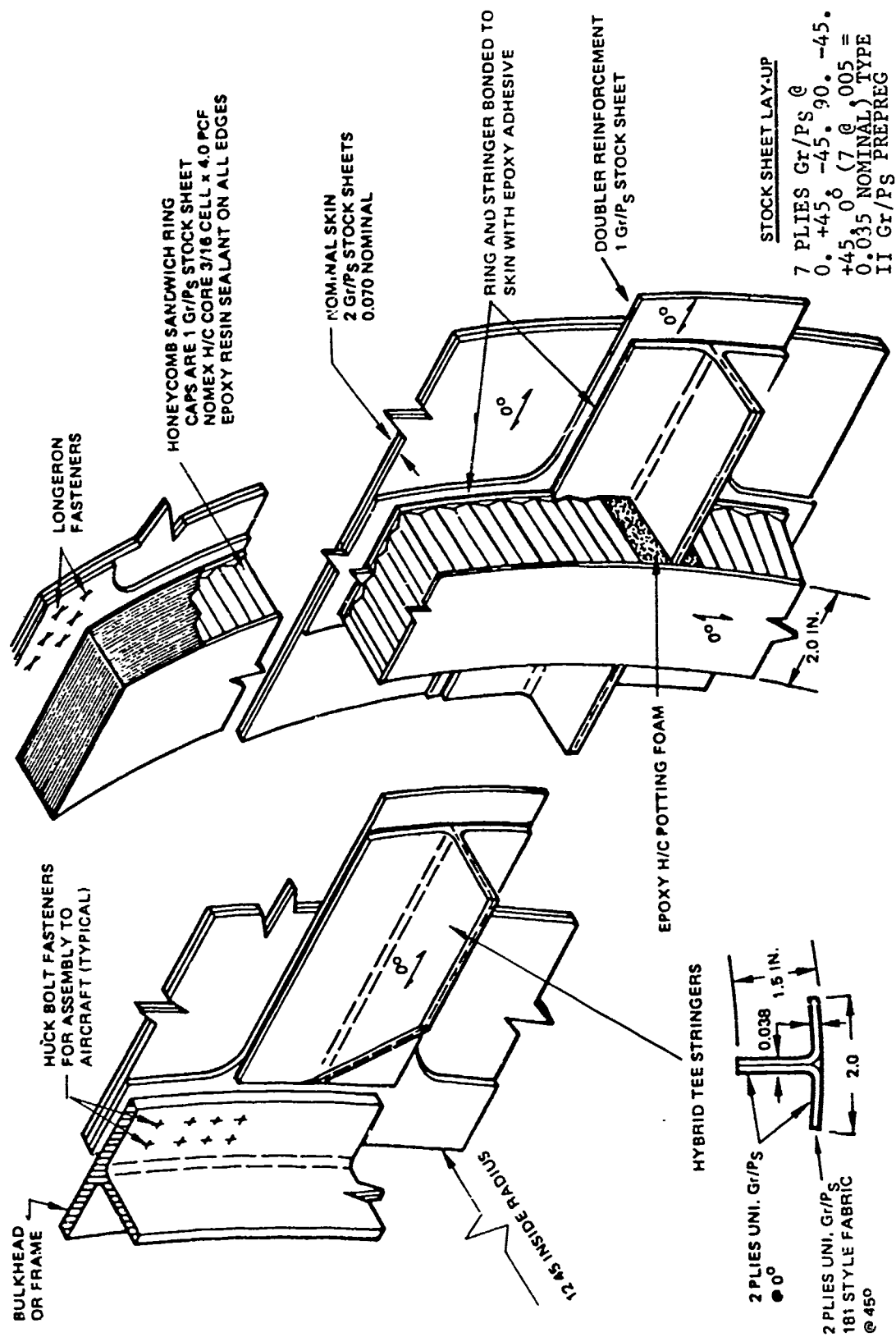


Figure 13. Prototype Gr/PS Component Design Concept Details

[illegible]

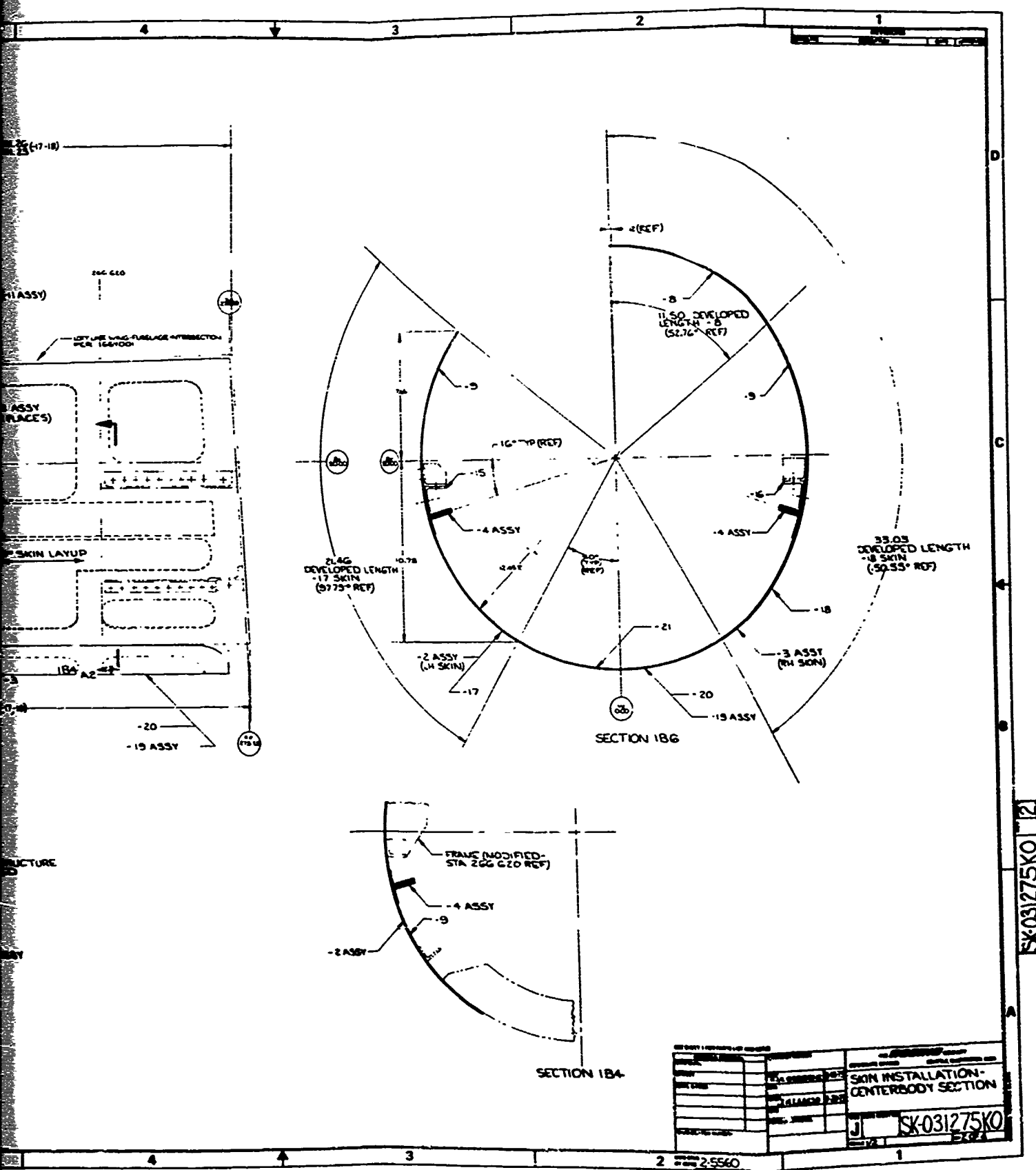
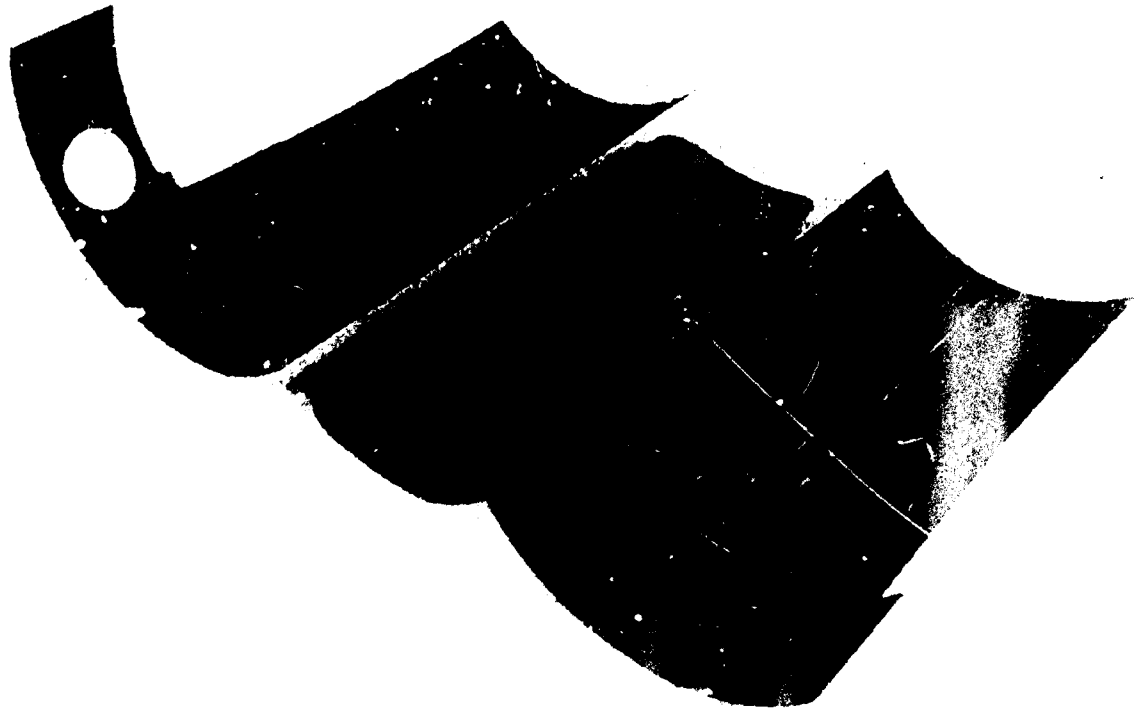


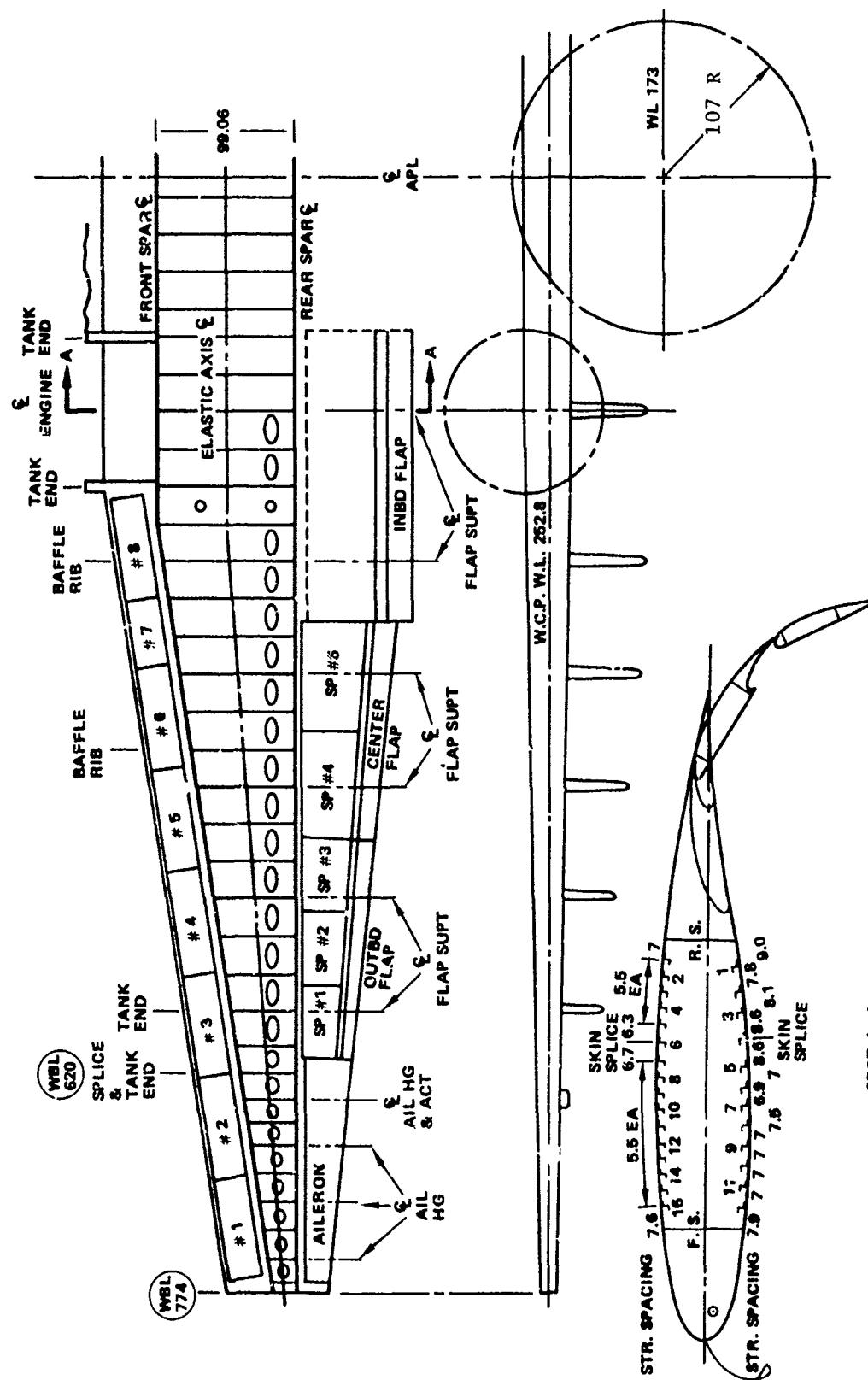
Figure 14. Skin Installation - Centerbody Section



*Figure 15. Delivered G RTP Components For The Fire: Drone
Center Body Section.*

Table 9. Fabrication Costs for Advanced Composite Designs Firebee Drone Body Component

ADVANCED COMPOSITE MATERIAL	NO. OF UNITS	PRODUCTION HRS.	MATERIAL DOLLARS	TOOLING HRS.	TOTAL COST DOLLARS
GRAPHITE/EPOXY	1	718	820	624	40,880
	10	5,109	8,200	624	178,189
	100	31,415	62,000	624	1,023,181
GRAPHITE/POLYSULFONE	1	386	527	1,131	46,337
	10	2,818	5,270	1,131	123,738
	100	17,327	52,700	1,131	606,428



SECT A-A
ALUM. BOX

Figures 16. YC-14 Wing Structure Diagram

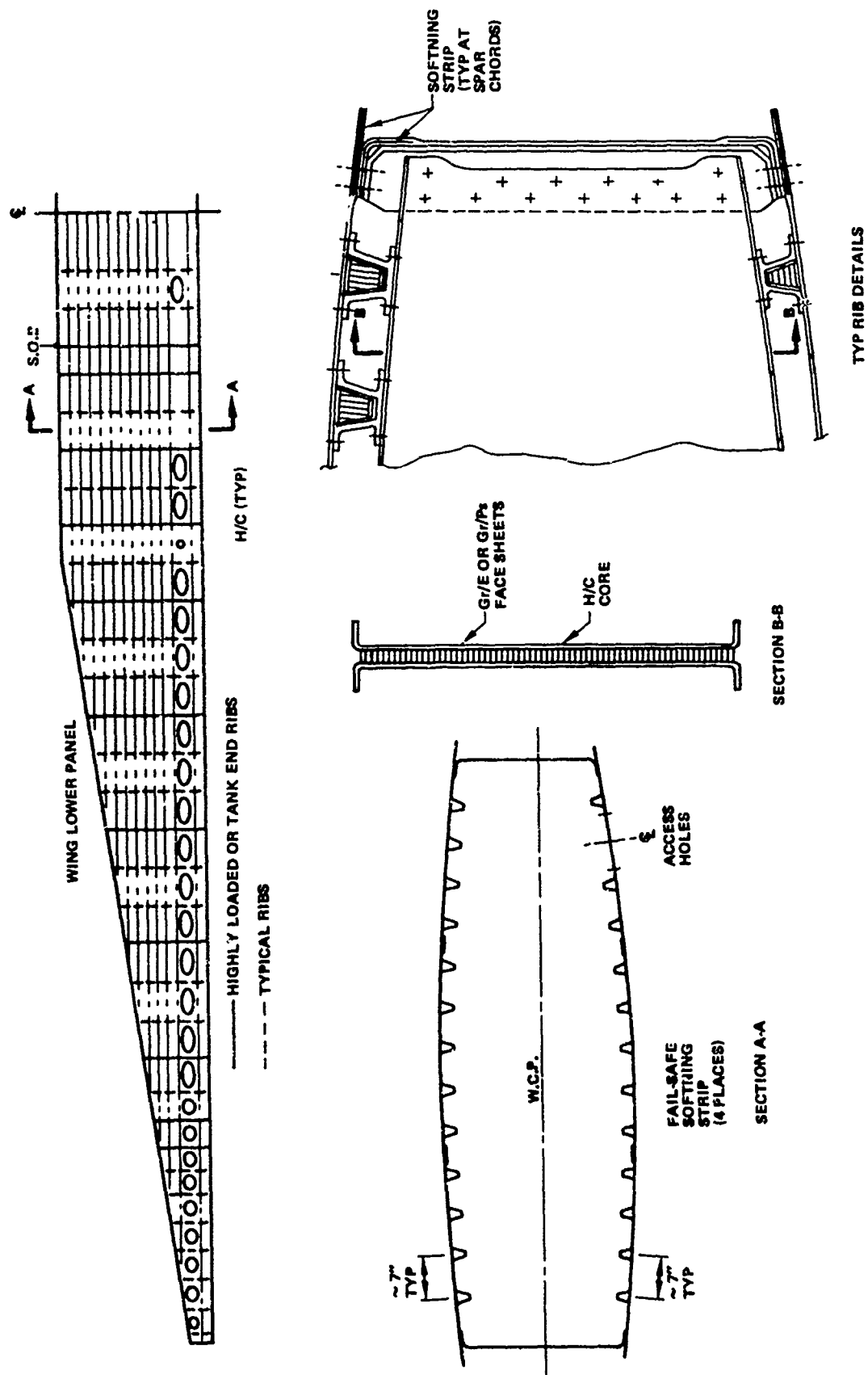
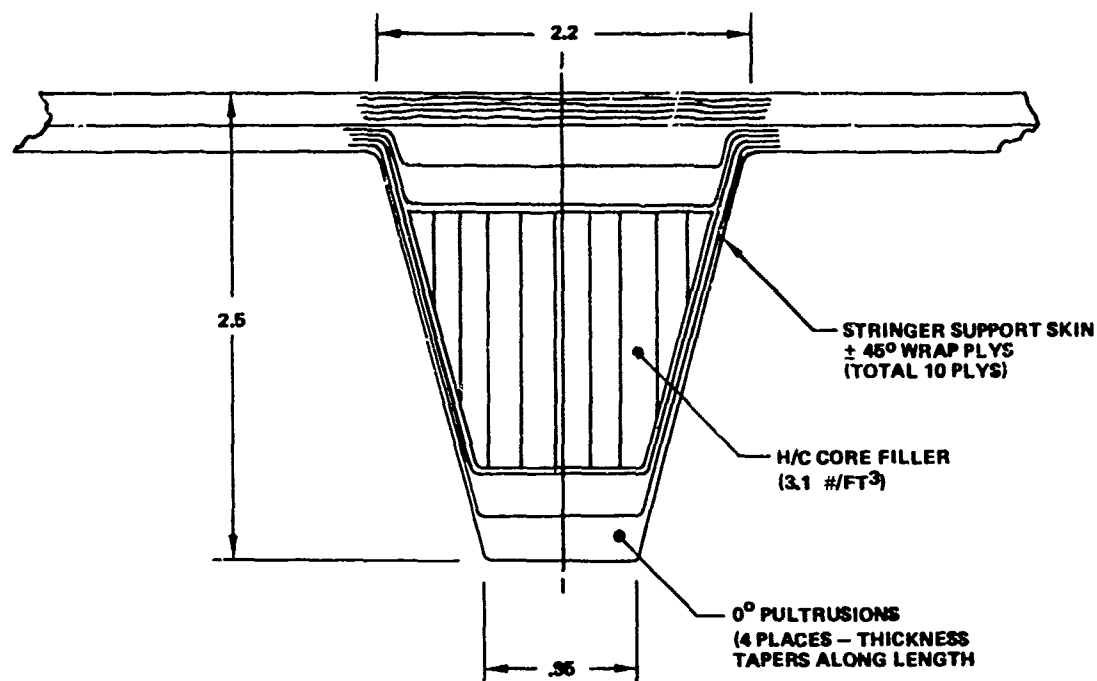


Figure 17. YC-14 Stiffened Laminate Wing Concept

A: UPPER PANEL STRINGERS



B: LOWER PANEL STRINGERS

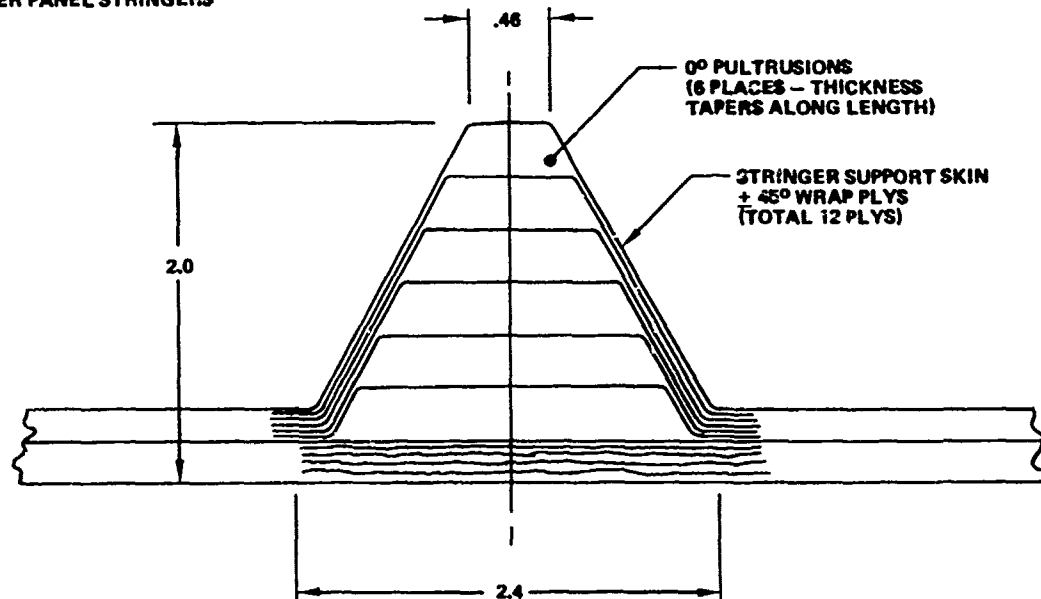


Figure 18. Stiffened Laminate Stringer Configurations

A weight estimate of the design is summarized in Table 10. As shown, the stiffened graphite laminate wing box is approximately 25 percent lighter than the equivalent aluminum design.

Estimates were made of the costs for this component fabricated using graphite-epoxy and graphite-polysulfone laminate and pultrusion material. Table 11 compared these estimates and shows the graphite-polysulfone is more cost effective by the tenth production component.

3.6 YC-14 HONEYCOMB WING BOX

A multi-spar-rib honeycomb wing box was developed for the YC-14 as shown in Figure 19. The box was designed to be fabricated as a single component from tip to tip. It consists of upper and lower skin panels, a front and rear spar, two intermediate spars, and twenty-four ribs. These are all HRH honeycomb parts with graphite laminate face skins. The intermediate spars are continuous members while the ribs act as intercostals between spars. The wing box design was sized to have the same bending and torsional stiffness as the YC-14 aluminum box. The surface panels were limited to $\epsilon_{\max} = 0.0044$ in./in. at ultimate load.

A weight estimate of the design was made and summarized in Table 12. The honeycomb wing box is approximately 29 percent lighter than the equivalent aluminum design.

Estimates were made of the costs for fabricating this component using graphite-epoxy and graphite-polysulfone face skins. Table 13 compares these two cost estimates. As shown, the graphite-polysulfone components are most cost effective than the graphite-epoxy components after the first few production parts. The graphite-epoxy component costs were based on data obtained from a 6-foot box section fabricated under Boeing in-house funding.

3.7 YC-14 HORIZONTAL STABILIZER

YC-14 horizontal stabilizer advanced composite designs were developed for evaluation. The stabilizer had a 17-1/2 ft. semi-span with a root chord of 5-1/2 feet and a tip chord of 3 feet. The designs were based on a multispar

Table 10. Wing Box Weight Summary—Stiffened Laminates Design
(Weight in Lbs.)

ITEM	AL	STIFFENED GRAPHITE	Gr/AL
UPPER PANEL	4211	3354	.80
LOWER PANEL	4214	3182	.75
SPARS	1540	943	.61
RIBS	1974	1482	.75
TOTALS	11,939	8961	.75
25% WEIGHT SAVING			

Table 11. Fabrication Costs for Advanced Composite Designs—Y/C-14 Stiffened Laminate Wing Box

ADVANCED COMPOSITE MATERIAL	NO. OF UNITS	PRODUCTION HRS.	MATERIAL DOLLARS	TOOLING HRS.	TOTAL COST DOLLARS
GRAPHITE/EPOXY	1	31,970	288,150	24,162	1,972,110
	10	227,498	2,881,500	24,162	10,431,315
	100	1,398,815	28,815,000	24,162	71,504,319
GRAPHITE/POLYSULFONE	1	20,225	246,000	44,158	2,177,490
	10	143,921	2,460,000	44,158	8,102,373
	100	884,925	24,600,000	44,158	52,472,479

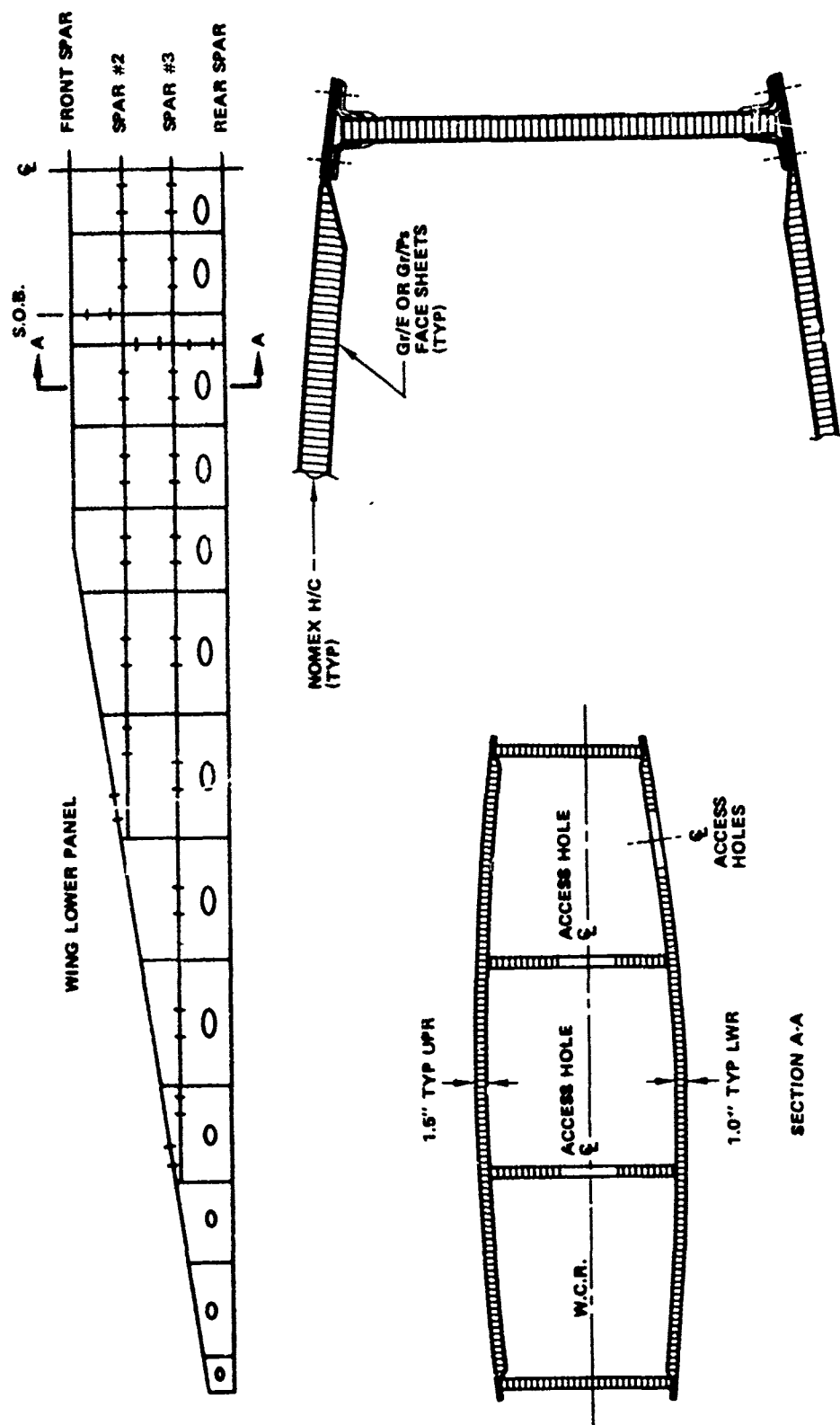


Figure 19. YC-14 Honeycomb Wing Concept

Table 12. Wing Box Weight Summary—Honeycomb Concept
(Weight in Lbs.)

ITEM	A1	HONEYCOMB GRAPHITE	Gr/AL
UPPER PANEL	4211	2975	.71
LOWER PANEL	4214	3052	.72
SPARS	1540	943	.61
RIBS	1974	1482	.75
TOTALS	11,939	8452	.71
29% WEIGHT SAVING			

Table 13. Fabrication Costs for Advanced Composite Design—YC-14 Honeycomb Wing Box

ADVANCED COMPOSITE	NO. OF UNITS	PRODUCTION HRS.	MATERIAL DOLLARS	TOOLING HRS.	TOTAL COST DOLLARS
GRAPHITE/EPOXY	1	24,945	245,870	24,344	1,724,540
	10	177,509	2,458,700	24,344	8,514,280
	100	1,091,443	24,587,000	24,344	58,060,625
GRAPHITE/POLYSULFONE	1	13,159	211,981	42,406	1,878,930
	10	93,639	2,119,810	42,406	6,201,173
	100	576,759	21,198,100	42,406	39,743,046

(4) concept and incorporated several full and partial ribs. A centerline diagram of the stabilizer is shown in Figure 20. Both the covers and the ribs were stiffened with beads. The spar webs were stiffened with "Tees" made of two back-to-back angles. Details of a typical spar/rib intersection are shown in Figure 21. The cover panels, spar and rib webs were all made of graphite/polysulfone fabric oriented at $\pm 45^\circ$.

The weights of both the Gr/E and GR/PS designs were determined. They were compared to the existing aluminum design and estimated to be approximately 35 percent lighter.

Cost studies were also performed which compared the fabrication cost of graphite-epoxy components with graphite-polysulfone components. The results obtained were consistent with the results obtained in previous cost studies.

Because of higher tooling cost the first unit production cost of a YC-14 horizontal stabilizer using graphite-polysulfone was higher than the design using graphite-epoxy. But, because the graphite-polysulfone design required fewer production hours, it could be produced at a lower net cost by the production of the tenth unit. Table 14 summarizes the data developed while evaluating YC-14 horizontal stabilizer production costs.

3.8 COMPASS COPE HORIZONTAL STABILIZER

A Compass Cope advanced composite horizontal stabilizer design was developed which used a honeycomb stabilized skin. The existing design utilizes fiberglass sandwich construction as shown in Figure 22. The stabilizer was 180 inches long and 20 inches between its forward and rear spars as shown in Figure 23. Typical details of the composite design are shown in Figure 24. The upper and lower panels were stabilized with 1/4 in. thick, 3 lb Nomex core. The face skins were $0/\pm 45/90$ graphite laminates. The rib webs are also stabilized with Nomex core.

The weights were determined for both the Compass Cope fiberglass honeycomb design and the graphite designs developed in this study. This data showed that the composite designs (graphite-epoxy and graphite-polysulfone) were 36 percent lighter than the fiberglass honeycomb design.

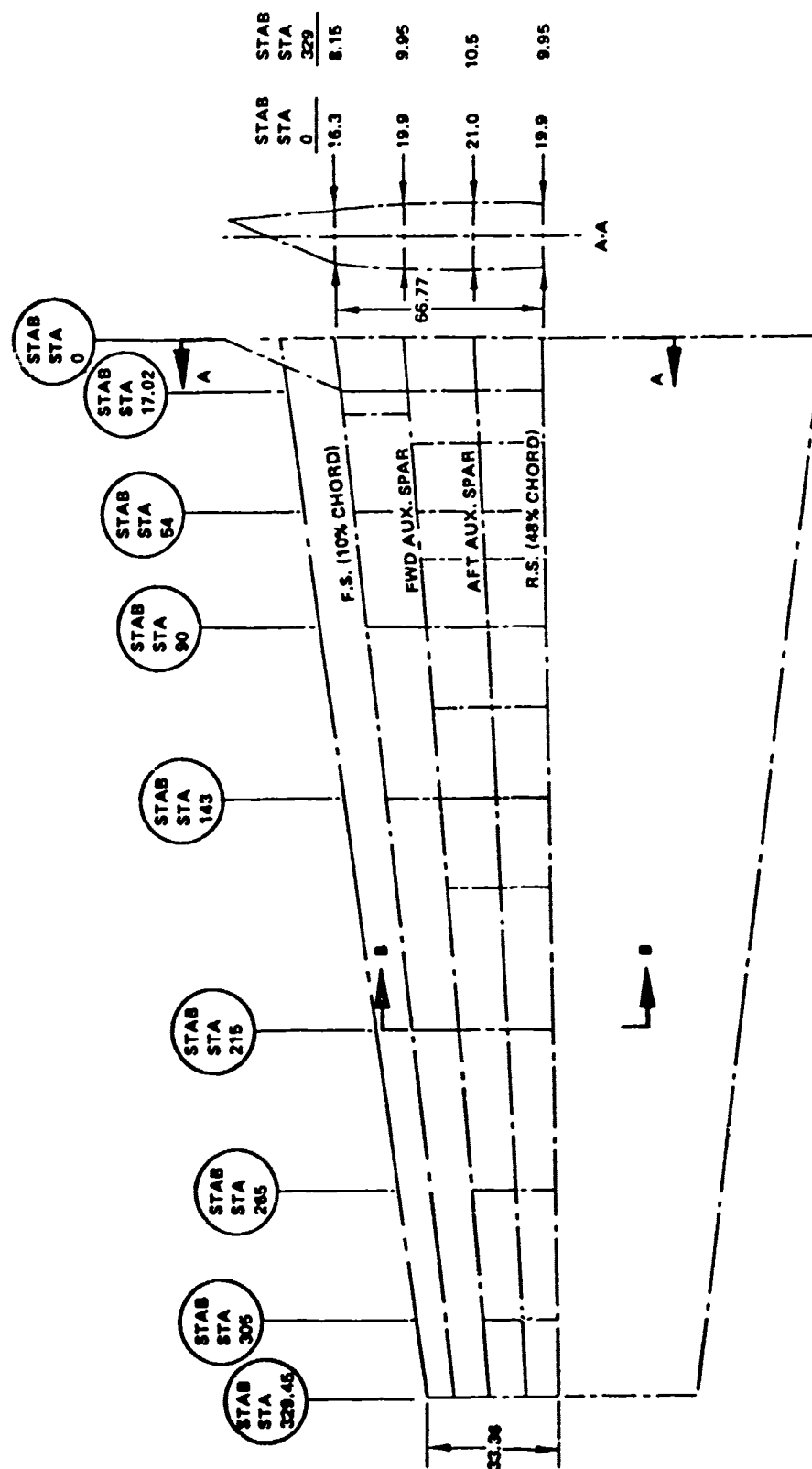


Figure 20. YC-14 Horizontal Stabilizer Centerline Diagram

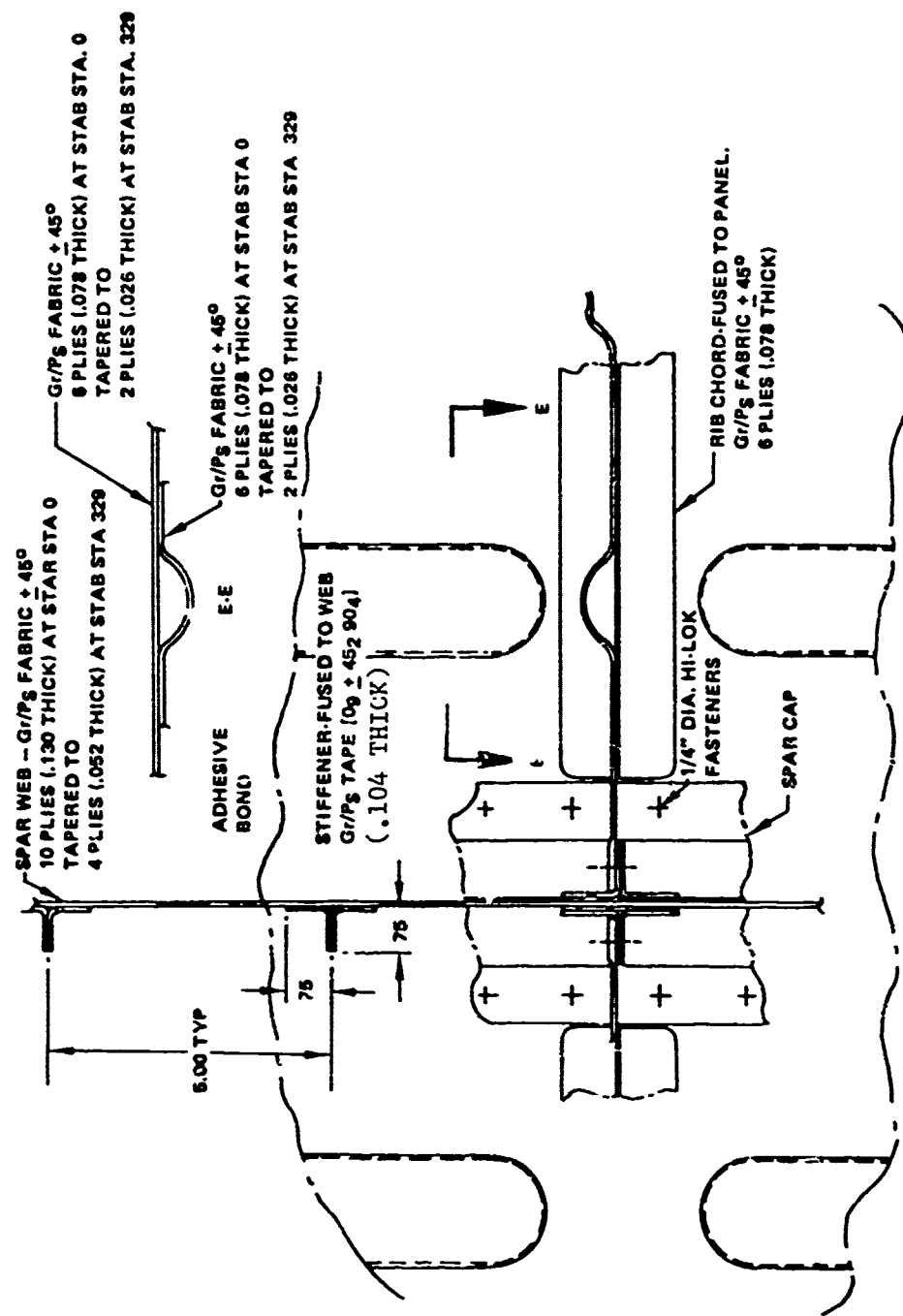
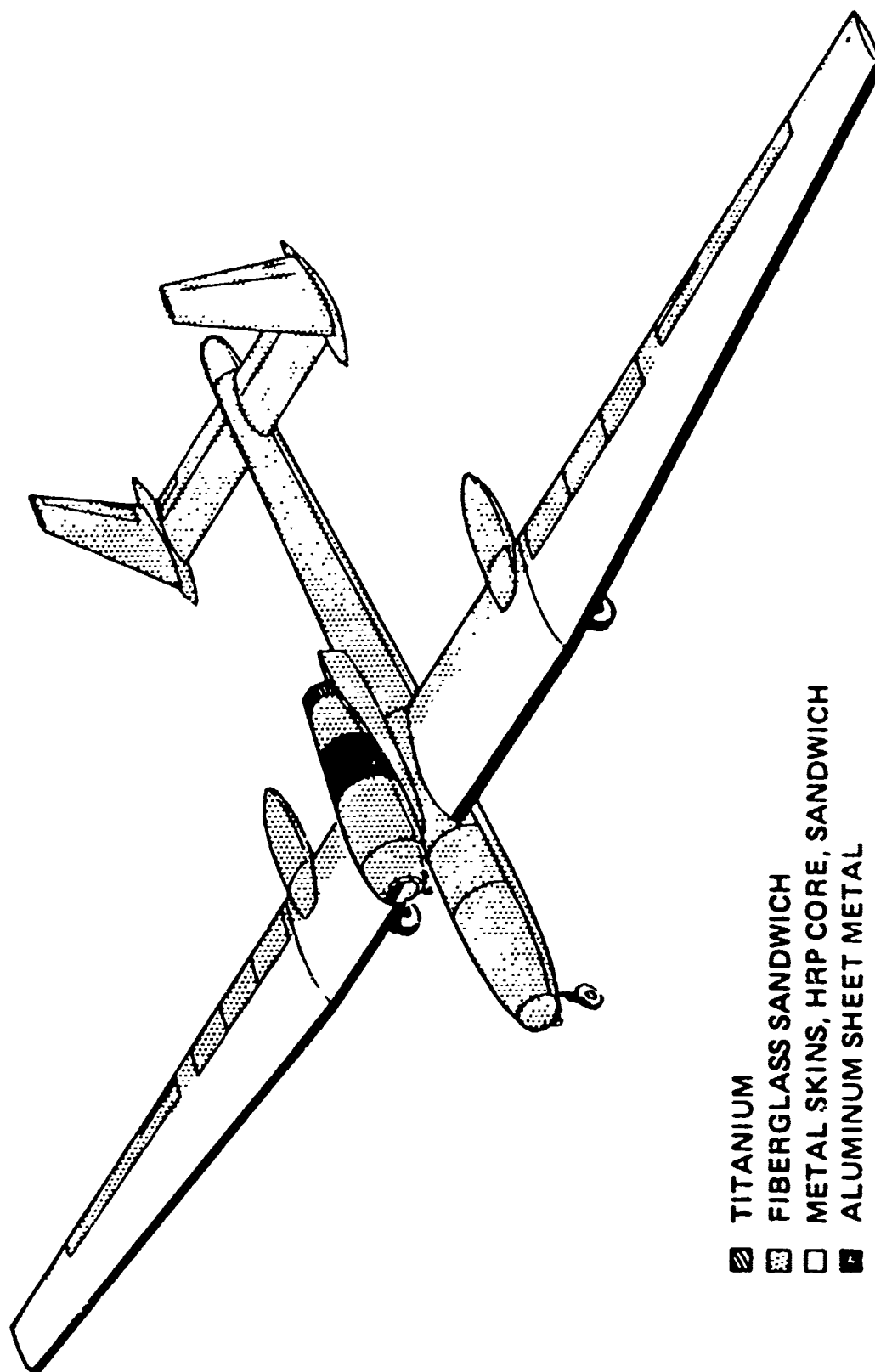


Figure 2'i. Typical Spar/Rib Attachment

Table 14. YC-14 Advanced Composite Horizontal Stabilizer Cost Estimate

ADVANCED COMPOSITE MATERIAL	NO. OF UNITS	PRODUCTION HOURS	MATERIAL DOLLARS	TOOLING HOURS	TOTAL COST DOLLARS
GRAPHITE/EPOXY	1	8,553	48,926	7,742	536,076
	10	60,936	469,260	7,742	2,529,550
	100	374,666	4,692,600	7,742	16,164,825
GRAPHITE/POLYSULFONE	1	6,050	40,015	11,726	573,295
	10	43,052	400,150	11,726	2,043,484
	100	264,712	4,001,500	11,726	12,294,631



- ▨ TITANIUM
- ▩ FIBERGLASS SANDWICH
- ▢ METAL SKINS, HRP CORE, SANDWICH
- ALUMINUM SHEET METAL

Figure 22. Compass Cope Material Systems

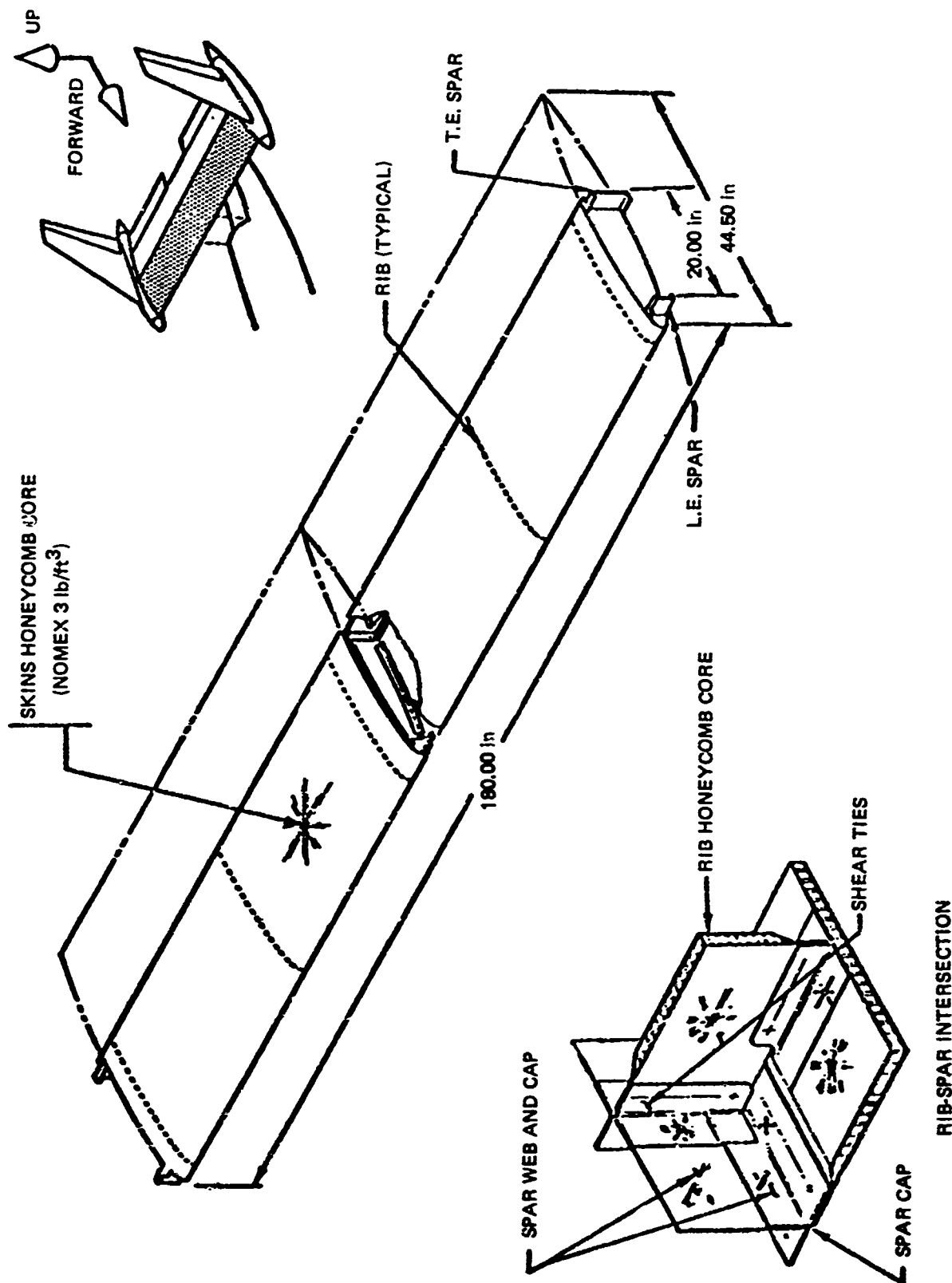


Figure 23. Compass Cope—Horizontal Stabilizer Composite Design

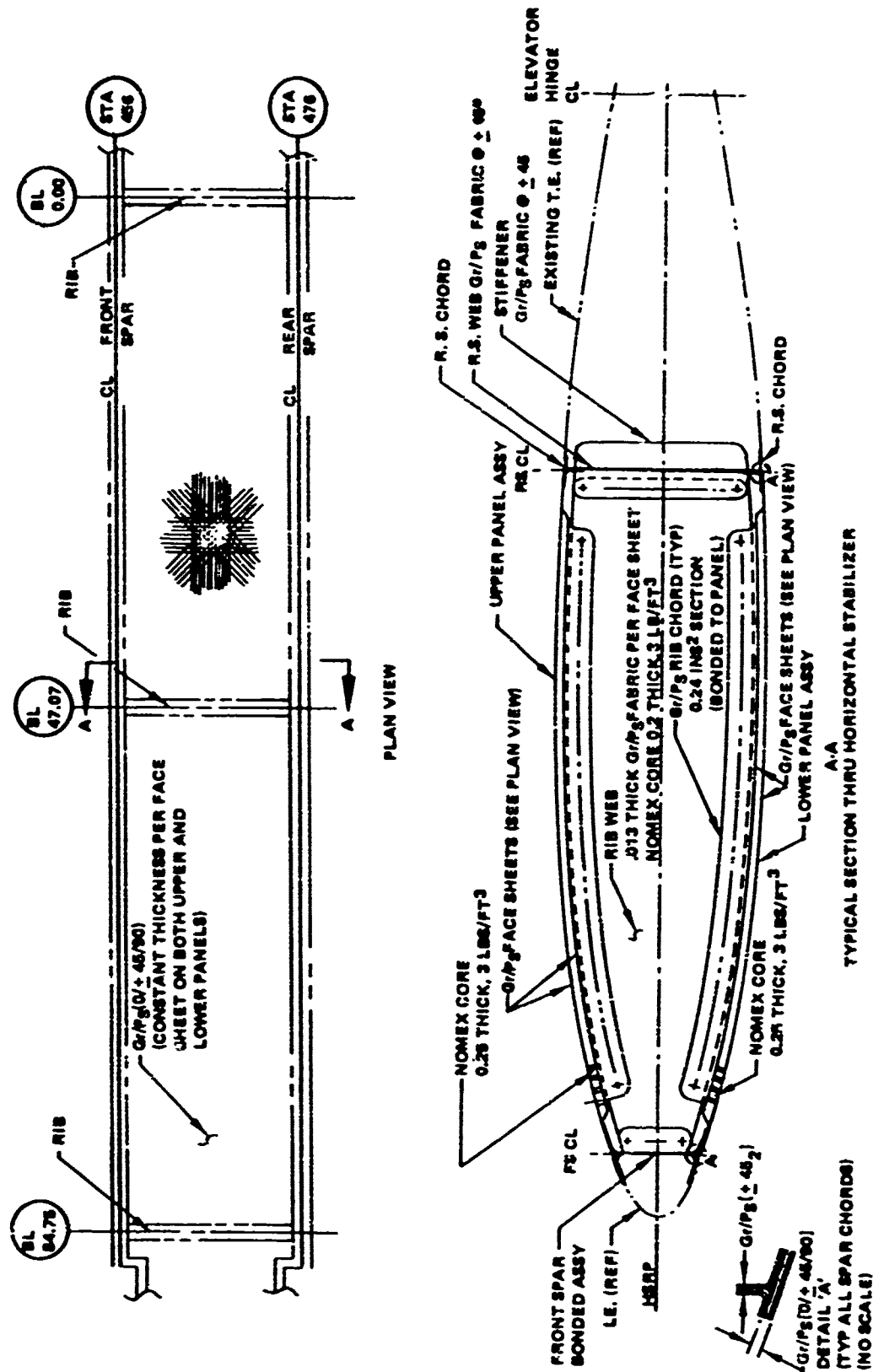


Figure 24. Compass Cope Horizontal Stabilizer Details

Studies were also performed to determine the relative costs between the graphite-epoxy and graphite-polysulfone designs. A summary of this data is shown in Table 15. As shown, the graphite-polysulfone design is more cost effective by the production of the tenth unit. The first unit is more expensive because of higher tooling cost. The significantly lower production hours required for producing the graphite-polysulfone parts amortizes the difference in tooling in a manner which makes the tenth production part more cost effective than the equivalent graphite-epoxy part.

Another cost study was made in which the cost of producing the fiberglass/epoxy honeycomb design was compared to the graphite-polysulfone design. In this study the fiberglass/epoxy material costs were based on aerospace quality material of \$12/lb and the graphite-polysulfone at today's cost of \$65/lb. The cost data is summarized in Table 16. As shown, the low production cost of the graphite-polysulfone design offsets the increase in material and tooling cost by the fabrication of the tenth part.

3.9 CONCLUSIONS

Seven aircraft and missile structural components were evaluated in this program (Table 1). The evaluation compared advanced composite component designs with existing aluminum or fiberglass designs. In all cases the results showed that the composite designs were lighter than the more conventional designs. The weight savings were from 5 percent for replacement body panels on the Firebee Drone to 36 percent provided by a new composite design of the Compass Cope's horizontal stabilizer.

One of the major objectives of this study was to obtain the relative costs between producing components utilizing graphite-epoxy materials and graphite-polysulfone. The study results consistently showed that using an 85% learning curve, the graphite-polysulfone parts were more cost effective by the production of the tenth unit. The tooling costs were higher for the graphite-polysulfone because of higher process temperatures and pressures. This additional cost was offset by the lower production costs, thereby producing a lower cost part by the production of the tenth unit. In general, the first unit cost of a thermoplastic component was 14 percent higher than the epoxy component. By the production of the tenth unit, the cost of thermoplastic parts averaged 33 percent less than the epoxy parts.

Table 15. Compass Cope Advanced Composite Horizontal Stabilizer Cost Estimate

ADVANCED COMPOSITE MATERIAL	NO. OF UNITS	PRODUCTION HOURS	MATERIAL DOLLARS	TOOLING HOURS	TOTAL COST DOLLARS
GRAPHITE/EPOXY	1	1,068	1,213	810	57,553
	10	10,680	12,130	810	264,426
	100	46,730	121,300	810	1,547,478
GRAPHITE/POLYSULFONE	1	775	1,060	1,690	75,010
	10	5,515	10,600	1,690	226,747
	100	33,909	106,000	1,690	1,173,980

Table 16. Compass Cope Horizontal Stabilizer Cost Estimate - Glass/Epoxy and Graphite/Polysulfone

ADVANCED COMPOSITE MATERIAL	NO. OF UNITS	PRODUCTION HOURS	MATERIAL DOLLARS	TOOLING HOURS	TOTAL COST DOLLARS
GLASS/EPOXY (\$12/LB.)	1	1,068	600	810	56,940
	10	7,600	6,000	810	258,296
	100	46,730	60,000	810	1,486,178
GRAPHITE/POLYSULFONE (\$65/LB.)	1	775	2,760	1,690	76,710
	10	5,515	27,600	1,690	243,747
	100	33,909	276,000	1,690	1,343,980

4.0 MANUFACTURING DEVELOPMENT

A series of studies were performed to evaluate graphite thermoplastic processing methods. The areas of study included laminate consolidation, post-forming bonding and joining methods and chopped fiber molding fabrication. A summary of the areas investigated is shown in Table 17.

4.1 CONSOLIDATION

Four laminate consolidation methods were investigated. They were accomplished by press, autoclave, pultrusion and roll-forming.

4.1.1 Press Consolidation

Press lamination studies were performed which resulted in a two-hour cycle for a 4 ft² laminate (0.5 hr/ft²). The time per unit area was dependent upon the capacity and capability of the press utilized. If the press had rapid heating or cooling capability, the cycle time could have been reduced. The two-hour cycle was based on a part/mold assembly heatup rate of 100°F/min from room temperature to +650°F and cooldown to +100°F. The cycle time could have been reduced to 1.25 hr if the part/mold was preheated to +350°F in an oven or other facility prior to insertion in the press and then molded at 600°F/200 psi, and removed at +300°F on the cooldown cycle.

Consolidation costs could have been further reduced by laminating multi-sheets at one time using a separator ply between layers. This technique would have increased the cycle time due to heat flow but the time per ft² of laminate would have decreased significantly as shown in Table 18. This table assumed three sheets were molded simultaneously.

Figures 25 and 26 show the cross section of a press consolidated unidirectional laminate and a 181-style fabric laminate respectively.

Table 17. Task IV-Manufacturing Development

LAMINATE CONSOLIDATION:	<ul style="list-style-type: none"> o ROLL LAMINATION o PULTRUSION o AUTOCLAVE LAMINATION o PRESS LAMINATION
POST-FORMING METHODS:	<ul style="list-style-type: none"> o PRESS (MATCHED-DIE) o AUTOCLAVE MOLDING o VACUUM FORMING o PULTRUSION
BONDING/JOINING METHODS	<ul style="list-style-type: none"> o FUSION o ADHESIVE BONDING o MECHANICAL FASTENING
CHOPPED FIBER MOLDING:	<ul style="list-style-type: none"> o INJECTION MOLDING o MATCHED-DIE
ASSEMBLY METHODS:	<ul style="list-style-type: none"> o FUSION o ADHESIVE BONDING
QUALITY ASSURANCE TECHNIQUES:	

Table 18. Processing Time for Consolidation

		HR/FT ²
PRESS	- SINGLE SHEET	.5
	- SINGLE SHEET W/PRE-HEAT	.32
	- MULTIPLE SHEET	.10
AUTOCLAVE	- SINGLE SHEET	0.125
	- MULTIPLE SHEET	0.041
PULTRUSION	-	2-6 INCHES/min.
ROLL-FORMING	-	Not established



Figure 25. Press Consolidated Unidirectional Laminate



Figure 26. Press Consolidated 181 Style Graphite Fabric Laminate

4.1.2 Autoclave Consolidation

Autoclave laminating has an advantage because large areas can be laminated at one time. The cycle time on Boeing's small autoclave (4 ft dia x 8 ft long) was 4 hr. This included bagging and debagging and allowed for a heat rise of 100°F/min with a 30 min hold at temperature followed by a 120/min cooldown to room temperature. Laminating 32 ft² resulted in costs of 0.125 hr/ft² to 0.041 hr/ft² when three sheets were laminated simultaneously. This low cost consolidation was accomplished without major tooling expense.

4.1.3 Pultrusion Compaction

Existing graphite-epoxy pultrusion equipment was modified to provide higher temperature and pressure capabilities needed for making graphite thermoplastic pultrusions. The existing microwave pultrusion chamber was used as a first stage preheat in series with a second stage where resin softening and compaction occurred. The new second-stage cure chamber consisted of 30-in.-long electric conduction heated chrome steel platens, which were hydraulically actuated with a 200 psi pressure facility. The first 15 inches of the platen was heated while the remaining 15 inches were force-air cooled. The pultrusion puller system was modified to provide increased pulling capability. A flow chart of the thermoplastic pultrusion facility is shown in Figure 27.

Three basic polysulfone/graphite pultruded shapes were fabricated in these studies. These were 3-in. wide solid laminates, 1-in. x 1-in. angles, and 0.040-in. x 3-in. wide sandwich. Three-inch wide tape, 0.005-in. thick was used for making the solid laminates. Eleven- and eighteen-ply laminates were made at speeds varying from 1/2 in. to 6 in. per minute. The best results were obtained at temperatures of 600°F and pressures of 200 psi at pull speeds of 2 in. per min. Angle sections were also made using 12 plies of 0.005 inches thick tape. The best results were obtained using approximately the same process parameters described above. The above sections were also made using polysulfone impregnated woven fabric. This form of material proved to be much more difficult to handle since it would neck down when pulled through the dies. This was solved by using a supporting teflon fabric on both sides of the laminate.

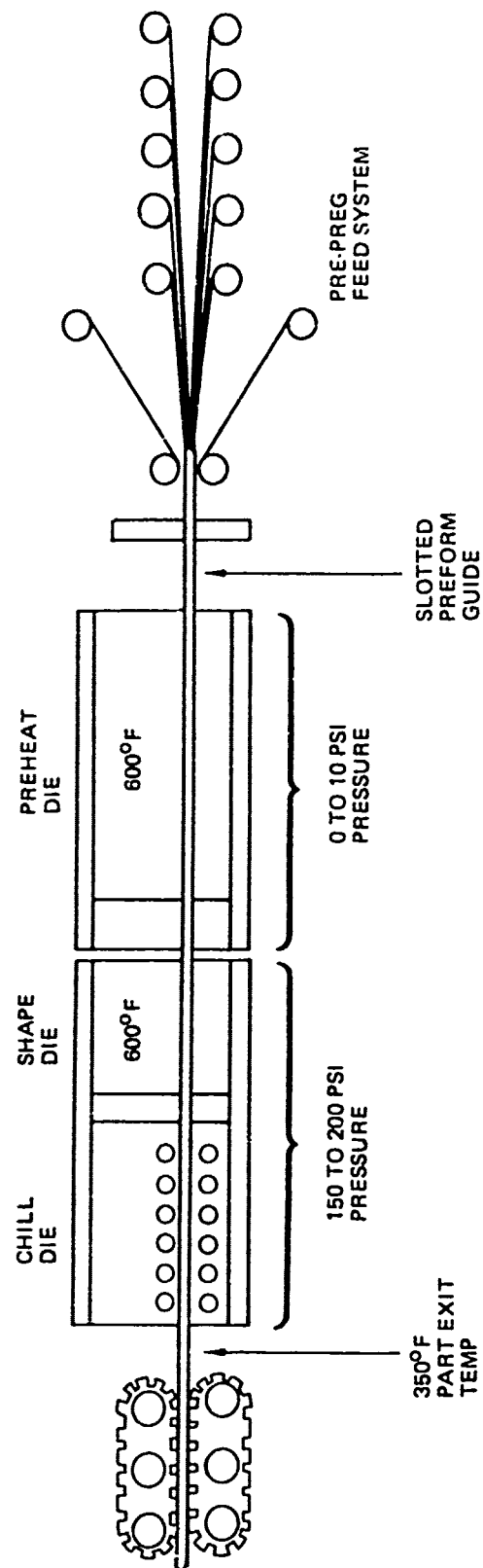


Figure 27. Thermoplastic Pultrusion Facility

Sandwich panels were made using woven fabric face skins and polyimide core. Although the feasibility of producing sandwich sections was established, the finished parts had insufficient peel strength between the face skins and the core due to inadequate adhesive filleting. This characteristic could be improved by using face skin material with a polysulfone resin rich surface on the core interface for a more compatible adhesive system. A photograph of the three sections pultruded is shown in Figure 28. These parts were sectioned; inspection showed them well compacted and free of voids.

Flat platens with side bar inserts were used for producing the flat laminate pultrusions and two-part dies for the shape pultrusions. Ceramic platens or dies were used in the first stage (MW heated) and chrome plated steel in the second stage (electric cartridge) heater.

The studies demonstrated the feasibility of producing pultruded graphite polysulfone structural shapes. Future potential improvements include extruded sandwich panels whose face peel strengths were low but which could be remedied by using prepreg that was resin rich on the core side; or by providing an adhesive system which would provide better filleting and one that would be compatible with the short processing times in the pultrusion equipment. This could be either a thermoset or a thermoplastic adhesive system. The pultruding equipment could also be further improved by using longer platens which would allow an increase in pull force by reducing platen friction. This also could be accomplished by developing an air bearing platen.

4.1.4 Roll Forming Compaction

A survey was performed to find a commercial source with the equipment and capability to perform continuous roll compaction. Several companies were contacted which had adequate rolling equipment but lacked the temperature capability since they were steam heated. This effort was discontinued.

4.2 POST FORMING

The post-forming methods investigated were (a) press match die, (b) autoclave, (c) vacuum forming, and (d) pultrusion forming which was discussed in the previous section and therefore will not be covered here.



Figure 28. Graphite Thermoplastic Pultruded Sections

4.2.1 Press Match Die Post Forming

Several parts were made by post forming in a press with match dies. This technique consists of preheating a consolidated laminate and then placing it in warm dies located in a press for forming. The consolidated material is heated to approximately 500⁰F while the die is restricted to the 300⁰ to 325⁰F temperature range. The die tends to cool the part below the polymer softening point (345⁰F) after forming. This method will produce typical parts in a time span of 6 to 8 minutes which is considered highly acceptable for production. The channel shown in Figure 29 was produced by this procedure. The eight-ply laminate used to produce the channel was preheated, placed over a female metal die, and then pressed to its final shape with a silicone plug. The silicone plug enabled the fabric to fill in all corners of the mold with uniform pressure resulting in a well compacted high tolerance part. Figure 30 shows a double contoured part that was successfully produced by this method.

4.2.2 Autoclave Post Forming

Several parts were successfully post formed in an autoclave in this program. The process is similar to the press die forming except autoclave pressure is used to form the part. The cycle time in the autoclave was approximately 3.0 hours which was less than used for consolidation because the hold time is not required. Also, the forming temperature was reduced since parts are heated to slightly above the softening temperature. The autoclave post forming cycle is significantly less time than the cure cycle for epoxy parts and therefore has economical advantages for producing large composite parts. Costs are saved in shorter cycle times thus providing more facilities usage; less labor costs and on some cases less total energy usage.

Figures 31 and 32 show two parts that were formed by using autoclave pressure. In Figure 31, a web is shown which was formed out of graphite-polysulfone tape oriented at (0⁰,90⁰). Figure 32 shows a shear web formed out of fabric using the same tooling. Both parts were carefully examined and no delaminations or serious fiber distortions were found.

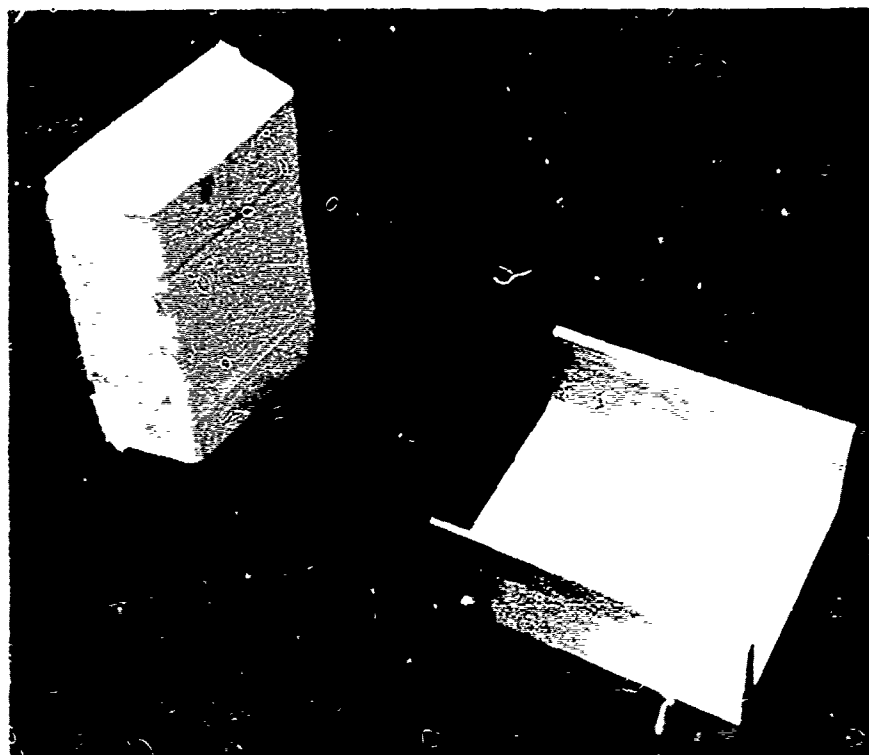


Figure 29. Press Match-Die Molded Post Formed Channel



Figure 30. Press Molded Shapes-Silicone Plug Mold

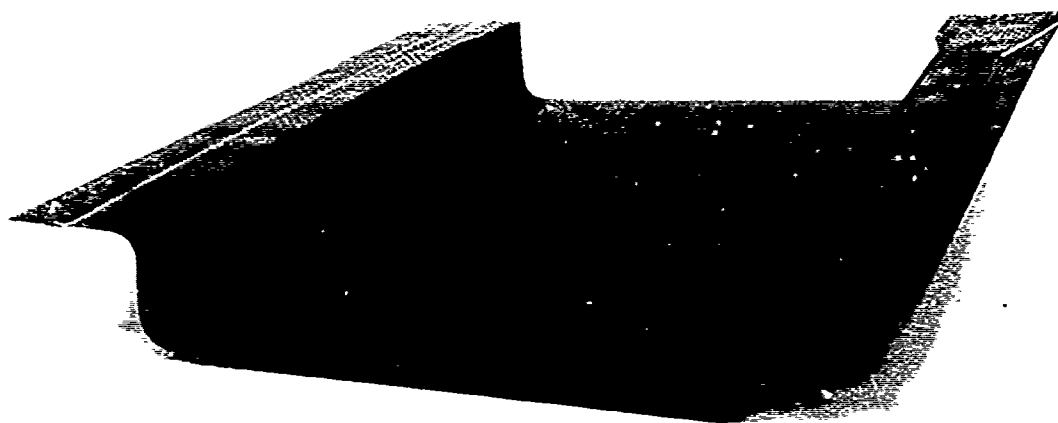


Figure 31. Shear Web Molded From (0/90)_S Graphite Tape Composite

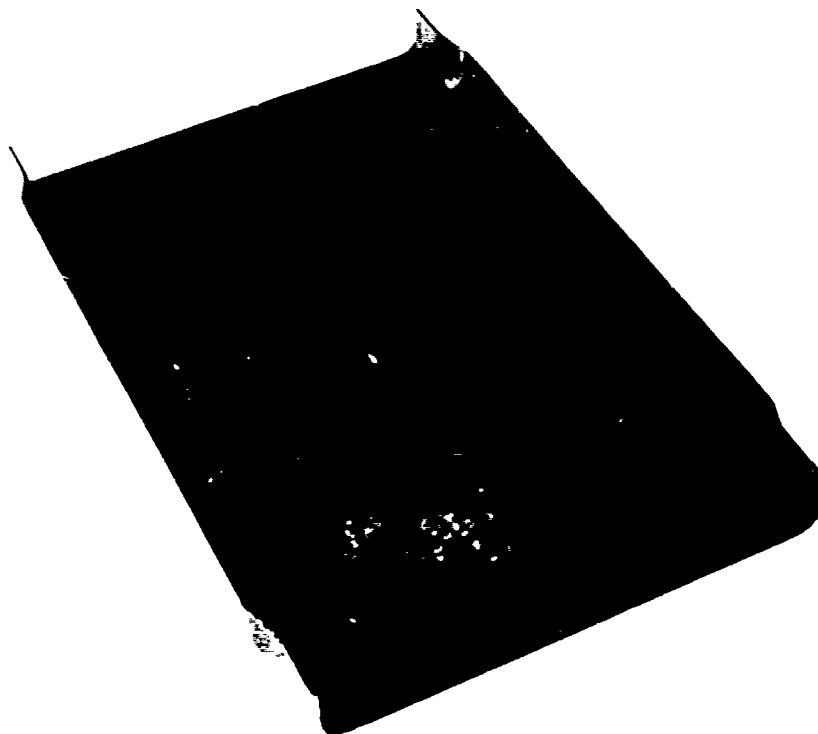


Figure 32. Shear Web Molded Form Graphite Fabric

4.2.3 Vacuum Forming

Vacuum forming proved to be a cost-effective method of making formed parts. Figure 33 shows shear-web 0.040 in. thick which was formed from 0° to 90° sheet stock made from tape. A graphite fabric laminate part is shown in Figure 34. Both parts were vacuum formed using a 10-minute cycle. Figure 35 shows a schematic of the vacuum forming equipment. It consists of three stages. The laminate was loaded in Zone 1 where it was then moved to Zone 2 which consists of an oven. The laminate was heated with radiant lamps to 550 to 600°F and then moved to Zone 3 where the actual forming takes place. The hot laminate was formed over an aluminum tool with vacuum pressure. When full vacuum was on the part, the forming cavity was pressurized with plant air (80 psi) to consolidate the part. Figure 36 shows a schematic of the forming chamber. The laminate was then cooled and removed as shown in Figure 37.

Time studies on a production basis showed parts could be produced on a 10-12 minute cycle. The main factor governing the cycle time was part thickness and the time associated with bringing the laminate up to forming temperature.

Vacuum forming provides extremely accurate and reproducible parts. The process could be improved by increasing the auxiliary air pressure from 80 to 150 psi. This increased air pressure produces a very high quality structural laminate in all configurations.

4.3 BONDING/JOINING METHODS

Three methods of load transfer were investigated. They were by fusion bonding, adhesive bonding, and mechanical attachments.

4.3.1 Fusion Bonding

Fusion joints were formed by using heat and pressure to fuse the composite matrix material. A previous contract (NASC Contract No. N00019-72-C-0526) demonstrated that lap bond strengths in excess of 8,000 psi could be developed in unidirectional graphite P1700 composites. This value was obtained by fusion at 550°F and 200 psi. The efforts in this program were directed toward forming fusion bonds using techniques requiring less pressure and more conducive to multi-part production.

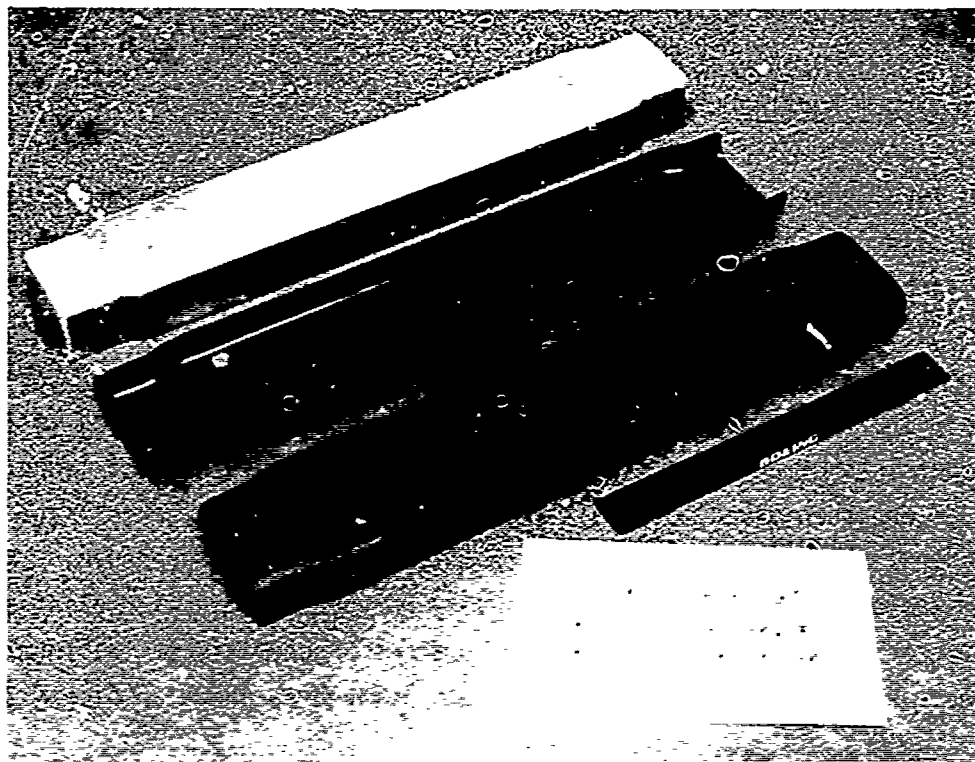


Figure 33. Vacuum Formed Shear Web (0/90)_S Sheet Stock

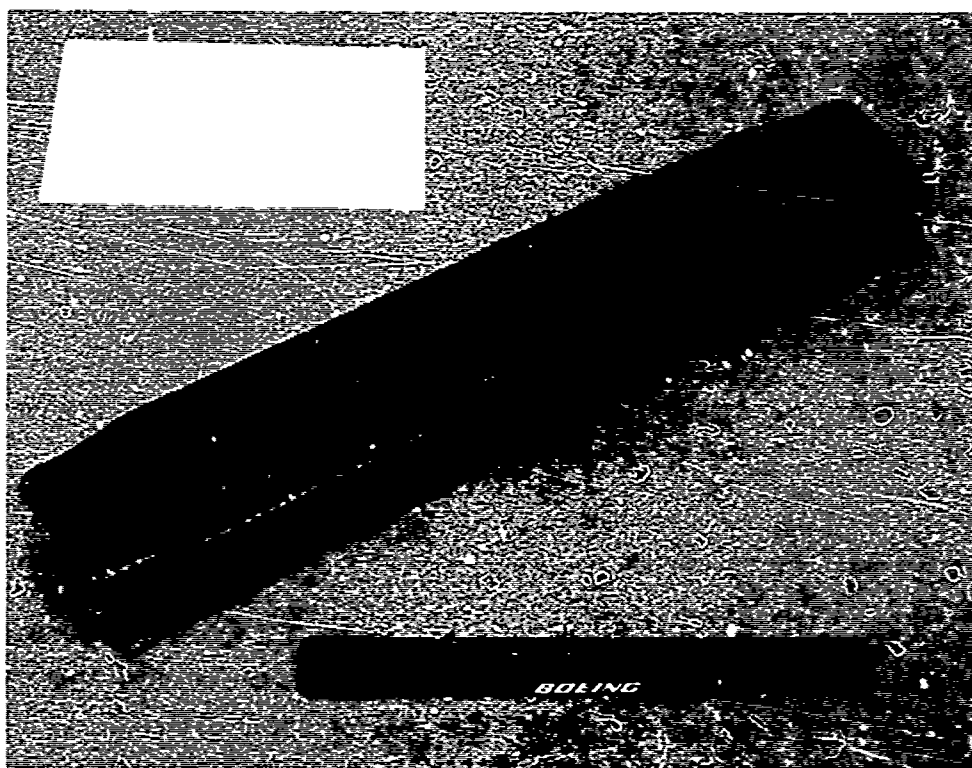


Figure 34. Vacuum Formed Shear Web Graphite Fabric

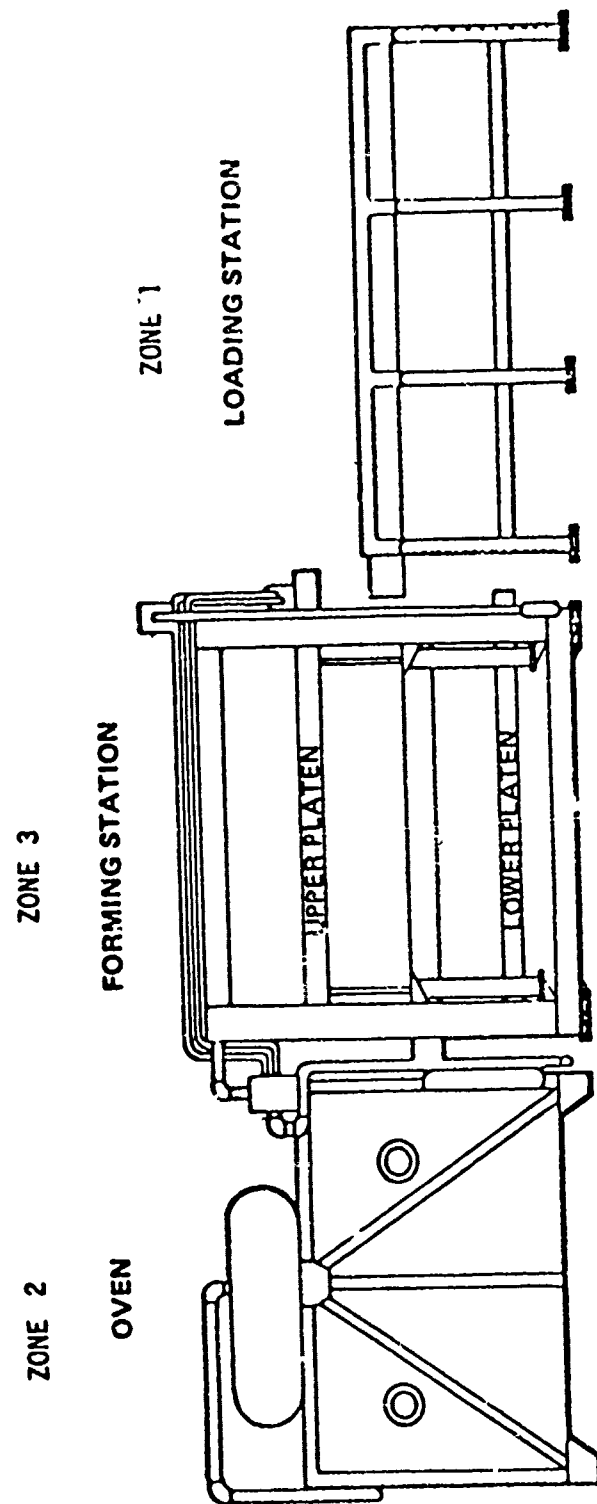


Figure 35. Chemithon Thermoforming Machine

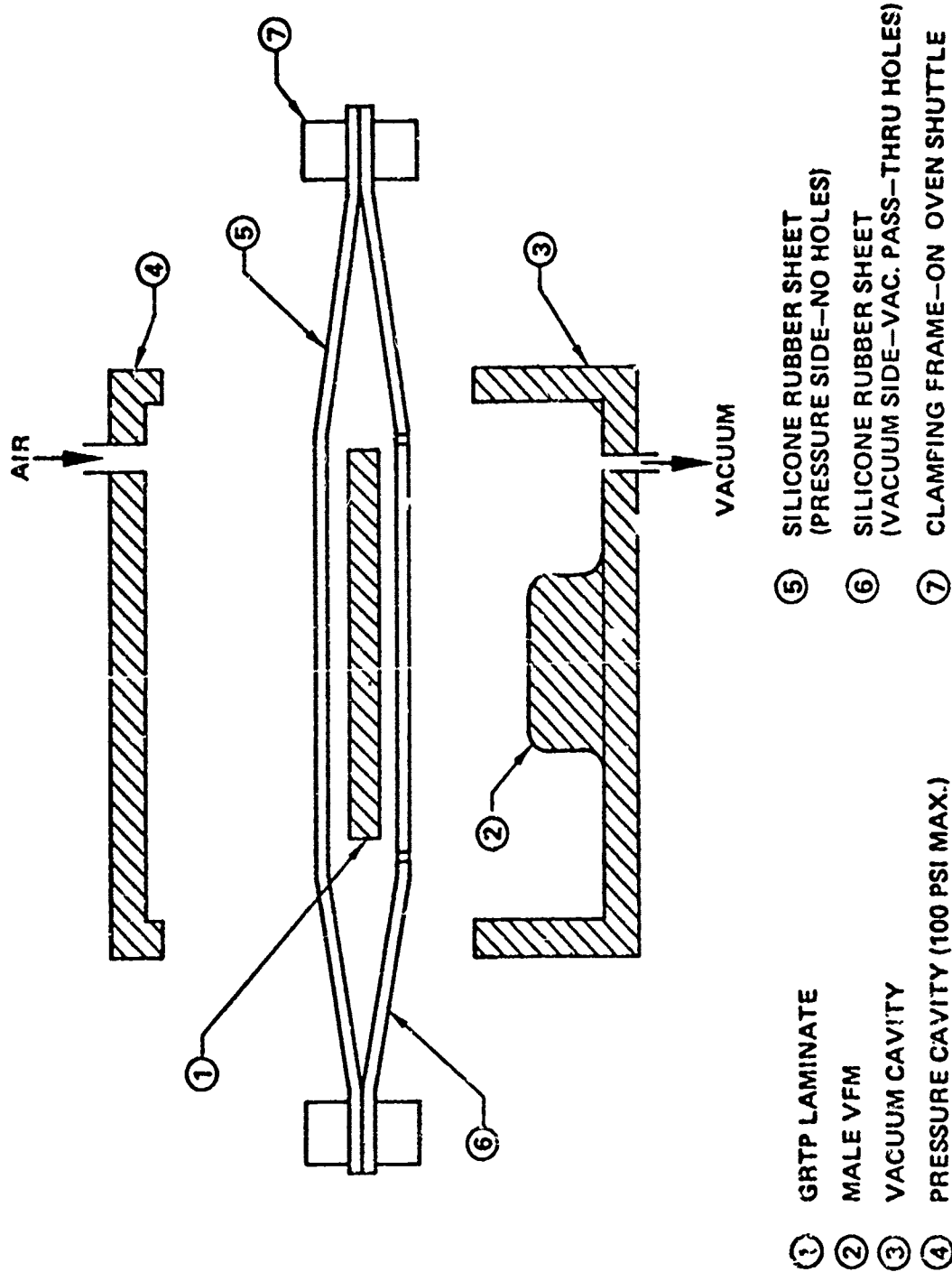


Figure 36. Vacuum Forming Chamber — Schematic

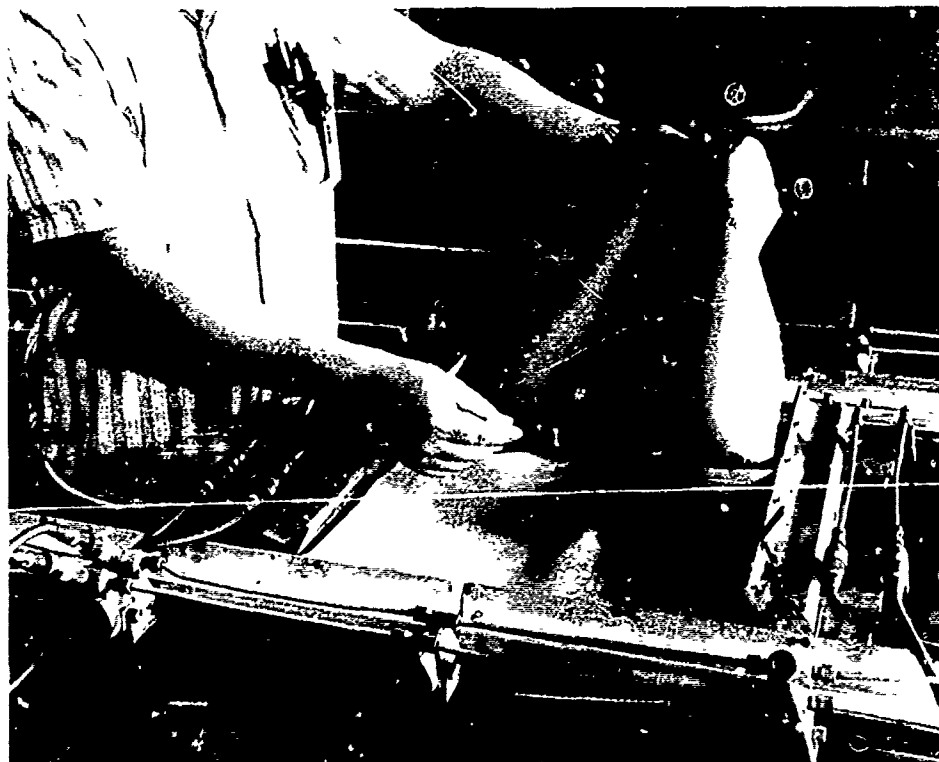


Figure 37. Graphite Thermoplastic Vacuum Forming—Part Removal

One approach investigated placed resistance wires at the bond interface and applied a potential across the joint interface. As a result the heated wires softened the polysulfone which fused and formed the joint. Figure 38 shows a polysulfone adhesive film 2.5 mils thick with the resistance wires embedded. Figure 39 shows a joint made with this type of film and minimum contact pressure. Lap shear values in the range of 1,400 psi were obtained with specimens made from this joint. However, the interface in this joint had only 25 percent of the area fused. The wire (28 ohms/ft) did not generate enough uniform heat. Based on this data it seemed likely that if total area fusion was obtained then shear strengths in the range of 4,000 to 5,000 psi were possible. Figure 40 shows a cross-section of the fused area in the joint. Some voids are evident but in general excellent fusion was obtained.

Another series of specimens was made in which stainless steel screen (80 mesh) was used as a resistant heater. This type of adhesive screen is shown in Figure 38. This joint was formed in 90 seconds using a pressure of 10 psi. The composite overheated as shown in Figure 41 but lap shear values of 3,800 psi were obtained. All failures were adhesive at the wire mesh interface. The 80-mesh wire is a very close weave and therefore very little penetration of the screen occurred. Additional joints were made at a lower power setting to prevent overheating the composite. This worked very well but the joint strength was not increased and the failure mode remained the same. Although additional work could not be performed in this program, the resistance wire heating technique proved very promising and warrants further research.

Another joining technique that was investigated and proved promising was electromagnetic bonding. With this method, a lap shear value of 3,750 was obtained.

Electromagnetic bonding utilizes the principle of induction heating between two abutting thermoplastic surfaces, to fusion temperature, via a heat-activated electromagnetic adhesive layer. The electromagnetic material at the bonding interface consists of a dispersion of finely divided metal particles in a thermoplastic matrix. When the interface is subjected to a high frequency alternating current, fusion temperature is instantly achieved. Under slight pressure a bond is formed. Figure 42 shows a cross section of a bond that was

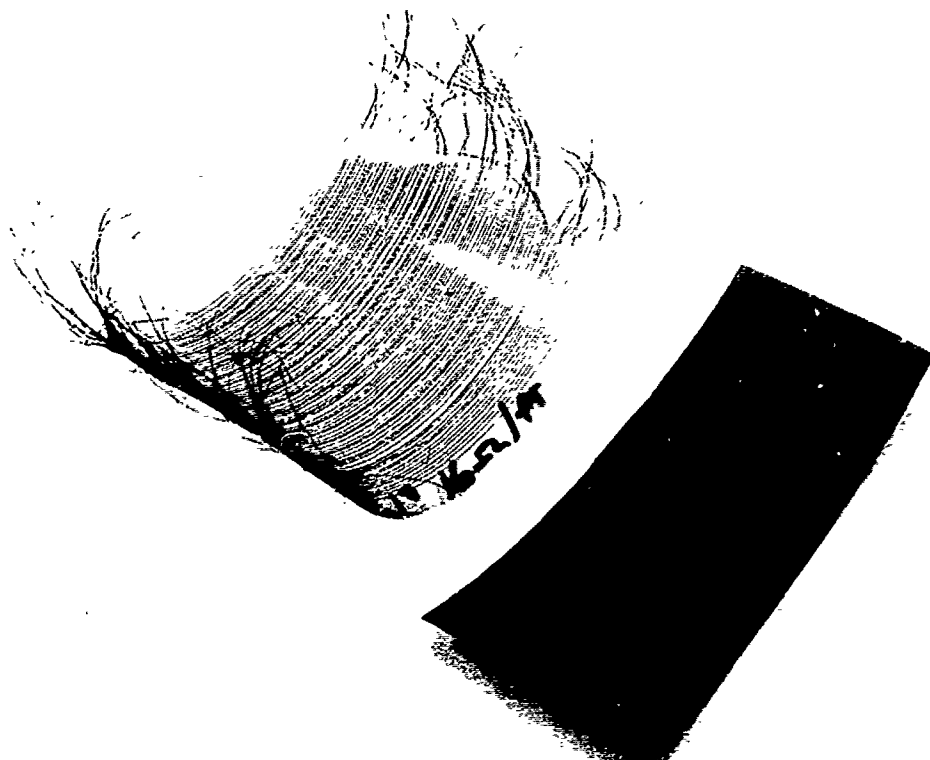


Figure 38. Polysulfone Adhesive Films with Self Contained Heating Wires and Screen

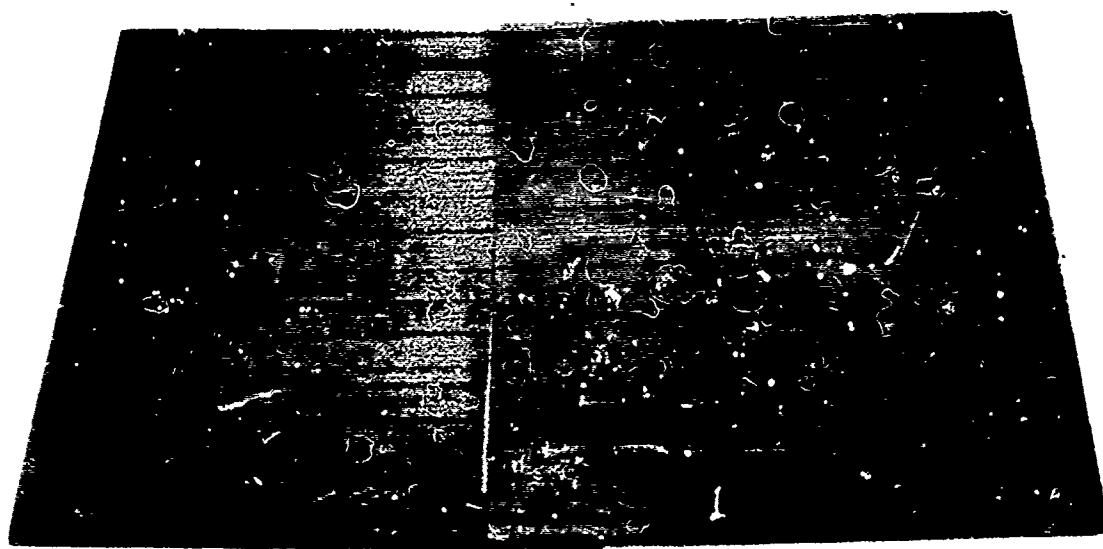


Figure 39. Fusion Joint-Resistant Heating Wires

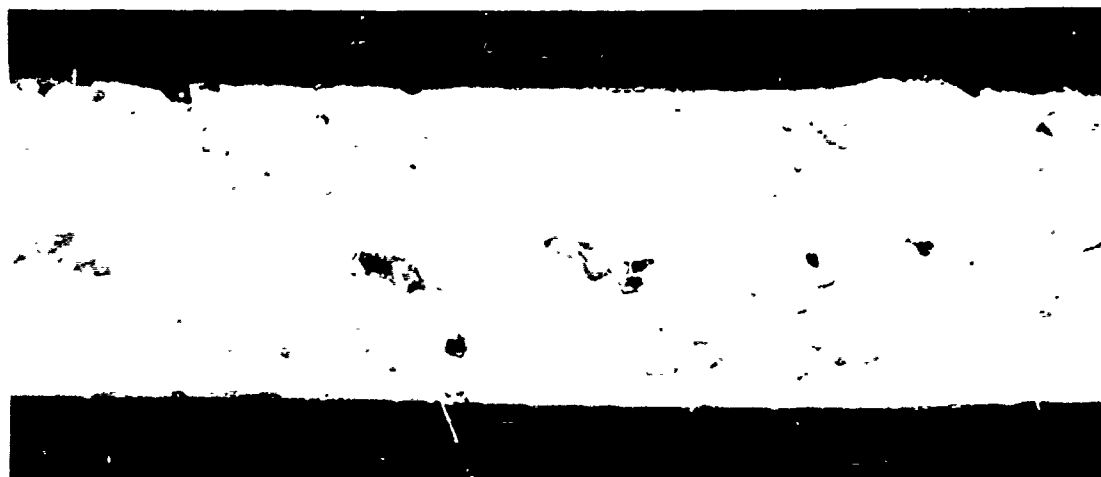


Figure 40. Fusion Joint—Close Up

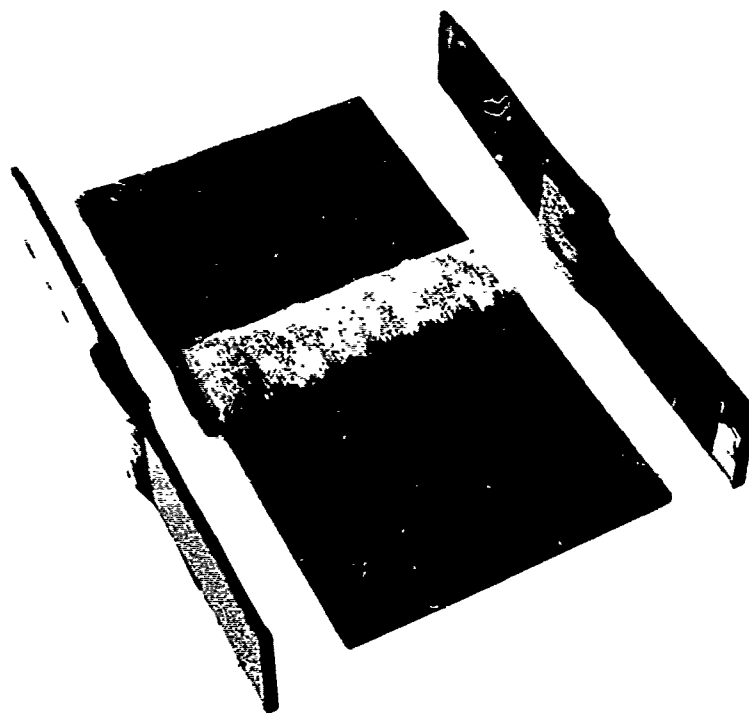


Figure 41. Fusion Joint—Resistant Heating Screen

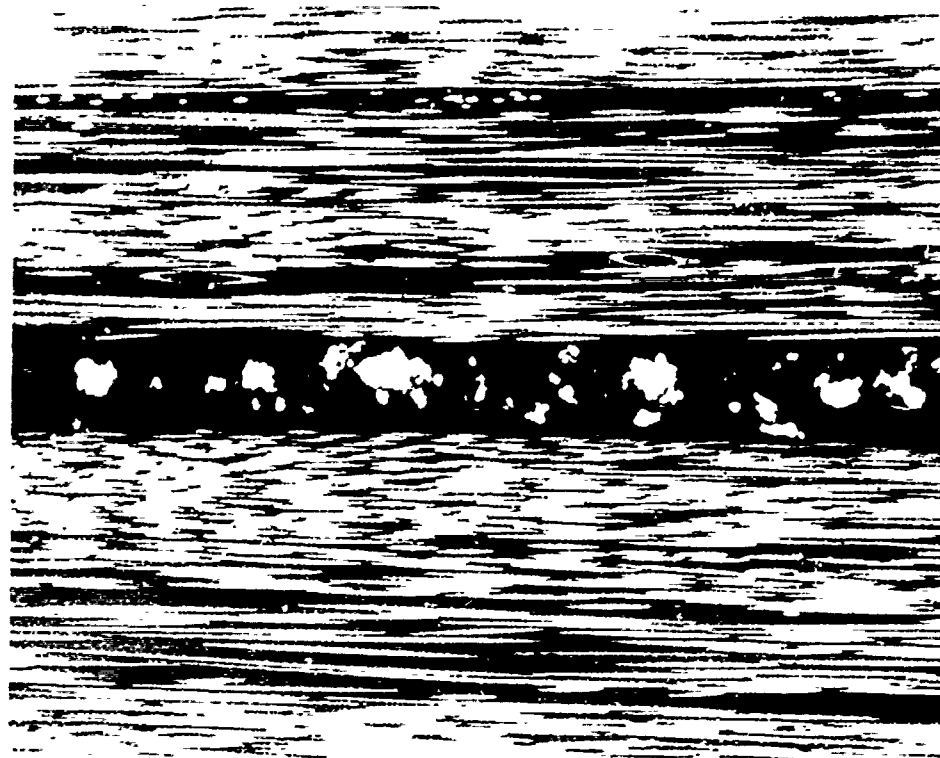


Figure 42. Electromagnetic Bonding


formed in a matter of 5 seconds. The joint shows some porosity, indicating more pressure or process refinements are required but the composite-adhesive interface is not discernible. The light particles in Figure 42 are the polycarbonate electromagnetic filler used in the adhesive.


4.3.2 Adhesive Bonding

Several specimens were fabricated and tested to obtain load transfer capabilities for graphite-polysulfone adhesive bonded joints. A room temperature curing adhesive, Hysol EA 934, was evaluated to obtain data for developing field repair techniques discussed later in this report. The average lap shear values obtained are summarized in Table 19. An elevated temperature (250°F) cure adhesive was also tested to obtain data for primary joints in the design of components. This data is also summarized in Table 19. Specimens were also fabricated with tape orientated at (0°). A summary of this data is shown in Table 20 along with data from other joining methods.

4.3.3 Mechanical Fastening

A study was made to evaluate the effect of die-punching holes in a thermoplastic laminate in contrast to the conventional method of drilling and reaming. Holes 1/4 in. in diameter were die-punched in laminates of three different thicknesses, 0.022, 0.044, and 0.066 in. The laminates were then tested in tension and compared to an unpunched laminate. Similar tests were conducted using a 1/4 in. drilled and reamed hole. The results are shown in Table 21. The punched hole was more effective on the thin laminates (0.022) than the drilled and reamed hole since the drill has a tendency to "bite" into the thin material. The two methods of hole preparation appear comparable on the 0.044 in. thick laminate. With the thicker laminate (0.066 in.), the force to die-punch the material appears to do considerable damage around the hole, resulting in a loss in laminate properties. Figures 43 and 44 show a comparison of a punched and drilled/reamed hole on a 0.066 in. laminate. Subsequent tests determined that a punched hole cleaned by reaming, is similar to a drilled/reamed hole (see Table 22).

Table 19. Adhesive Lap Shear Strengths 

ADHESIVE	CURE TEMPERATURE deg F	PRESSURE APPLICATION	AV SHEAR STRENGTH (PSI) 
HYSOL EA 934	R.T.	VACUUM BAG	2025
HYSOL EA 934	R.T.	SPRING CLAMPED	1850
HYSOL 9628	250 deg	AUTOClave 90 PSI	2640

 SINGLE 1/2 in OVERLAP SHEAR TESTS

 ADHERENDS - (± 45) FABRIC

Table 20. Bonding Methods - Typical Values

BONDING METHOD	LAP SHEAR STRENGTH psi
FUSION BOND	8000
RESISTANT HEATED BOND	3800
ELECTROMAGNETIC FUSION	3750
EPOXY ADHESIVE	4200
ULTRASONIC BONDING	1400

Table 21. Attachment Studies – Hole Fabrication Evaluation

	THICKNESS (in)	CONTROL (psi)	DRILLED & REAMED (psi)	PUNCHED (psi)
4 PLY 0°/90° LAMINATE	0.022	71,000	44,300	52,000
8 PLY 0°/90° LAMINATE	0.044	70,000	64,000	62,400
12 PLY 0°/90° LAMINATE	0.066	88,000	76,000	66,000



Figure 43. Punched Hole – 1/4 Diameter (50X)



Figure 44. Drilled/Reamed Hole – 1/4 Diameter (50X)

Table 22. Attachment Studies – Reamed Hole Evaluation

HOLE CONDITION - 12 PLY (0°, 90°) TESTED IN TENSION AT + 70°F	CONTROL	88,000 psi
	PUNCHED 1/4"	66,000 psi
	DRILLED & REAMED	76,000 psi
	PUNCHED & REAMED	77,000 psi

4.4 CHOPPED FIBER MOLDING

Present elevator fittings are machined metal designs which are quite costly to produce. Studies were therefore made to evaluate the potential of reducing these costs by producing the fittings by injection molding or close die molding using chopped fiber thermoplastic materials. Although most of the effort was expended on close die molding evaluation, some injection molding material properties were developed.

4.4.1 Injection Molding

One injection molding material was tested to establish its properties. This material was Ryton PPS made by Phillips Petroleum. Flexure specimens were cut from injection molded sheets approximately 0.17 inches thick. The specimens were oriented in both the 0° and 90° directions and were tested at room temperature and 180°F . A summary of this data is shown in Table 23.

4.4.2 Close Die Molding

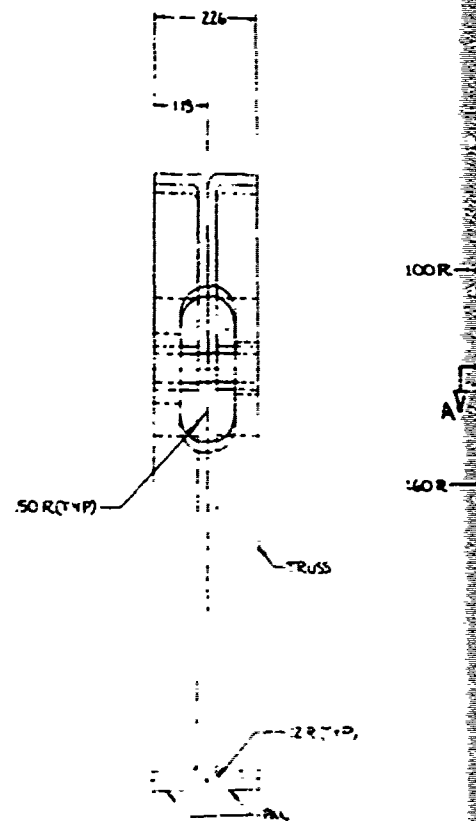
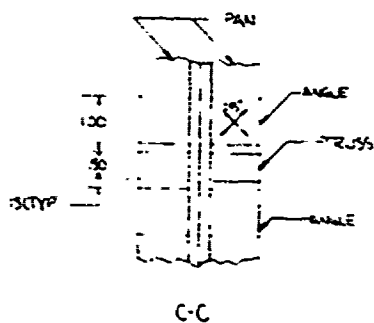
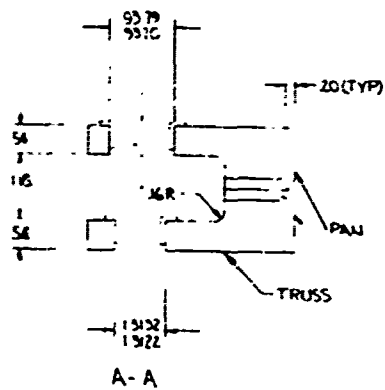
A close die molded fitting design was developed which incorporated two molded pans fused back-to-back to provide the main load path for transmitting hinge loads to the elevator box assembly. Two molded trusses were also incorporated by fusion bonding to provide additional bearing area at the load pick-up point and also, additional lateral stiffness. Details of the design are shown in Figure 45.

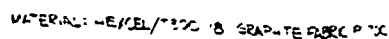
Two types of fittings were produced. Both incorporated the two three-sided molded fabric pans fused back-to-back. One type of fitting incorporated fabric molded trusses and a second chopped fiber molded trusses.

The three-sided pan details were fabricated by first making a preform and then compacting it in an autoclave. Fabric plies were cut to the proper shape and then formed and stacked into a preform as shown in Figure 46. The preform was then placed on a tool and covered with caul plates (Figure 47). This assembly was then bagged and placed in an autoclave and the pan compacted at 200 psi and 600°F for 30 minutes. Figure 48 shows a pan after compaction. It was then trimmed to the proper configuration prior to installation in the fitting fusion tool.

Table 23. Injection Molding Material Flexural Properties – Ryton PPS (Phillips)

DIRECTION	TEMPERATURE	ULT. STRESS (PSI)	MODULUS (X 10 ⁶)
0°	RT	18.2	1.8
0°	180°F	16.5	1.3
90°	RT	7.6	1.1
90°	180°F	9.7	0.76





1. PREPAREMENTS & TOLERANCES 2. FINISHES 3. UNIT OR SYSTEM VOLTAGE 4. UNIT OR SYSTEM CAPACITY 5. REQUIREMENTS ARE IN INCHES 6. VOLTAGES ARE IN VOLTS 7. DEGREES °C 8. DEGREES °F 9. JOINT & BOLT FORCE MARCH 1, 1961 10. NO. OF BOLT 100 11. NO. OF BOLT 100 12. NO. OF BOLT 100 13. NO. OF BOLT 100 14. NO. OF BOLT 100 15. NO. OF BOLT 100 16. NO. OF BOLT 100 17. NO. OF BOLT 100 18. NO. OF BOLT 100 19. NO. OF BOLT 100 20. NO. OF BOLT 100 21. NO. OF BOLT 100 22. NO. OF BOLT 100 23. NO. OF BOLT 100 24. NO. OF BOLT 100 25. NO. OF BOLT 100 26. NO. OF BOLT 100 27. NO. OF BOLT 100 28. NO. OF BOLT 100 29. NO. OF BOLT 100 30. NO. OF BOLT 100 31. NO. OF BOLT 100 32. NO. OF BOLT 100 33. NO. OF BOLT 100 34. NO. OF BOLT 100 35. NO. OF BOLT 100 36. NO. OF BOLT 100 37. NO. OF BOLT 100 38. NO. OF BOLT 100 39. NO. OF BOLT 100 40. NO. OF BOLT 100 41. NO. OF BOLT 100 42. NO. OF BOLT 100 43. NO. OF BOLT 100 44. NO. OF BOLT 100 45. NO. OF BOLT 100 46. NO. OF BOLT 100 47. NO. OF BOLT 100 48. NO. OF BOLT 100 49. NO. OF BOLT 100 50. NO. OF BOLT 100 51. NO. OF BOLT 100 52. NO. OF BOLT 100 53. NO. OF BOLT 100 54. NO. OF BOLT 100 55. NO. OF BOLT 100 56. NO. OF BOLT 100 57. NO. OF BOLT 100 58. NO. OF BOLT 100 59. NO. OF BOLT 100 60. NO. OF BOLT 100 61. NO. OF BOLT 100 62. NO. OF BOLT 100 63. NO. OF BOLT 100 64. NO. OF BOLT 100 65. NO. OF BOLT 100 66. NO. OF BOLT 100 67. NO. OF BOLT 100 68. NO. OF BOLT 100 69. NO. OF BOLT 100 70. NO. OF BOLT 100 71. NO. OF BOLT 100 72. NO. OF BOLT 100 73. NO. OF BOLT 100 74. NO. OF BOLT 100 75. NO. OF BOLT 100 76. NO. OF BOLT 100 77. NO. OF BOLT 100 78. NO. OF BOLT 100 79. NO. OF BOLT 100 80. NO. OF BOLT 100 81. NO. OF BOLT 100 82. NO. OF BOLT 100 83. NO. OF BOLT 100 84. NO. OF BOLT 100 85. NO. OF BOLT 100 86. NO. OF BOLT 100 87. NO. OF BOLT 100 88. NO. OF BOLT 100 89. NO. OF BOLT 100 90. NO. OF BOLT 100 91. NO. OF BOLT 100 92. NO. OF BOLT 100 93. NO. OF BOLT 100 94. NO. OF BOLT 100 95. NO. OF BOLT 100 96. NO. OF BOLT 100 97. NO. OF BOLT 100 98. NO. OF BOLT 100 99. NO. OF BOLT 100 100. NO. OF BOLT 100 101. NO. OF BOLT 100 102. NO. OF BOLT 100 103. NO. OF BOLT 100 104. NO. OF BOLT 100 105. NO. OF BOLT 100 106. NO. OF BOLT 100 107. NO. OF BOLT 100 108. NO. OF BOLT 100 109. NO. OF BOLT 100 110. NO. OF BOLT 100 111. NO. OF BOLT 100 112. NO. OF BOLT 100 113. NO. OF BOLT 100 114. NO. OF BOLT 100 115. NO. OF BOLT 100 116. NO. OF BOLT 100 117. NO. OF BOLT 100 118. NO. OF BOLT 100 119. NO. OF BOLT 100 120. NO. OF BOLT 100 121. NO. OF BOLT 100 122. NO. OF BOLT 100 123. NO. OF BOLT 100 124. NO. OF BOLT 100 125. NO. OF BOLT 100 126. NO. OF BOLT 100 127. NO. OF BOLT 100 128. NO. OF BOLT 100 129. NO. OF BOLT 100 130. NO. OF BOLT 100 131. NO. OF BOLT 100 132. NO. OF BOLT 100 133. NO. OF BOLT 100 134. NO. OF BOLT 100 135. NO. OF BOLT 100 136. NO. OF BOLT 100 137. NO. OF BOLT 100 138. NO. OF BOLT 100 139. NO. OF BOLT 100 140. NO. OF BOLT 100 141. NO. OF BOLT 100 142. NO. OF BOLT 100 143. NO. OF BOLT 100 144. NO. OF BOLT 100 145. NO. OF BOLT 100 146. NO. OF BOLT 100 147. NO. OF BOLT 100 148. NO. OF BOLT 100 149. NO. OF BOLT 100 150. NO. OF BOLT 100 151. NO. OF BOLT 100 152. NO. OF BOLT 100 153. NO. OF BOLT 100 154. NO. OF BOLT 100 155. NO. OF BOLT 100 156. NO. OF BOLT 100 157. NO. OF BOLT 100 158. NO. OF BOLT 100 159. NO. OF BOLT 100 160. NO. OF BOLT 100 161. NO. OF BOLT 100 162. NO. OF BOLT 100 163. NO. OF BOLT 100 164. NO. OF BOLT 100 165. NO. OF BOLT 100 166. NO. OF BOLT 100 167. NO. OF BOLT 100 168. NO. OF BOLT 100 169. NO. OF BOLT 100 170. NO. OF BOLT 100 171. NO. OF BOLT 100 172. NO. OF BOLT 100 173. NO. OF BOLT 100 174. NO. OF BOLT 100 175. NO. OF BOLT 100 1	
--	--

73

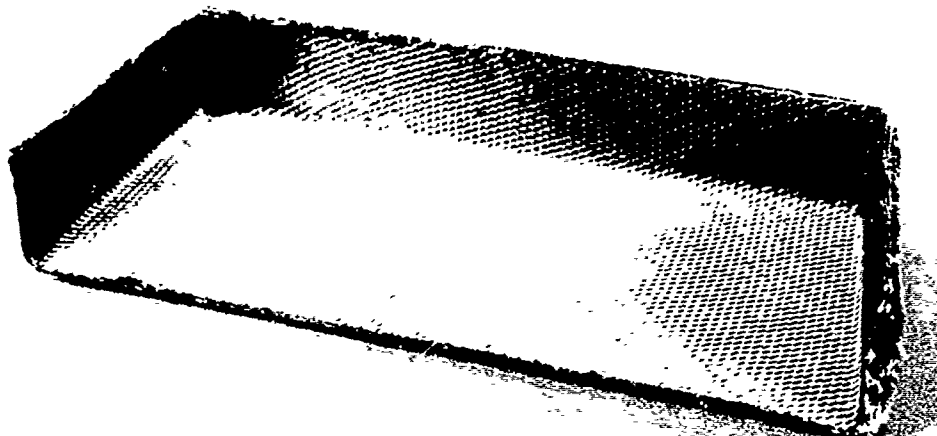


Figure 46. Molded Fitting — Preformed Fabric Pan

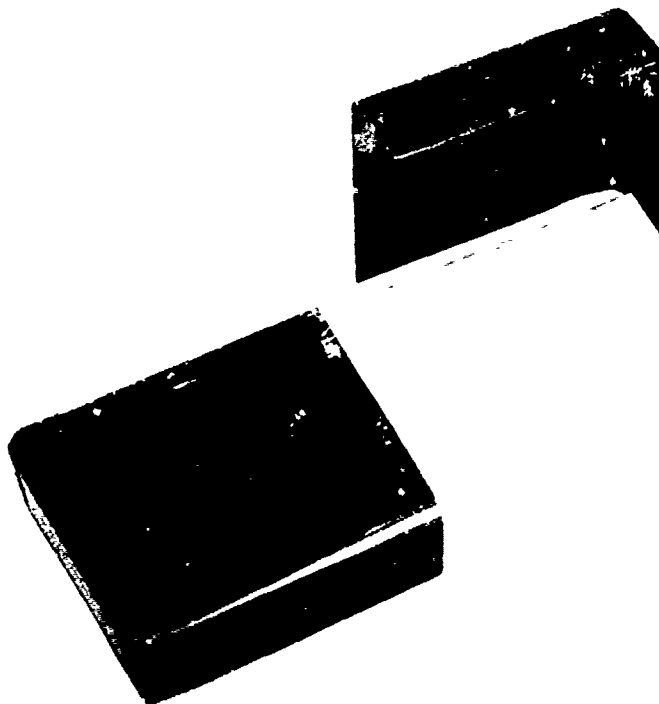


Figure 47. Molded Fitting — Pan Compaction Tool and Caul Plates

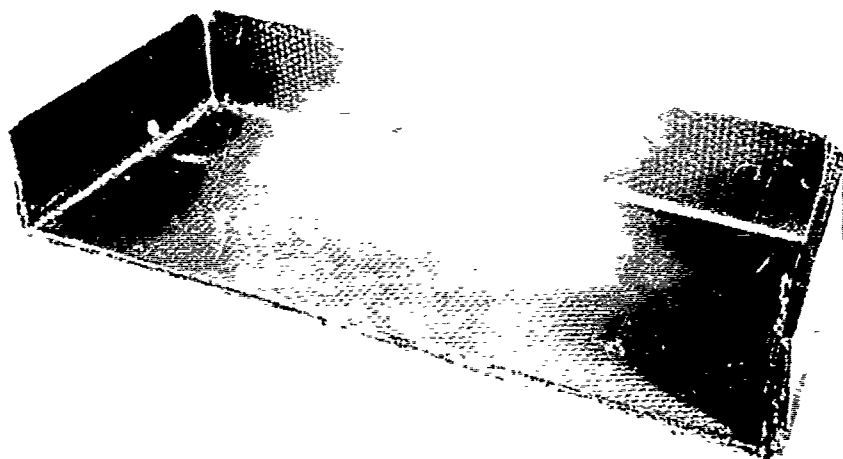


Figure 48. Molded Fitting – Compacted Pan Prior to Trim

Chopped graphite molding material was used to make the trusses for one of the fittings. The required amount of chopped fiber molding material was weighed and placed in a compaction tool. This assembly was placed in a press and run at 600°F for 30 minutes. Figure 49 shows a pile of the molding material and a completed truss. Figure 50 shows the truss compaction tool.

A second fitting was made using fabric molded trusses. The plies of graphite-polysulfone fabric were first cut to shape in a dinking die. They were then placed in the tool shown in Figure 50 and compacted at 600°F for 30 minutes. Figure 51 shows the dinked out plies and a completed fabric truss.

The fitting detail parts were then assembled in the molded fitting fusion assembly tool. Figure 52 shows the detail parts. Figure 53 shows them in the tool and Figure 54 after the pans have been placed in position. The fusion pool was then assembled as shown in Figure 55 and then placed in a press. Fusion was performed in the press at 600°F for 30 minutes. A completed graphite-polysulfone molded fitting is shown in Figure 56.

The first two fittings produced were not up to the desired quality. Web and flange thicknesses were not consistent. The insert tooling was changed to improve the containment of the fitting molding material by cutting back the amount of silicone used. Two more fittings were produced with the modified inserts. Their quality was much better than the original two produced.

The initial two fittings produced were tested to establish their load carrying capabilities. The fitting with the fabric molded trusses was tested for two YC-14 elevator fitting ultimate load conditions, four lifetime fatigue cycles and finally a pull-out test to failure. The first fitting (fabric truss) was bolted to a test fixture as shown in Figure 57. This fixture was then mounted in a test machine at an angle that would provide the required load components. Figure 58 shows a photo of a typical test set-up. Figure 59 shows the fitting positioning used to provide the ultimate load conditions. The fitting was loaded to two different ultimate load conditions (see Figure 59) without apparent damage. The fitting was then subjected to 120,000 fatigue load cycles at 42% of ultimate at the position #2 load condition (see Figure 59) without apparent damage. This represents four times the required

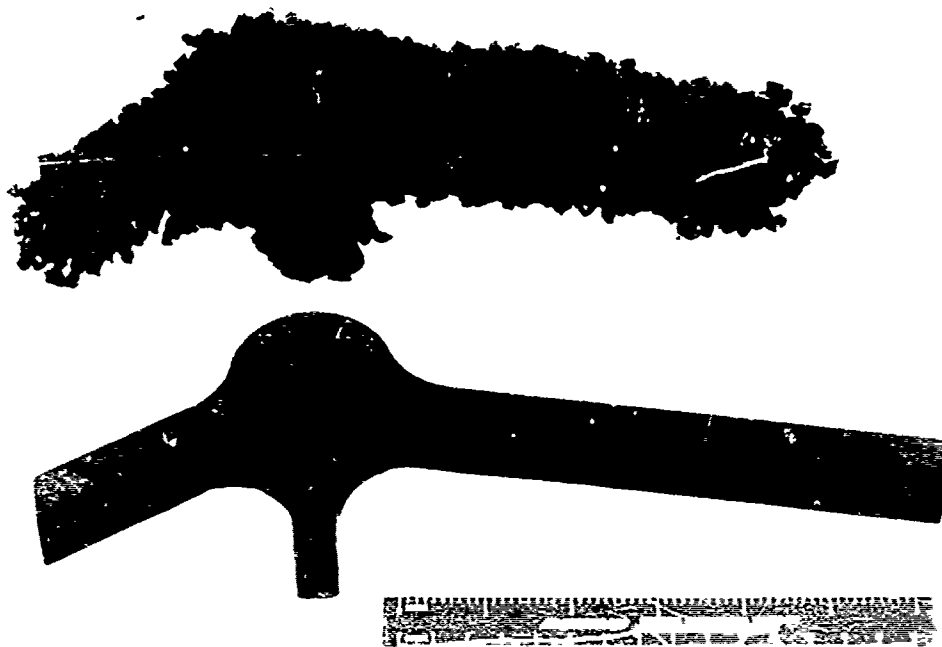


Figure 49. Molded Fitting – Chopped Graphite Fiber Molded Truss

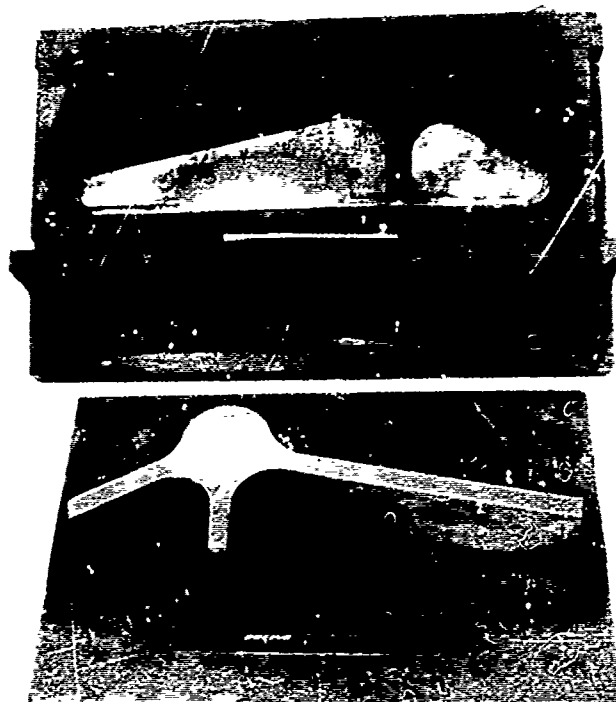


Figure 50. Molded Fitting – Truss Compaction Tool

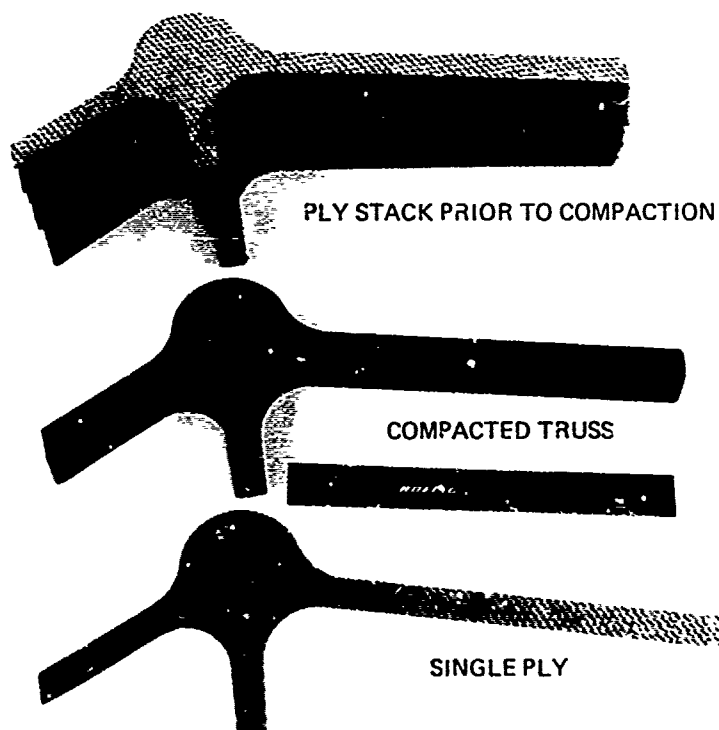


Figure 51. Molded Fitting – Fabric Truss

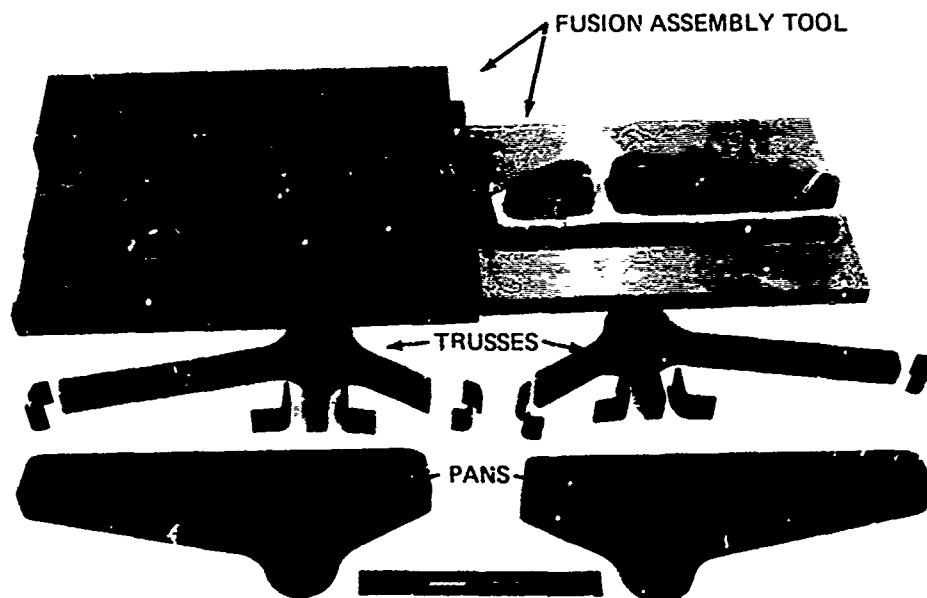


Figure 52. Molded Fitting - Detail Parts and Fusion Assembly Tool

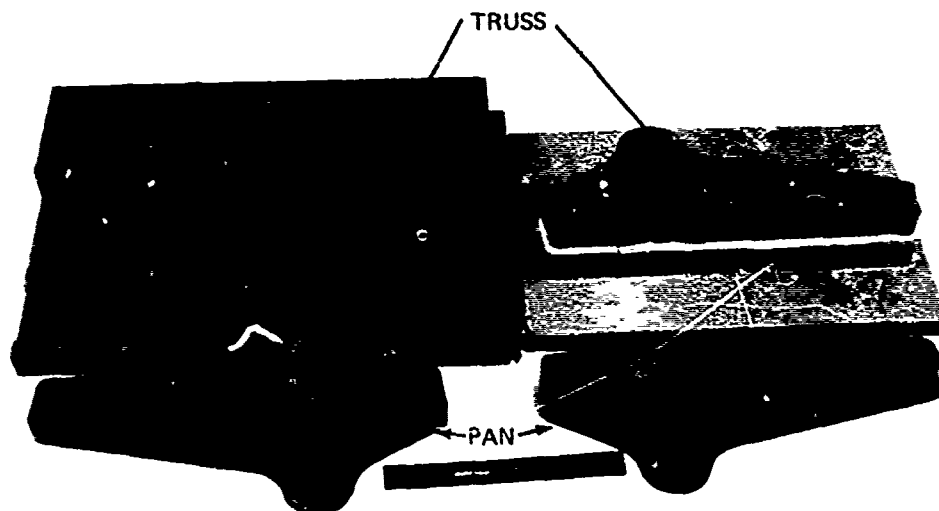


Figure 53. Molded Fitting - Fusion Tool With Details Installed



Figure 54. Molded Fitting – Details and Pans in Tool

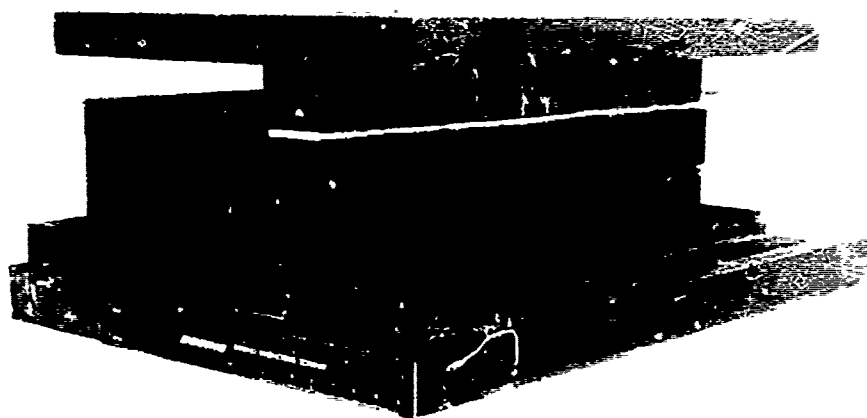


Figure 55. Molded Fitting – Fusion Assembly Tool Ready For Press

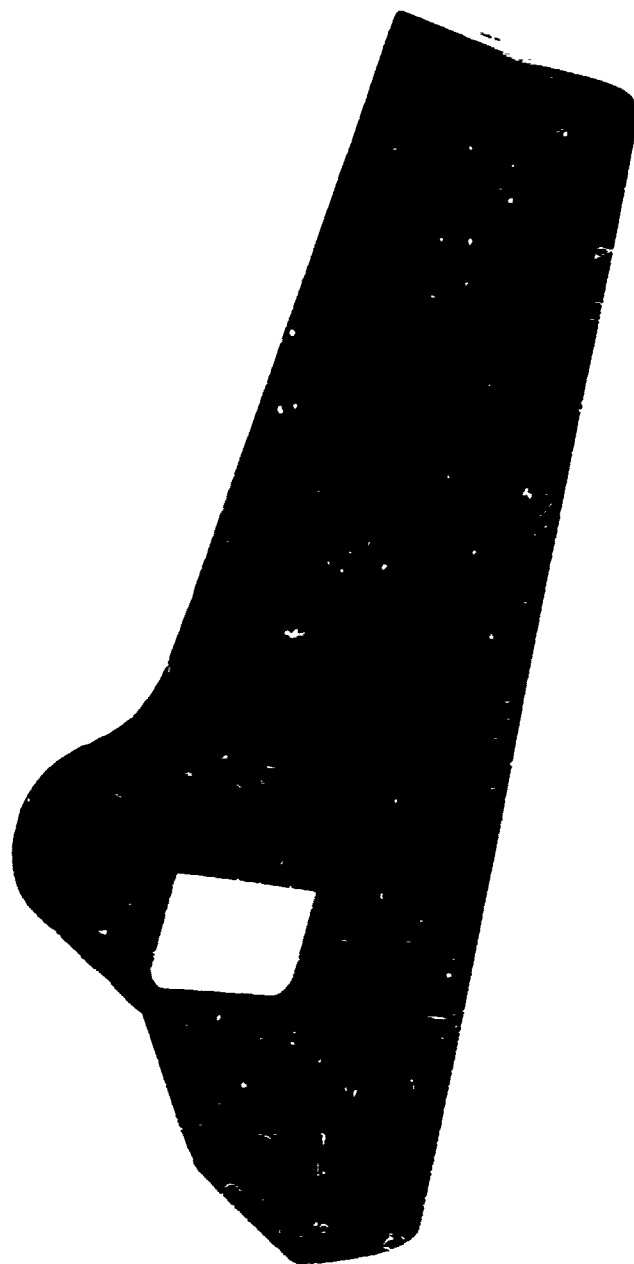


Figure 56. Molded Fitting — Graphite/Polysulfone

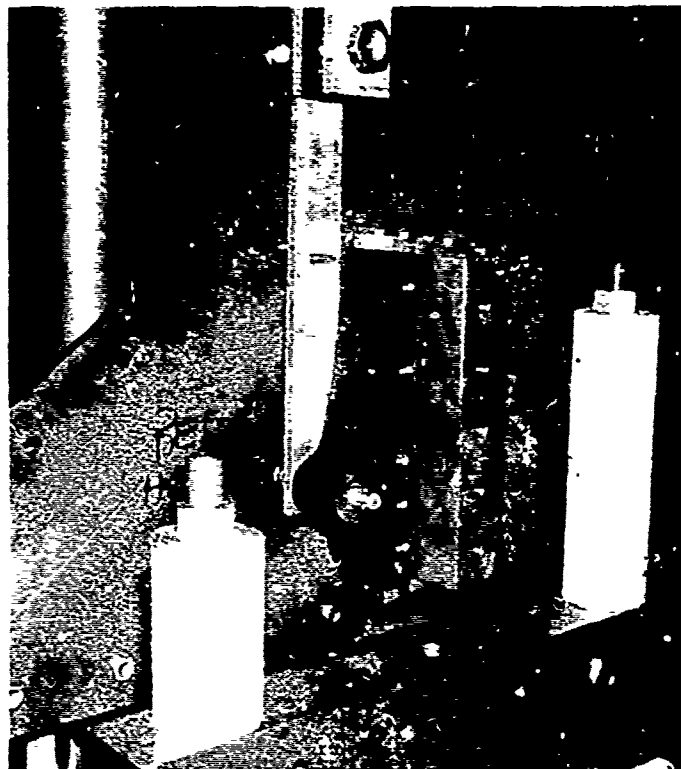


Figure 57. Molded Fitting - Test Set-Up Without Side Plate

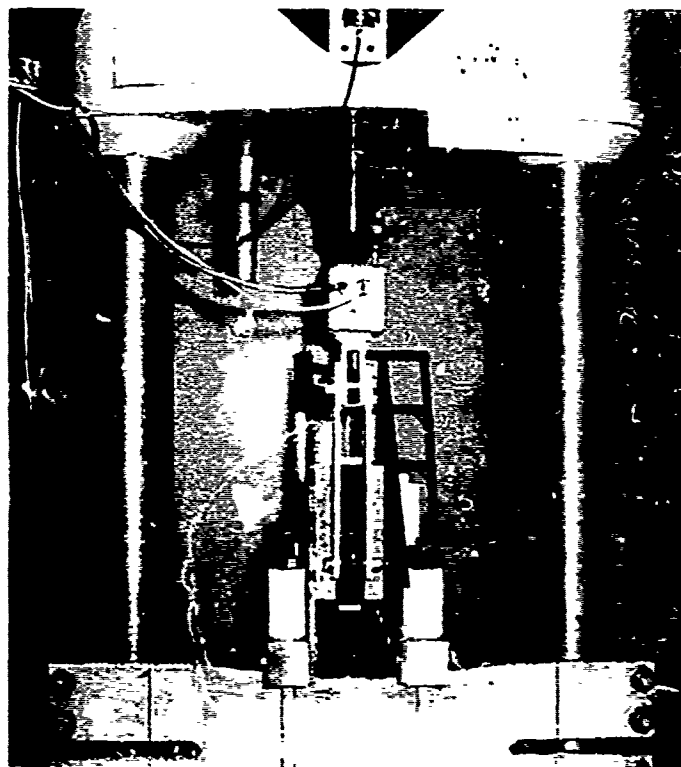
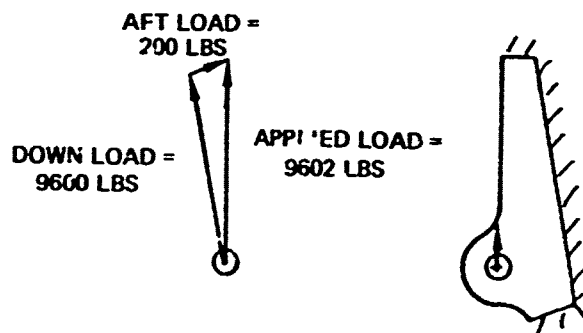
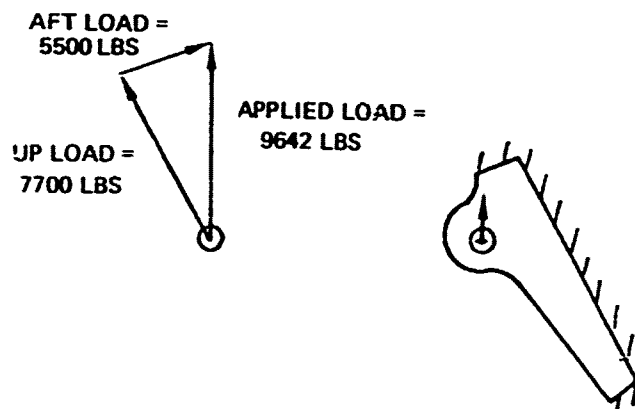


Figure 58. Molded Fitting - Test Set-Up

ULTIMATE LOAD TEST,
POSITION No. 1



ULTIMATE LOAD TEST,
POSITION No. 2



TEST TO FAILURE,
POSITION No. 3

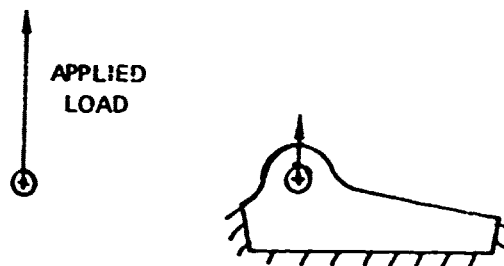


Figure 59. Molded Fitting — Test Load Conditions

design life cycles of the elevator fitting. The fitting was then repositioned to position #3 as shown in Figure 59. A pull-out load was applied until failure occurred at 15,050 lb, as shown in Figure 60. The fitting failed in the web-flange radii. A close-up of the failure is shown in Figure 61.

A fitting with the chopped fiber trusses was also tested to failure. This fitting was mounted in a test machine in position #3 (Figure 59). A pull-out load was applied until failure occurred at 11,600 lb. The fitting failed in tension in the lug area. A close-up of the failure is shown in Figure 62.

Both the fabric truss fitting and chopped fiber truss fitting failed above the highest ultimate load component even though they were loaded in a more severe direction. The fitting failure modes showed that the fabric truss concept provided better load transfer capability from the lug to the bolted flange area.

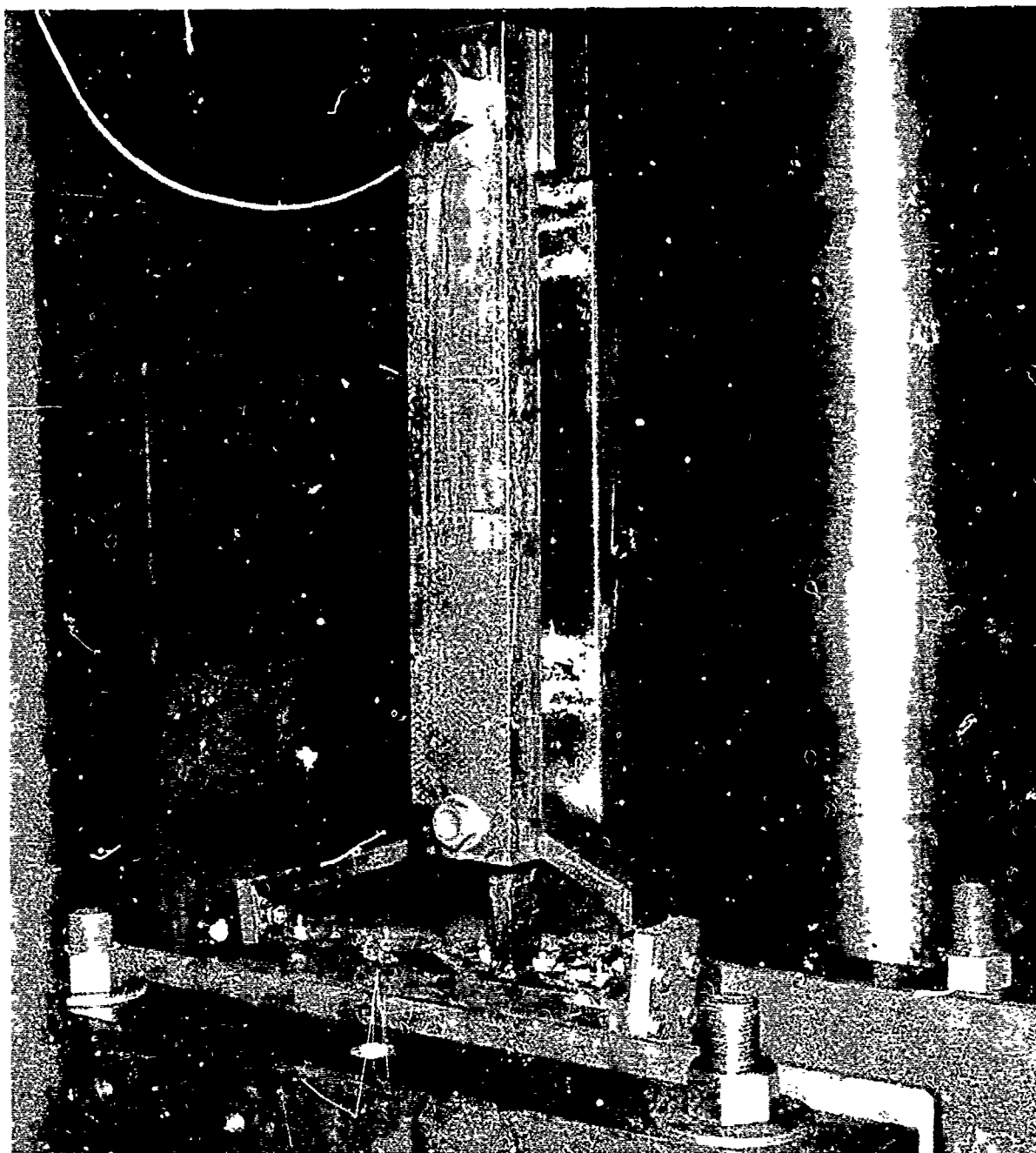


Figure 60. Molded Fitting – Pull-Out Test

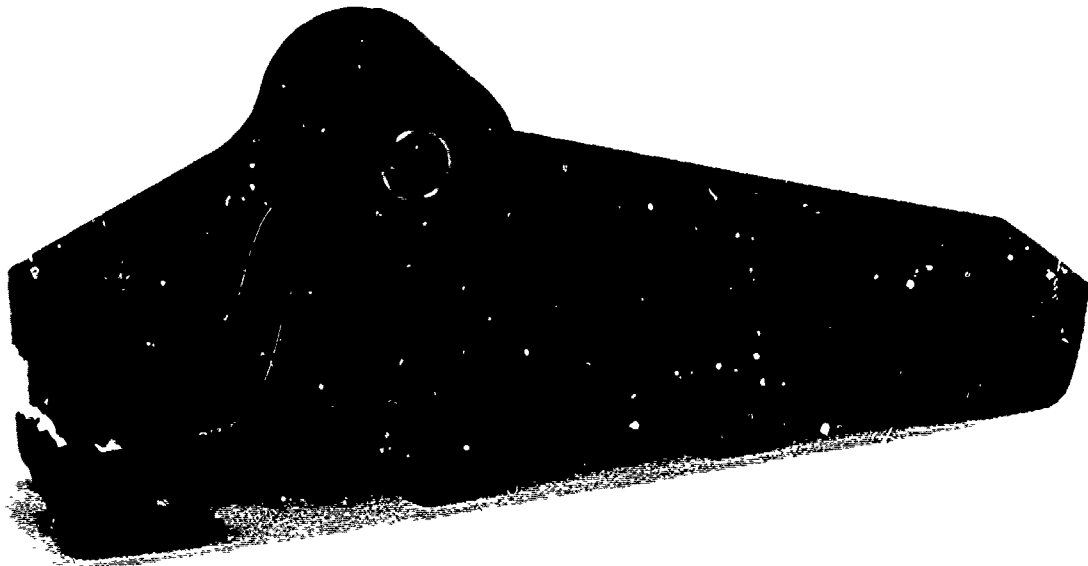


Figure 61. Fabric Truss Molded Fitting Failure

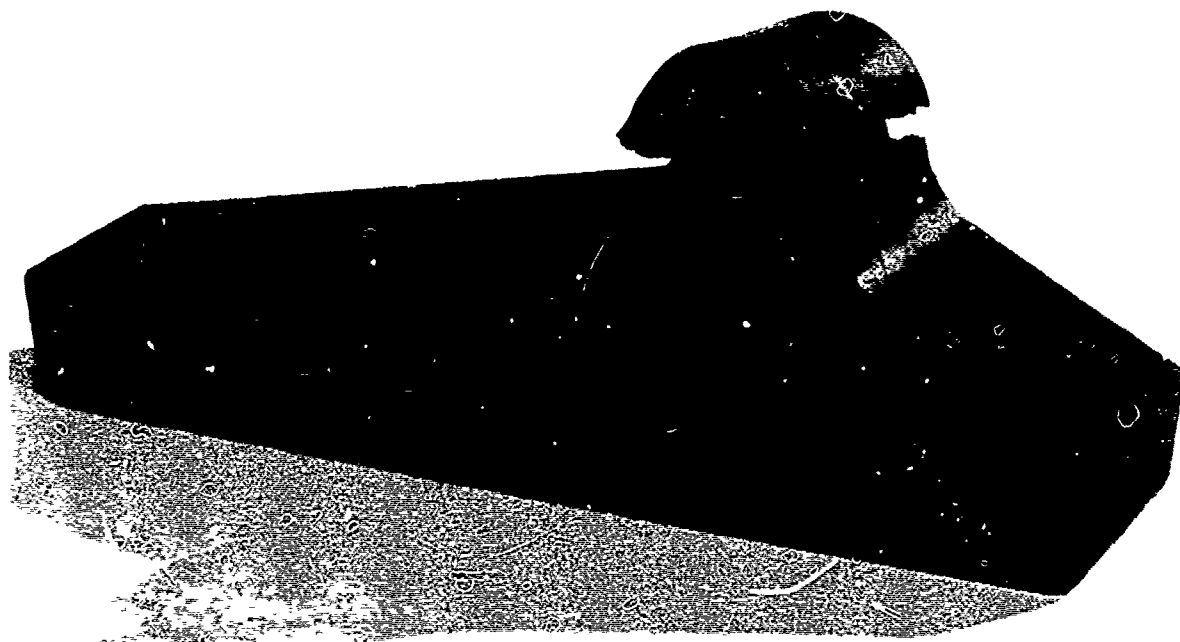


Figure 62. Chopped Fiber Truss Molded Fitting Failure

5.0 FIELD MAINTENANCE/REPAIR METHODS

Studies were initiated on field repair and maintenance procedures for graphite reinforced thermoplastic composites. The methods emphasized were the repair of laminate penetration or major damage under field conditions. Accordingly, facility limitations were imposed which only permitted the use of portable vacuum pressure and heat sources.

Several panels were tested that incorporated repaired areas. The panels were made of 4 plies of 181 style graphite fabric orientated at $(0^0, 90^0)$ and were 6 in. wide and 16 in. long. Damaged areas 1 in., and 3 in. in diameter were repaired. The frayed area of damaged zone was removed with a hole saw of the appropriate diameter. The edges were then scarfed by making several hole saw cuts each successive one being larger in diameter and one ply deep. The end result was a stepped joint of four concentric circles as shown in Figure 63. The area around the hole was then solvent cleaned with Methanol. Individual plies of fabric prepreg were then fitted to the hole. The repair was then accomplished by adhesive or fusion bonding using a portable vacuum and heat source. A typical repaired damage is shown in Figure 63.

Several different heat sources were evaluated. They consisted of a heating blanket, localized (spot) resistance heater, hot air gun and resistance wire. Of these, the hot air gun (Figure 64) proved to be the best. The location and rate of heating was most easily controlled by this method since the operator had good visibility of the area being repaired. The other heating methods caused panel distortion due to rapid rate of heating and/or non-uniform heating.

Using a heat gun as the heat source, a patch could be heated to a temperature of 500 to 550°F. It was found that a more uniform patch could be achieved if an aluminum back-up plate (x 0.060 in. thick) was used. The plate helped distribute the heat and minimize distortions. A standard fusion repair could be made in 15 to 30 minutes. Figure 63 shows a completed repair made by fusion. A cross section of a repair patch made by this method is shown in Figure 65.

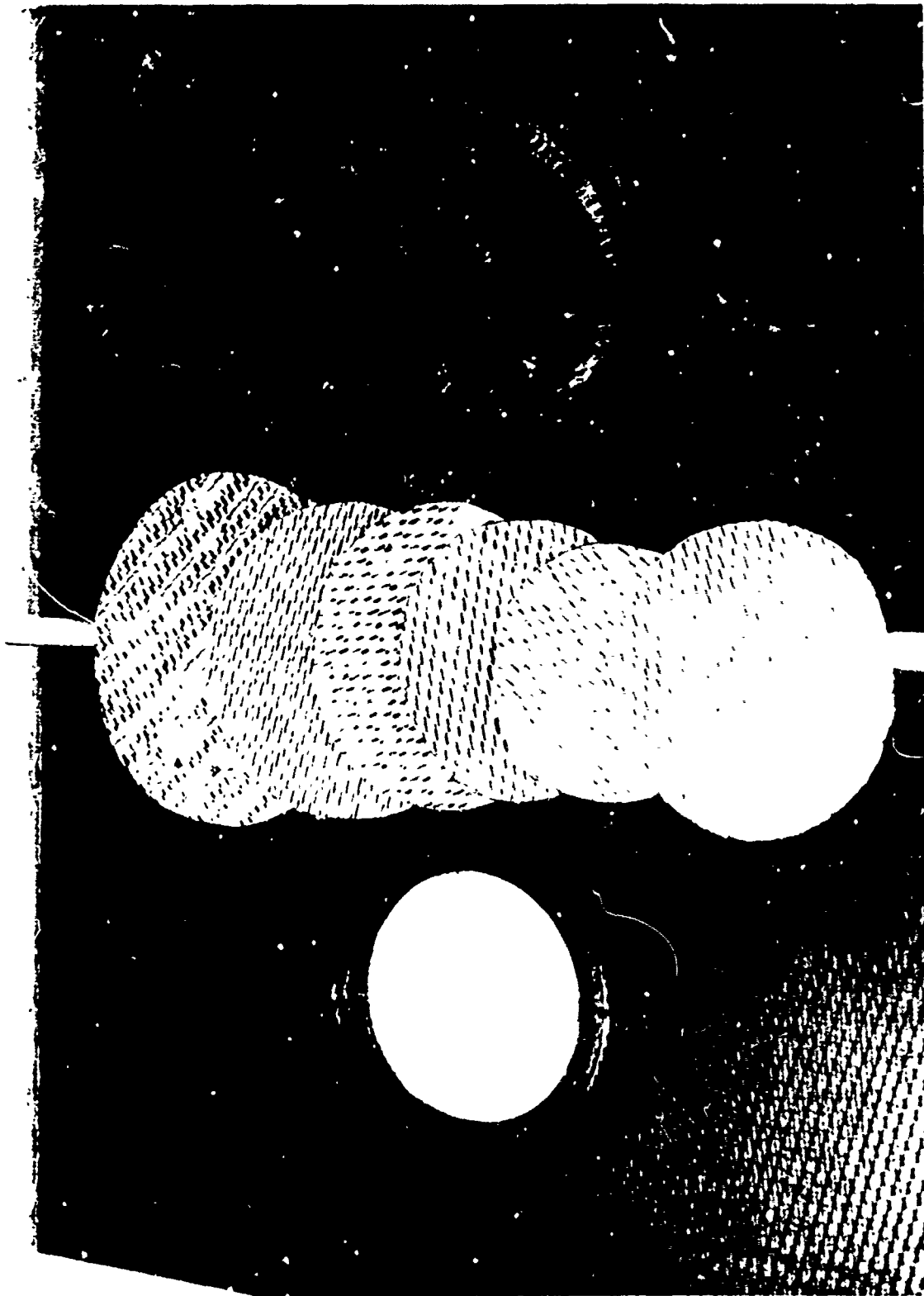


Figure 63. Fusion Bond Damage Repair

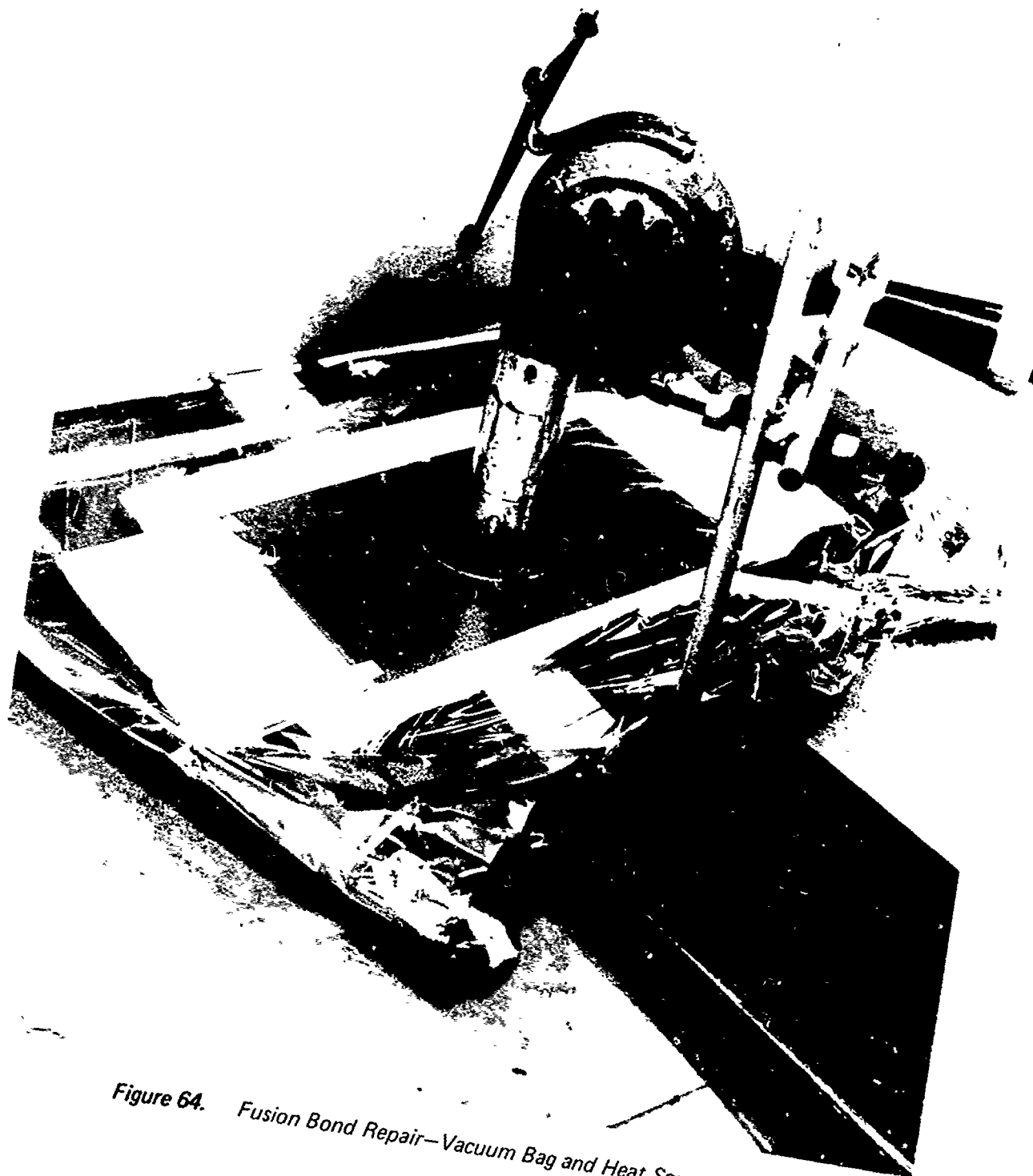


Figure 64. Fusion Bond Repair—Vacuum Bag and Heat Source

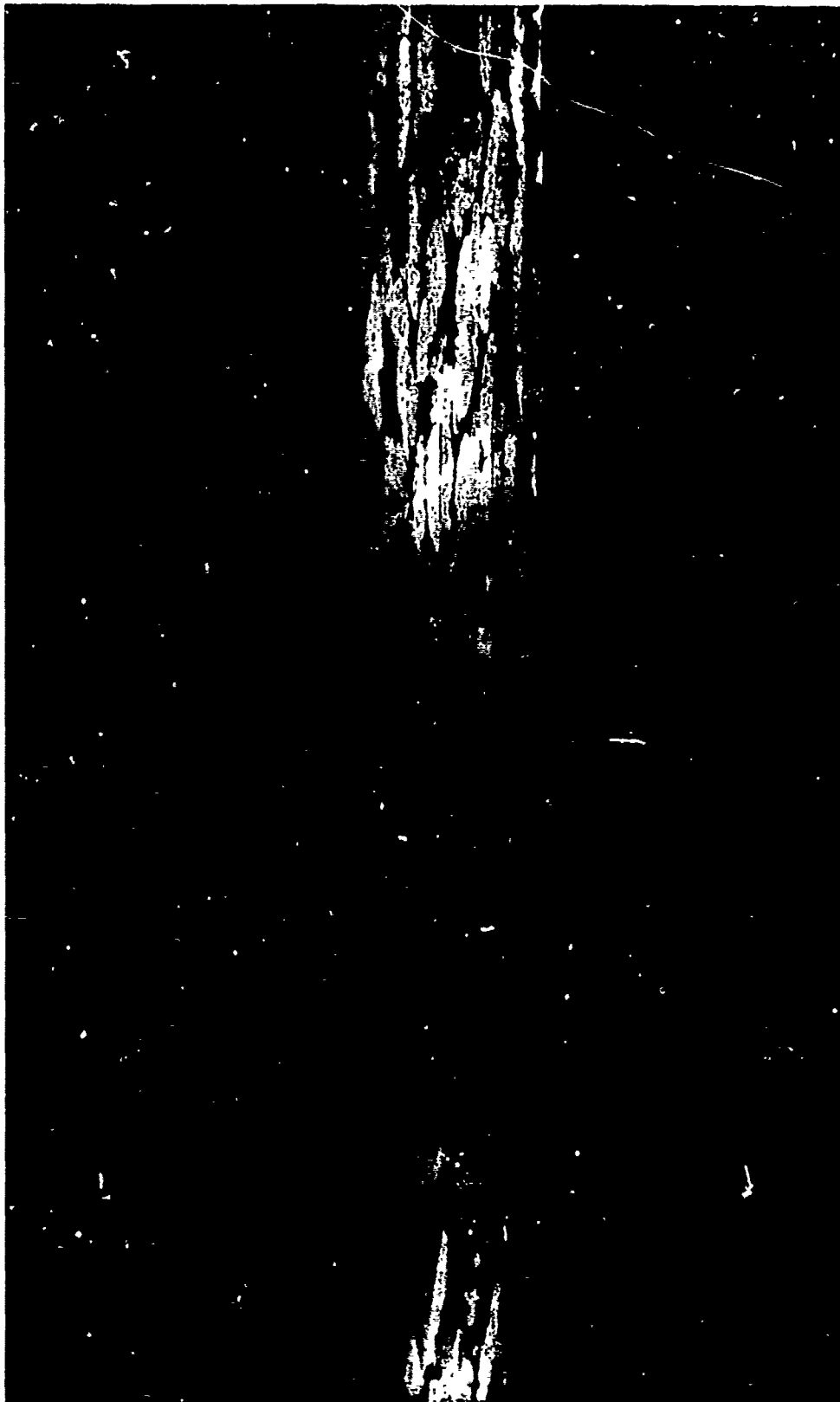


Figure 65. Fusion Bond Repair Cross Section

Repairs were also made using epoxy adhesives EA934 and EA9628 (Hysol). The hole preparations were the same as used for the fusion repair. The replacement patches, however, were preconsolidated in a press (consolidated patches can also be used in the fusion process), as shown in Figure 66. EA9629 adhesive was applied between each layer of the patch. It was then vacuum bagged and then cured 90 minutes at +250°F with a heating blanket. Similar procedures were used with EA934 adhesive except the patch was cured at room temperature.

A total of 12 panels were tested. Two were used as controls. Eight repair panels were static tested. They were conducted in a 120,000 lb capacity Baldwin Universal test machine at room temperature and with a deflection rate of 0.05 in./min. Two repair panels were fatigue tested. Fatigue tests were run in a 40 kip capacity hydraulic fatigue machine with a servo load controller. The repair panel test data is summarized in Tables 24 and 25. A photo of some of the failed specimens is shown in Figure 67.

Two control panels were tested in tension, one to obtain basic panel strength and one with a 1 in. diameter hole. The first control panel was tested and initially failed in the grip area. It developed a maximum gross stress of 66,000 psi. This panel was then repaired and necked down to a 3 in. width in the test area. It failed at a lower gross stress of 50,948 psi in the necked down region in the second test. A second control panel with a 1 in. diameter hole was also tested. This panel developed a gross stress of 26,593 psi at failure.

Panels with a 1 in., 2 in., and 3 in. hole were repaired by fusion bonding. Panels with 1 in. diameter holes were also repaired by adhesive bonding. The panels with the fusion and adhesively bonded 1 in. diameter repaired holes were static tested and achieved gross strengths equivalent to that attained in the second test of the control panel. The panels with the 2 in. diameter repairs attained static strengths that were 56 percent of ultimate and panels with the 3 in. repaired holes attained strengths that were 42 percent of ultimate. The net stress of these panels based on areas after the laminates

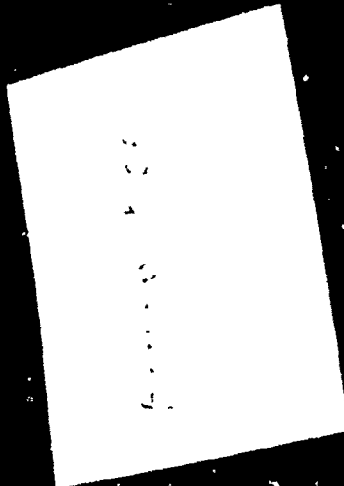


Figure 66. Adhesive Bond Repair


Table 24. Repair Panel Static Tests^(a)


PANEL	AREA (IN ²)	LOAD (LB)	GROSS STRESS (PSI)	NET STRESS (PSI)
CONTROL NO. 1	0.1635	8,330 ^(b)	50,948	50,948
CONTROL NO. 2 (1-IN HOLE, NO REPAIR)	0.3276	8,830	26,593	32,343
1-IN HOLE REPAIR - FUSION	↓	16,540	50,438	60,585
1-IN HOLE REPAIR - FUSION		17,100	52,197	62,636
2-IN HOLE REPAIR - FUSION		9,260	28,266	42,399
2-IN HOLE REPAIR - FUSION		9,600	29,304	43,956
3-IN HOLE REPAIR - FUSION		7,420	22,649	45,298
3-IN HOLE REPAIR - FUSION		6,720	20,512	41,024
1-IN HOLE REPAIR - BOND		17,250	52,655	63,186
1-IN HOLE REPAIR - BOND		16,220	49,511	59,413

(a) FOUR PLYS OF FABRIC AT (0,90)

(b) FIRST TEST FAILED IN GRIPS AT 66,000 PSI,
MACHINED TO 3 IN WIDTH FOR SECOND TEST

Table 25. Repair Panel Fatigue Tests

FATIGUE SPECIMEN	GROSS AREA IN ²	MEAN + ALT. LOAD, KIPS	MAXIMUM STRESS (GROSS AREA) PSI	CYCLES TO FAILURE	NOTES
					
B-1	.3282	3.00 ± 2.00	15,000	7,749,000	NO FAILURE
↓		3.90 ± 2.60	20,000	3,823,000	NO FAILURE
↓		4.92 ± 3.28	25,000	2,779,000	NO FAILURE
B-1		5.91 ± 3.94	30,000	106,700	TEST FIXTURE FAILED, SPECIMEN BROKEN
B-2	.3245	5.83 ± 3.89	30,000	5,847,000	NO FAILURE

 1-INCH HOLE REPAIR FUSION
FOUR PLYS OF FABRIC AT
(0,90)

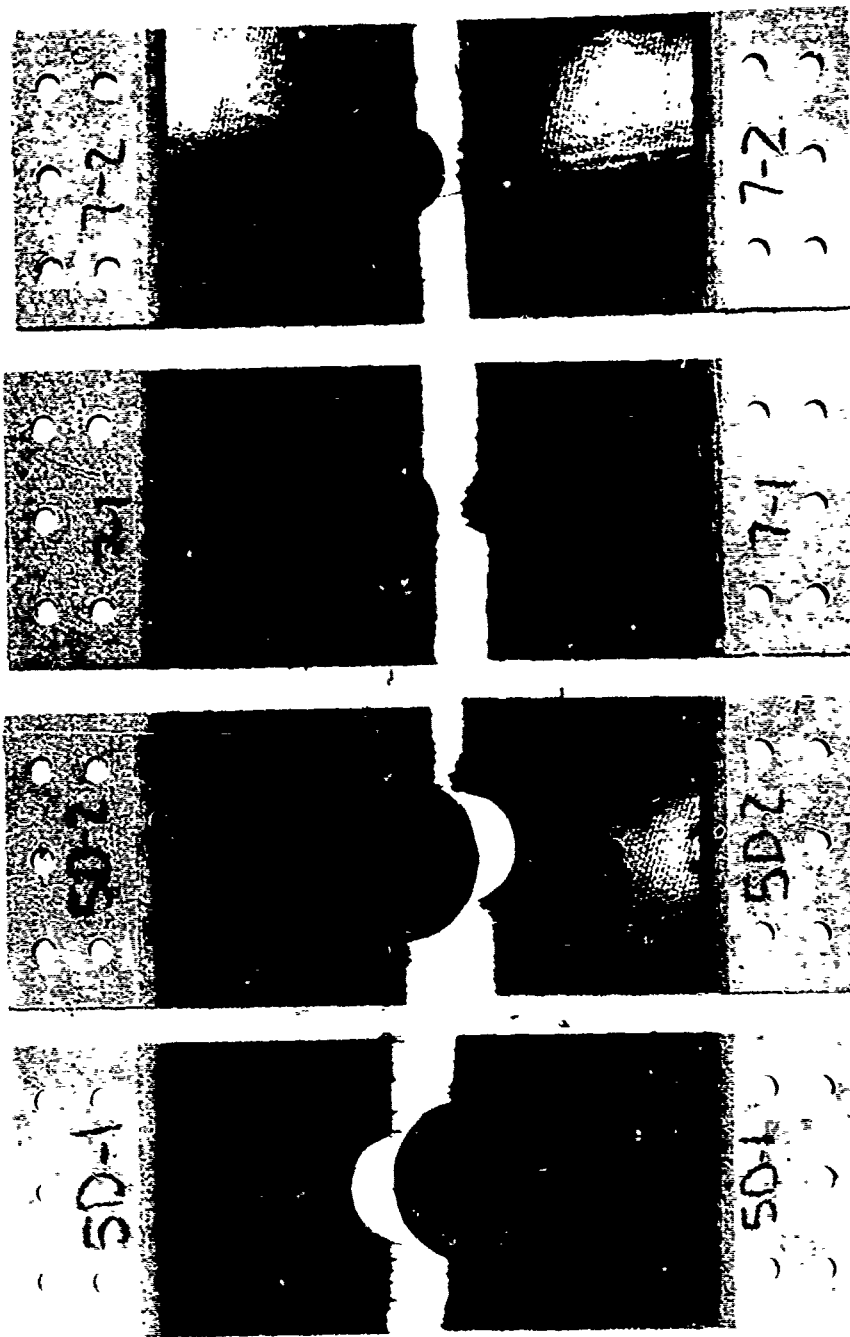


Figure 67. Repair Panel Failed Specimens

had been stepped to accept the repair patches are approximately the same. They showed a significant improvement when compared to the net stress in the control panel incorporating the 1 in. diameter hole. This improvement was developed in spite of the more severe boundary conditions on the panels with the large holes by the constant 6 in. panel width.

Panels with 1 in. hole repairs were fatigue tested. The fatigue tests were run in a 40 kip capacity hydraulic fatigue machine with a servo load controller. Specimens were loaded with a sinusoidally varying load at an $R = 0.2$ and a frequency of 10 Hz. The first panel was tested at increasing maximum stress levels until failure occurred. The panel finally attained 2.8×10^6 cycles at 25,000 psi gross stress which was well beyond the safe life (4 lives) required for design. When the next load level (30,000 psi) was attempted the test fixture failed which caused the panel to break in bending. The second panel was fatigued at a maximum stress level of 30,000 psi and attained 5.8×10^6 cycles without failure.

6.0 SUBCOMPONENT EVALUATION

A subcomponent test program was performed to establish the data required to finalize the design of an AF RTP YC-14 outboard elevator. The tests in this program included static and fatigue rail shear tests, static and fatigue lap shear bond tests, mechanical attachment tests, shear buckling tests, compression buckling tests, load introduction tests and fracture panel tests. A summary of the tests performed is shown in Table 26.

6.1 IN-PLANE SHEAR TESTS

To obtain in-plane graphite composite shear data, several rail shear specimen configurations were tested (Figure 68). All of the specimens incorporated laminates consisting of Gr/Ps fabric oriented at $\pm 45^\circ$ which was representative of the construction anticipated for the elevator surfaces. Standard rail shear specimens 3 in. x 6 in. were tested and developed an average ultimate shear stress of 31,000 psi. Figure 69 shows a closeup of a typical rail shear static test setup. Rail shear specimens were tested with the attachment areas reinforced, and they showed an approximately 10 percent improvement. One specimen was tested with the rails bonded in place to minimize the stress concentration due to the attachment and this one also showed some improvement. A summary of the rail shear static tests is shown in Table 27. Photos of the failed specimens are shown in Figures 70 through 72. The specimens attained strength levels sufficient to show design compliance. The failure stresses were 2 to 3 times greater than required for the YC-14 elevator design.

An additional set of rail shear specimens was tested to obtain additional strength, shear stiffness data and temperature effects. This data is also included in Table 27 (Specs 11 through 14). These specimens tested slightly higher than the initial bolted rail specimens. The specimens tested at 160°F showed no significant drop in strength and only a slight drop in shear stiffness.

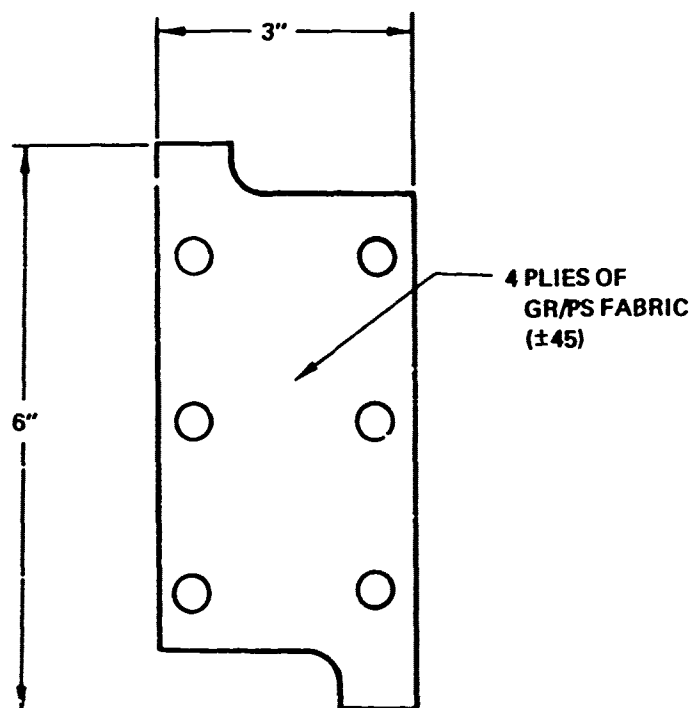
Rail shear specimens incorporating the same laminate design as the static specimens were tested in fatigue. The fatigue tests were conducted in a Sonntag SF-10 fatigue test machine at a loading frequency of 30 Hz and a $R(\text{minimum load/maximum load})$ of 0.05. Test specimens were clamped between

Table 26. Subcomponent Tests

TEST	SPECIMEN	NO. OF TESTS
IN-PLANE SHEAR JOINT STRENGTH	RAIL SHEAR	17
FUSION BOND	LAP SHEAR	24
ADHESIVE BOND	LAP SHEAR	9
MECHANICAL ATTACH.	PULL OUT	13
SHEAR BUCKLING	CANTILEVER BEAM	3
COMPRESSION BUCKL'G	STIFF. COMPRESSION PANEL	3
LOAD INTRODUCTION	BOX BEAM	1
FRACTURE	SLOTTED PANEL	3

Table 27. Rail Shear Static Tests – ±45 Graphite Fabric/P1700

SPEC. NO.	NO. PLIES		TEST TEMP	MAX. SHEAR STRESS	SHEAR MODULUS 10 ⁶
1	4	STD. BOLTED RAILS	R.T.	30,900	
2	4	STD. BOLTED RAILS	R.T.	31,100	
3	8	DOUBLERS – BOLTED RAILS	R.T.	33,000	
4	8	DOUBLERS – BOLTED RAILS	R.T.	35,400	
5	4	BONDED RAILS	R.T.	35,600	
11	4	BOLTED RAILS	R.T.	32,520	4.0
12	4	BOLTED RAILS	R.T.	35,430	3.9
13	4	BOLTED RAILS	160°F	31,890	3.7
14	4	BOLTED RAILS	160°F	33,430	3.5
15	4	BOLTED RAILS – 5/16" DIA. HOLE	R.T.	33,400	
16	4	BOLTED RAILS – 5/16" DIA. HOLE	R.T.	33,700	



RAIL SHEAR SPECIMEN

SPECIMEN	TEST	TEST TEMP	NO. OF TEST
NO HOLE	STATIC	R.T.	4
NO HOLE	FATIGUE	R.T.	5
HOLE	STATIC	R.T.	2
HOLE	FATIGUE	R.T.	2
NO HOLE	STATIC	160°F	2
NO HOLE	FATIGUE	160°F	2
		TOTAL	17

Figure 68. In-Plane Shear

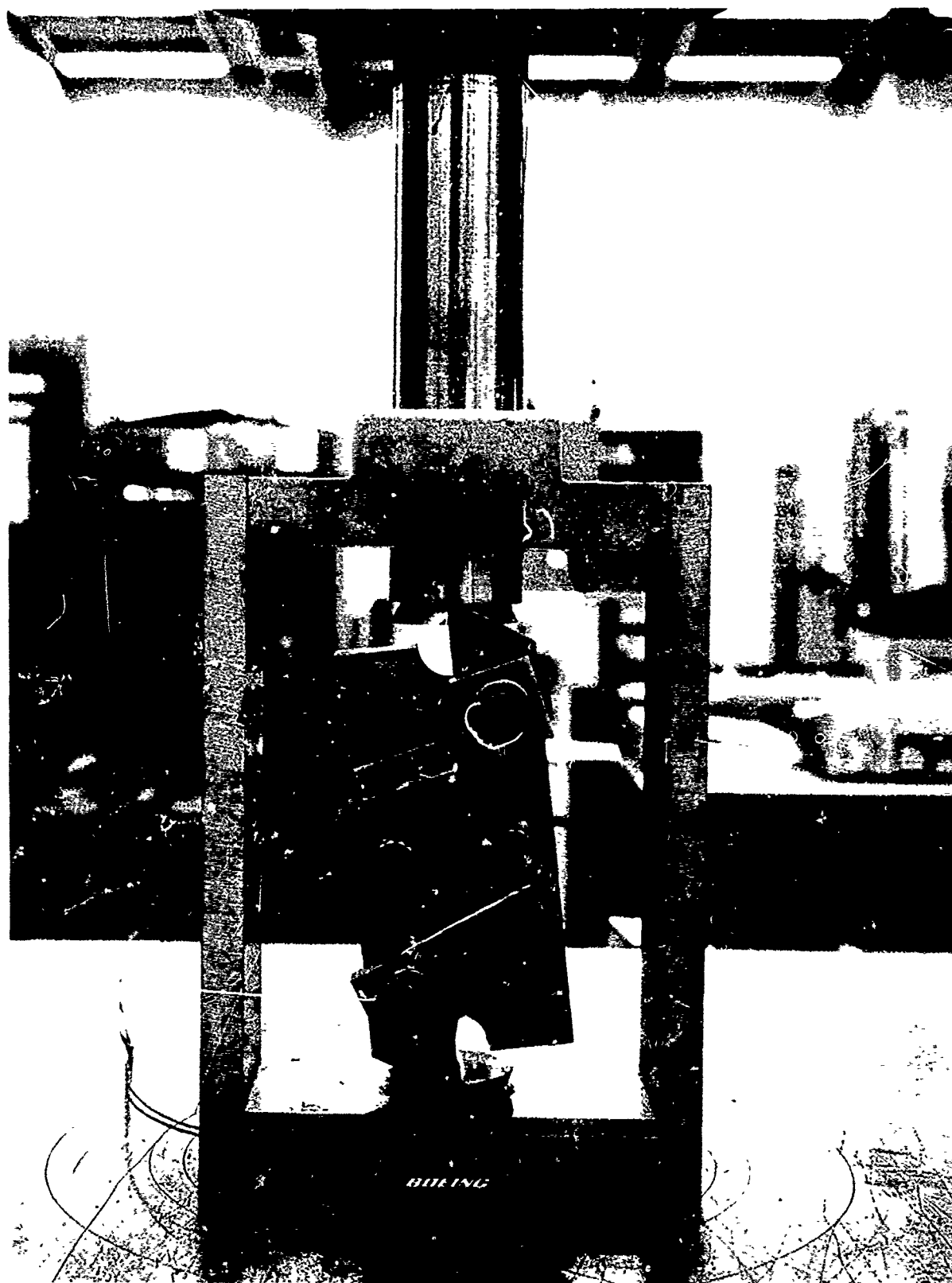


Figure 69. Rail Shear Static Test Set-Up

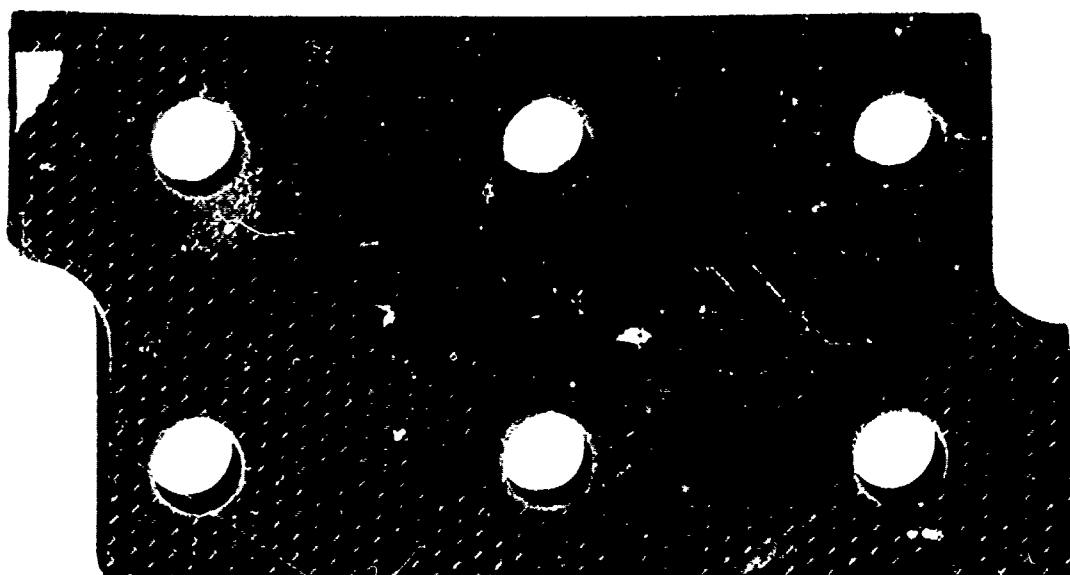
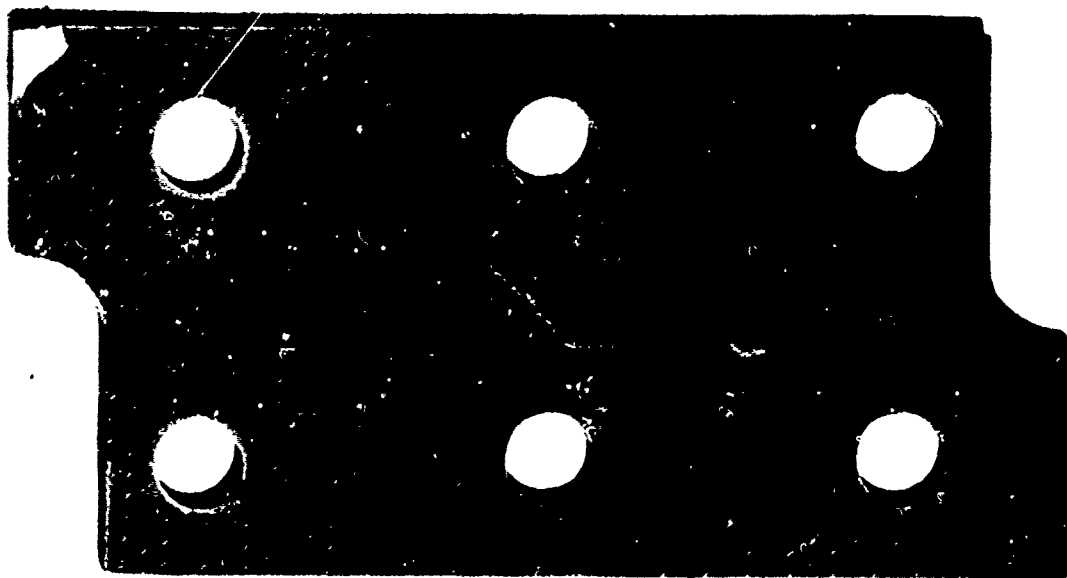


Figure 70. Failed Rail Shear Specimens

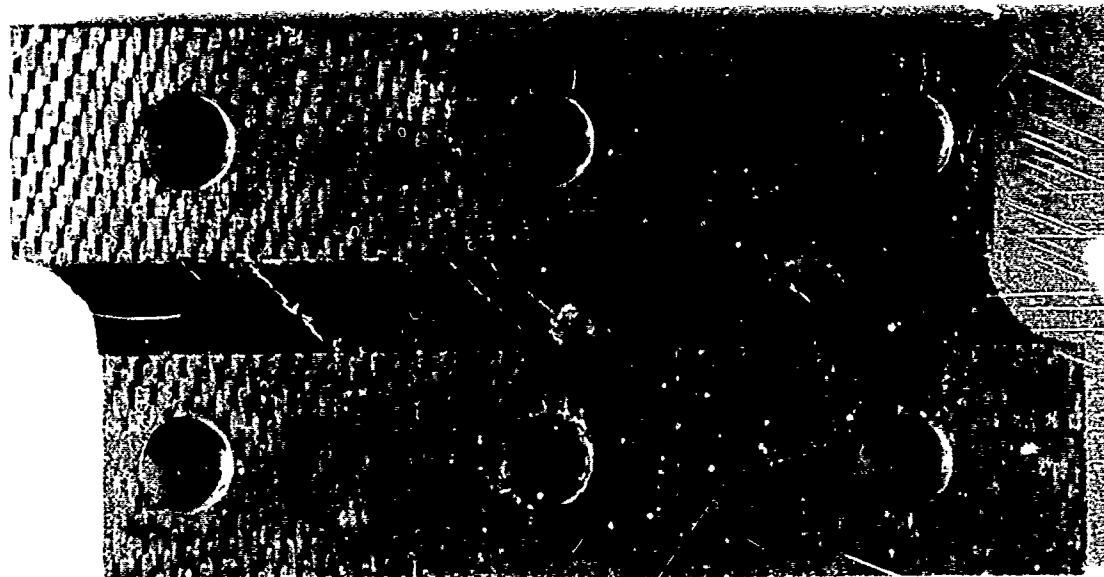
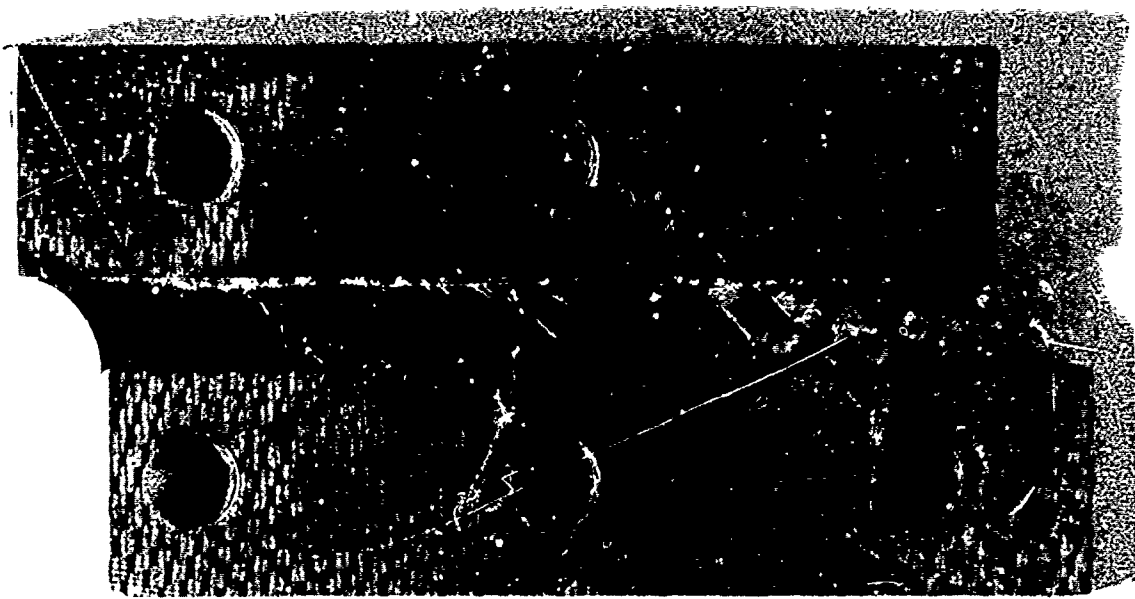


Figure 71. Failed Rail Shear Specimens – Doublers Bonded in Attachment Areas

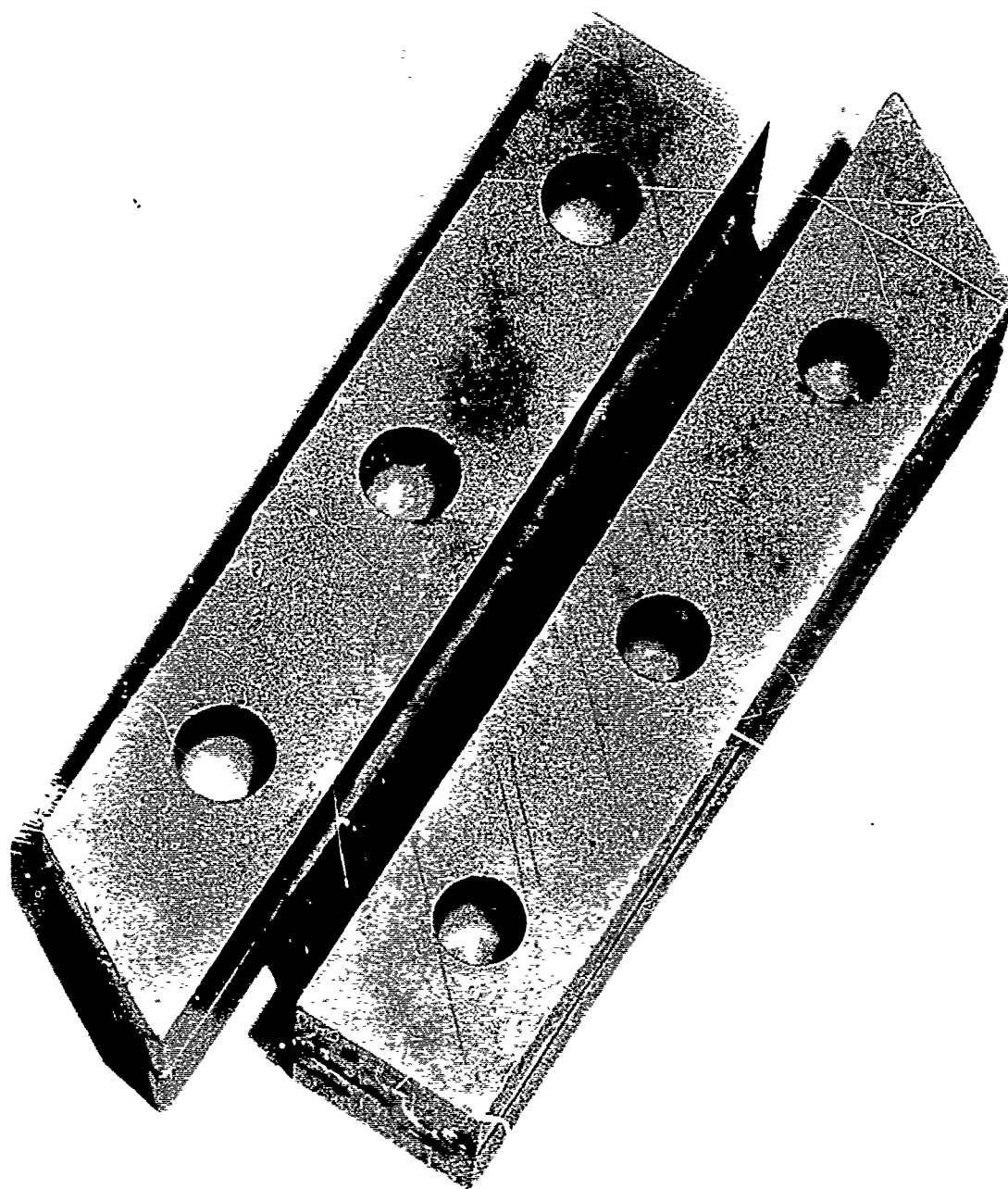


Figure 72. Failed Rail Shear Specimen — Rails Bonded In-Place

rails which were attached to the test machine through spherical ball bearings such that the load time was geometrically the same as used in the static rail shear test fixtures. The upper end was connected to the fixed end of the test machine through a strain gaged load cell to monitor test loads. The lower end was connected to the test machine loading platen, which applied mean and alternating loads. An automatic control system continuously made adjustments to maintain the proper load levels throughout the test duration.

Five rail shear specimens without holes were tested in fatigue. An endurance limit was attained at a maximum cyclic fatigue stress of 16,000 psi. A summary of this data is shown in Figure 73. Two rail shear specimens with a 5/16-in. diameter hole in the center of the test section were tested in fatigue. One was cycled to a maximum stress level of 23,000 psi and failed after 71,000 cycles. This data point plotted slightly below the S-N curve is shown in Figure 73. A second specimen with a hole in the test area was cycled at a maximum stress of 16,000 psi. This specimen failed after 6×10^6 cycles. Typical failed static and fatigue rail shear specimens are shown in Figure 74.

6.2 JOINT TESTS

Specimens were tested to obtain fusion bond, adhesive bond, and mechanical attachment joint strength data. Lap shear specimens were tested to obtain both static and fatigue properties.

6.2.1 Bonded Joints

Several lap shear specimens were tested to obtain properties of adhesive and fusion bonded joints. Both static and fatigue tests were performed.

The adhesive bond shear tests were performed using a 1 in. by 6 in. specimen with a 0.5 inch overlap as shown in Figure 75. Fiberglass end tabs were incorporated to facilitate gripping.

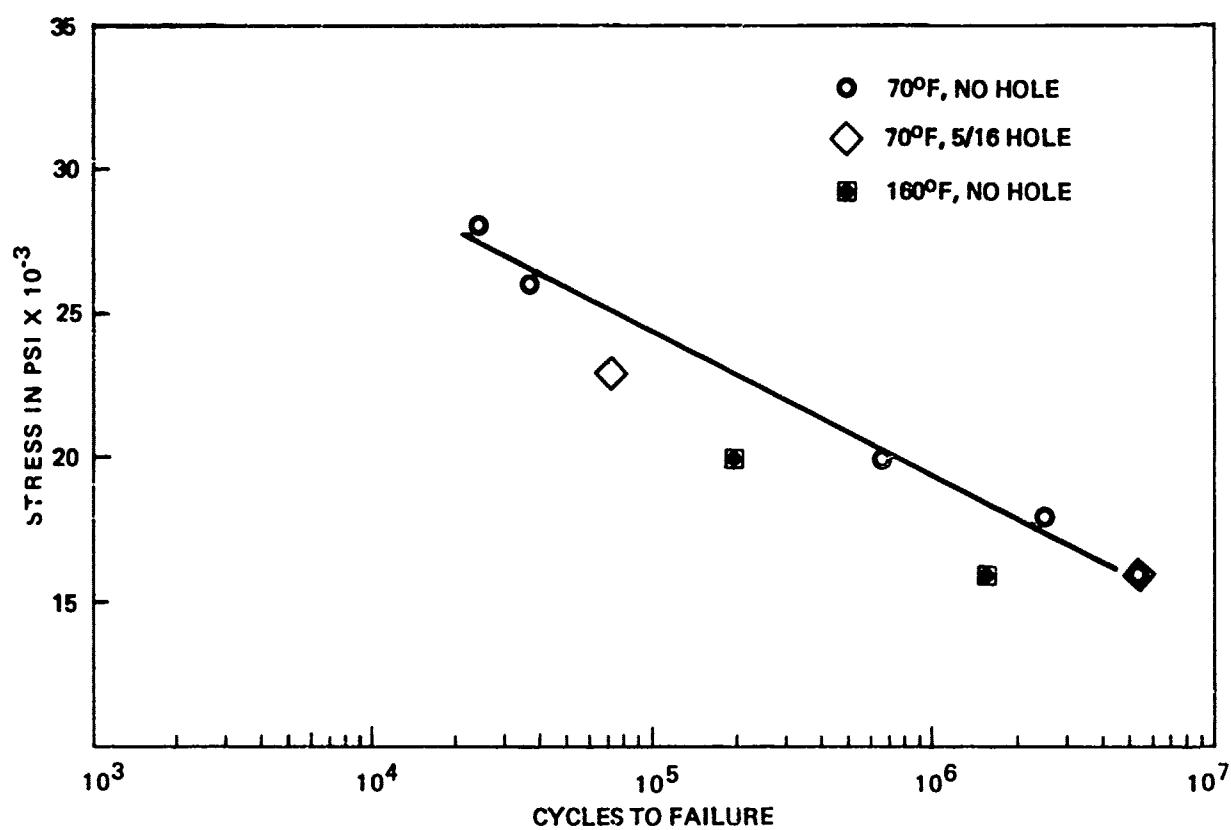
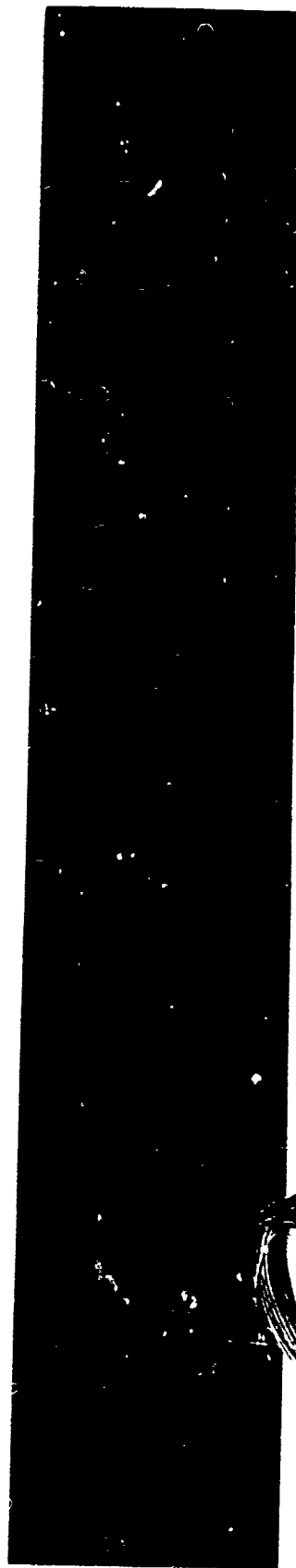
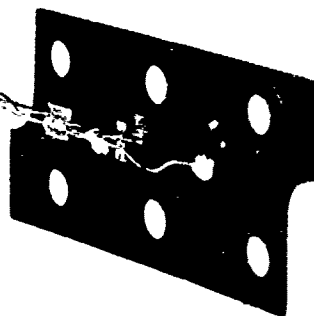


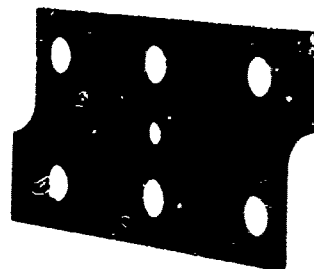
Figure 73. Rail Shear Fatigue Data



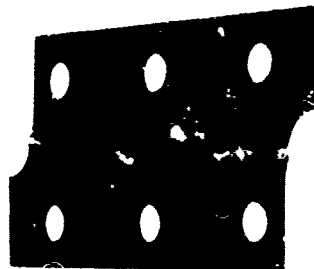
18
19
20
21
22
23
24
25
26
27
28
29
30
31
32
33
34
35
36
37
38
39
40
41
42
43
44
45
46
47
48
49
50
51
52
53
54
55
56
57
58
59
60
61
62
63
64
65
66
67
68
69
70
71
72
73
74
75
76
77
78
79
80
81
82
83
84
85
86
87
88
89
90
91
92
93
94
95
96
97
98
99
100



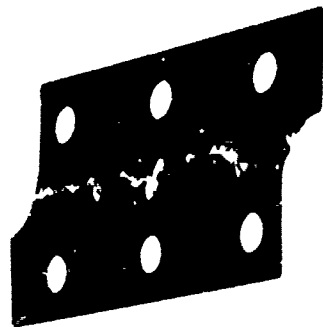
STATIC TEST
@ 160°F



STATIC TEST
WITH HOLE



FATIGUE TEST
@ 70°F



FATIGUE TEST
WITH HOLE

Figure 74. Rail Shear Failed Specimens

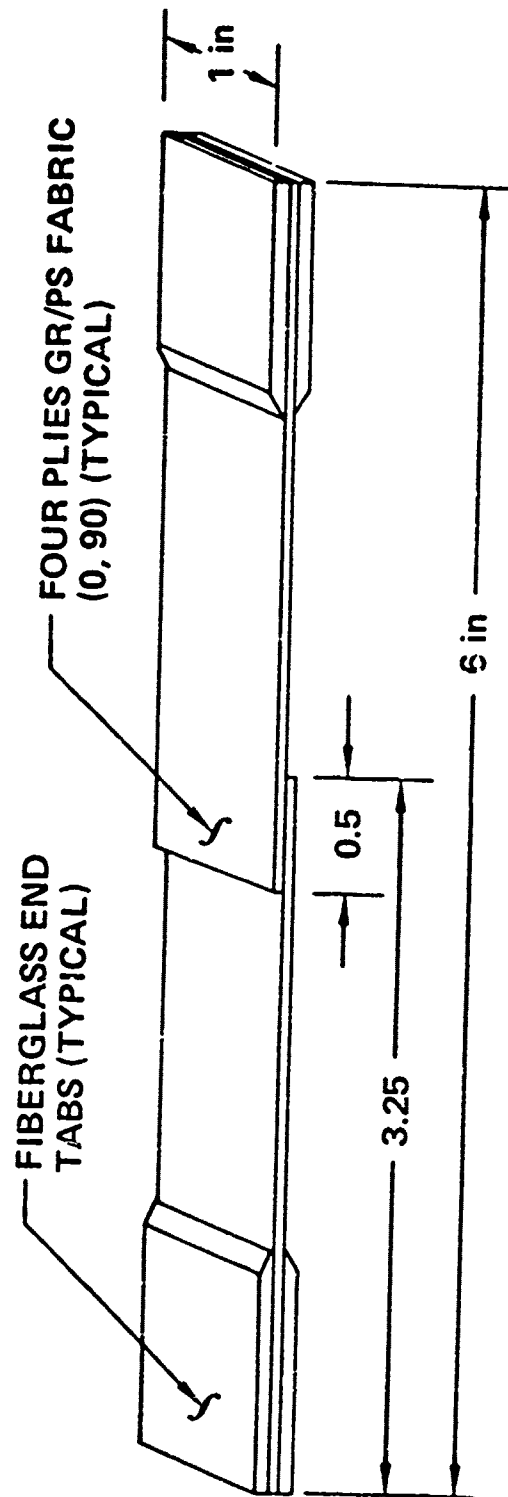


Figure 75. Lap Shear Specimen

A series of tests was performed to obtain the shear strength of adhesives cured using different process parameters. The specimens incorporated fabric laminates oriented at $(0^{\circ}, 90^{\circ})$. Some were made using room temperature curing adhesive, Hysol EA934, that were processed with vacuum bag pressure and others processed with spring-clamped pressure. The vacuum bagged specimens had an average strength of 2,025 psi and the spring clamped specimens averaged 1,850 psi. These strengths are well above that required by design. A series of specimens were also made that were bonded with Hysol 9628 adhesive. The adhesive in these specimens was cured at 250°F and an autoclave pressure of 90 psi. These specimens were tested and ultimate shear strengths averaged 2,640 psi. A summary of the above test data is shown in Table 28.

Several additional lap shear specimens were tested to obtain the shear properties at temperatures covering the YC-14 elevator design temperature range. These specimens were tested at -65°F , room temperature and 180°F . They incorporated graphite fabric laminates oriented at $\pm 45^{\circ}$ to simulate the most severe load transfer condition in the final design. Specimens were bonded with AF126 adhesive cured at 250°F , with Hysol EA9628 adhesive cured at 250°F and Hysol EA934 cured at room temperature. Several specimens were also fabricated that were fusion bonded at 500°F and 100 psi. Figure 76 shows a cross-section of a typical fusion joint. All of the specimens tested attained shear strengths above that required for design.

The data obtained from the above tests showed that the AF126 adhesive produced the highest shear strengths. This adhesive is considered to be the most flexible of the group tested and therefore best able to contend with the high in-plane strains produced by the $\pm 45^{\circ}$ laminates. The Hysol EA934 adhesive cured at room temperature attained room temperature strengths averaging 1,060 psi which is more than sufficient to meet field repair design requirements. The fusion bond specimens attained room temperature strengths of 1,210 psi and retained the highest percentage of their room temperature strength at 180°F . In general, all of the specimens tested developed strengths that would meet design requirements. A summary of this test data is shown in Table 29.

Table 28. Adhesive Lap Shear Strengths

Adhesive	Cure temperature of	Pressure application	Average shear strength (psi) ^a
Hysol EA 934	R.T.	Vacuum bag	2,025
Hysol EA 934	R.T.	Spring-clamped	1,850
Hysol 9628	250°	Autoclave 90 psi	2,640

^a Single 1/2-in overlap shear tests Fabric (0, 90).



Figure 76. Fusion Bonded Joint

Table 29. Lap Shear Strength (psi) (4 Plies \pm 45 Fabric)

Adhesive cure temperature		Test temperature		
		-65°F	R.T.	180°F
AF126	250°F	2,270	2,170	920
EA9628	250°F	1,500	1,290	580
EA934	R.T.	1,190	1,060	700
Fusion	500°F @ 100 psi	1,640	1,210	860

Several lap shear specimens were fatigue tested. These specimens incorporated graphite fabric laminates oriented at $\pm 45^\circ$ and were assembled by fusion bonding. The specimens were fatigued in tension with a load ratio of $R = 0.05$. Endurance limit attained was approximately 450 psi. This is well above the limit load levels used in the thermoplastic elevator design. A summary of the fatigue data is shown in Figure 77.

The rail shear specimens were fabricated with 0.3-in. wide fusion bond along the center of their sections. Figure 78 shows the specimen cross-section. These specimens were tested and attained shear strengths of 3,220 psi and 2,990 psi which are consistent with the strengths achieved with the lap specimens. The failures occurred within the first ply of one of the specimen halves.

6.2.2 Mechanical Attachment Joints

Several mechanical attachment joint specimens were fabricated and tested. A summary of this data is shown in Figure 79. All of the specimens failed in either a shear-out of tension mode or in the specimens with doublers in the basic $\pm 45^\circ$ laminate. The specimens that incorporated $\pm 45^\circ$ laminates at the attachment (No.'s 1, 2, and 3) failed at higher loads than those with $(0^\circ, 90^\circ)$ laminates (No.'s 4, 5, and 6). The specimens with doublers in the attachment areas failed in the basic laminates and carried the highest loads. A photo of the failed specimens is shown in Figure 80.

Nine graphite-polysulfone to aluminum lap joint specimens fastened with 1/4-in bolts were tested to determine their fatigue lives and failure modes. The nine specimens consisted of three groups of three each having different laminate construction representative of various types that had a possibility of being used in the elevator design. The first group incorporated $\pm 45^\circ$ laminates, the second $(0^\circ, 90^\circ)$ laminates and the third 45° laminates with a $(0^\circ, 90^\circ)$ doubler in the attachment area. The first two groups were attached with standard head bolts and the third with countersunk bolts. All specimens were 1.50 inches wide and had a 0.50-inch edge margin ($e/d = 2$).

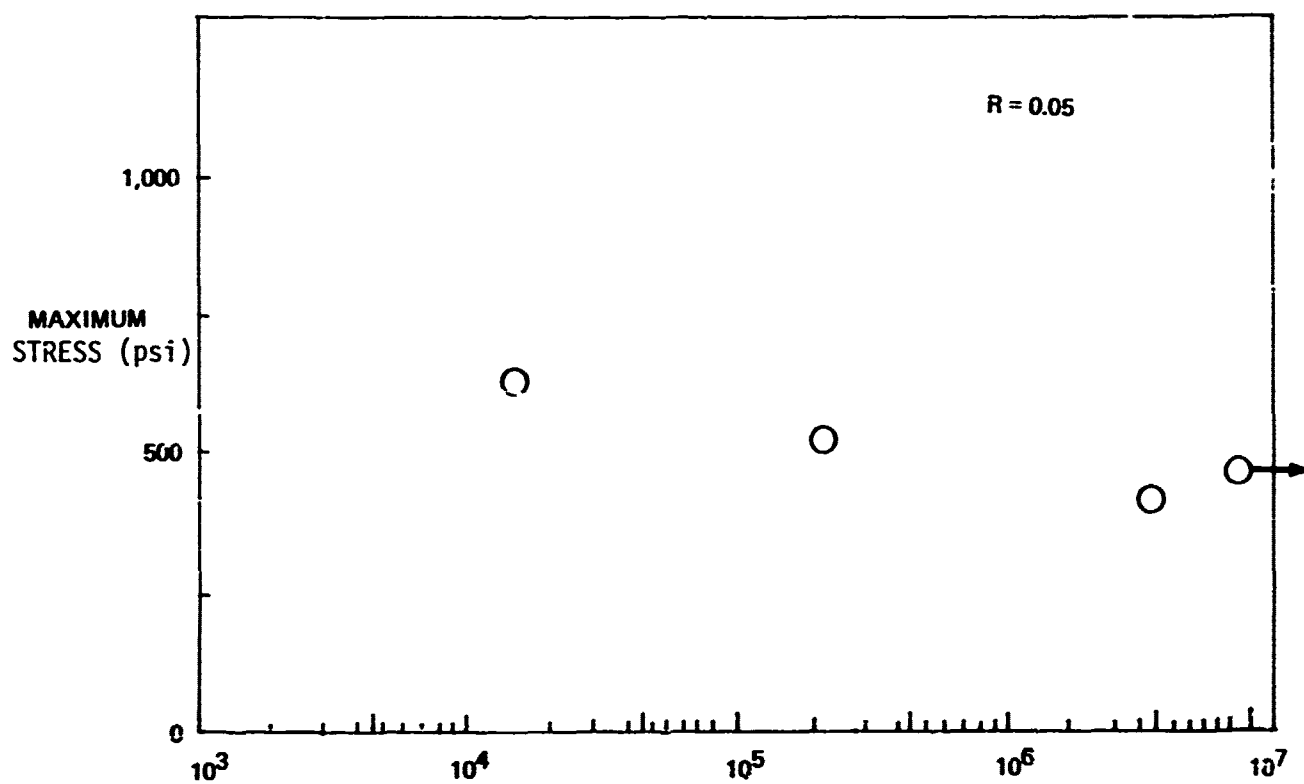


Figure 77. Fusion Bond Lap Shear Fatigue (Fabric at ± 45)

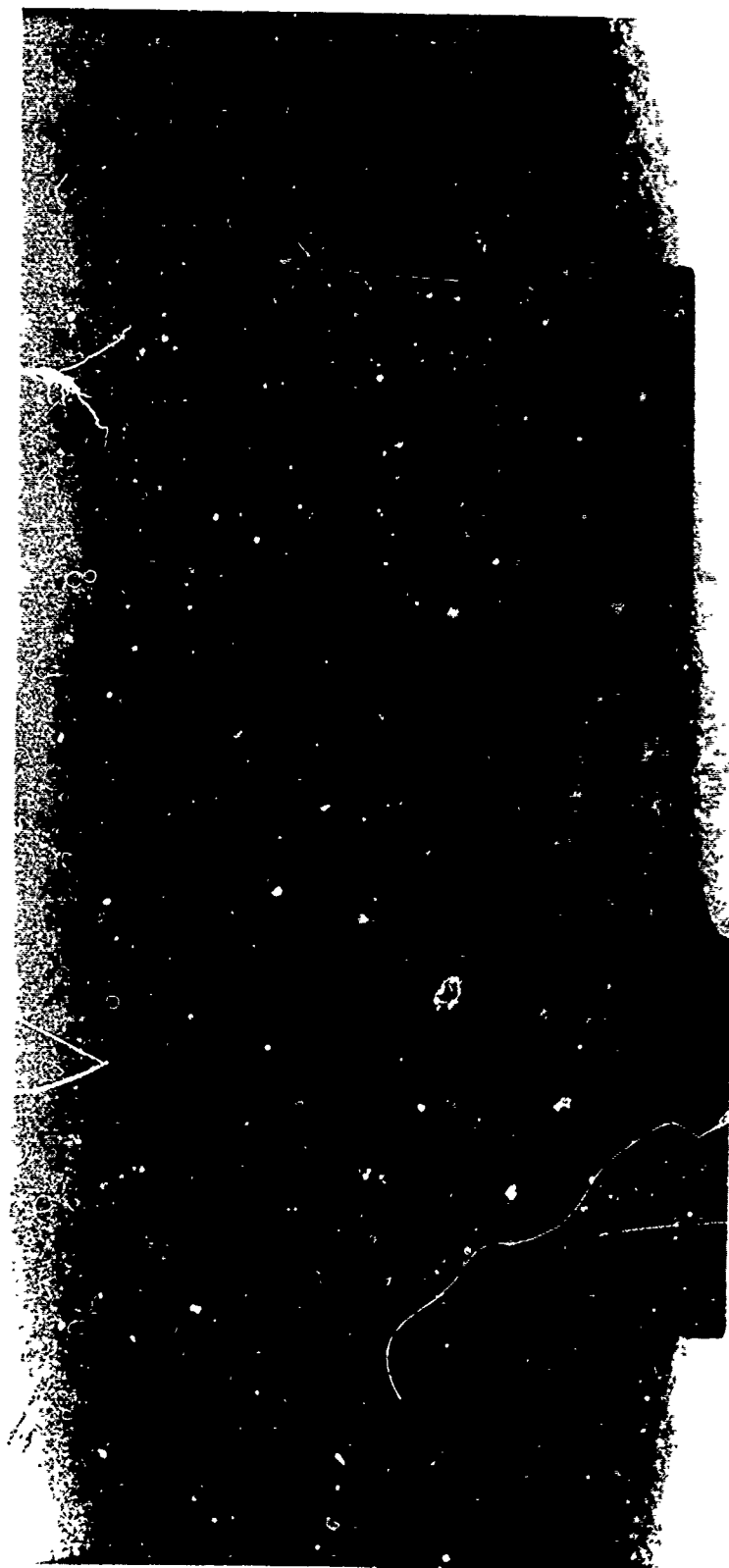
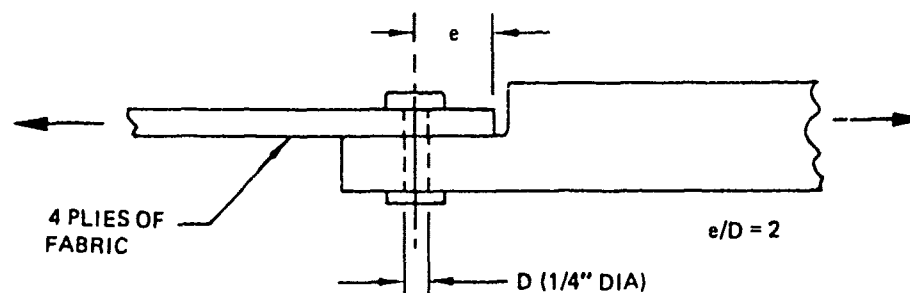


Figure 78. Fusion Bond—Rail Shear Specimen



SPEC.	LAMINATE 4 PLY	MAXIMUM STRESS (KSI)			FAILURE MODE
		BEARING	SHEAR OUT	TENSILE	
1	± 45	71.8	17.9		
2	± 45	75.0	18.8		
3	± 45	65.1	16.4		
4	0, 90	51.1	12.8		
5	0, 90	59.9	15.0		
6	0, 90	53.2	13.4		
7		69.1		22.8	BASIC LAMINATE
8		63.8		21.4	BASIC LAMINATE
9		68.9		22.9	BASIC LAMINATE

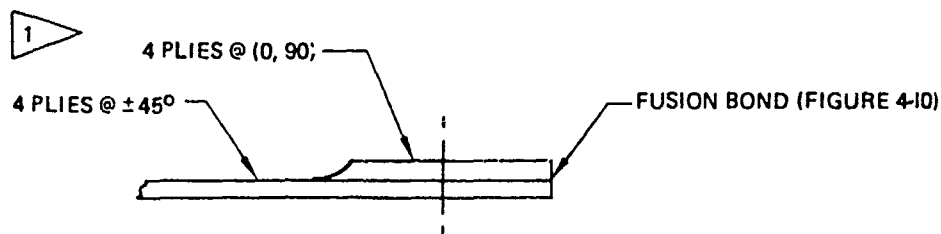


Figure 79. Mechanical Attachment Joint Test Data

Specimen No. 121-122-123-124-125-126-127-128-129-130-131-132-133-134-135-136-137-138-139-140-141-142-143-144-145-146-147-148-149-150-151-152-153-154-155-156-157-158-159-160-161-162-163-164-165-166-167-168-169-170-171-172-173-174-175-176-177-178-179-180-181-182-183-184-185-186-187-188-189-190-191-192-193-194-195-196-197-198-199-200-201-202-203-204-205-206-207-208-209-210-211-212-213-214-215-216-217-218-219-220-221-222-223-224-225-226-227-228-229-230-231-232-233-234-235-236-237-238-239-240-241-242-243-244-245-246-247-248-249-250-251-252-253-254-255-256-257-258-259-260-261-262-263-264-265-266-267-268-269-270-271-272-273-274-275-276-277-278-279-280-281-282-283-284-285-286-287-288-289-290-291-292-293-294-295-296-297-298-299-300-301-302-303-304-305-306-307-308-309-310-311-312-313-314-315-316-317-318-319-320-321-322-323-324-325-326-327-328-329-330-331-332-333-334-335-336-337-338-339-340-341-342-343-344-345-346-347-348-349-350-351-352-353-354-355-356-357-358-359-360-361-362-363-364-365-366-367-368-369-370-371-372-373-374-375-376-377-378-379-380-381-382-383-384-385-386-387-388-389-390-391-392-393-394-395-396-397-398-399-400-401-402-403-404-405-406-407-408-409-410-411-412-413-414-415-416-417-418-419-420-421-422-423-424-425-426-427-428-429-430-431-432-433-434-435-436-437-438-439-440-441-442-443-444-445-446-447-448-449-450-451-452-453-454-455-456-457-458-459-460-461-462-463-464-465-466-467-468-469-470-471-472-473-474-475-476-477-478-479-480-481-482-483-484-485-486-487-488-489-490-491-492-493-494-495-496-497-498-499-500-501-502-503-504-505-506-507-508-509-510-511-512-513-514-515-516-517-518-519-520-521-522-523-524-525-526-527-528-529-530-531-532-533-534-535-536-537-538-539-540-541-542-543-544-545-546-547-548-549-550-551-552-553-554-555-556-557-558-559-560-561-562-563-564-565-566-567-568-569-570-571-572-573-574-575-576-577-578-579-580-581-582-583-584-585-586-587-588-589-590-591-592-593-594-595-596-597-598-599-600-601-602-603-604-605-606-607-608-609-610-611-612-613-614-615-616-617-618-619-620-621-622-623-624-625-626-627-628-629-630-631-632-633-634-635-636-637-638-639-640-641-642-643-644-645-646-647-648-649-650-651-652-653-654-655-656-657-658-659-660-661-662-663-664-665-666-667-668-669-670-671-672-673-674-675-676-677-678-679-680-681-682-683-684-685-686-687-688-689-690-691-692-693-694-695-696-697-698-699-700-701-702-703-704-705-706-707-708-709-710-711-712-713-714-715-716-717-718-719-720-721-722-723-724-725-726-727-728-729-730-731-732-733-734-735-736-737-738-739-740-741-742-743-744-745-746-747-748-749-750-751-752-753-754-755-756-757-758-759-760-761-762-763-764-765-766-767-768-769-770-771-772-773-774-775-776-777-778-779-780-781-782-783-784-785-786-787-788-789-790-791-792-793-794-795-796-797-798-799-800-801-802-803-804-805-806-807-808-809-810-811-812-813-814-815-816-817-818-819-820-821-822-823-824-825-826-827-828-829-830-831-832-833-834-835-836-837-838-839-840-841-842-843-844-845-846-847-848-849-850-851-852-853-854-855-856-857-858-859-860-861-862-863-864-865-866-867-868-869-870-871-872-873-874-875-876-877-878-879-880-881-882-883-884-885-886-887-888-889-890-891-892-893-894-895-896-897-898-899-900-901-902-903-904-905-906-907-908-909-910-911-912-913-914-915-916-917-918-919-920-921-922-923-924-925-926-927-928-929-930-931-932-933-934-935-936-937-938-939-940-941-942-943-944-945-946-947-948-949-950-951-952-953-954-955-956-957-958-959-960-961-962-963-964-965-966-967-968-969-970-971-972-973-974-975-976-977-978-979-980-981-982-983-984-985-986-987-988-989-990-991-992-993-994-995-996-997-998-999-1000

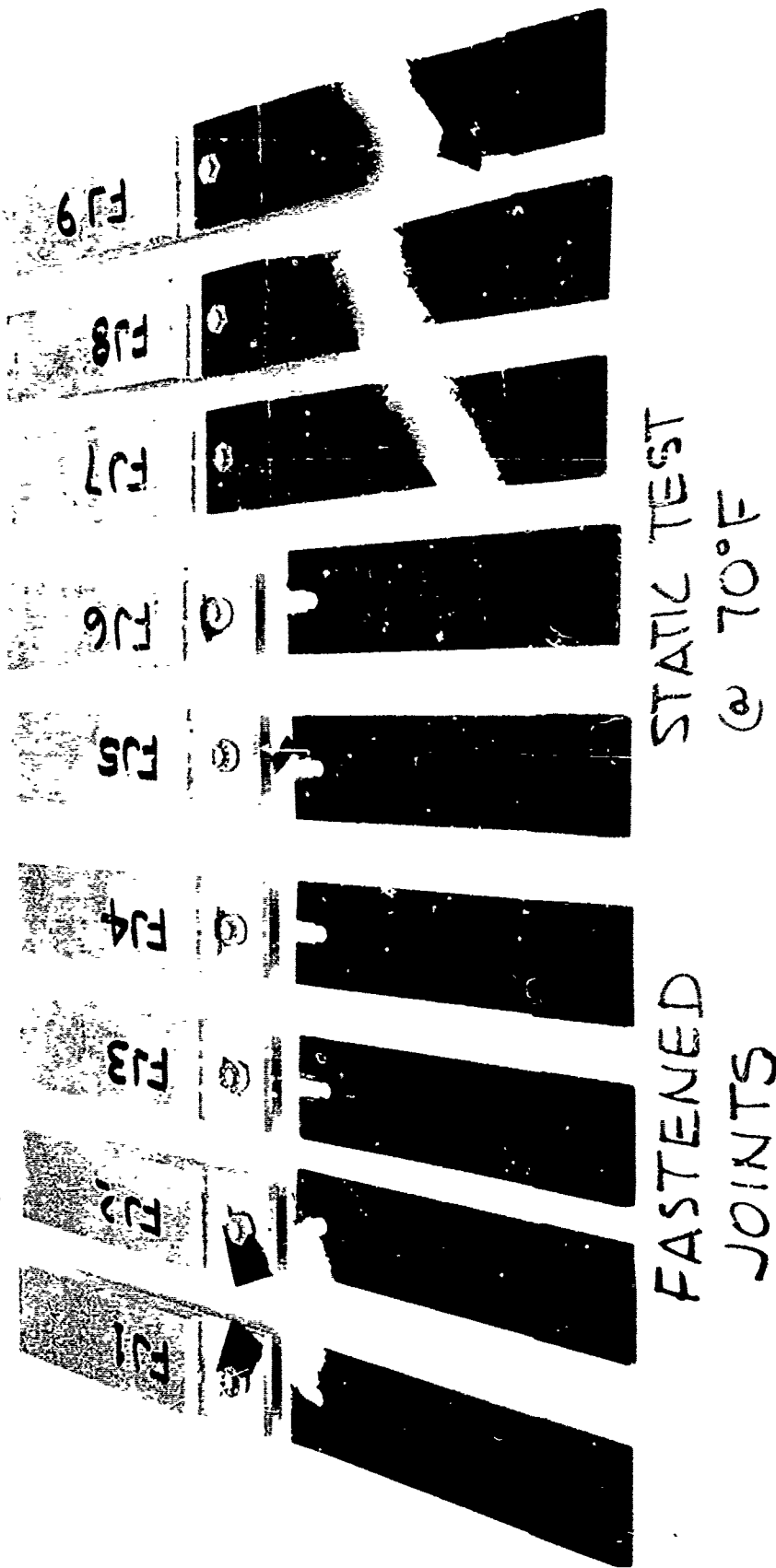


Figure 80. Failed Mechanical Attachment Specimens

The tests were performed at room temperature in a Sonntag SF-1 machine at a frequency of 30 Hz. The initial load on all the specimens was equal to or greater than the load expected under service conditions. All specimens were tested at these load levels to at least 2.5 million cycles and then the load was increased to higher levels to induce failure. The fatigue loads, number of cycles and types of failure for each specimen are shown in Table 30. A photo of the failed specimens is shown in Figure 81.

As noted in Table 30, all of the specimens sustained 2.5 million cycles at service load levels and failed at loads significantly higher. The results obtained from the mechanical attachment fatigue tests showed that this method of load transfer can be used successfully with the types of construction to be used in the elevator design.

6.3 SHEAR PANEL BUCKLING TESTS

Three graphite-polysulfone beams were fabricated and tested to obtain shear buckling and fatigue data. The design of the shear panels in the beams was representative of the spar webs in the elevator design. Each beam used a different stiffener concept. The results obtained from all the tests showed structural capabilities that were predictable and sufficient to meet elevator design requirements.

The three beams were approximately 13 in. high and 24 in. long. The beam chords consisted of two angles made of 4 plies of graphite fabric oriented at $\pm 45^\circ$ and 16 plies at $(0^\circ, 90^\circ)$. The webs were made of 4 plies of fabric oriented at $\pm 45^\circ$ and were divided into 3 bays by stiffeners. Each beam had a different stiffener design, one of which was a $(0^\circ, 90^\circ)$ ply tee stiffener, one a $(0^\circ, 90^\circ)$ angle stiffener and the third a $\pm 45^\circ$ ply angle stiffener. Figure 82 is a sketch describing the beam details.

Three shear buckling beams were fabricated. The beams were approximately 13 in. high and 24 in. long. The chords consist of two angles made of 4 plies of graphite fabric oriented at $\pm 45^\circ$ and 16 plies of fabric oriented at $(0^\circ, 90^\circ)$. The webs were made of 4 plies of fabric oriented at $\pm 45^\circ$ and are divided into 3 bays by web stiffeners.

Table 30. Mechanical Attachment Fatigue Data

SPECIMEN NO.	SPECIMEN CONFIGURATION	MAXIMUM LOAD (LBS)	MEAN LOAD + ALTERNATING (LBS)	NUMBER OF CYCLES	TYPE OF FAILURE
FJ10	4 Ply, $\pm 45^\circ$	240	126 ± 114	7,600,000	No failure
		480	252 ± 228	42,000	1 ▶
FJ11		360	189 ± 171	2,661,000	No failure
		480	252 ± 228	4,996,000	No failure
		540	284 ± 256	109,000	2 ▶
FJ12	4 Ply, $\pm 45^\circ$	420	220 ± 200	2,500,000	No failure
		480	252 ± 228	74,000	2 ▶
FJ13	4 Ply, $0-90^\circ$	240	126 ± 114	7,126,000	No failure
		480	252 ± 228	5,136,000	No failure
		540	284 ± 256	1,292,000	3 ▶
FJ14		360	189 ± 171	2,500,000	No failure
		540	284 ± 256	1,000	3 ▶
FJ15	4 Ply, $0-90^\circ$	420	220 ± 200	7,710,000	No failure
		540	284 ± 256	355,000	3 ▶
FJ16	4 Ply, $\pm 45^\circ$	240	126 ± 114	2,600,000	No failure
	4 Ply, $0-90^\circ$	540	284 ± 256	95,000	1 ▶
	Doubler				
FJ17		360	189 ± 171	2,500,000	No failure
		540	284 ± 256	10,000	1 ▶
FJ18	4 Ply, $\pm 45^\circ$	420	220 ± 200	10,300,000	No failure
	4 Ply, $0-90^\circ$	480	252 ± 228	4,700,000	No failure
	Doubler	540	284 ± 256	3,479,000	1 ▶

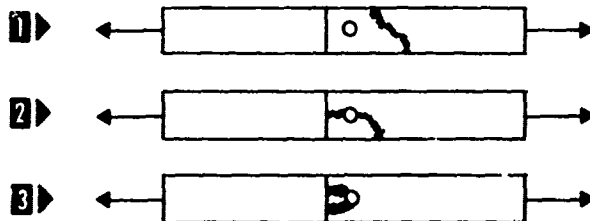




Figure 81. Mechanical Attachment Fatigue Specimen Failures

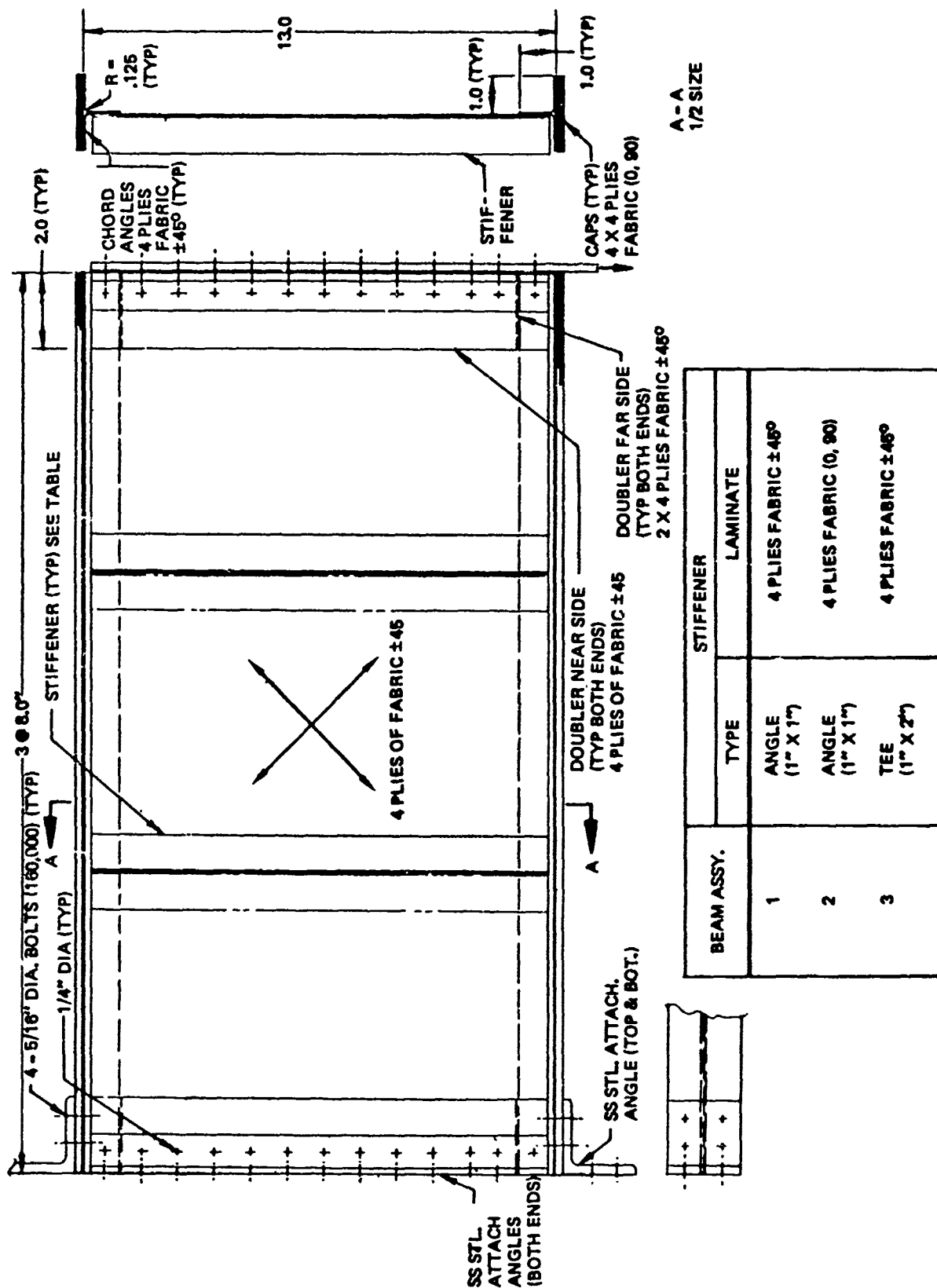


Figure 82. Shear Beam Element

The chord angle and cap details were assembled by fusion bonding. Figure 83 shows the chord details before and after assembly. Figure 84 shows all the beam element details. Figure 85 shows a completed beam element assembly.

Static tests were conducted on all three graphite-polysulfone shear beams to determine their buckling characteristics. Load introduction and reaction plates were bolted to the test beams as shown in Figure 86. This assembly was then installed in a test frame as shown in Figure 87. The base plate was bolted to the bottom of the fixture and the load jack was attached to the load introduction plate. The loads were applied in a horizontal plane.

The center panel of each beam was instrumented with two sets of back-to-back strain gages. They were also instrumented with three deflection indicators to obtain out-of-plane deflections. A fourth deflection indicator was used to obtain load jack deflections. Figure 88 shows the location of the above instrumentation.

A Moire' displacement study was also conducted on the center bay of the test panels during loading. The stiffener side of the center bay was sprayed with a coating of flat white paint to obtain greater shadow contrast. A high frequency Moire' grid was mounted parallel to the webs and displaced from this surface 1/8 inch. The grid was supported from the panel at three points to permit it to follow the panel motion without imposing bending. The grid was illuminated with a Xenon lamp. The test setup is shown schematically in Figure 89 and a photograph of the actual setup is shown in Figure 87.

The Xenon light was directed to the panel surfaces by two mirrors which were adjusted to obtain an angle of incidence of 60° . A 100 LPI linear amplitude grid provided a sensitivity of 0.0058 in. out-of-plane displacement per fringe order. The fringe patterns produced at the load increments were photographed using a Hasselblad 500 EL camera and Kodak Tri-X film.

Each beam was loaded in 10 percent increments to an ultimate design load of 4,180 lb. The panels were unloaded and held at load increments at 60%, 40%, and zero. Moire' fringe patterns as well as strain gage and lateral deflection readings were recorded at each load increment. Figures 90 through 92 show some of the fringe patterns recorded on the panel with the tee stiffeners. Figure 90 is a typical pattern of a center panel with zero load. Figure 91



Figure 83. Chord Details- Beam Element



Figure 84. Beam Element Details

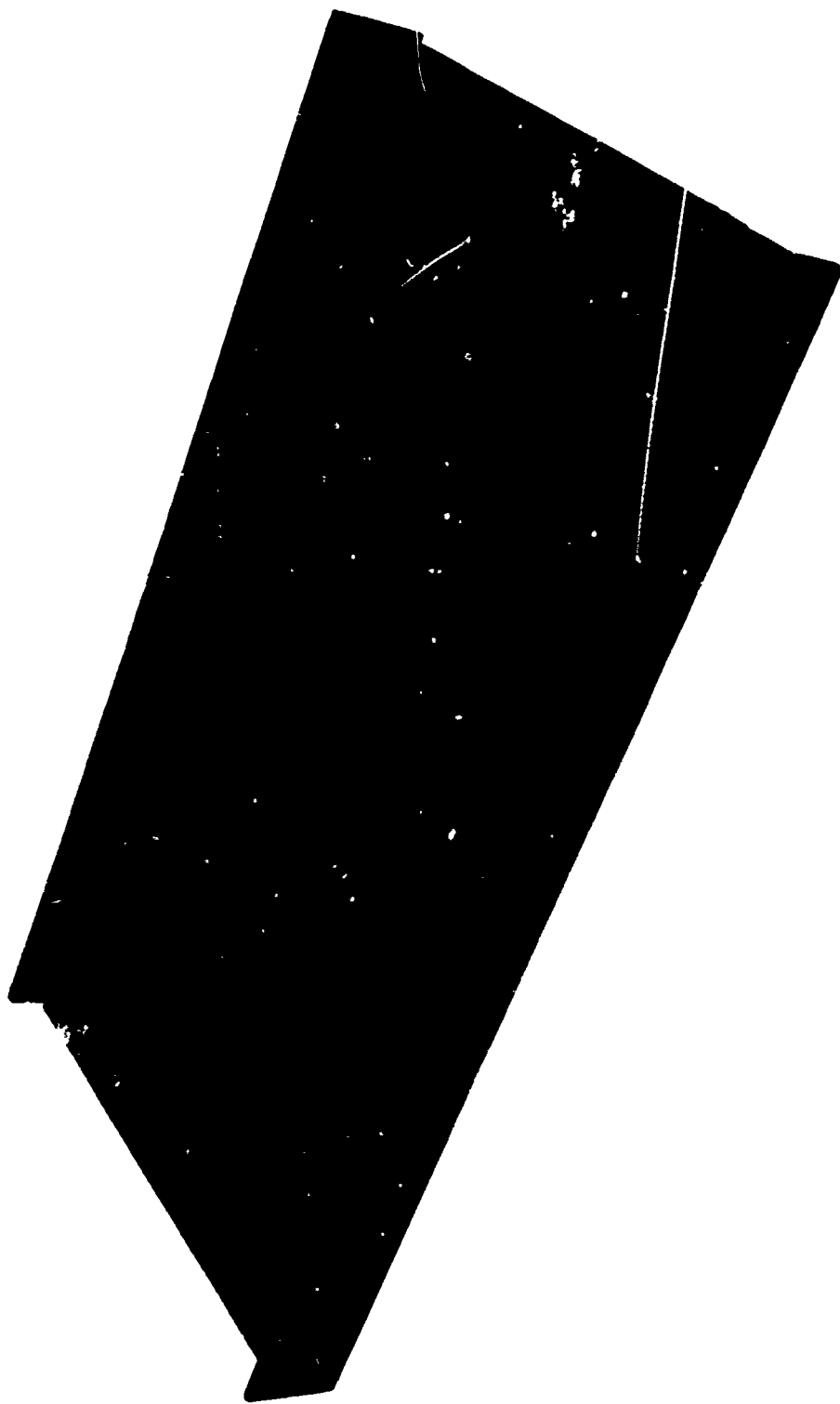


Figure 85. Beam Element Assembly

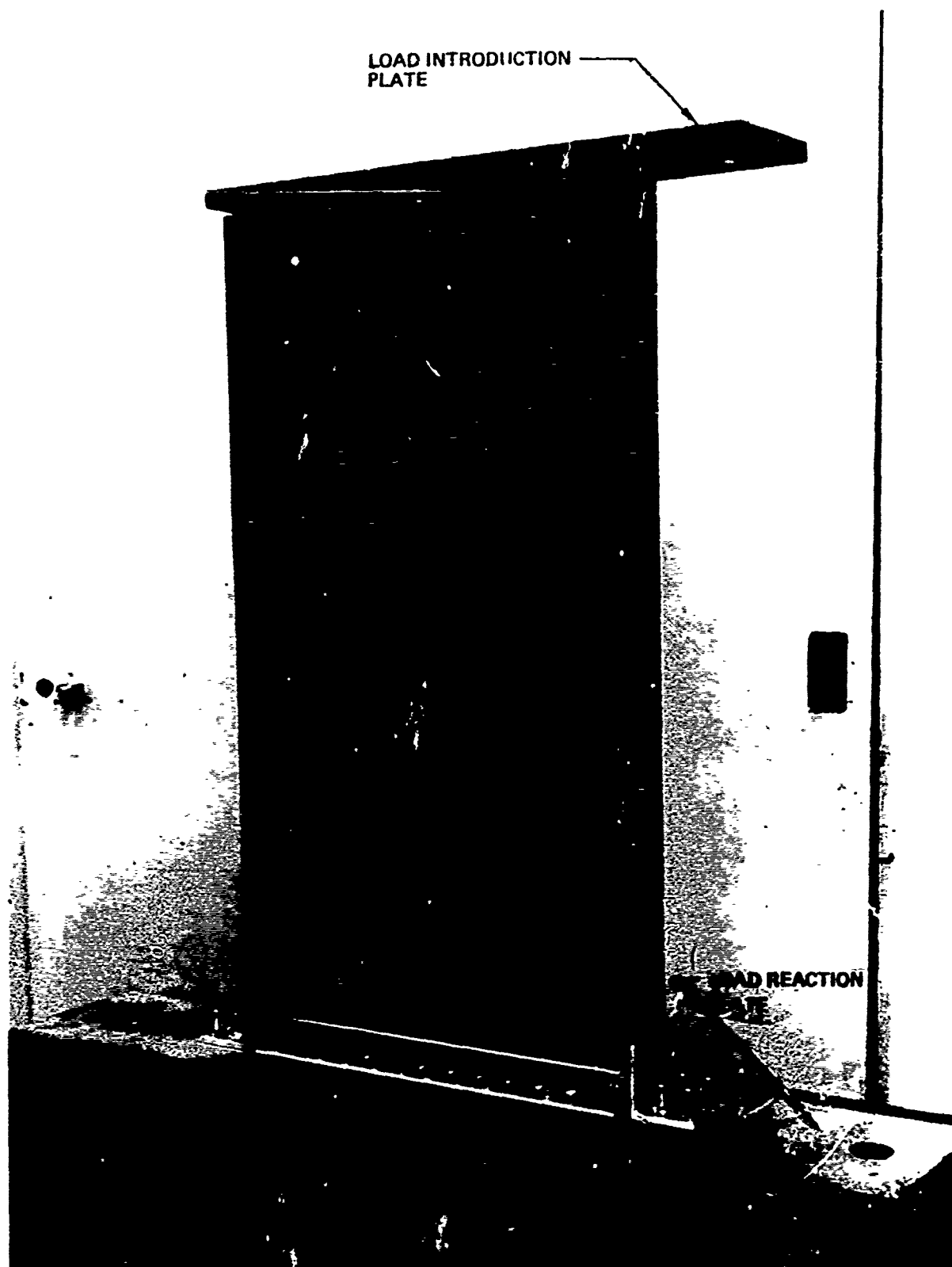


Figure 86. Beam Element—Test Setup

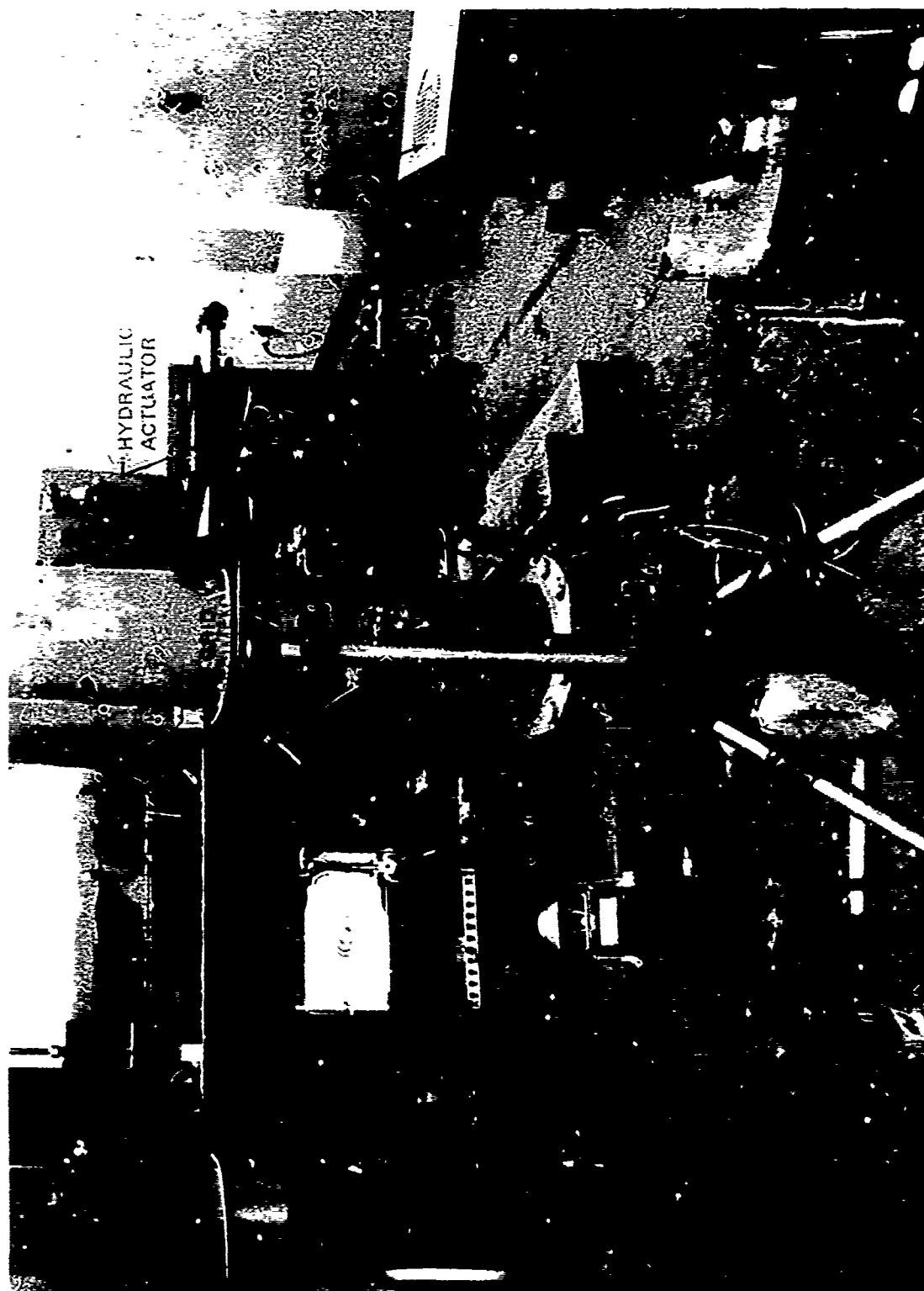


Figure 87. Shear Beam Overall Test Set-Up

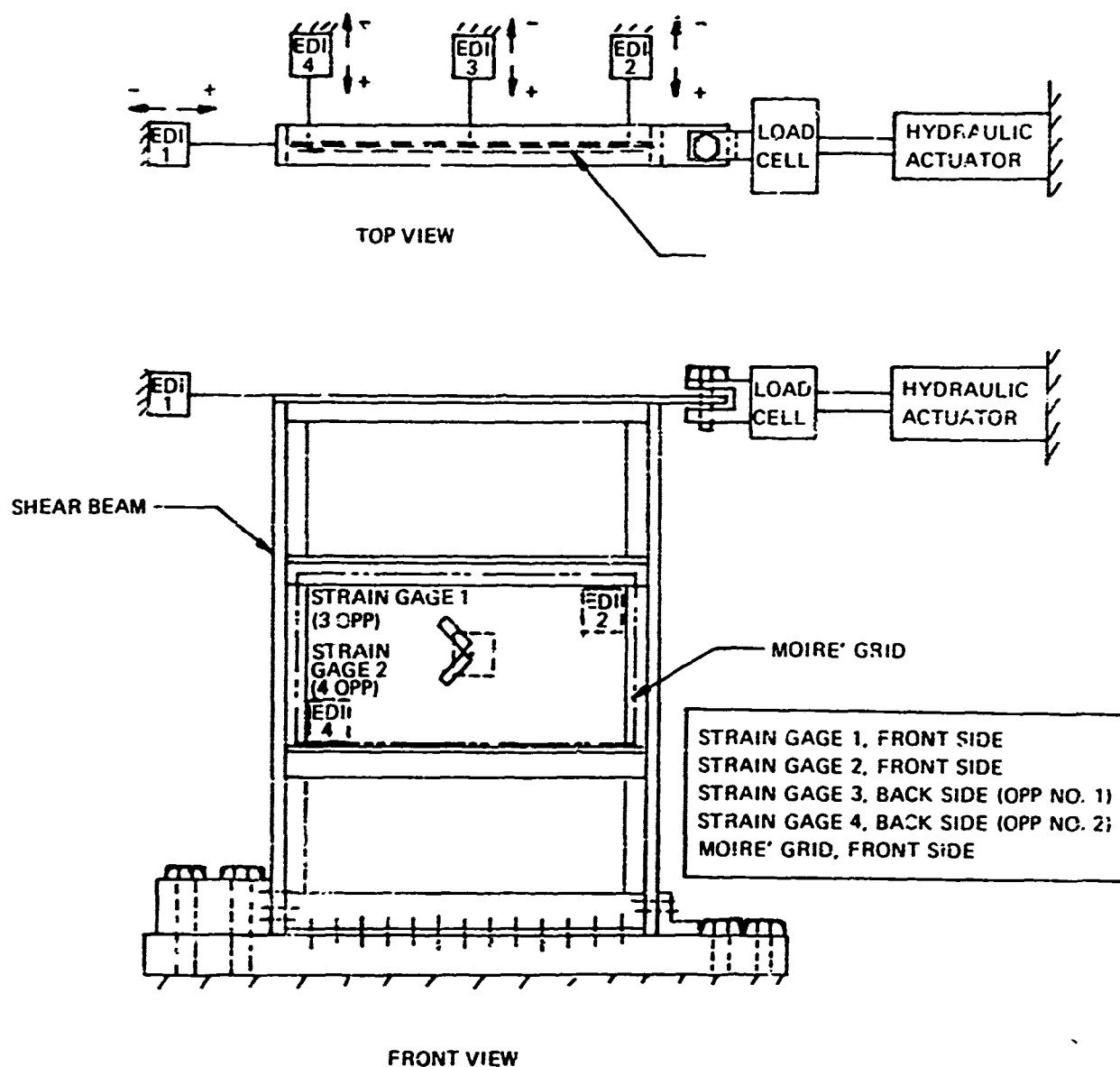


Figure 88. Shear Panel Instrumentation

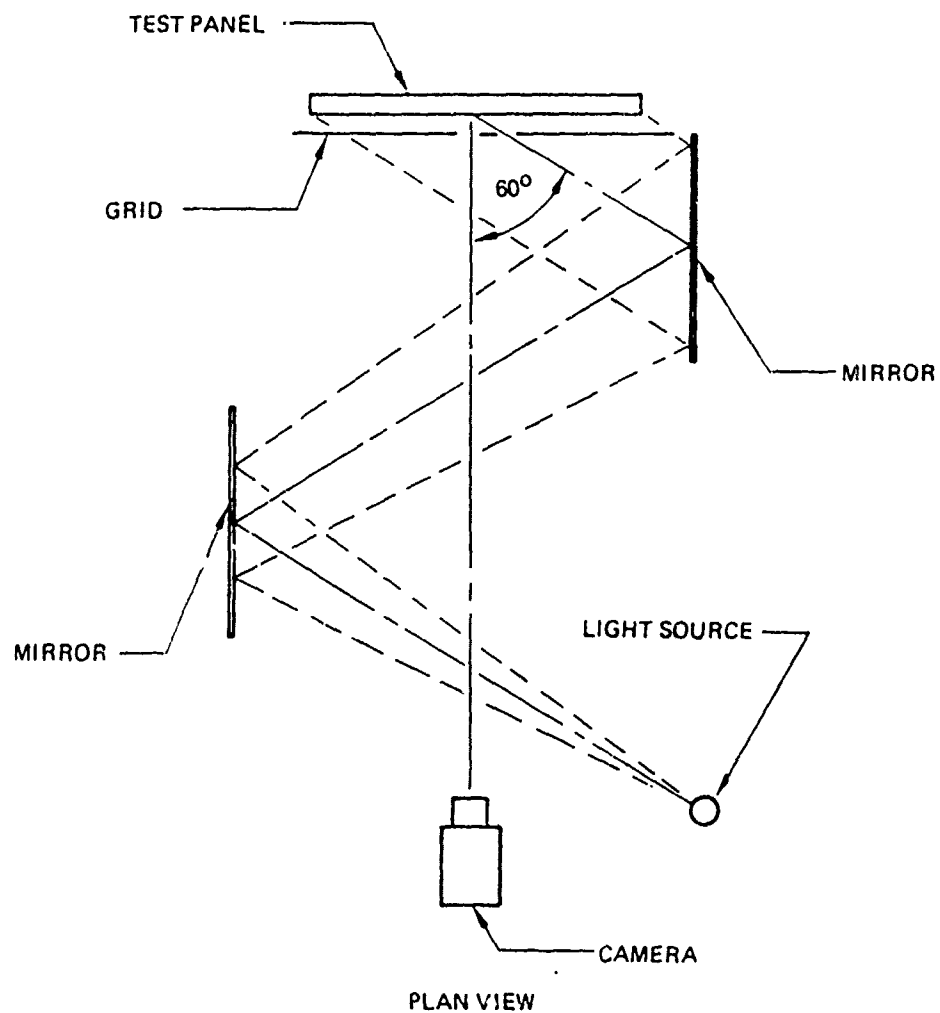


Figure 89. Shear Beam Test Schematic - Moiré' Displacement

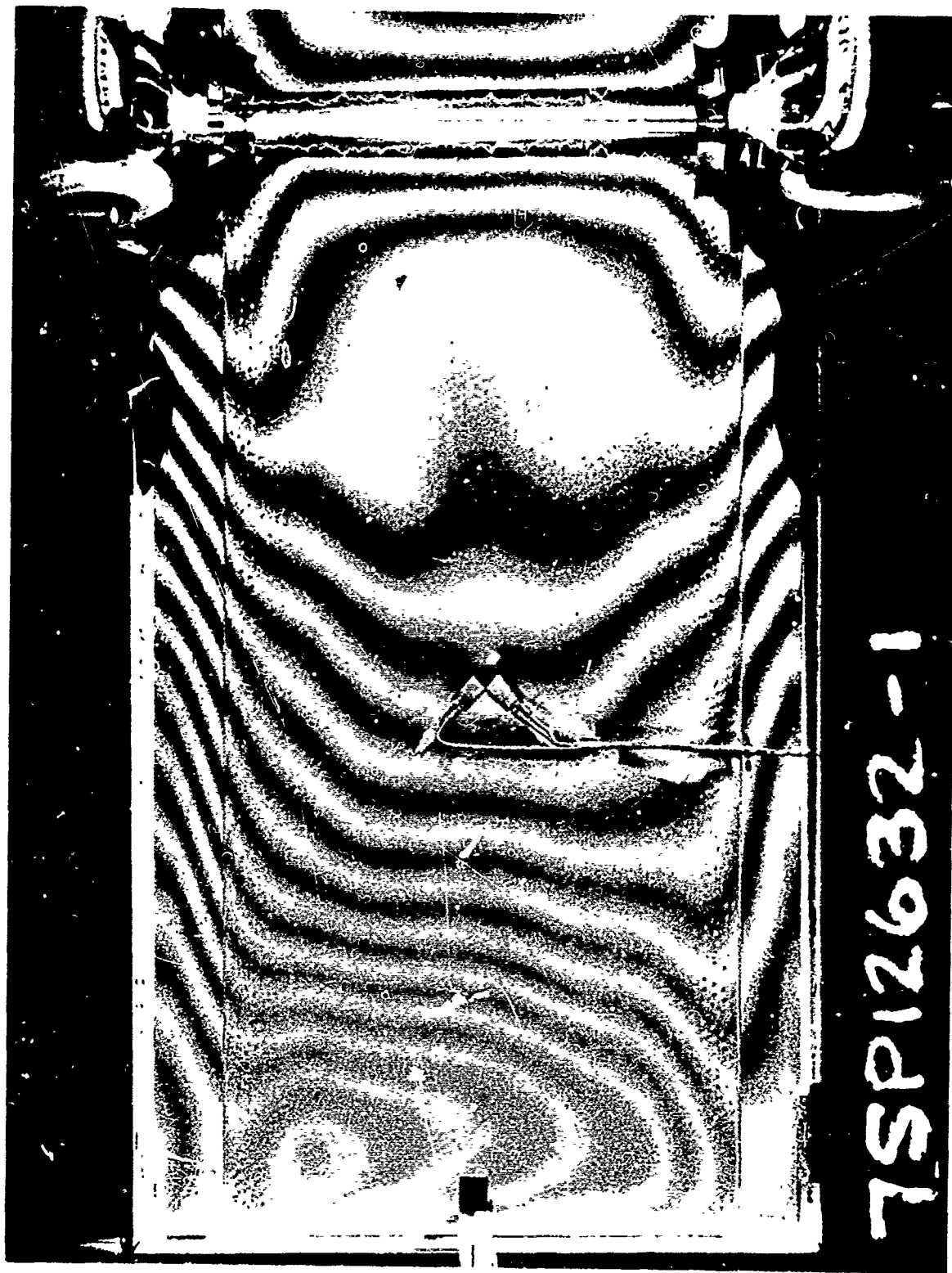


Figure 90. Shear Panel Moiré Fringe Zero Load

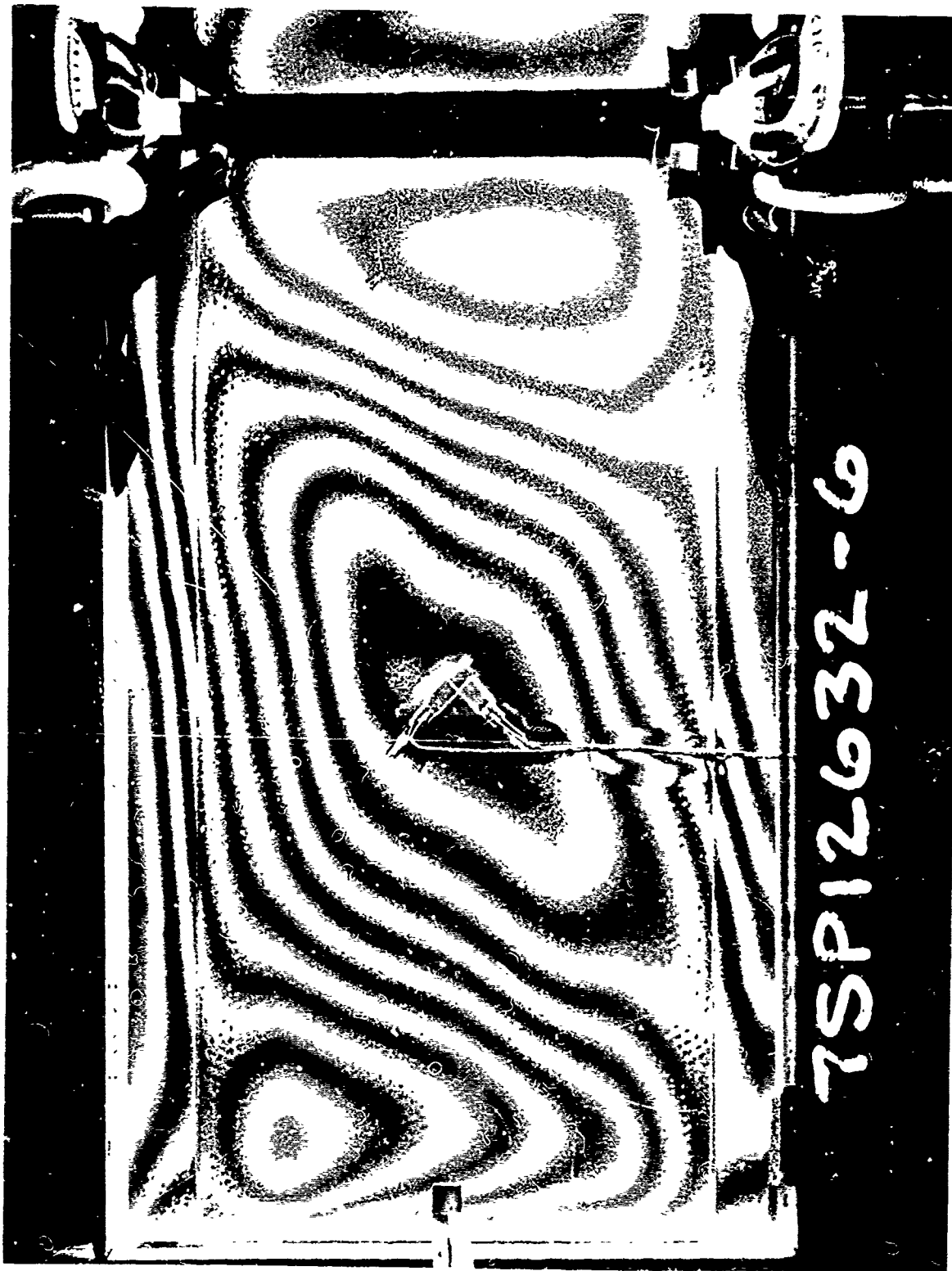


Figure 91. Shear Panel Moiré Fringe 50% Ultimate Load

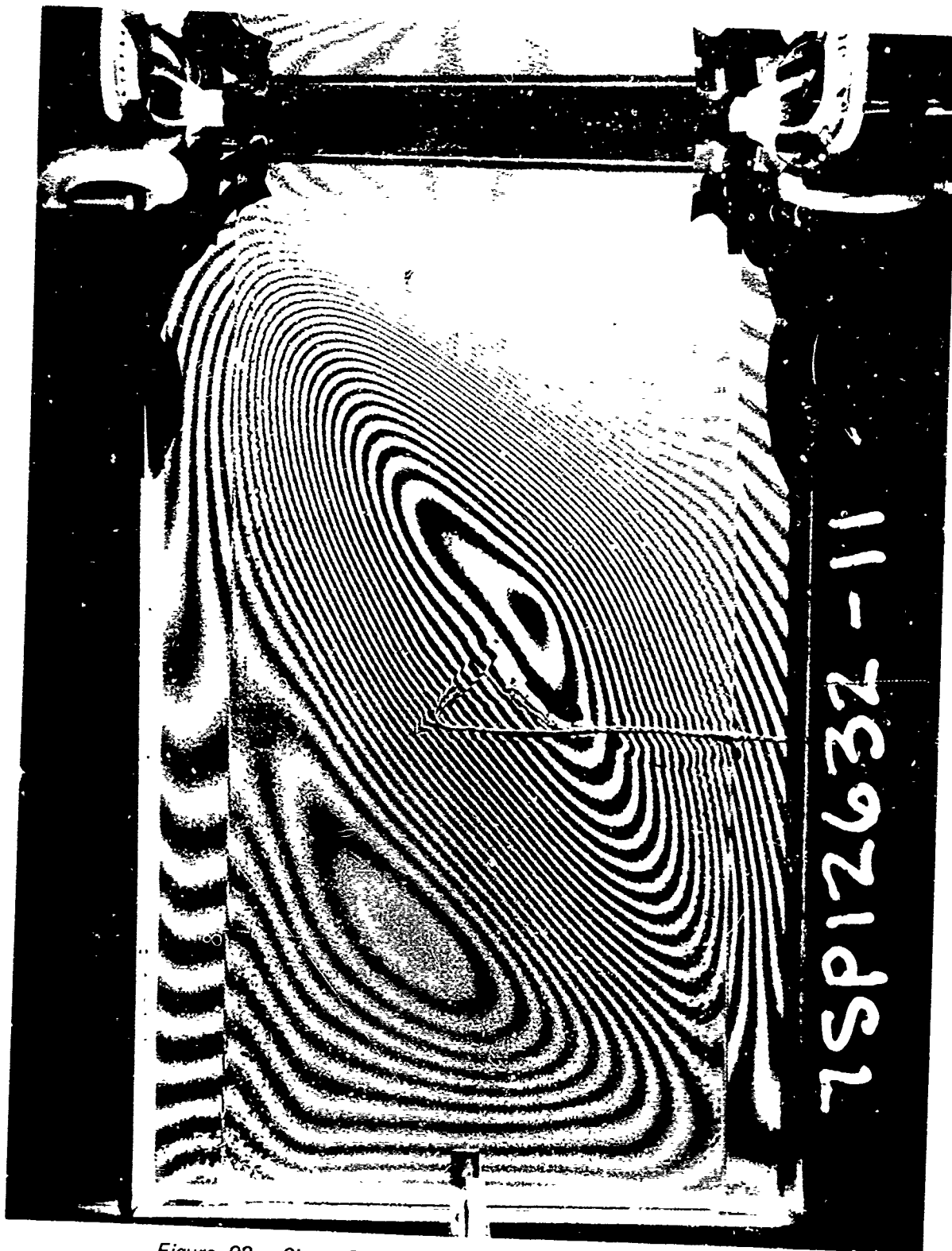


Figure 92. Shear Panel Moiré Fringe 100% Ultimate Load

is a photograph of a typical pattern at 50% load and Figure 92 is a typical pattern at 100% load. The lateral displacement profiles were developed for each of the panels along a center panel diagonal using the Moire' fringe data. Figure 93 shows the location of the diagonal on which the lateral displacement was determined. Figure 94 shows a typical plot of the lateral displacement developed from the Moire' fringe data.

The out-of-plane deflections of the center panels in the shear beams were also obtained by electronic deflection indicators (Figure 88). A typical plot of this data obtained from the beam with the $\pm 45^\circ$ laminate tee stiffeners is shown in Figure 95. A buckling analysis of the beam shear web was also performed using the STAGS-C computer program. Figure 95 shows a comparison of the analytic prediction and the test data and demonstrates the excellent capability for predicting structural response of graphite thermoplastic structures.

The shear beam with the $\pm 45^\circ$ angle stiffeners was fatigue tested to demonstrate design safe life compliance. Figure 96 shows the load spectrum required to demonstrate a safe life of four life times. At the lower load level (118 lb/in) the center panel was at buckling onset as indicated by Figure 91 showing the Moire' fringe pattern at the approximately same load level. The beam was cycled at both required load levels for 10^6 cycles which was approximately 16 times greater than required to demonstrate safe life requirements. The center panel of the beam visually buckled at every cycle. The beam was then cycled at twice the design loads for 2×10^6 cycles without failure. A summary of this fatigue test is shown in Figure 96.

6.4 COMPRESSION PANEL BUCKLING TESTS

Three graphite-polysulfone compression panels were fabricated and tested to obtain compression buckling and fatigue data. Their details were representative of the YC-14 elevator cover panels. The data obtained was used to finalize the graphite-polysulfone elevator design and to demonstrate design compliance.

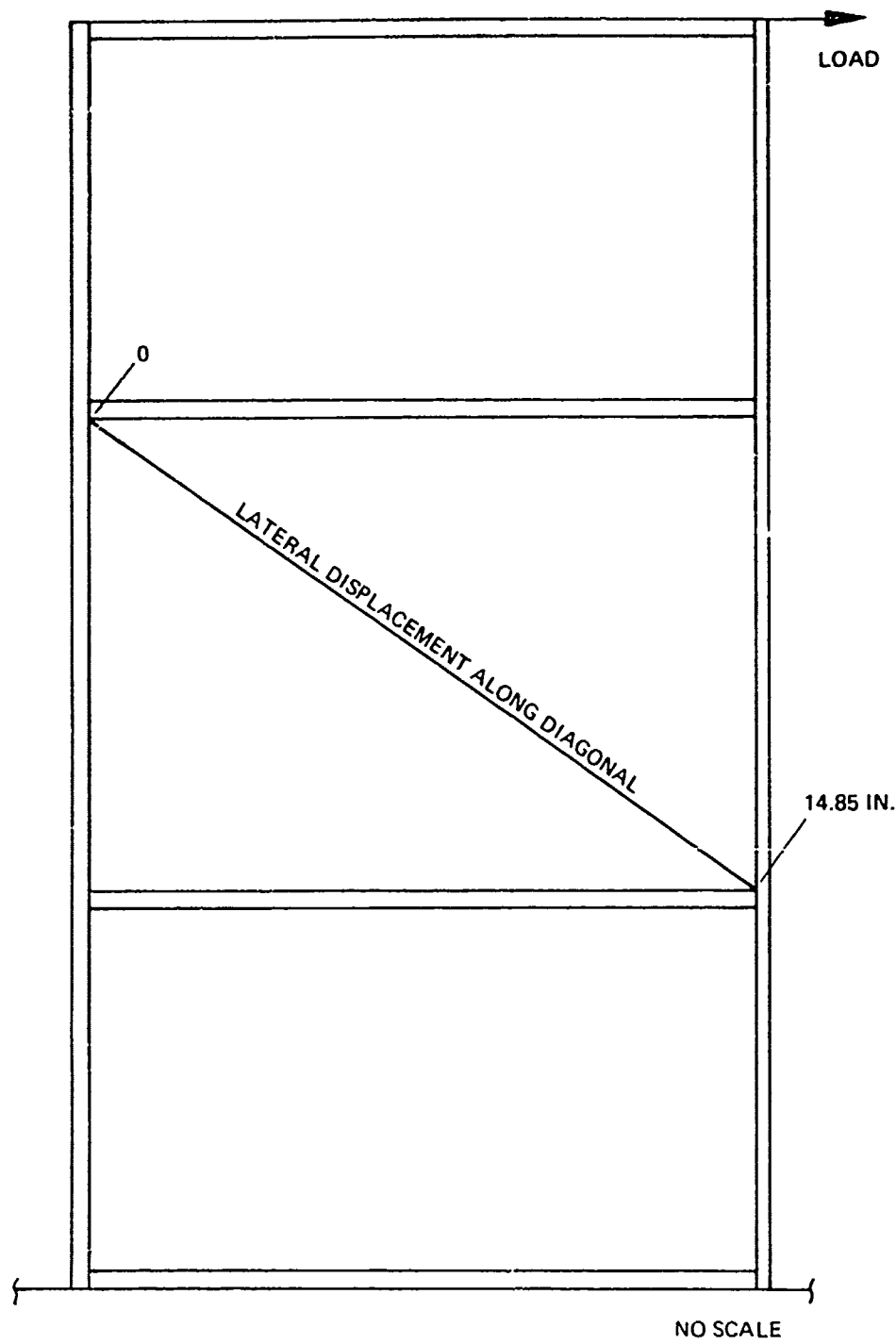


Figure 93. Shear Panel Schematic - Lateral Displacement Line

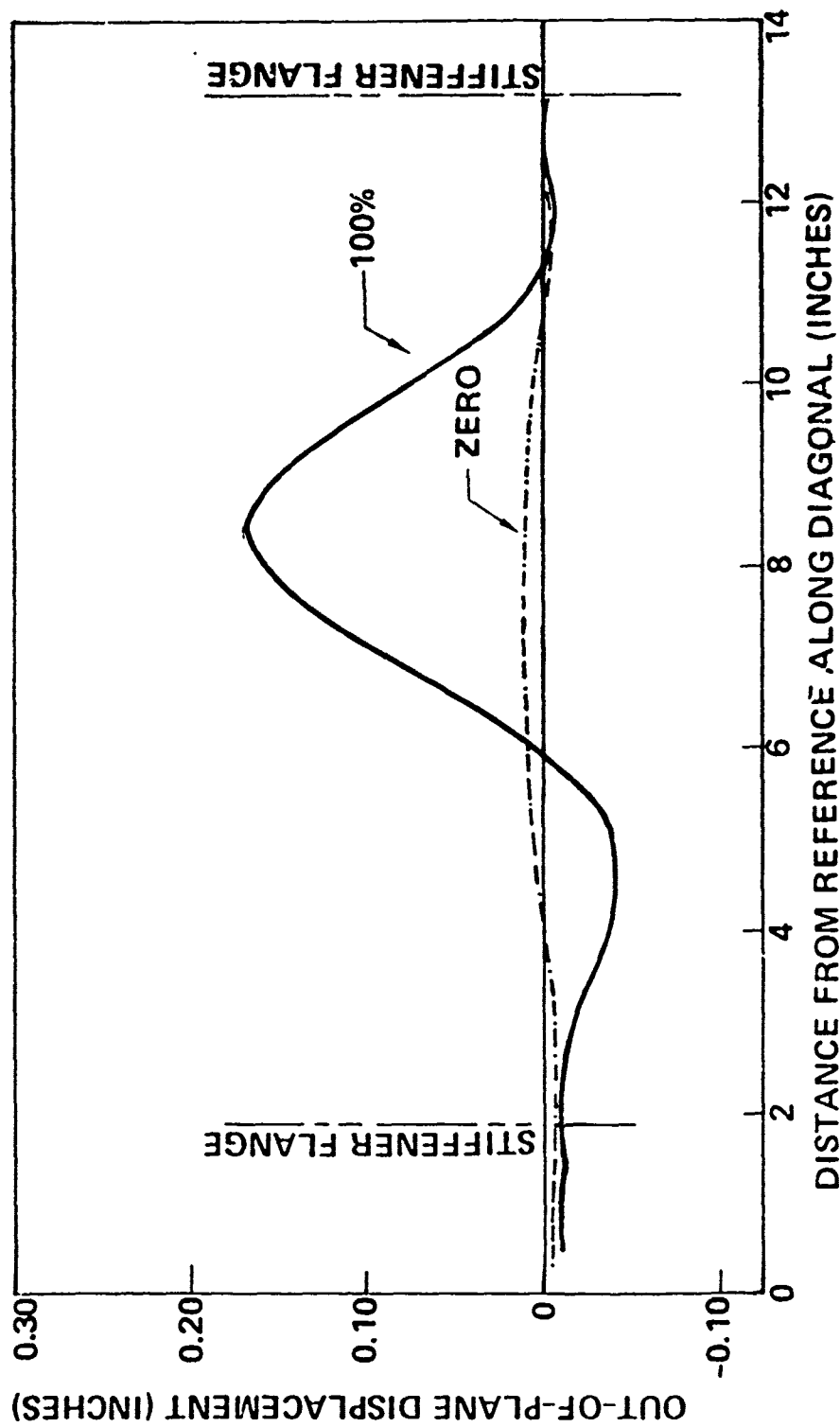


Figure 94. "T" Stiffener Panel Displacement Profile Zero and 100% Shear Load

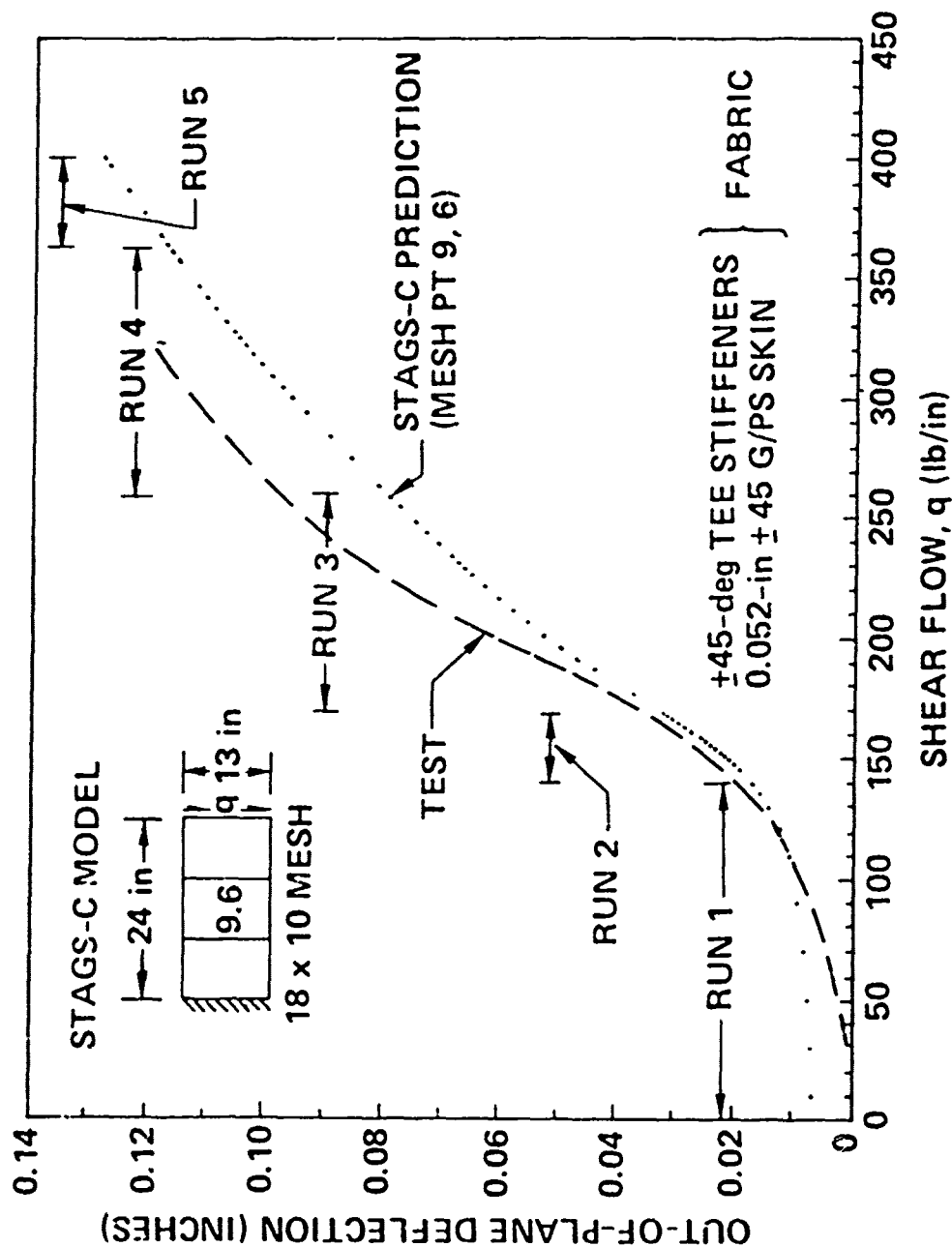


Figure 95. Shear Buckling - Theory vs Test

REQUIRED

75 CYCLES AT 160 lb/in (STOL)
125 CYCLES AT 118 lb/in (CTOL)

X600 = FOUR LIFE TIMES

TEST

STATIC TEST
320 lb/in

118 lb/in FOR 10^6 CYCLES
160 lb/in FOR 10^6 CYCLES

236 lb/in FOR 10^6 CYCLES
320 lb/in FOR 10^6 CYCLES

Note: Onset buckling = 120 lb/in

Figure 96. Shear Buckling Fatigue Test

The three graphite-polysulfone compression panels tested each incorporated a different stiffener design. One consisted of $\pm 45^\circ$ laminate tee, one a $\pm 45^\circ$ fabric laminate angle and one a $(0^\circ, 90^\circ)$ fabric laminate angle. The compression panels were 13 in. wide and 24 in. long. Stiffeners were incorporated to stabilize the web. The stiffeners were 12 in. long thereby allowing room for the edge support along the sides of the panels. Glass epoxy pads were bonded at the ends of the panels to prevent brooming during loading. Figure 97 shows the compression panel design details.

Static load tests were conducted on all three graphite-polysulfone compression panels in a ten-kip capacity Ametek test machine. Steel channel edge constraints were used to stabilize the edges of the panels.

The center bay of the panels were instrumented with back-to-back strain gages to obtain panel buckling data and with deflection indicators to obtain out-of-plane deflections. Figure 98 shows a schematic of the compression panel test setup and the location of the panel instrumentation. In addition to the above instrumentation, Moire' fringe data was obtained to develop out-of-plane deflection data. The center bays of the compression panels were sprayed with a flat white paint coating to obtain a distinctive shadow image. A high frequency Moire' grid was mounted parallel to the webs by a three-point support. The grid was illuminated with an Xenon lamp. The light was directed to the panel surfaces by mirrors which were adjusted to obtain an incidence angle of 60° . The 100 LPI linear amplitude grid provided a sensitivity of 0.0058 in. of out-of-plane displacement per fringe with a Hasselblad 500 EL camera and Kodak Tri-X film. A photograph of the overall test setup is shown in Figure 99. Figure 100 shows a panel from the back side. In this photograph the steel channel edge constraints can be seen bolted in place and also the deflection indicators.

Each compression panel was loaded in 10 percent increments to an ultimate design load of 3,380 lb. Load, strain and deflection data was recorded at each load increment. Photos of the Moire' fringe patterns were also taken at each load increment. The three panels were loaded to ultimate load without difficulty. Onset buckling occurred at a very low load level (16 percent ultimate) as predicted by the panel analysis. A typical Moire' fringe pattern at 100 percent of ultimate load is shown in Figure 101. A typical lateral deflection plot of the center bay is shown in Figure 102.

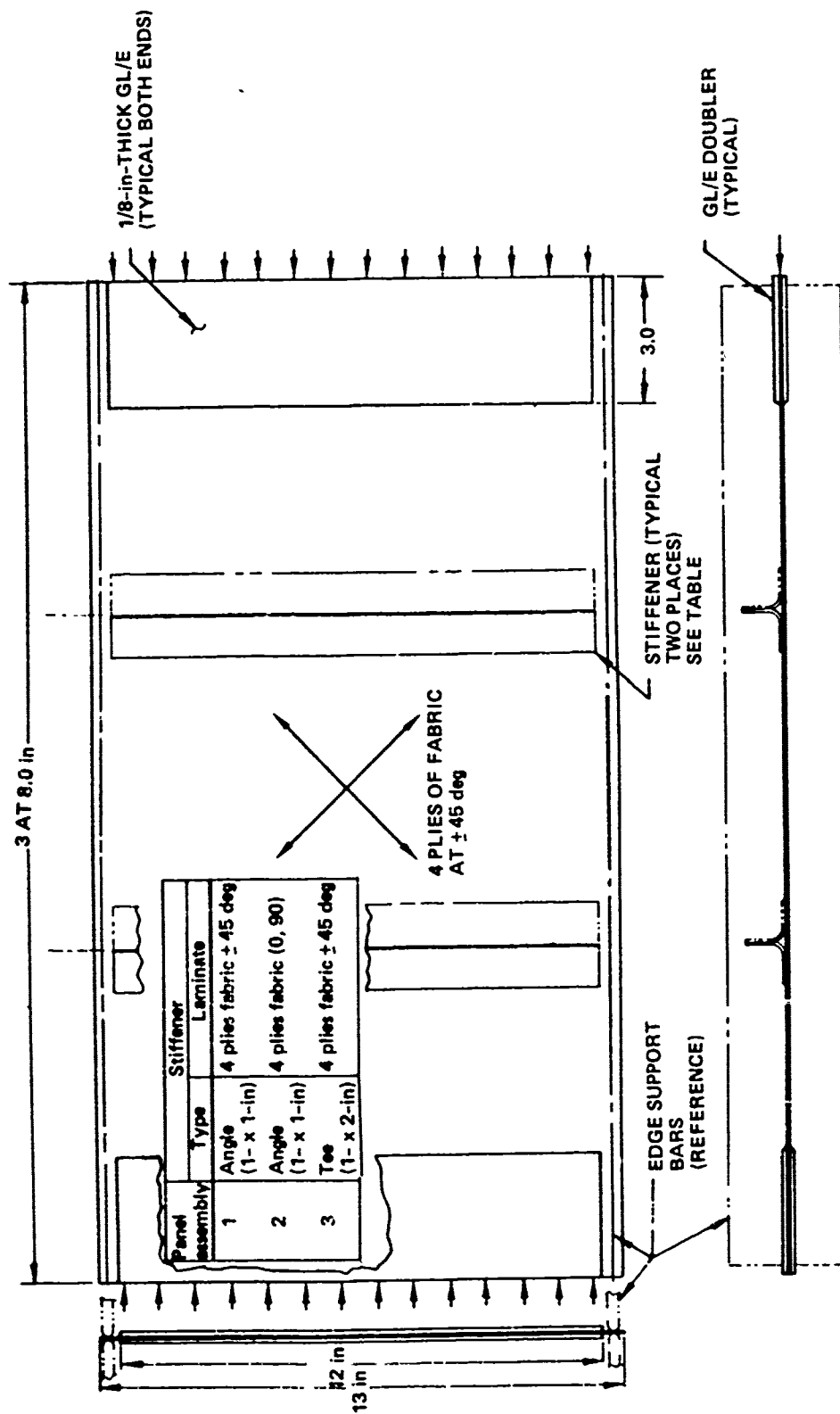


Figure 97. Compression Buckling - Panel Element

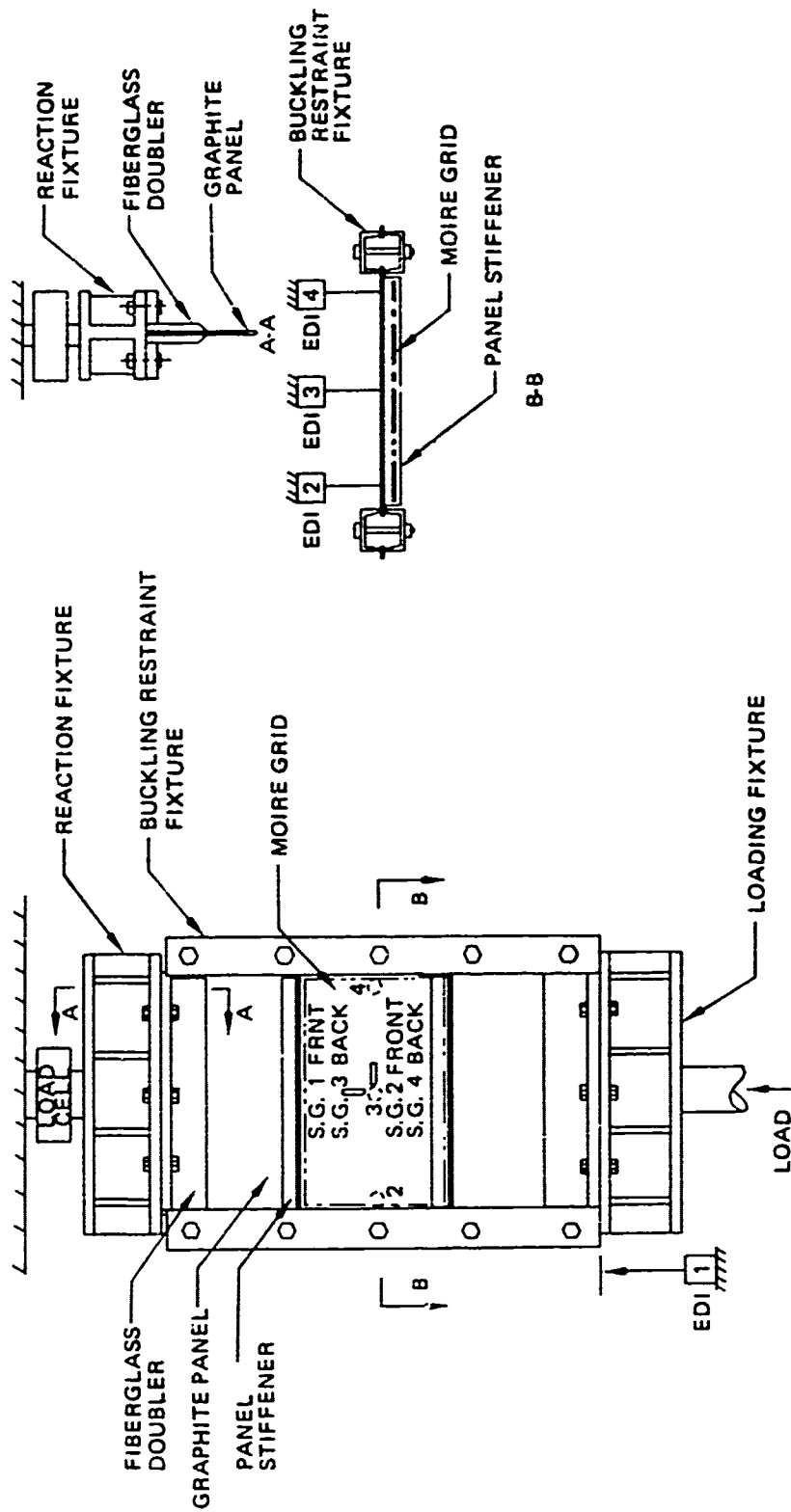


Figure 98. Compression Panel Instrumentation

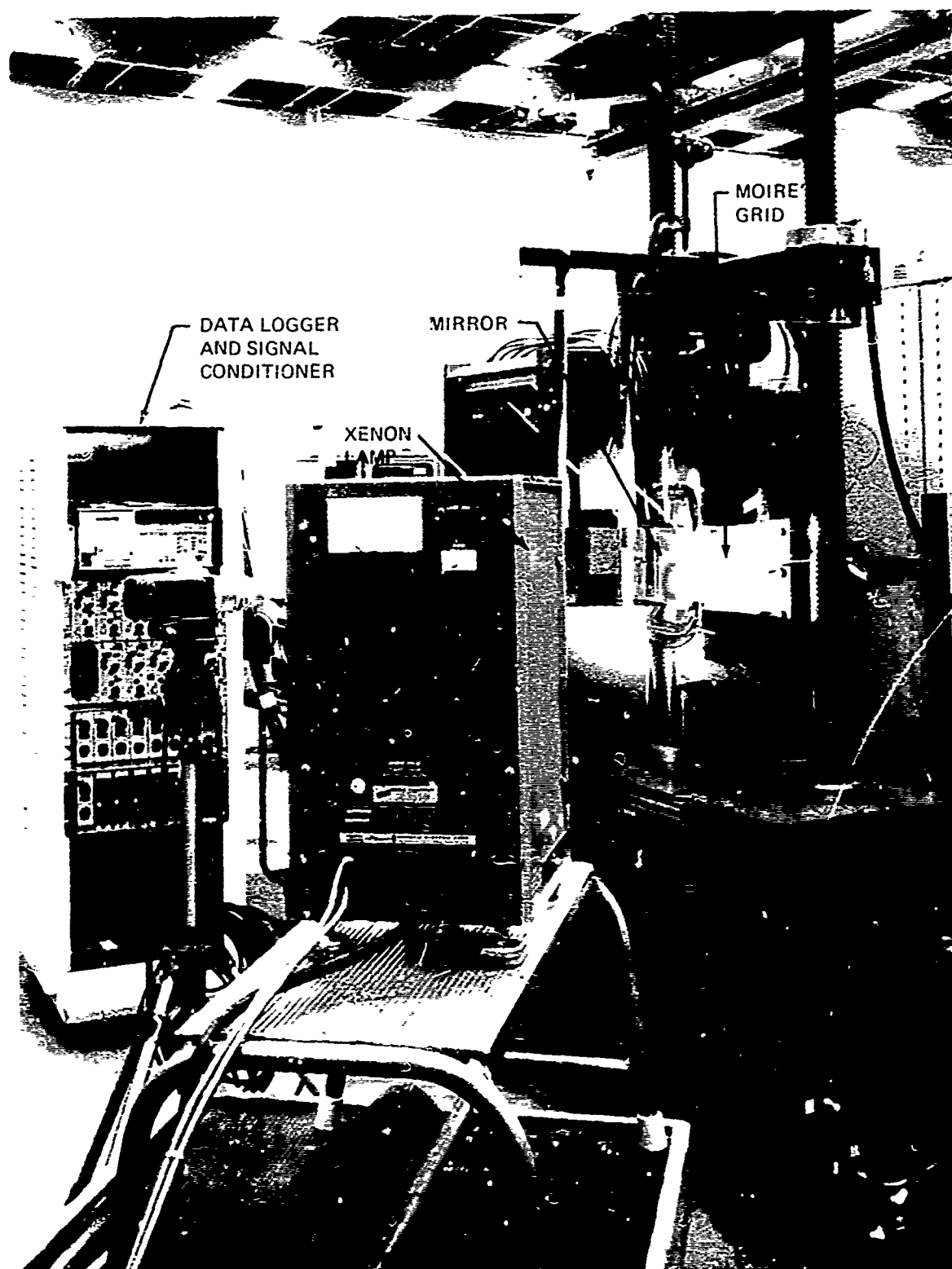


Figure 99. Compression Panel Test Set-Up

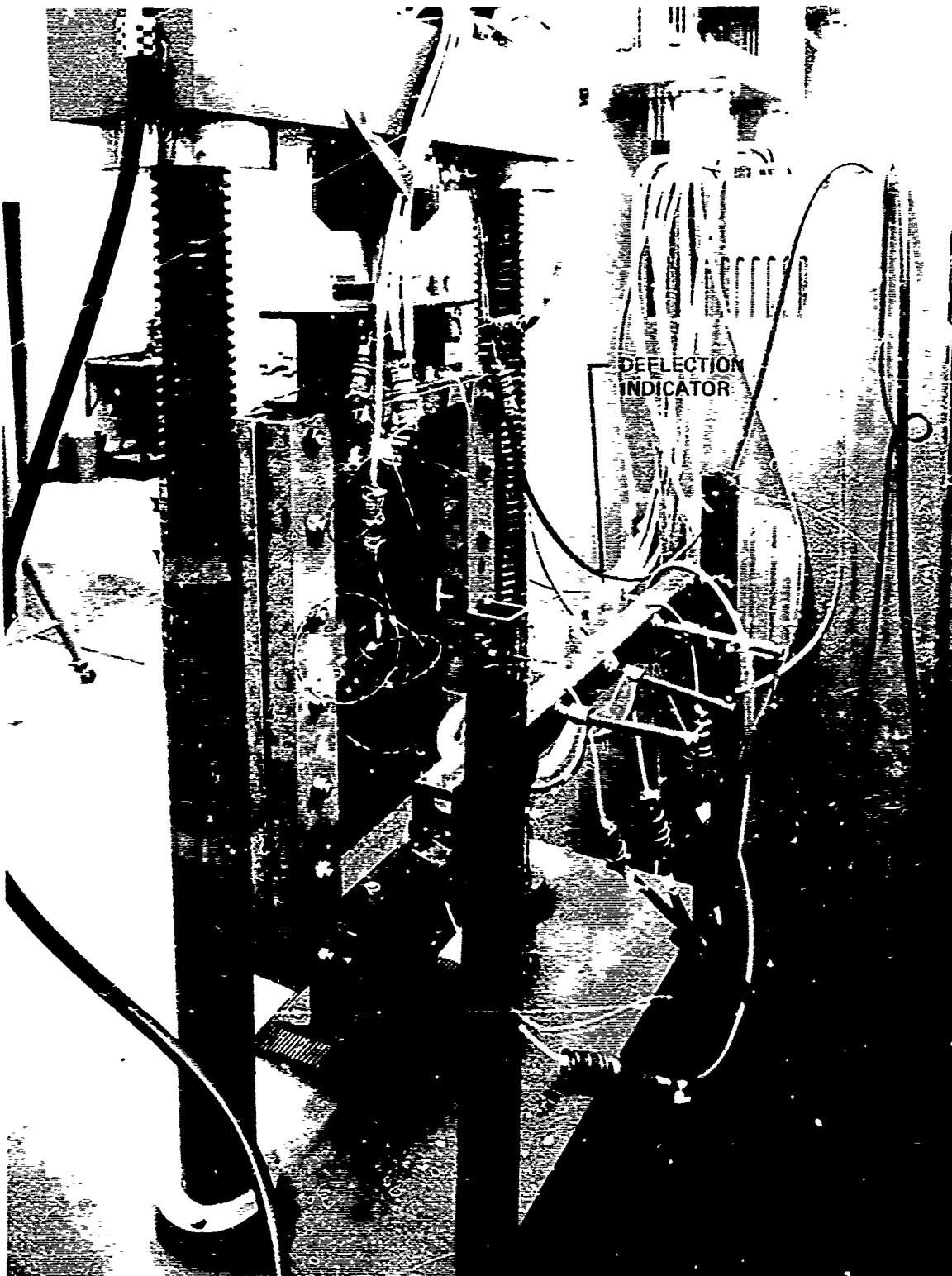


Figure 100. Compression Panel Test—Back Side



Figure 101. Compression Panel Moiré Fringe—100% Ultimate Load

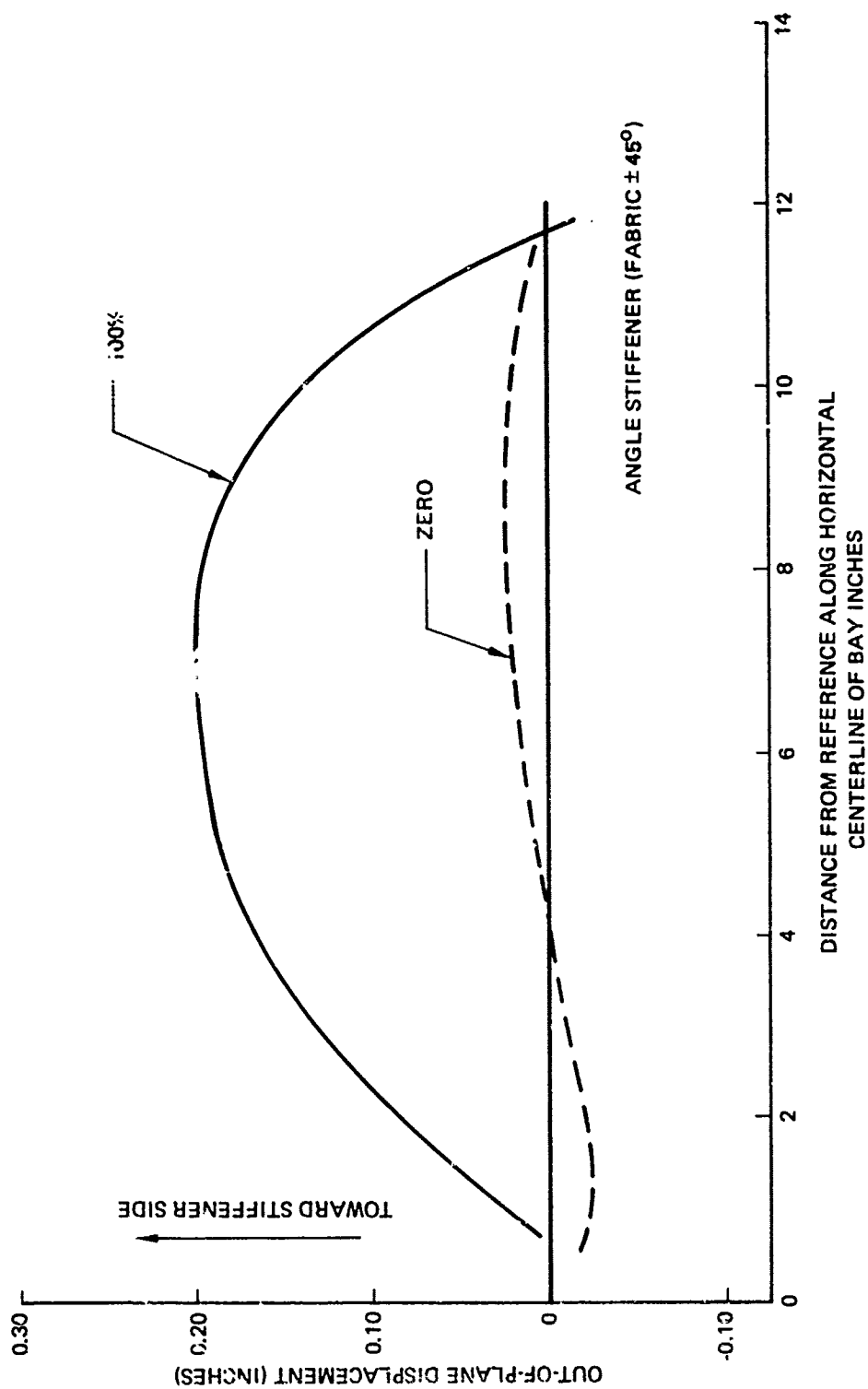


Figure 102. Compression Panel Lateral Displacement Profile - Zero and 100% Ultimate Load

The panel with the $\pm 45^\circ$ fabric laminate stiffeners was fatigue tested to demonstrate safe life compliance of the graphite-polysulfone elevator design. Figure 103 shows the load spectrum required to demonstrate a safe life of four life times. At the lower fatigue load level (40 percent of the ultimate) the center bay of the panel was well beyond on-set buckling. The panel therefore buckled during each of the fatigue cycles. It was successfully cycled for one million cycles at each of the load levels specified in Figure 103 which was several factors greater than required to demonstrate safe life compliance.

6.5 FRACTURE PANEL TESTS

Three slotted panels were fabricated and tested to obtain fracture data. Two of the panels incorporated four plies of $\pm 45^\circ$ fabric and the third, four plies of $(0^\circ, 90^\circ)$ fabric. The panels were 6 in. wide and 16 in. long. The panels incorporated slots that consisted of a 1/2 in. diameter hole with saw cut extensions. The distance between the ends of the saw cuts was 1 in. The slotted panel details are shown in Figure 104.

The panels were tested in tension. The panel with the $(0^\circ, 90^\circ)$ fabric laminate failed at the same gross stress level attained with the control specimen incorporating a 1 in. diameter hole (section 3). The two panels with the $\pm 45^\circ$ laminates failed at gross stress levels of 15,628 psi and 17,155 psi. A summary of the fracture panel test data is shown in Table 31. A photo of the failed panels is shown in Figure 105.

The data from the panels with the $\pm 45^\circ$ laminates is shown plotted with equivalent graphite-epoxy panel data in Figure 106. As shown, the residual strength of the damaged graphite-polysulfone fabric panels are equivalent to the graphite-epoxy panels and well above the limit strain used in design.

6.6 LOAD INTRODUCTION TESTS

A load introduction test element was designed, fabricated, and tested. Its configuration was representative of load introduced by a fitting in the AF RTP-YC-14 elevator box design. It incorporated front and rear spars which

75 CYCLES @ 53.3% PULT

125 CYCLES @ 40% PULT

x 600 = FOUR LIFETIMES

PULT = 260 LB/IN

NOTE: ONSET BUCKLING = 42 LB/IN

Figure 103. Compression Panel Fatigue

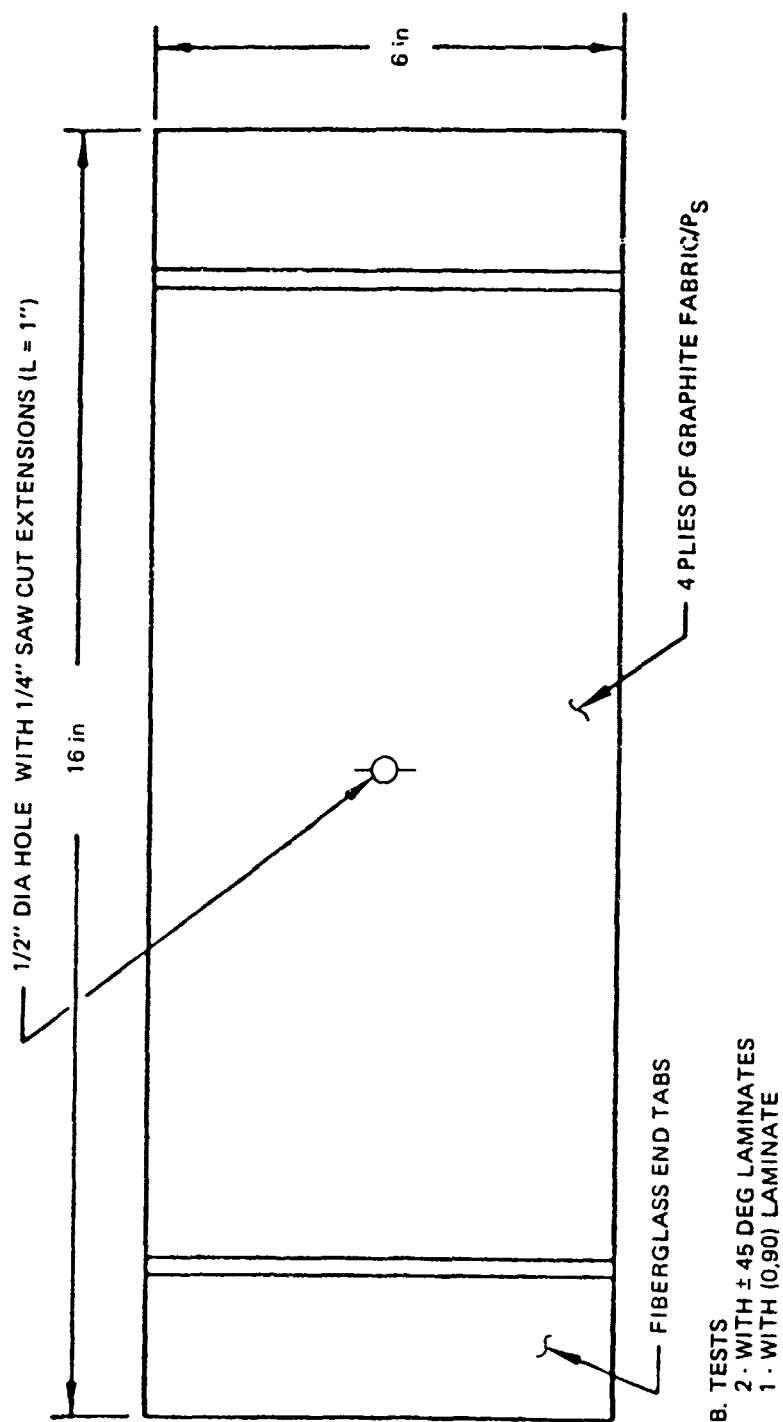


Figure 104. Slotted Panel Test Specimen

Table 31. Fracture Panel Tests

Panel	Fabric laminate (deg)	Failure load (lb)	Gross stress (psi)
No. 1	(0-90)	8,140	24,847
No. 2	±45	5,120	15,628
No. 3	±45	5,620	17,155

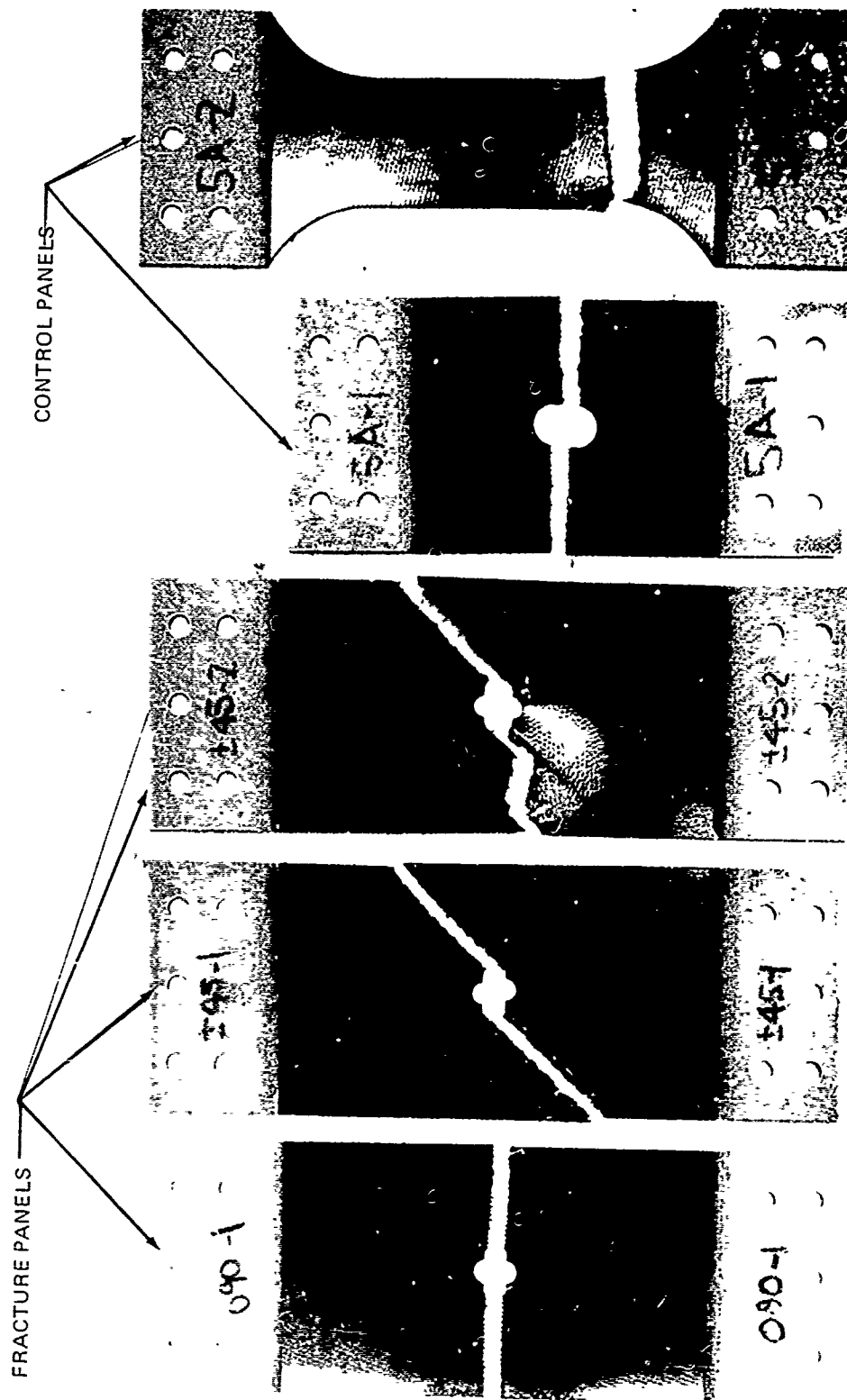


Figure 105. Fracture Panel Failure and Control Panels

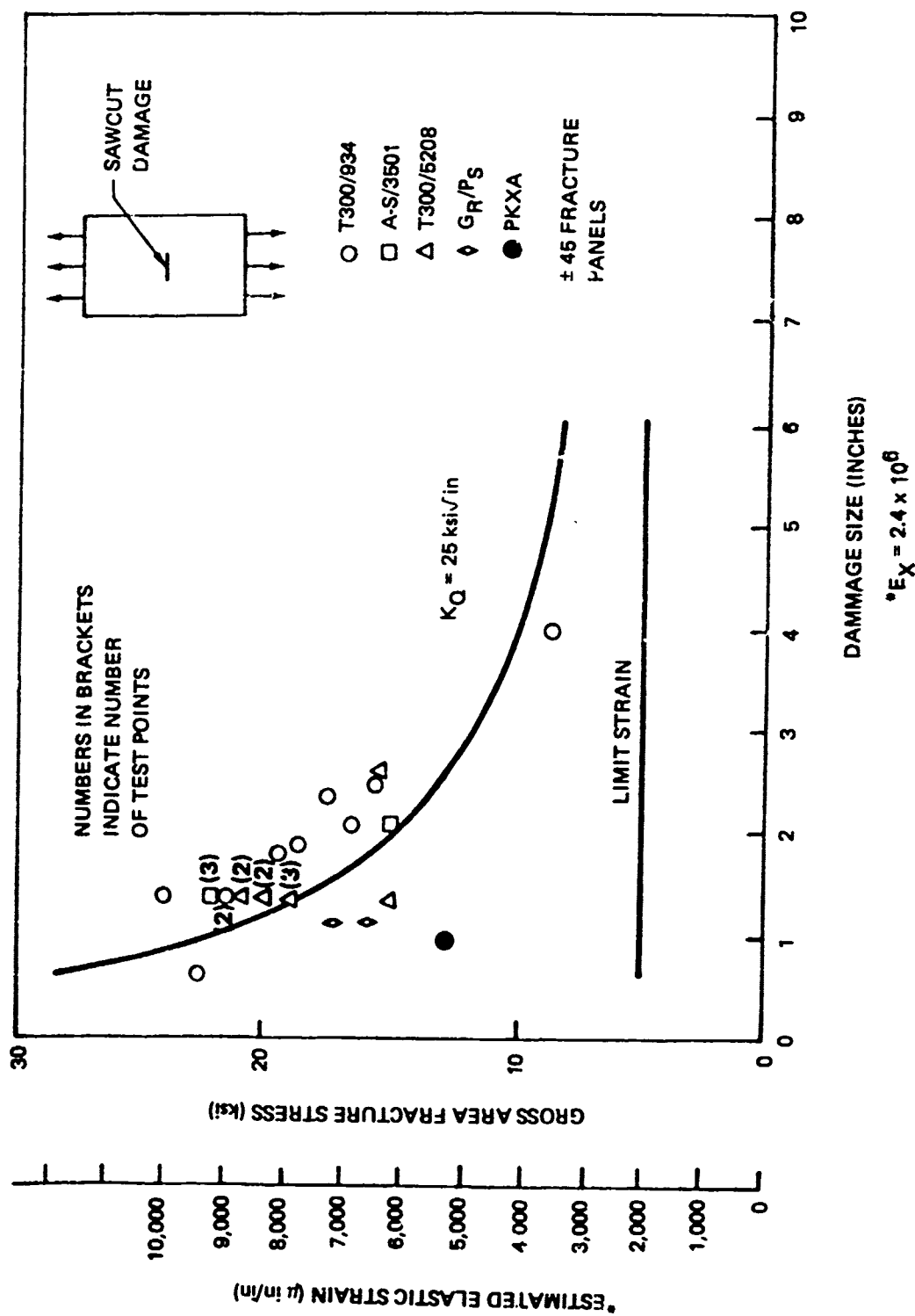


Figure 106. ± 45 Graphite/Epoxy Center Notched Panel Fracture Response

included graphite-polysulfone webs made of fabric oriented at $\pm 45^\circ$. The spar chords were "Tees" made of fabric oriented at $(0,90)$. The spars were connected by top and bottom covers made from 4 plies of fabric ($\pm 45^\circ$). The box was 16.0 in. long and 10 in. long, 10 in. wide and 8.0 in. high. A typical rib was installed in the center of the box to distribute fitting loads. A drawing showing all the design details is shown in Figure 107. The load introduction box element was fabricated using the same detail fabrication and assembly procedures that were used in the full-scale demonstration components. The assembly was accomplished using fusion, adhesive bonding, and mechanical attachments. After the box fabrication was completed, an aluminum fitting was installed at the rib location at the center of the box.

Both static and fatigue tests were performed on the test element. The box was bolted to metal plates at its ends. The edges of the end plates were mounted at the angle required to introduce the fitting loads at the desired angle.

Two static tests were conducted in a test machine using the fixtures depicted in Figures 108 and 109. The fixtures were designed to position the box element so that a single actuator could apply the resultant of the desired load components in the forward-aft and up-down directions. Loads were applied by a hydraulic actuator and controlled by an MTS, Model 436 servo controller. A load cell was connected between the actuator and the load link to measure applied load. Photographs of the above test set-ups are shown in Figures 110, 111, and 112. A third static side load was also applied. The test box and side plates were placed in a 10 Kip capacity Tinius Olsen test machine and a side load was applied to the fitting lug by a load rod extending through a hole in the side plate as shown in Figure 113.

The fatigue testing was accomplished in the 90 in. machine using the same set-up as the second static test Figure (109), except that a MTS Model 430 was used to indicate the maximum and minimum peak loads.

In the first static test, an ultimate fitting load of 9,602 lb was applied. This resultant loading was equivalent to a 200-lb component into the box in the aft direction and 9,600 lb component in the down direction relative to the box. Loads were applied in 10 percent increments. The load introduction box accepted the ultimate fitting load without any difficulty.

ASSEMBLY SEQUENCE

1) DETAIL ASSEMBLY

A. (2) SPARS

- FUSION BOND SPAR CHORDS 2 L's AND CAP
- FUSION BOND CHORDS TO RES
- FUSION BOND IT TO ONE SPAR

B. PR AND LNR COVERS

- FUSION BOND END DOUBLERS TO COVER PLATES

2) ELEVATOR BOX ASSEMBLY

A. FUSION BOND SPARS TO LOWER COVER

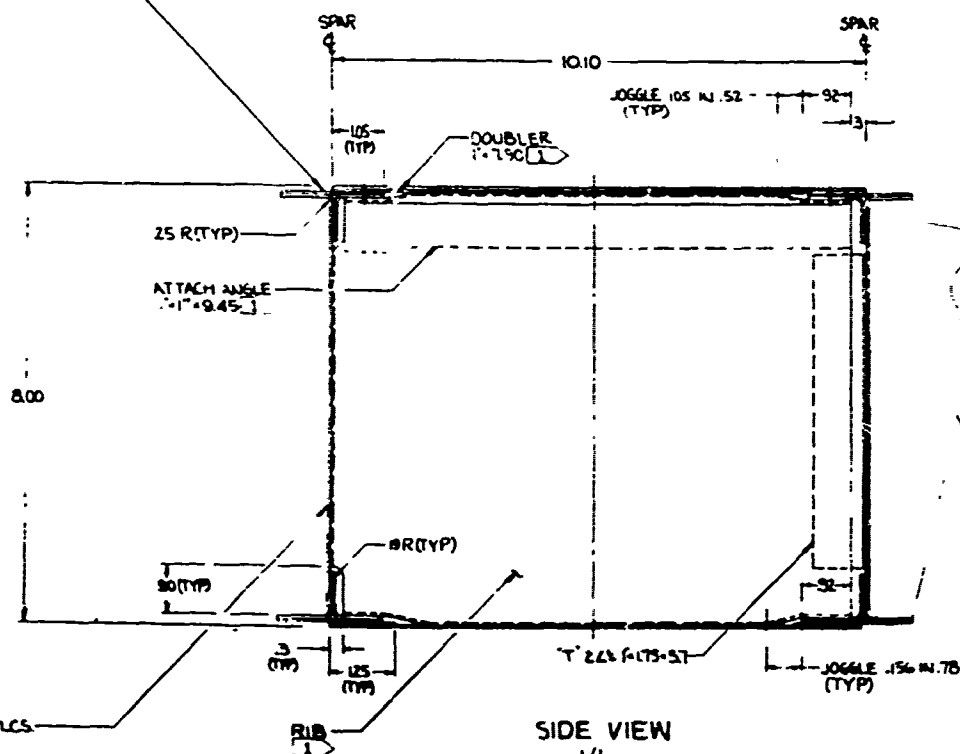
- INSTALL RB AND ATTACHMENT ANGLE BY FUSION BONDING
- INSTALL UPPER COVER USING BOND VEHICLE ATTACHMENT.

UPPER COVER

- 1) 4 PLES, 245°, 60/PS FIBRE PER VAC. SPECIFICATION "GRAPHITE FIBRE PREIMPREGNATED, THERMOPLASTIC" D 80-19348-3

SPAR CHORD TYP 4 PLCS

- (1) CAP 2"x16"
- (2) L's 1"x16"



SIDE VIEW

1/1

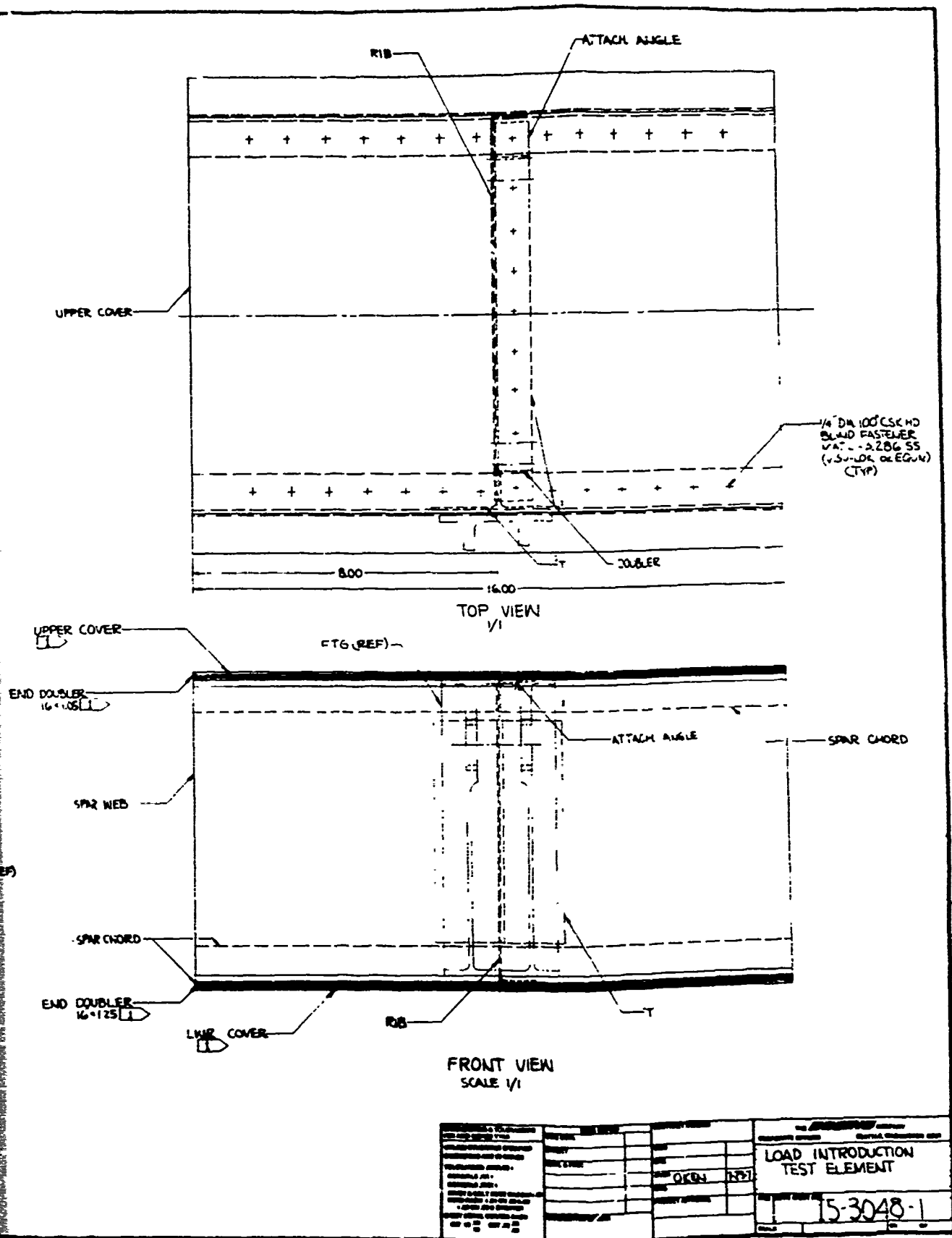


Figure 107. Load Introduction Test Element

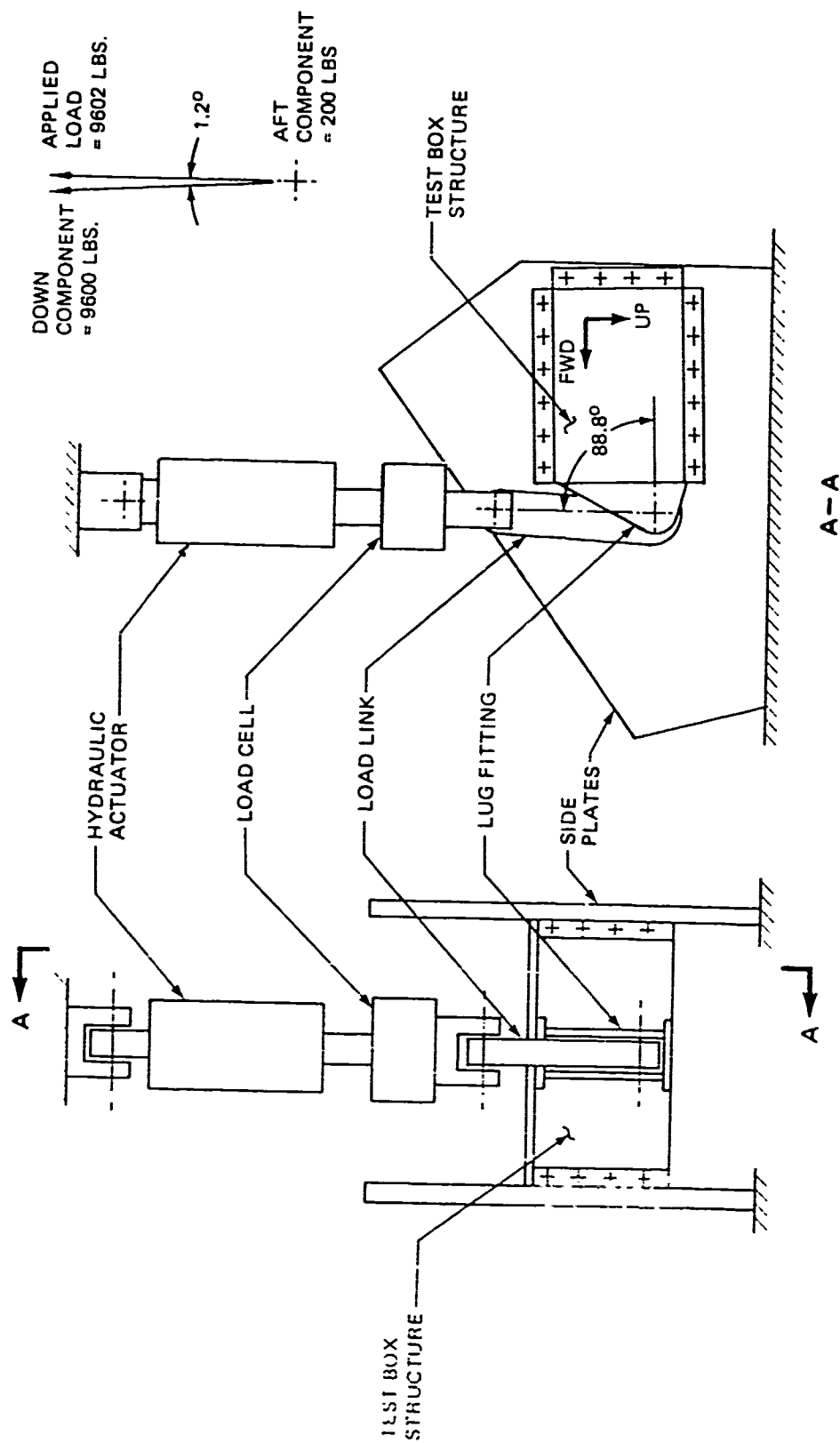


Figure 108. Static Test No. 1 Setup

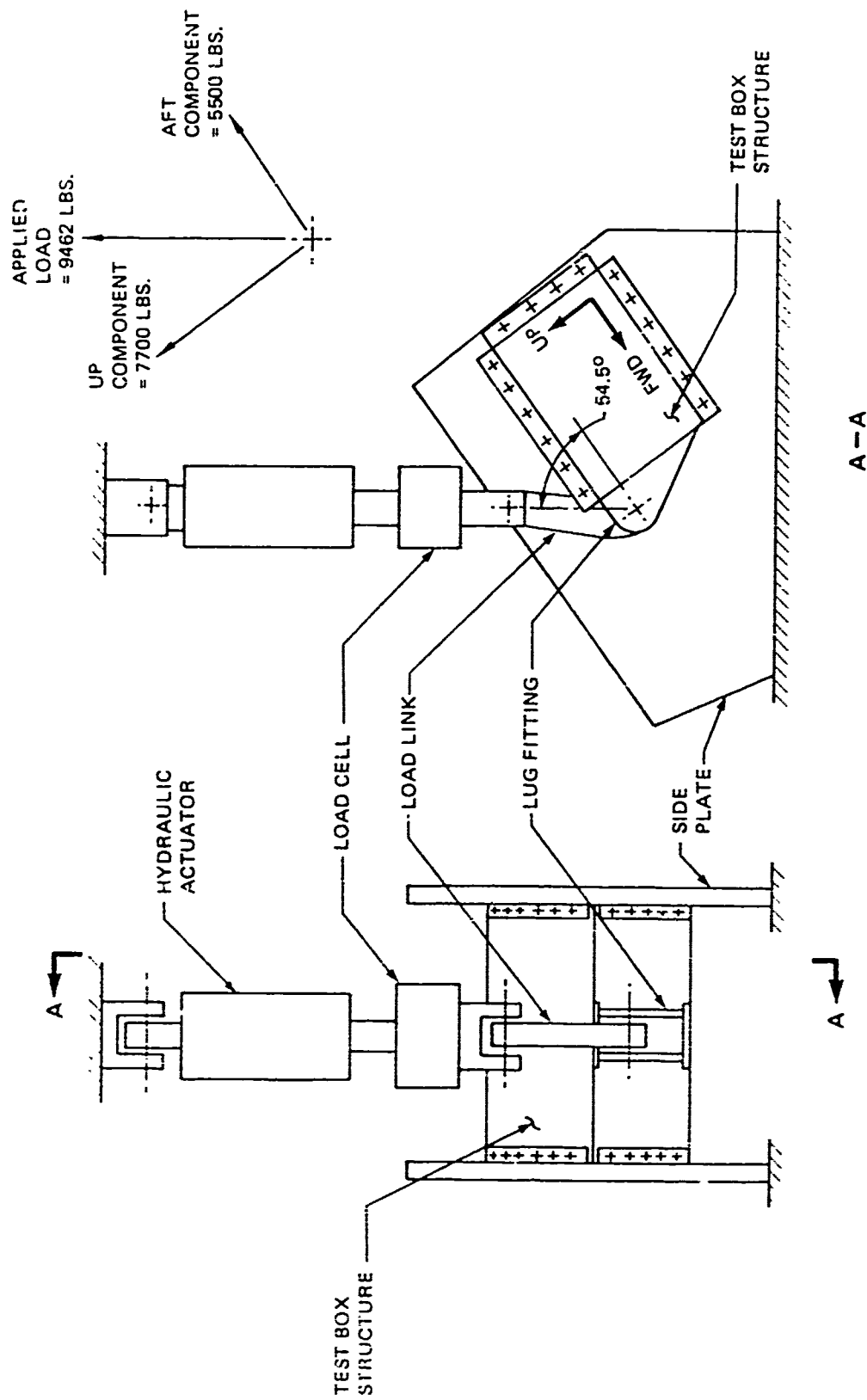


Figure 109. Static Test No. 2 and Fatigue Test Setup



Figure 110. Load Introduction Box - Test Set-Up

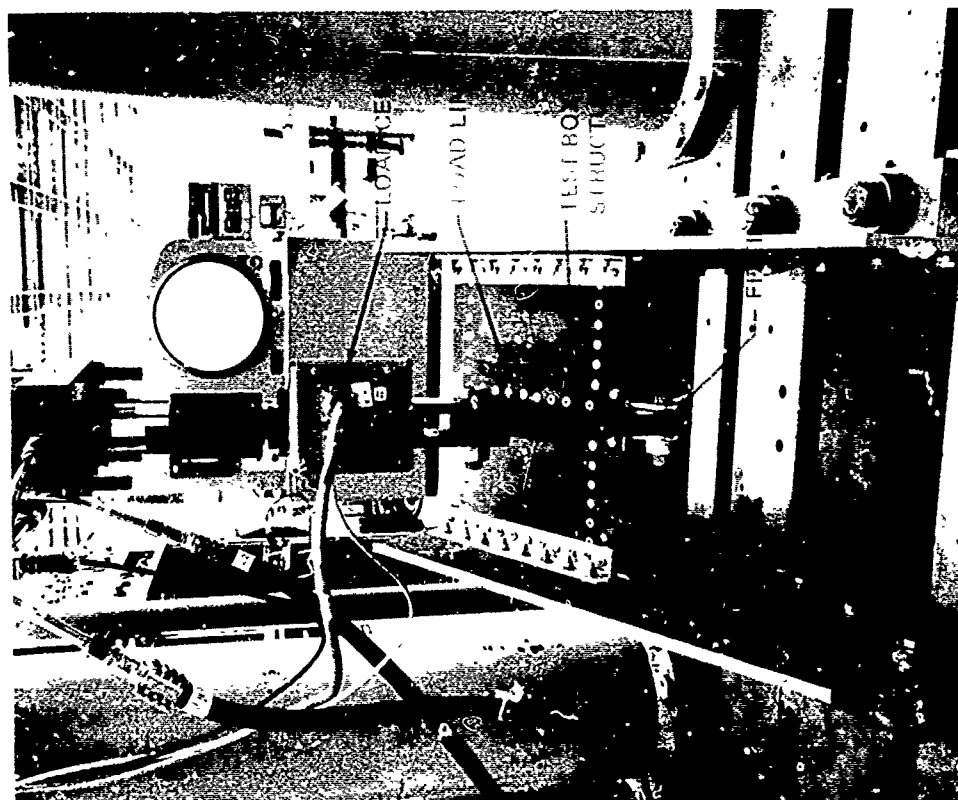


Figure 111. Load Introduction Box - Test Set-Up, Front View

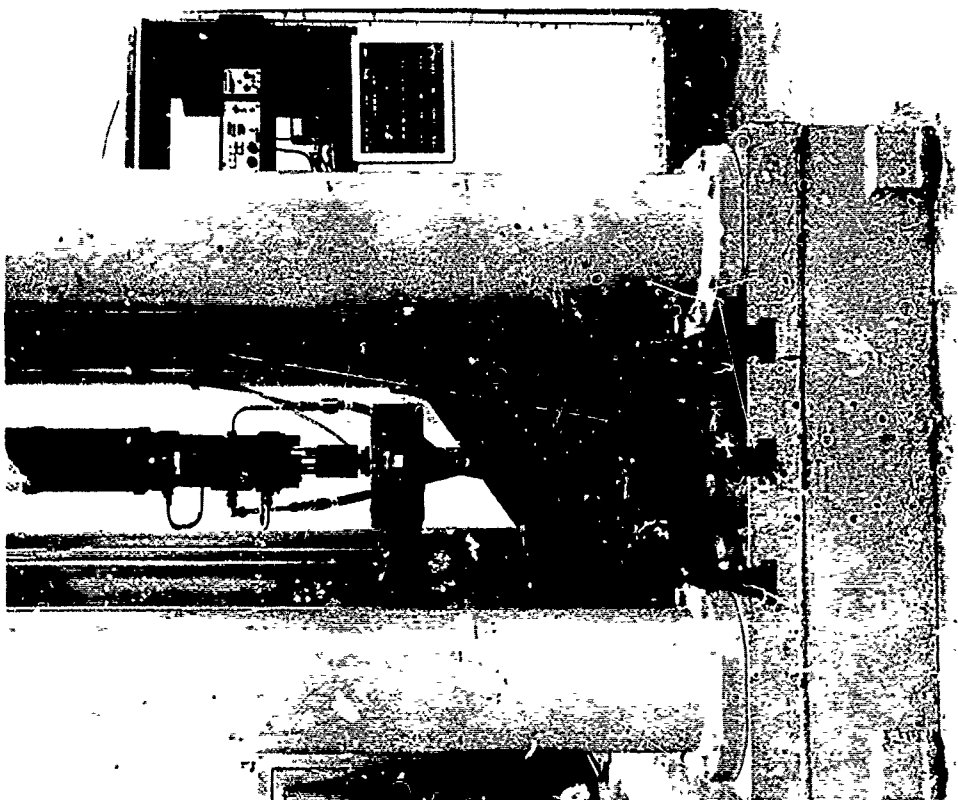


Figure 112. Load Introduction Box - Test Set-Up, Side View

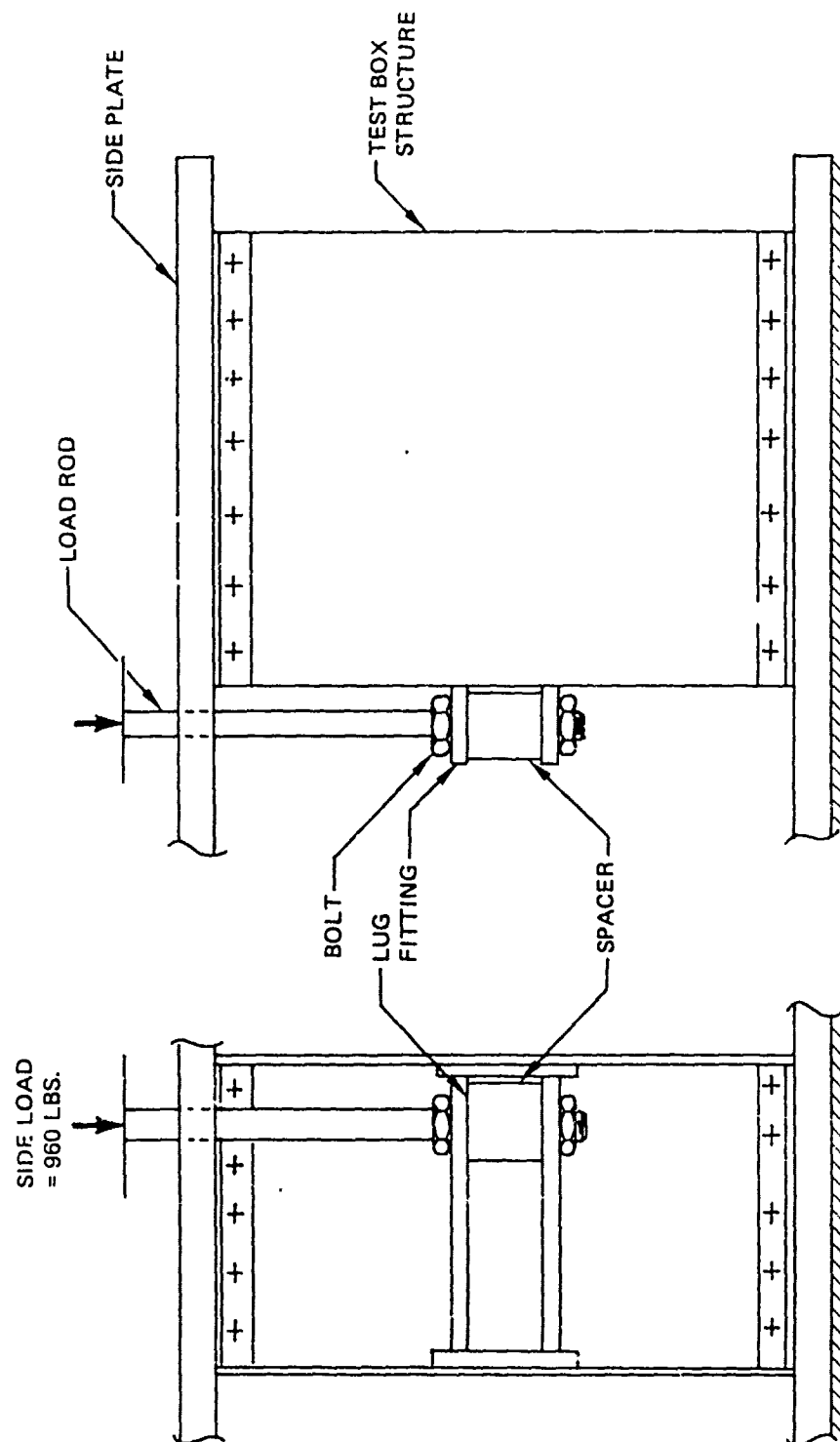


Figure 113. Static Test No. 3, Side Load Test Setup

After the successful initial static test the box was repositioned (Figure 109) and a second ultimate static loading condition was applied. Load was applied in 10 percent increments to a maximum load of 9,462 lb. This load was equivalent to components of 5,500 lb into the box in the aft direction and 7,700 lb in the up direction.

The third static test was an ultimate side load condition. A maximum load of 960 lb was successfully applied to the side of the lug fitting.

A fatigue test was performed in which 120,000 load cycles were applied with a maximum load equal to 42% of the second ultimate static load condition. This was equivalent to four life cycles at the maximum load in each ground-air-ground load spectrum. The load was varied sinusoidally between 3,974 lb and 200 lb at a frequency of 5 Hz. The fatigue test was successfully completed without damage to the box.

7.0 YC-14 ELEVATOR FULL-SCALE DESIGN AND FABRICATION

Three graphite thermoplastic YC-14 outboard elevator designs were developed and evaluated and one was selected for further development. The three concepts were a corrugated stiffened concept, a stabilizer honeycomb concept and a "Z" stiffened concept. All of the concepts were designed using the same requirements and criteria that was for the existing flight hardware.

7.1 DESIGN REQUIREMENTS AND CRITERIA

The composite outboard elevators were designed to be a direct replacement of the existing aluminum outboard elevator on the YC-14. They were developed to utilize existing metal hinges, actuator and reaction links. The composite elevator design envelopes matched the external mold line surfaces of the aluminum design. The basic elevator structures consisted of a two-spar box similar to the aluminum design.

Design Loads

The GRTP elevators were designed for the same ultimate load conditions as the YC-14 outboard elevator aluminum design.

Ultimate Load Factor

The ultimate loads were based on an ultimate factor of safety of 1.50 applied to the limit loads.

Fitting Factors

The fitting factors used on the aluminum design were used to ensure durability and rigidity. The factors were applied to the internal limit structural loads obtained by analysis for both normal and fail-safe flight conditions.

Fail-Safe Requirements

The G RTP designs were capable of carrying limit loads with the following hinge failures occurring independently (same as aluminum design):

<u>F/S Condition</u>	<u>Failed Hinge Station</u>
1	115
2	143
3	171
4	215
5	265

Temperatures

The temperature range criteria for the composite designs was -65°F to 160°F.

Design Service Life

The design service life goal of the composite designs was the same as the C-14 (production) aluminum design:

	<u>YC-14</u>	<u>C-14</u>
Cumulative flight hours	1,000	30,000
Total number of landings	2,000	17,000
Total service life years	10	20

The composite elevators were designed to have an operational life to exceed the design service life per MIL-STD-1530 and MIL-A-8866(A). The objective of the Design Service Life requirement was to minimize potential cracking problems that could reduce the functional capability or increase the operational cost of the elevator.

Flutter

The GRTP elevators had equal or greater flutter margins than the aluminum design. In order to satisfy this criterion, the unbuckled box torsional stiffness (GJ) distribution was equal to or higher than the aluminum design.

Control System Effectiveness

Control system effectiveness was maintained by providing equivalent local stiffnesses in the actuator load loop structural elements.

Permanent Deformations

The composite laminate layups were configured so that no significant ply yielding would occur due to transverse and/or shear ply strains under applied limit elevator loads. For $\pm 45^\circ$ laminates, the maximum strain in the 0° or 90° directions shall be 2,000 microstrain at limit load.

Spar Webs

Spar webs of other than stiffened monocoque construction were designed to be buckle resistant. Intermediate elastic buckling of stiffened monocoque laminate webs was allowed. The maximum ratio of applied-to-critical shear buckling loads was 5.0. The strength of the critical web panel was established by nonlinear deflection analysis using a maximum ply strain failure criterion. The web strength analysis was substantiated by shear web subcomponent testing.

Cover Panels

All cover panels were designed to be buckle resistant or intermediate elastic buckle design. The cover panel strength analysis was substantiated by subcomponent testing.

Rib and Actuator Beams

All ribs and actuator beams were designed to be buckle resistant.

Design Allowables

Design data and properties for GRTP composites were determined from test data for the materials, processes, and composite configurations used in the elevator. Joint design allowables were based on element test data. Nominal ply dimensions were used for analytical calculations to substantiate structural integrity.

Damage Tolerance

The materials, design concepts and stress levels for the composite design were selected so that the probability of failure of the component is minimized due to the propagation of undetected or inservice inflicted damage. These damage tolerance requirements were achieved (1) through the use of fail-safe design in the case of a hinge failure, (2) by designing to strain levels at limit load that are below critical flaw growth levels, and (3) by requiring that damage caused by impact with small debris or hail would not reduce the strength below limit load requirements.

Corrosion

Aluminum fittings would be de-coupled from the GRTP elevator materials by two coats of corrosion resistant primer. Special consideration would be given to the fitting connection fasteners with respect to material selection and wet-primed installation.

Panel Sizing

The cover panels and spar webs were sized to provide torsional stiffness (GJ) greater than the aluminum design at reduced structural weight. For a design goal target, the GJ distribution for the YC-14 graphite-epoxy elevator shown in Figure 114 was adopted. The EI_y and EI_z distributions for the graphite-thermoplastics designs are shown in Figure 115. These distributions

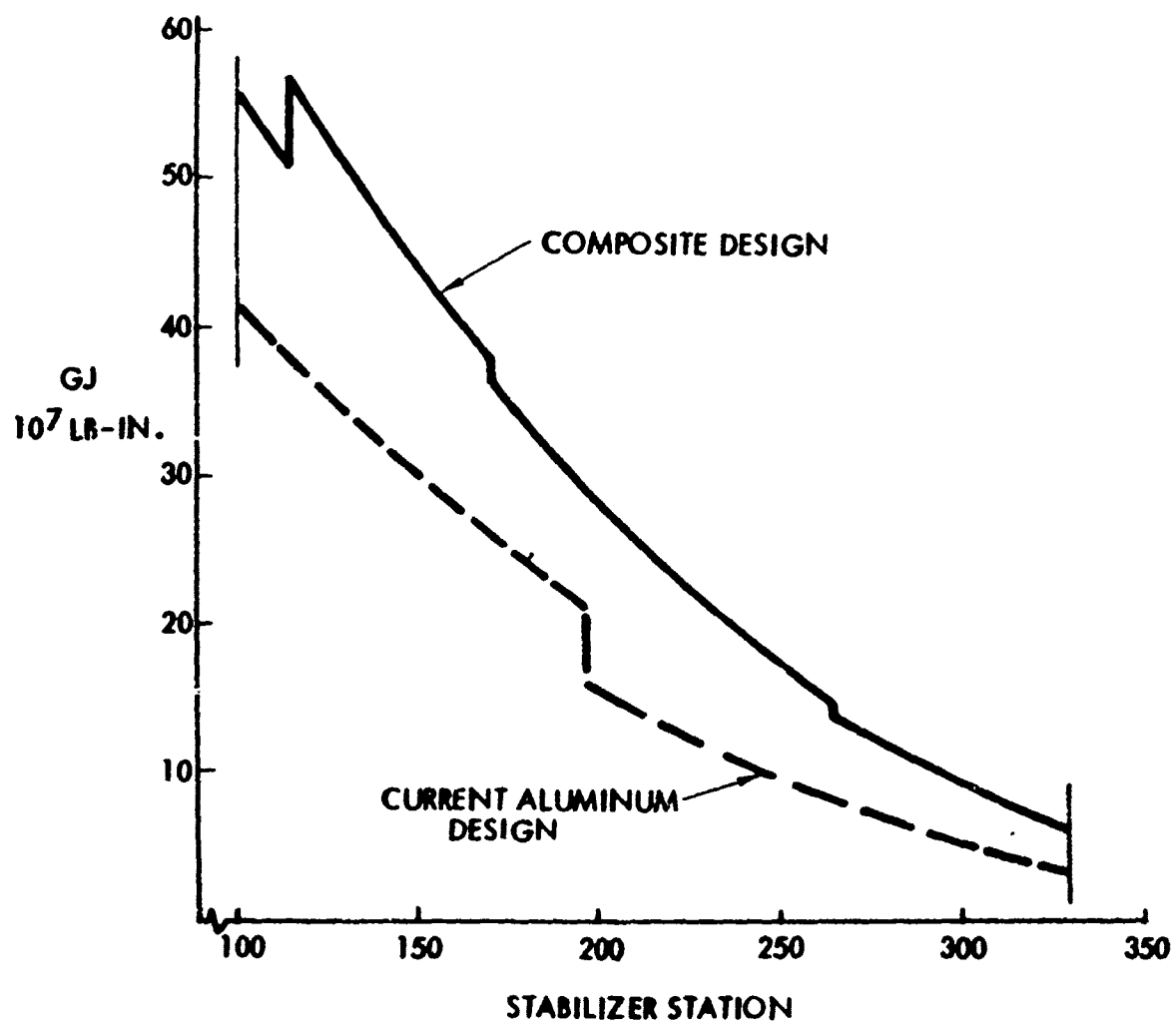


Figure 114. YC-14 Outboard Elevator GJ Comparisons

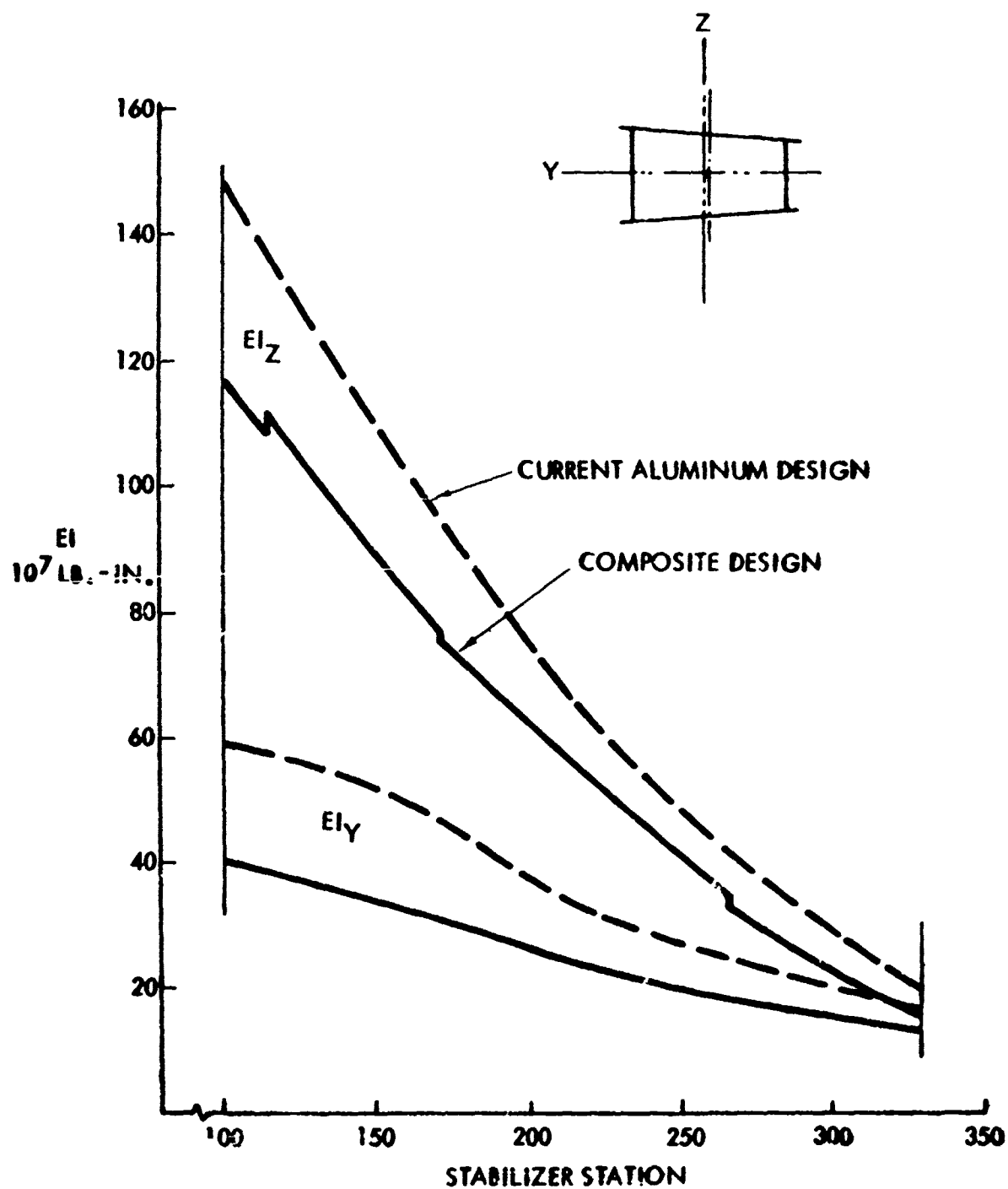


Figure 115. YC-14 Outboard Elevator EI Comparisons

are lower than the current aluminum design. The combined EI, GJ distribution shown for the composite design are known to provide flutter margins in excess of the design criteria requirements.

The cover panels and spar webs were also sized to ensure integrity at ultimate design loads. Classical orthotropic panel analysis methods were used to determine critical general and local instability loads. The stiffened monocoque panel concept allowed intermediate buckling as stated in the design criteria.

Fatigue and Fracture

A study of the YC-14/C-14 G RTP elevator component designs indicated they would meet service life requirements. The elevator skin and spar webs were designed to a stiffness requirement resulting in low laminate operating stresses. Limit strains for the basic skin laminates were about 2,000 in./in. due to axial and torsional loading. In order to assess the general fatigue behavior of the skin laminates, available data from the Advanced Composites Design Guide was reduced as shown in Figure 116. The reduced data does not include thermoplastic laminate data but initial studies and element tests have shown equivalent fatigue response for G RTP laminates.

As shown in the above figure all the laminates presented, including those containing holes, did not fail at maximum peak strain values below 4,000 μ in./in. The typical maximum fatigue load anticipated in each flight is expected to be only about one-half of limit load with only small load reversal resulting from take-off rotation. The maximum skin strain will be considerably below the fatigue limit. The laminates shown did not include the all $\pm 45^\circ$ layup used in the preliminary design but did include testing of $\pm 45/90$ laminates which would be expected to have similar performance. It is anticipated from this comparison that the basic laminates will have sufficient fatigue margin.

The preliminary G RTP design concepts with $\pm 45^\circ$ laminate skins surpass the requirements for in-service damage tolerance. Fracture data developed in the element tests (Section 6.0) substantiated this capability.

DATA FROM: ADVANCED COMPOSITES
DESIGN GUIDE

INTERMEDIATE STRENGTH G_r/E_p

$R = 0.05$

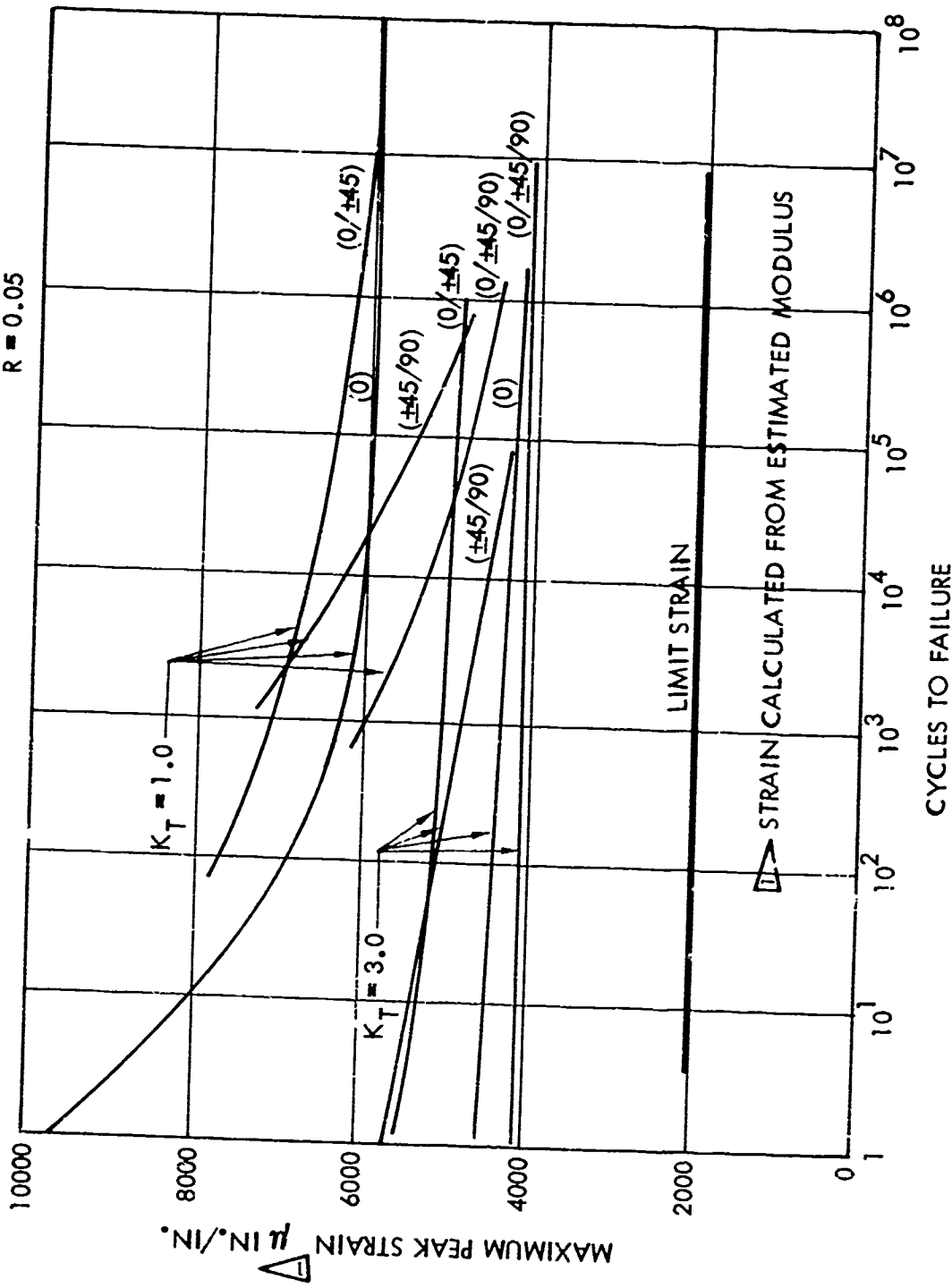


Figure 116. Fatigue of Intermediate Strength Graphite/Epoxy

7.2 PRELIMINARY DESIGN

Three YC-14 outboard elevator preliminary conceptual designs incorporating graphite thermoplastic materials were evaluated. The evaluation considered weight, cost, inspectability and repairability. As a result, one of the concepts was selected for further design refinement and hardware evaluation.

The laminate thicknesses and ply orientations in all three designs were selected to be as close to the existing aluminum design as practical. The YC-14 elevator is subjected to bending induced by loads from the horizontal stabilizer through the interfacing multi-hinge attachment. The induced bending loads can be minimized by reducing the elevator EI stiffness to an acceptable lower limit. In the design of the ply orientations a major consideration was the high torsional stiffness required because the elevator is actuated at the inboard end only; both the reduced bending stiffness and high torsional stiffness resulted from the use of $\pm 45^\circ$ plies in both the cover panels and spar webs. Figures 114 and 115 show a comparison of the bending and torsional stiffnesses between the composite designs and the existing aluminum design.

A detailed SAMECS finite element computer model has been built for internal loads analysis. A total of 16 flight maneuver and ground load cases were evaluated. Analysis results indicate the composite designs have cover panel and spar web ultimate shear load capabilities within 4 percent of the aluminum elevator loads. Torsionally, the composite design is considerably stiffer, showing 30 percent less windup than the aluminum design.

Figure 117 shows locations of hinge and actuator fittings and envelope control dimensions. These dimensions and locations were maintained throughout the program to assure interchangeability of GRTP and aluminum elevators.

7.2.1 "Z" Stiffened Panel Concept

A graphite-polysulfone YC-14 elevator design was developed incorporating a panel concept with chordwise stiffeners. The details of this design are shown in Figure 118. The covers and spar webs used graphite fabric oriented at $\pm 45^\circ$ to provide good torsional stiffness. Panel stability was provided by

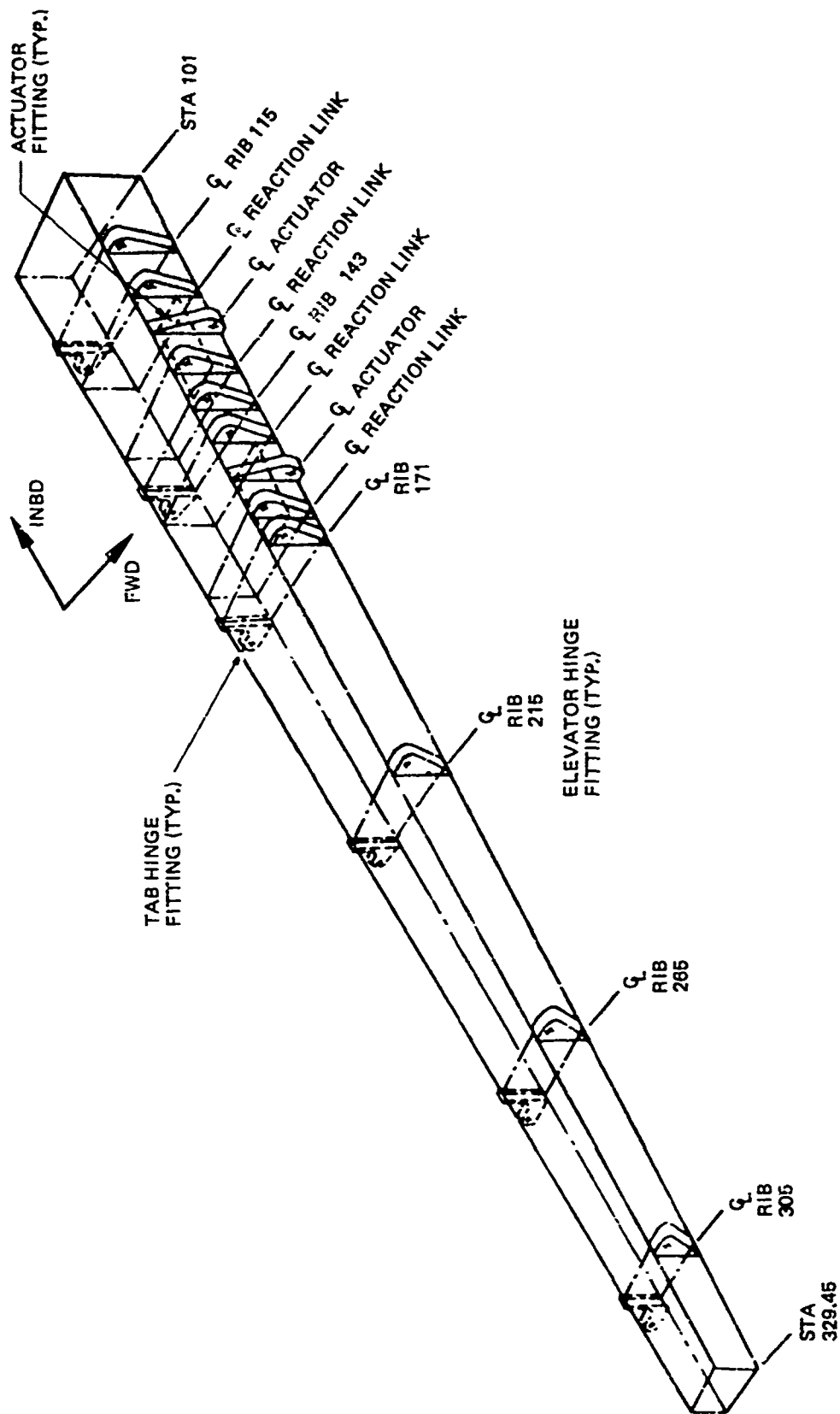
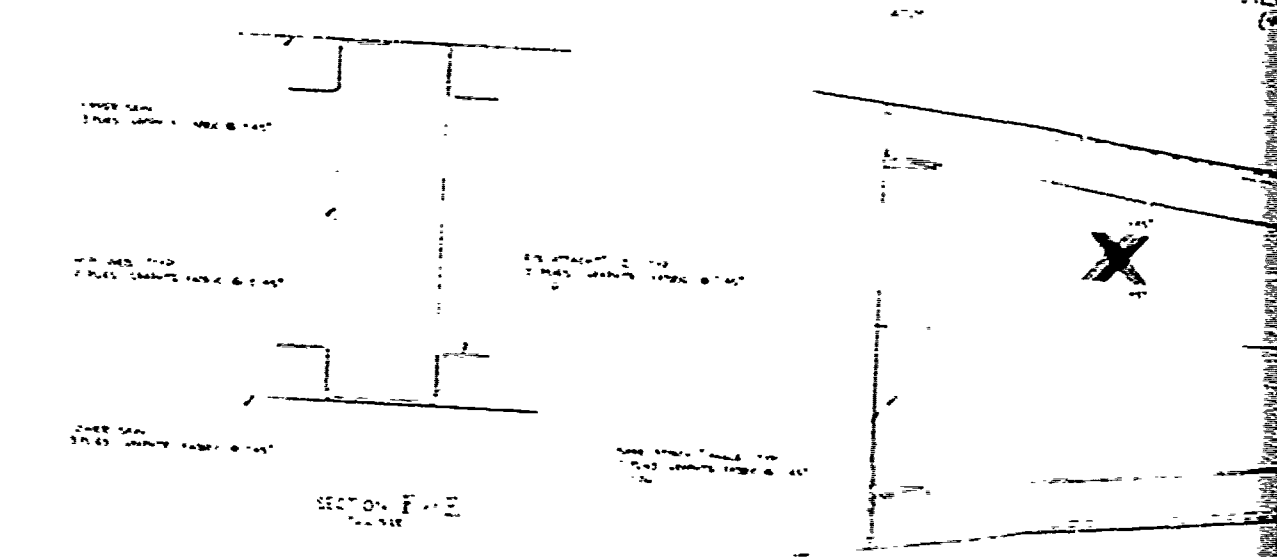
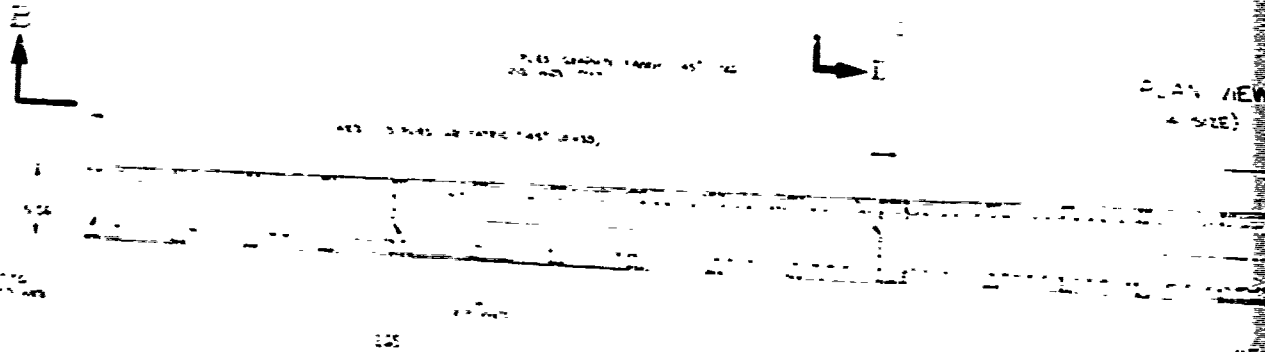
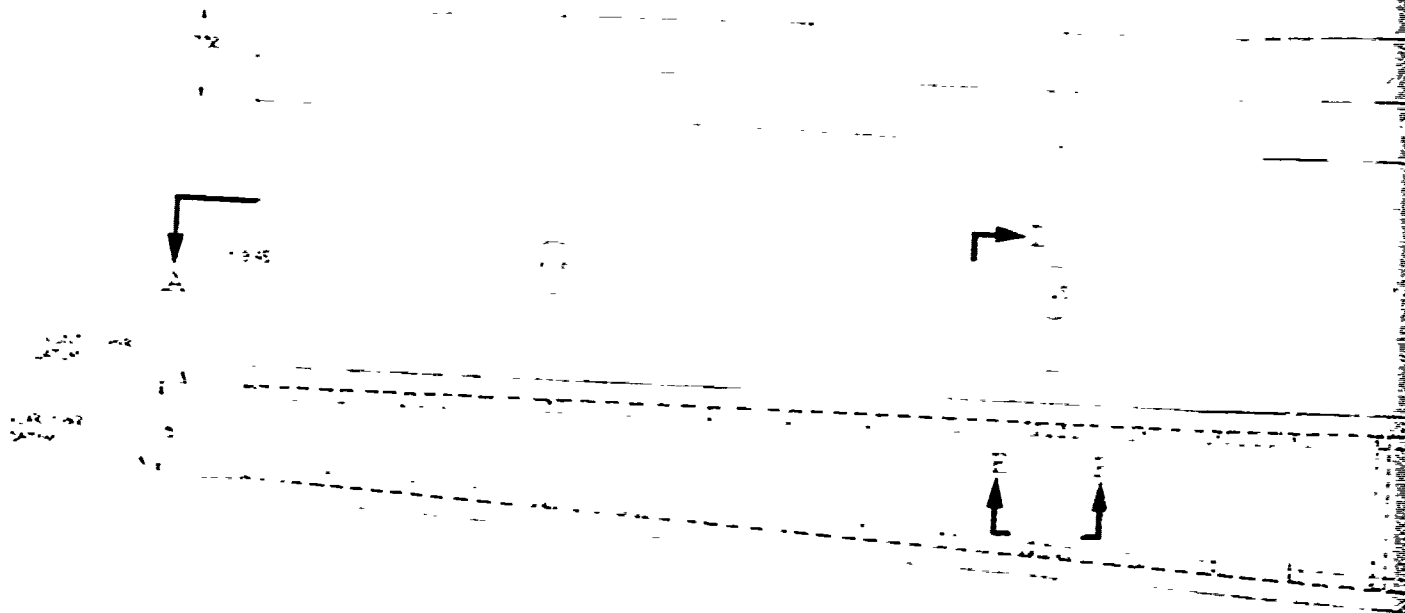


Figure 117. YC-14 Elevator Schematic

ALL DIMENSIONS ARE IN FEET



SECTION I-D
1/11/50
THICK 23 CONSTRUCTION

WEB - 4 PLYS GR FABRIC @ 45° (0.092)

WEB - 3 PLYS GR FABRIC

VIEW A-A

265

215

UPPER & LOWER SKIN PANELS
3 PLYS GRAPHITE FABRIC @ 45°

171

ALUM. HANGE FTE (TYP)

143

PLAN VIEW
(1/4" SIZE)

WEB - 4 PLYS GR FABRIC @ 45° (0.092)

WEB - 3 PLYS GR FABRIC

VIEW B-B
(1/4" SIZE)

035
R/S WEB (TYP)

FS
DATUM

SKIN STIFFENING 'Z' (TYP)
2 PLYS GRAPHITE FABRIC @ 45°
0.016

035
R/S WEB

032
R/S WEB

R/S
DATUM

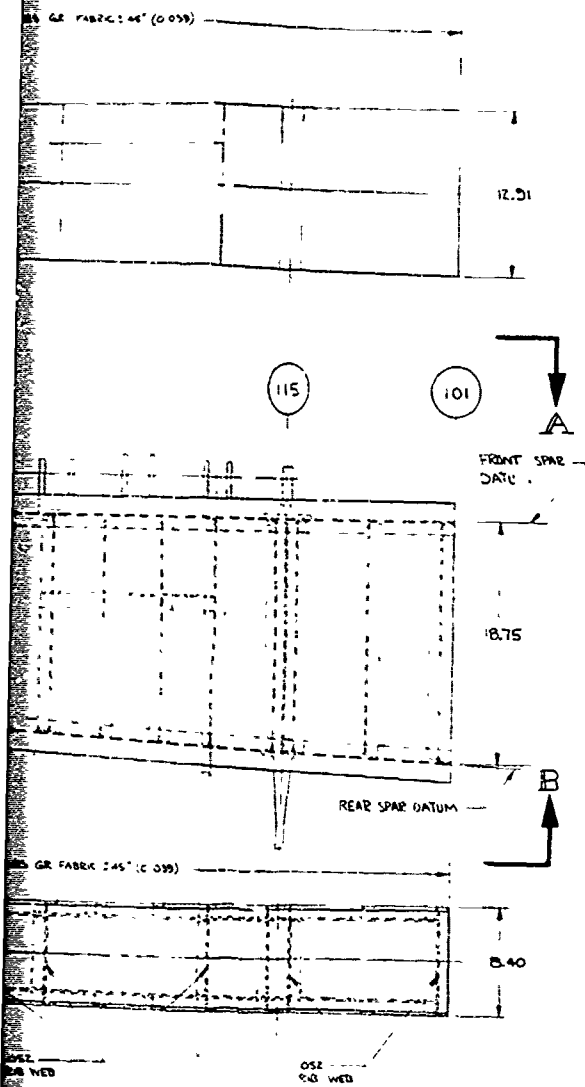
SKIN ATTACHMENT ANGLE (TYP)
2 PLYS GRAPHITE FABRIC @ 45°
0.016

4 PLYS GRAPHITE
(TYP FOR R/S-B)
0.092

SKIN CHORD (TYP)
4 PLYS GRAPHITE
(TYP FOR FS)
0.092

SECTION D-D
(FULL SIZE)
TYPICAL RIB CONSTRUCTION

SECTION C-C
(FULL SIZE)
TYPICAL CROSS SECTION



MATERIAL

GRAPHITE FABRIC - HENGER T100 31 STYLE / POLYSULFONE
GRAPHITE TAPE - HENGER A2 / POLYSULFONE

DETAIL FABRICATION

TOP & BOTTOM COVERS

- 1) SKIN CONSOLIDATION - HOT ROLLING, AUTOCLAVE OR PULTRUSION
- 2) TRIM
- 3) 'Z' SECTIONS (MAIN STIFFENERS & RIBS CHORDS) - PULTRUSIONS
- 4) ANGLE SECTIONS (SPAR CHORDS & STIFFENER ATTACHMENTS) - PULTRUSIONS
- 5) CUTOFF & TRIM 'Z' & ANGLE SECTIONS
- 6) ASSEMBLE 'Z' SECTIONS & ANGLE SECTIONS BY FUSION

RIBS

- 1) WEB LAMINATE CONSOLIDATION PER STEP 1) ABOVE
- 2) TRIM WEBS
- 3) ANGLE SECTIONS (RIB TO SPAR ATTACHMENT) - PULTRUSIONS
- 4) CUT OUT & TRIM ANGLE SECTIONS
- 5) ASSEMBLE ANGLES TO SPAR WEBS BY FUSION

SPARS

- 1) WEB LAMINATE CONSOLIDATION PER STEP 1) ABOVE
- 2) TRIM WEBS

ELEVATOR ASSEMBLY

- 1) TOP & BOTTOM COVERS, RIBS AND FRONT SPAR ASSEMBLED BY FUSION BONDING
- 2) REAR SPAR AND HINGE FITTINGS INSTALLED WITH MECHANICAL ATTACHMENTS

NOTE: THIS DESIGN WILL BE UPDATED AS MANUFACTURING DEVELOPMENT AND FEASIBILITY STUDY RESULTS ARE OBTAINED

DESIGNING & CONSTRUCTION FOR AND UNDER FILE	DATE	CONTRACT NUMBER	THE BOEING COMPANY CORPORATE OFFICES SEATTLE, WASHINGTON 98101
UNLESS OTHERWISE SPECIFIED DIMENSIONS ARE IN INCHES	STAGE	FILE	
TOLERANCES UNLESS OTHERWISE SPECIFIED: FRACTIONS ANGLES DECIMALS INCHES DECIMALS DEGREES	DATE & PRICE	ONE	YC-14 ELEVATOR GRAPHITE / POLYSULFONE Z STIFFENED COVER CONCEPT
SHIPLEY & BULLOCK ENGINEERING CO. 1000 1ST AVENUE, SUITE 1000 SEATTLE, WASHINGTON 98101	DATE	ONE	
SHEET METAL FABRICATOR 1000 1ST AVENUE, SUITE 1000 SEATTLE, WASHINGTON 98101	CHANGE ITEM NUMBER	PROCKET APPROVAL	DATE & PRICE BIZOS SK11-81477
DATE	BY	DATE	DATE

171 Figure 118. YC-14 Elevator Gr/Ps Z Stiffened Cover Concept

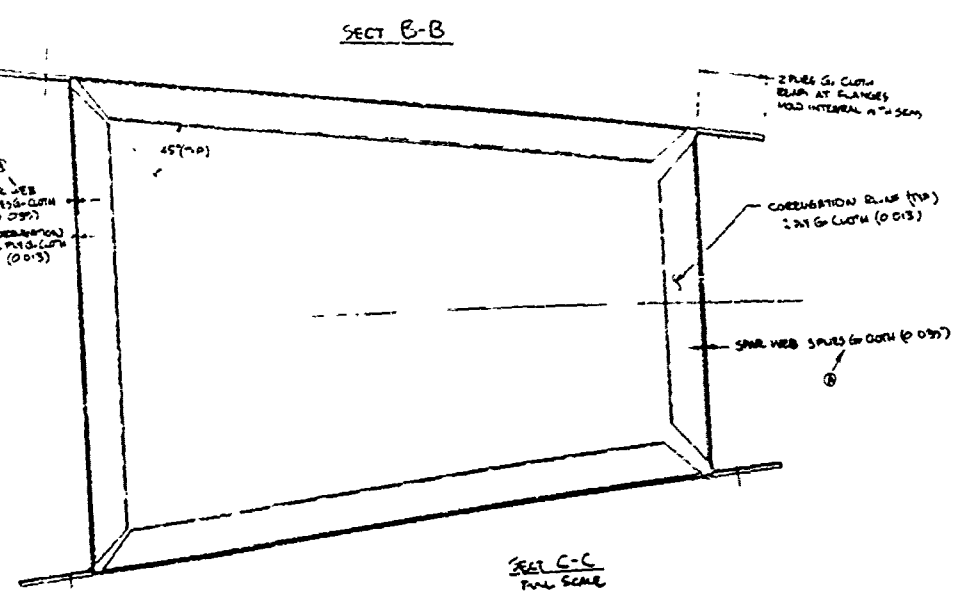
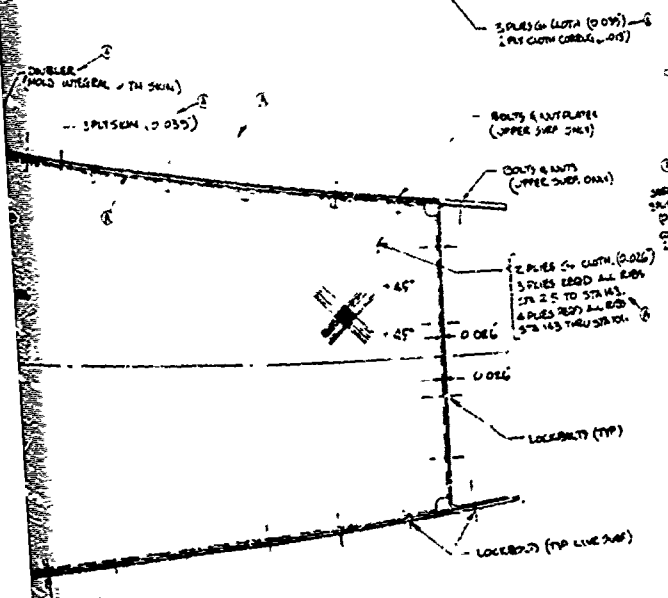
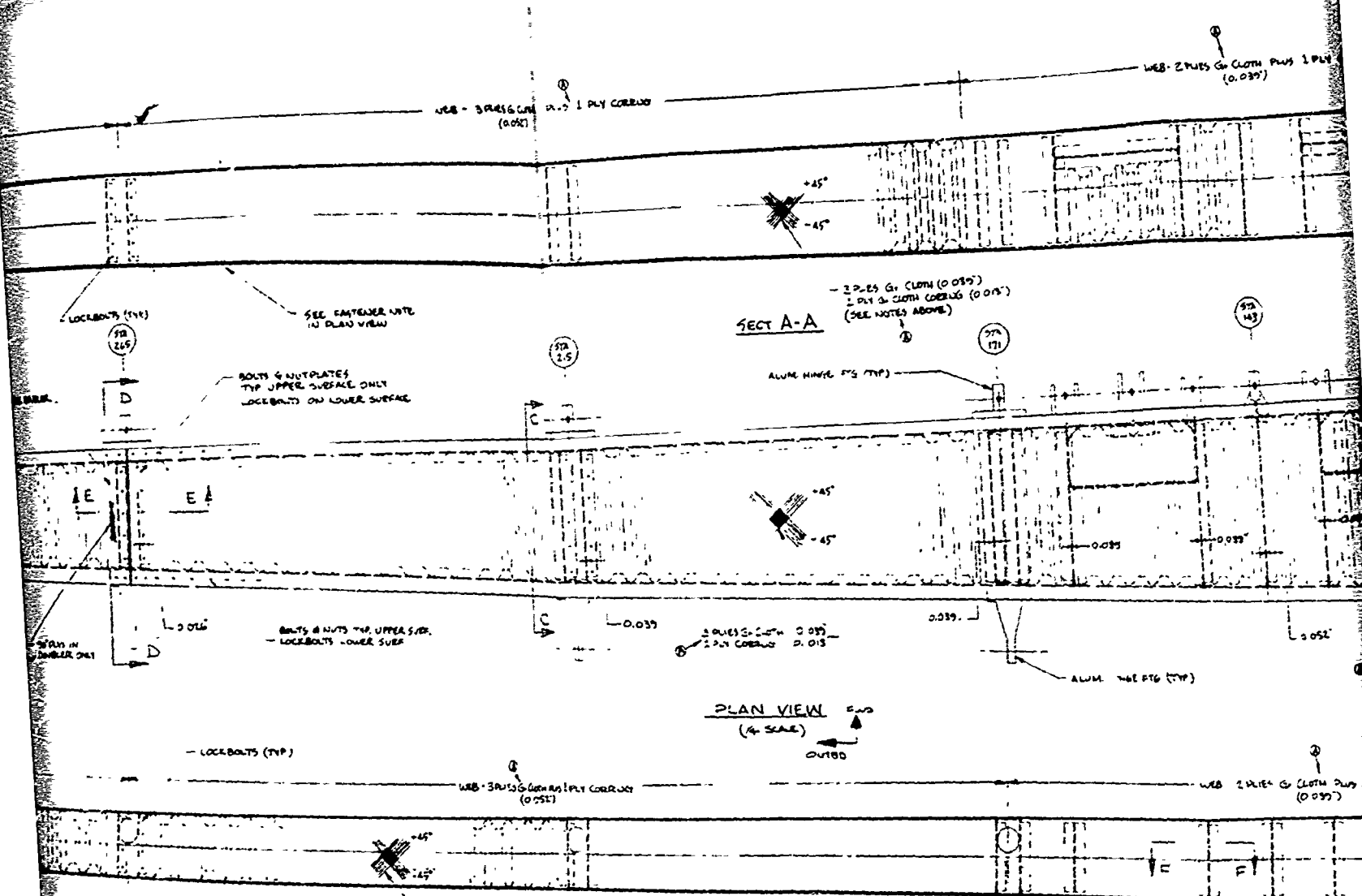
stiffeners installed by fusion bonding. Ribs, which also use graphite fabric oriented at $\pm 45^\circ$ were installed at each of the hinge locations. Some flanges on both the ribs and spars were post-formed as an integral part of these details. In most cases additional angle details were added by fusion bonding to provide a means for controlling assembly tolerances. Fusion bonding was used wherever practical for detail installation and component assembly. Mechanical fastening was held to a minimum and used primarily for close-out of the elevator box.

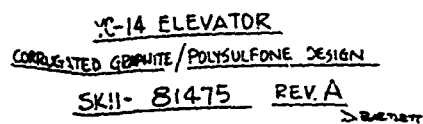
7.2.2 Corrugated Stiffened Panel Concept

The design shown in Figure 119 utilized a corrugated stiffened panel concept. The top and bottom covers, and the front and rear spar webs were designed with graphite fabric oriented at $\pm 45^\circ$ to provide good torsional stiffness. These laminates were then stiffened with corrugated panels made of graphite fabric. The corrugated panels were fusion bonded to the flat lamination. Ribs, which were also made of graphite fabric oriented at $\pm 45^\circ$ were installed at each of the hinge locations. The flanges on both the ribs and the spars were post formed and were made as an integral part of the spar and cap details. The overall elevator was assembled by mechanical attachments.

7.2.3 Honeycomb Stiffened Cover Panel Concept

A design was developed that incorporated a honeycomb stiffened cover panel concept. This design was based on a 8 ft long graphite-epoxy YC-14 elevator component that had been fabricated and tested. The component tests demonstrated complete design compliance. This component demonstrated a safe life capability (4 factors) in which two of the life cycles were performed with 2 in. long saw cuts in both the covers and spar webs. After the fatigue cycling was completed the component was tested to failure. Failure occurred at 60 percent above design ultimate. Figure 120 shows the portion of the elevator that was used for the graphite-epoxy elevator test component and the structural concept that was incorporated. Because of the excellent performance





175

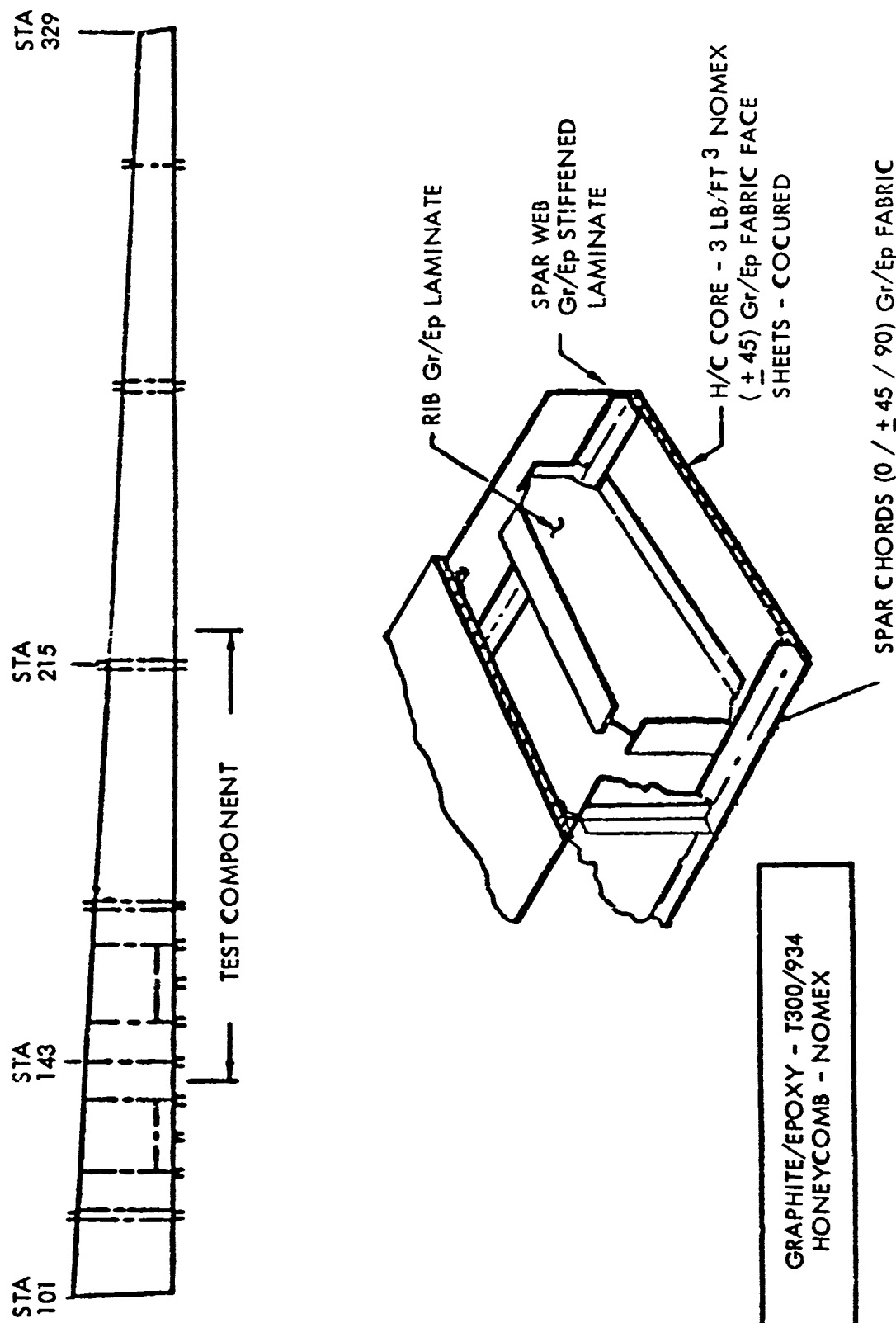


Figure 120. Graphite/Epoxy Elevator Test Component

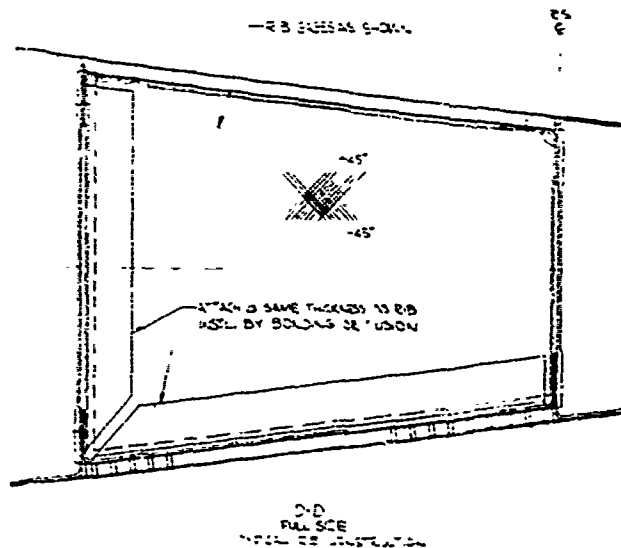
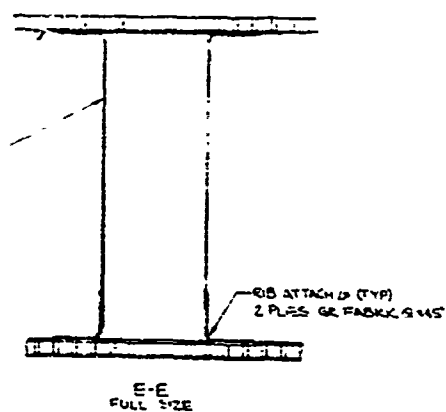
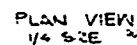
of this component, a graphite-thermoplastic design was developed based on the same concept. Figure 121 shows the details of this design. The top and bottom covers have graphite fabric polysulfone skins stabilized with Nomex honeycomb. The spars and ribs utilize graphite fabric/polysulfone laminates oriented at $\pm 45^\circ$. Stiffening is not required for these elements. The rear spar and the covers were assembled by fusion bonding. The front spar and hinge fittings were installed with mechanical attachments.

7.2.4 Preliminary Design Study Results

Three preliminary designs of a graphite thermoplastic YC-14 elevator were developed as described above. The three concepts were evaluated and the stiffener stabilized panel concept was selected for further evaluation.

Weights of the three designs were established. It was determined that all three concepts weighed within a few percentage points of each other. This study also showed that all three composite designs were approximately 25 percent lighter than the existing YC-14 aluminum elevator design.

A study was also performed to determine the costs for producing the three composite designs. Costs were based on the procedures described in Section 3.0. Costs were determined for the first unit production and then using an 85 percent learning curve for the 10th and 100th unit production. A summary of this data is shown in Table 32. These results show that for the first unit production the honeycomb design is the least costly, the "Z" stiffened next, and the corrugated design most costly. By the 10th unit production the honeycomb concept remains the least costly, the positions of the following two were reversed. The "Z" stiffened concept has the highest cost because it has the greatest number of details. These costs could have been reduced by simplifying the stiffener geometry and by using integral rib flanges to reduce the number of parts. Using these techniques, most of the 10 percent cost difference (10 unit) could be eliminated. The Z-stiffened is more applicable to other aircraft components than the other two concepts thereby permitting wider dissemination of the technology developed in this program. The data generated in this study indicated that all three concepts could be fabricated for approximately 25 percent less cost than the existing aluminum design.



WEB-4 PLYS GR FABRIC 245° (0.052)

WEB-3 PLYS GR FABRIC

A-A

265

215

171

45

OUTER SKIN 3 PLYS GRAPHITE FABRIC 0.039"
TYP TOP & BOTTOM COVERS

ALUM HINGE FTG. TYP.

0.039" TYP

PLAN VIEW
1/4" SIZE

WEB-4 PLYS GR FABRIC 245° (0.052)

WEB-3 PLYS GR FABRIC 245°

NOVEX CORE (3.10 IN.)

INNER SKIN 1 PLY GRAPHITE FABRIC 0.015" TYP.

B-B

2 B SIDES AS SHOWN

NOVEX CORE 25 THICK (3.10 IN.)
(TYP TOP & BOT)

2 PLYS GR CLOTH 445° (0.052) OUTER SKIN
1 PLYS GR CLOTH 445° (0.052) INNER SKIN
(TYP TOP & BOTTOM COVERS)

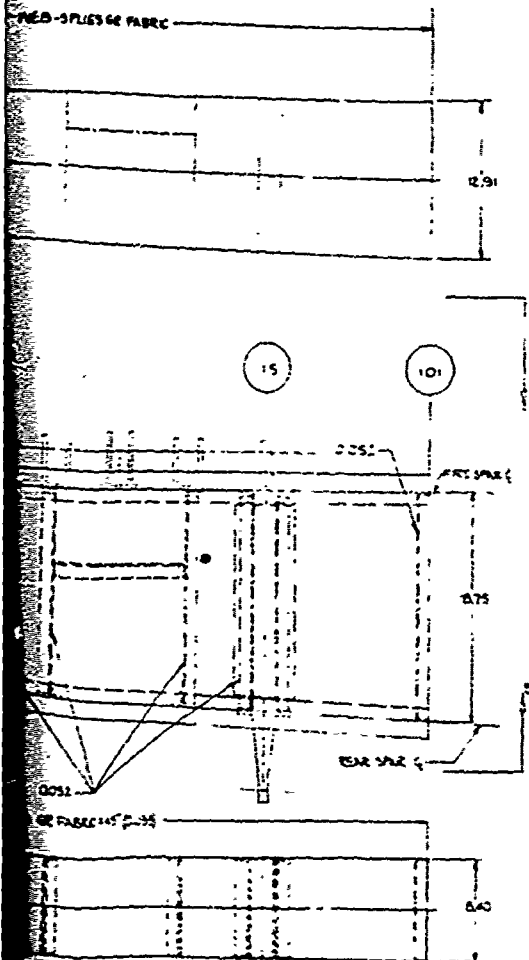
4 PLYS GR CLOTH 445°
(TYP FOR T.S. & R.S.)
(0.052)

CONCEPT NO. 1

FOR ATTACHMENT ALBIE
GR FABRIC 245° 4 PLYS

D-D
FULL SIZE
TYPICAL CROSS SECTION

FULL SIZE
TYP CROSS SECTION



MATERIAL
 GRAPHITE FABRIC-MERKEL T800 81 STYLE/POLYSULFONE
 GRAPHITE TAPE-MERKEL AS/POLYSULFONE
 HONEYCOMB-HONEY CORE 25 HONES THICK, 3.10:1.0, HIGHER DENSITY IN ATTACH AREA

DETAIL FABRICATION
 TOP & BOTTOM COVERS
 1) SKIN CONSOLIDATION - HOT PRESSING, AUTOCLAVE OR PULTRUSION
 2) MACHINE HONEYCOMB TO THICKNESS
 3) ASSEMBLE SANDWICH BY BONDING FIBER
 4) TON

OPTION 2
 1) MACHINE HONEYCOMB
 2) ASSEMBLE COVERS BY PULTRUSION
 3) STEM

SPARS
 1) LAMINATE CONSOLIDATION PER SP-1 SPEC
 2) STRAIN FIBERS
 3) POST FORM CHORD ANGLES
 4) BOND SPAR ASSEMBLY BY FUSION
 OPTIONAL: FIBERGLASS LAMINATE (CONSIDERATION AND FORMING ALTERNATE FLANGES) AT THE SAME TIME

RIBS
 1) LAMINATE CONSOLIDATION PER SP-1 SPEC
 2) LAMINATE'S BLANKED AND TONED
 3) FLANGES (2) POST FORMED
 4) RIB ANGLES (2) BUILT AND POST FORMED
 5) RIB ANGLES INSTALLED SEPARATELY TO PROVIDE TOLERANCE PAYOFF

ELEVATOR ASSEMBLY
 TOP & BOTTOM COVERS, REAR SPAR AND RIBS ASSEMBLED BY FUSION BONDING
 FRONT SPAR AND HUB FITTING INSTALLED AT MECHANICAL ATTACHMENTS

NOTE: THIS DESIGN WILL BE UPDATED MANUFACTURING DEVELOPMENT AND FEASIBILITY STUDY RESULTS ARE OBTAINED.

ITEM	DESCRIPTION	QUANTITY	UNIT	REMARKS
1	GRAPHITE FABRIC	100	sq ft	
2	GRAPHITE TAPE	100	sq ft	
3	HONEYCOMB CORE	100	sq ft	
4	FRONT SPAR	1	pc	
5	REAR SPAR	1	pc	
6	RIBS	10	pc	
7	FLANGES	20	pc	
8	STRAIN FIBERS	100	sq ft	
9	POST FORM CHORD ANGLES	10	pc	
10	BOND SPAR ASSEMBLY	1	pc	
11	FIBERGLASS LAMINATE	100	sq ft	
12	CONSIDERATION AND FORMING ALTERNATE FLANGES	100	sq ft	

Figure 121. Honeycomb Stiffened Design Concept

Table 32. Cost Summary -- Graphite/Polysulfone YC-14 Elevator

	UNIT	PRODUCTION HOURS	MATERIAL DOLLARS	TOOLING HOURS	TOTAL COST DOLLARS
HONEYCOMB	1	1,087	1,654	2,075	96,520
	10	7,735	16,540	2,075	310,840
	100	47,560	165,400	2,075	1,654,470
CORRUGATED	1	1,185	1,600	2,870	123,250
	10	8,432	16,000	2,870	355,075
	100	51,848	160,000	2,870	1,801,555
"Z" STIFFENED	1	1,468	1,650	2,106	108,870
	10	10,446	16,500	2,106	393,060
	100	64,230	165,000	2,106	2,155,080

Additional areas that were considered and evaluated prior to selecting a concept for further evaluation were inspectability and repairability. The stiffener stabilized panel concept scored highest in these areas. Both the honeycomb and corrugated designs incorporate areas that have restricted accessibility and were therefore more difficult to inspect. The stiffener concept resembles present metal construction and therefore would more likely lend itself to established repair procedures.

As a result of the preliminary design study, the stiffener stabilized panel concept was selected for further design refinement and hardware evaluation. The manufacturing techniques required for producing this concept were applicable to the other two. Techniques and processes in areas of consolidation, post-forming, bonding, and mechanical assembly would be applicable for all three. This concept was not the most cost effective of the concepts studied but it still represented a significant cost saving when compared to the existing aluminum design. This design has greater accessibility and therefore is easier to inspect. The configuration of the stiffener stabilized panel concept closely resembles commonly used metal designs and therefore its development would be more applicable to aircraft design.

7.3 DETAIL DESIGN AND ANALYSIS

A final design of a graphite-polysulfone YC-14 outboard elevator was prepared. It was based on a stiffener stabilized concept as a result of the conclusions reached in the preliminary design studies. The elevator component was designed to be a direct replacement for the existing YC-14 aluminum elevator. Design drawings were sufficiently detailed to supply all the manufacturing information required to fabricate the elevator component.

The composite design was analyzed to show that all design requirements were met. A finite element model of the elevator was prepared. A Structural Analysis Method for Evaluation of Complex Structures (SAMECS) computer program utilized this model to establish the structural stiffnesses and internal loads. These loads were used for performing detail stress analysis.

7.3.1 Design

The Gr/Ps YC-14 elevator was designed to be a direct replacement for the existing aluminum design. Its reaction link, actuator and rib hinge fitting stations were the same. It incorporated two splices at locations shown in Figure 122 to accommodate available facilities. It had the same envelope, spar and cover locations as the existing design. The composite design also provided the same clearances and offsets required to permit the installation of the adjacent fairings (Figure 123). Its torsional and bending stiffnesses closely matched existing aluminum design.

Design drawings were prepared in sufficient detail to supply the manufacturing information required to build the composite elevator. These drawings are shown in Figure 124 through 129.

A design study was made of the different thermal growth between the composite elevator and adjacent structures and the associated adjustments required in design. It was determined that for the maximum spread in design temperatures (-65° to 160°F) the differential growth between the composite elevator and interfacing aluminum structure would be 0.72 in. Two fitting designs had been developed on other programs which permitted the required differential movements. These fittings had been mocked-up as part of their evaluation and both were found functionally acceptable. The design selected for the AFRTF elevator is shown in Figure 130.

7.3.2 Analysis

A "SAMECS" finite element model of the YC-14 graphite-polysulfone elevator box was developed and used to determine deflections and internal loads for use in designing the box. Figure 131 shows a plot of the model, which contains 565 nodes, 623 plates, 634 beams, and 32 load cases. Every rib and stiffener in the elevator box had been included in the finite-element model. The load cases considered include air pressure loads, actuator loads and imposed deflections at hinge points due to stabilizer deflection. The internal loads developed from the "SAMECS" analysis were used to check the buckling strength of the upper and lower surface skins and the spar webs using the "STAGS-C" finite-difference buckling analysis program. The finite-element model was also used in determining the ability of the design to attain ultimate load conditions.

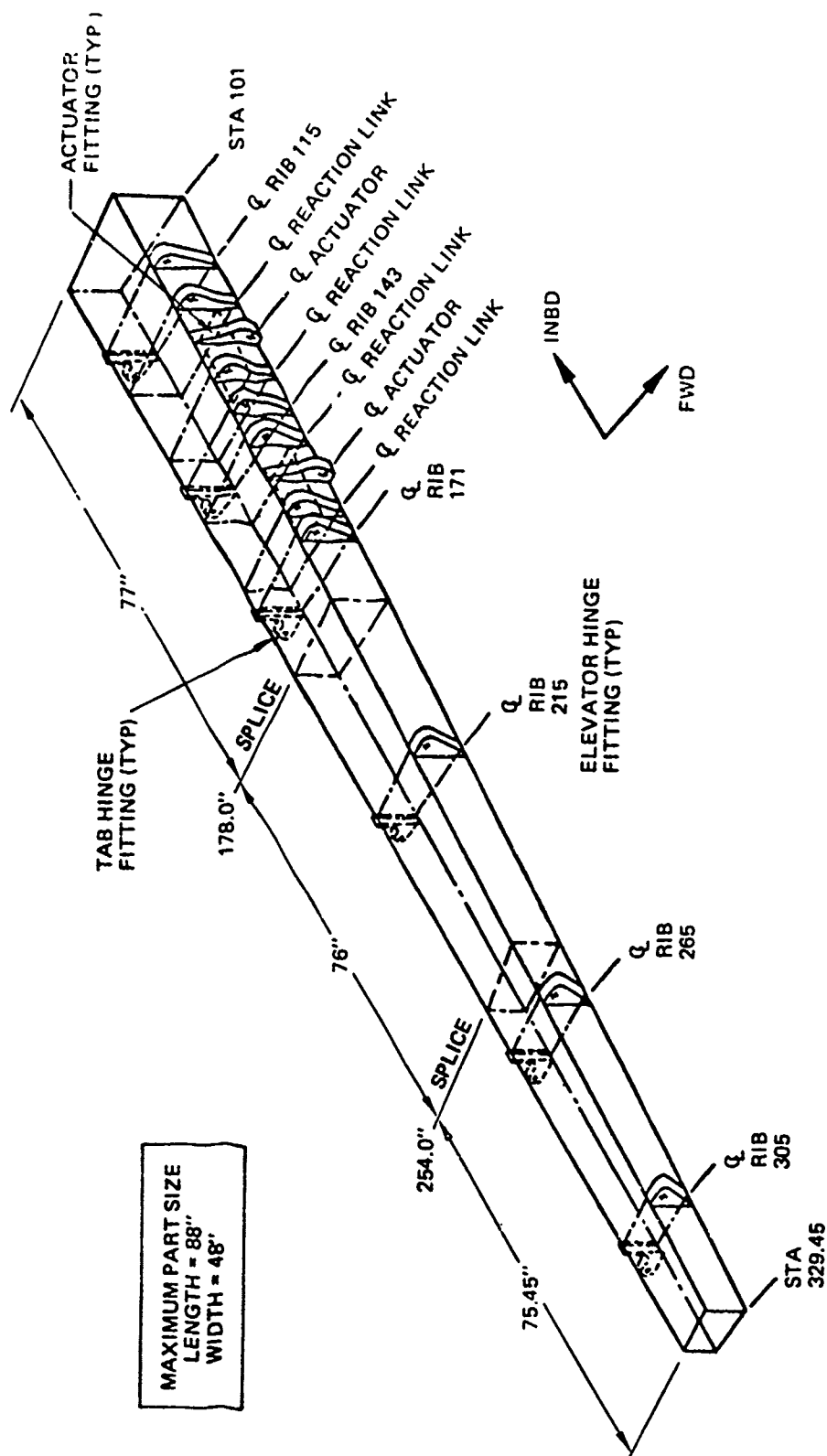


Figure 122. Elevator Splice Locations

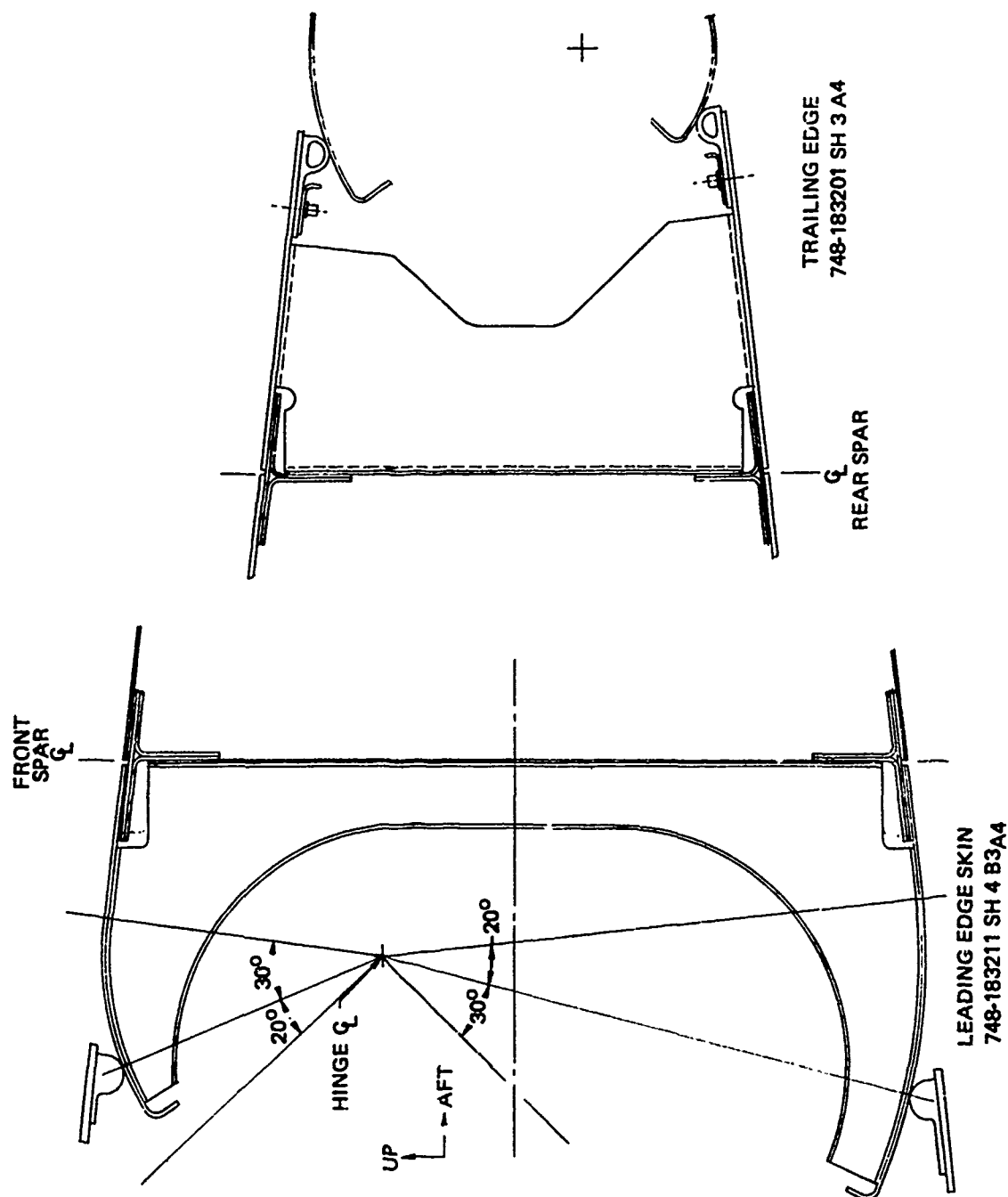
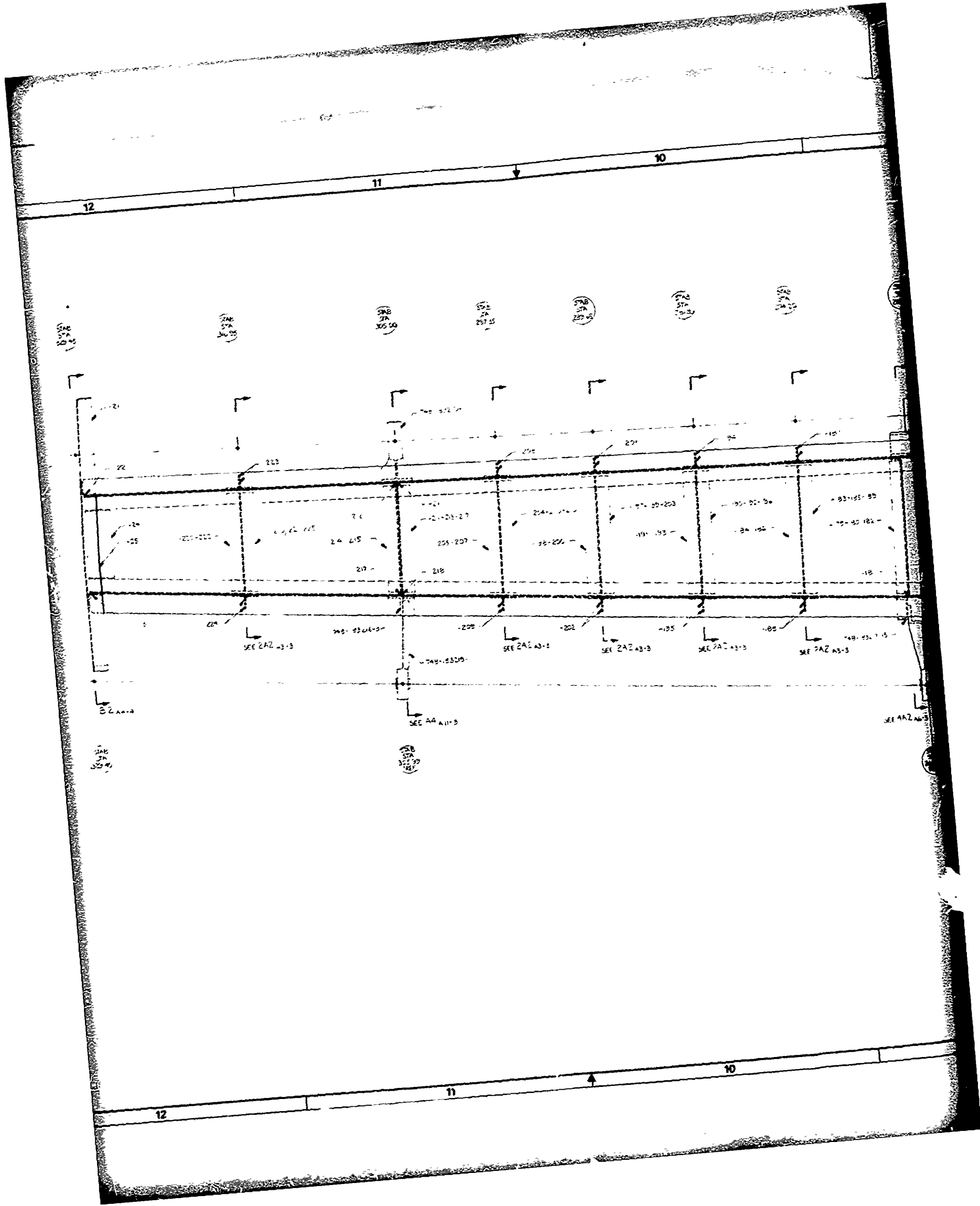


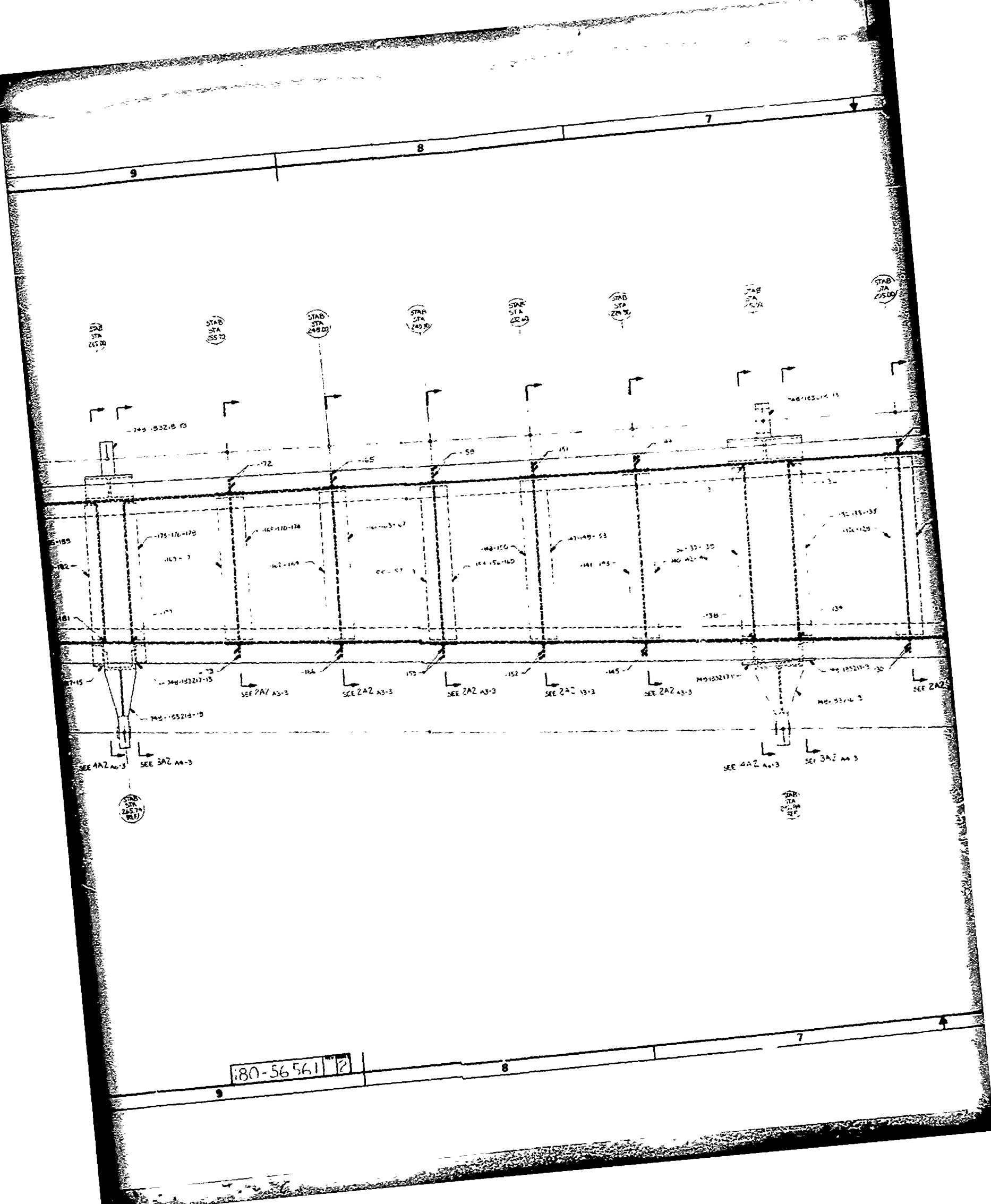
Figure 123. YC-14 Elevator Fairings

[illegible]

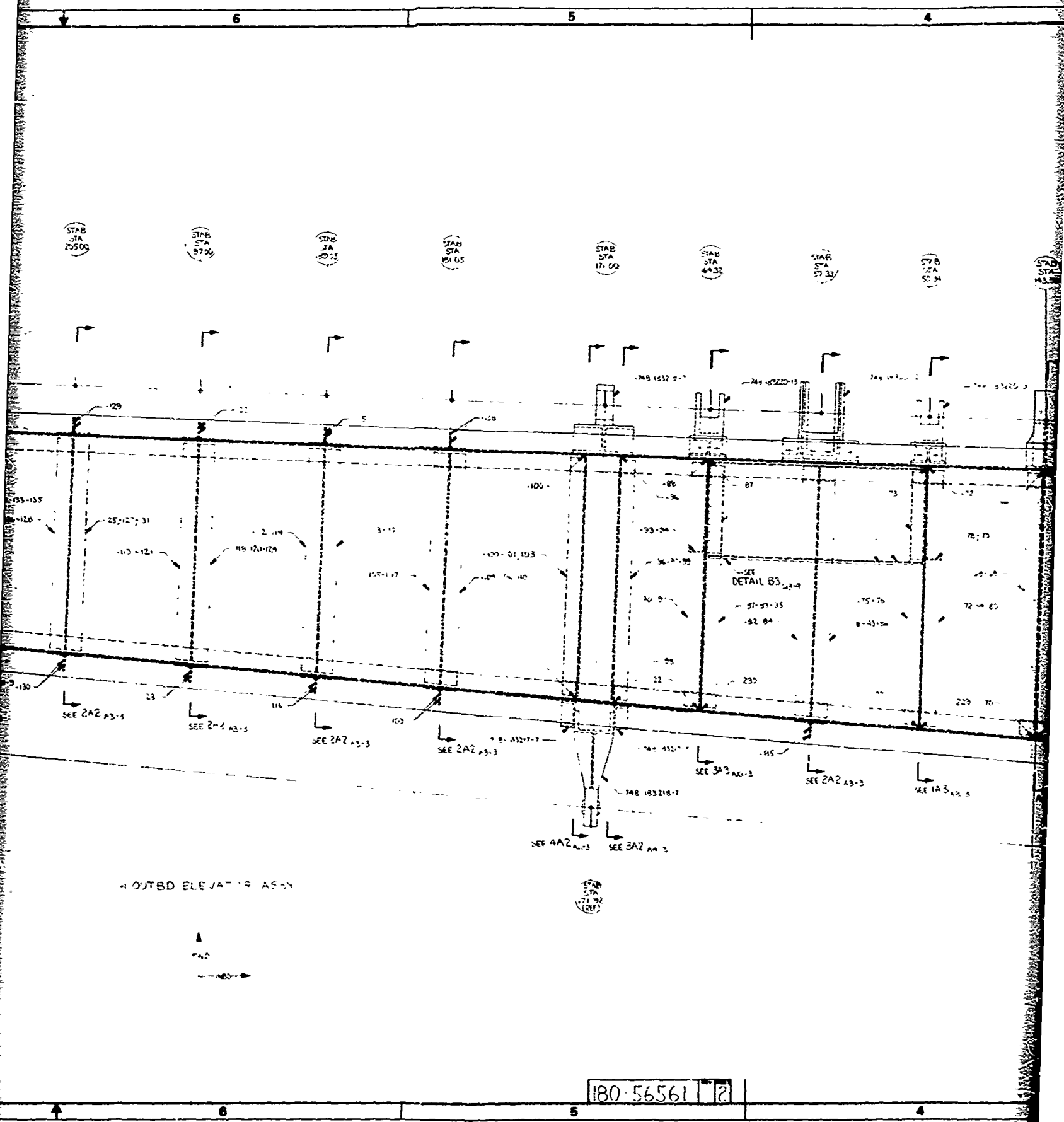
6											5																																																																																																																																																																																																																																																																																																																																																																																																																																																																																																																																																																																																																																																																																																																																																																																																																																																																																																																																																																																																																																																																																																																																																																																																																																																																																																																																																																																																				
									2																																																																																																																																																																																																																																																																																																																																																																																																																																																																																																																																																																																																																																																																																																																																																																																																																																																																																																																																																																																																																																																																																																																																																																																																																																																																																																																																																																																																						

130	56,56	19,95	1
-----	-------	-------	---





180-56561 2



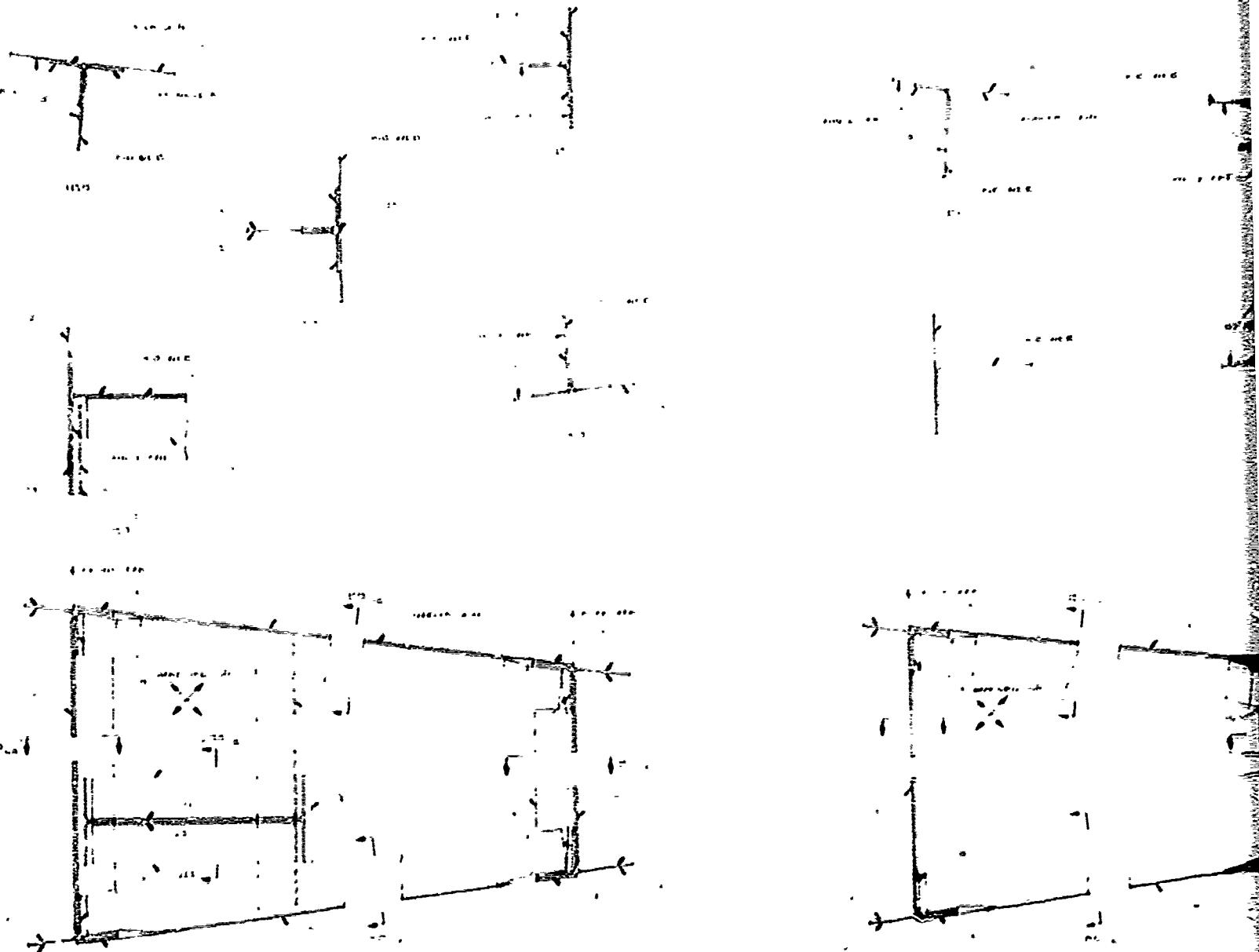
H OUTSD ELEVATION AS SH



STAB
STA
171.02
(REF)

180-56561 2

TABLE V



NOTES: 1. THE ABOVE DIAGRAMS ARE FOR INFORMATION ONLY. 2. THE ABOVE DIAGRAMS ARE NOT TO BE USED FOR DESIGN PURPOSES. 3. THE ABOVE DIAGRAMS ARE NOT TO BE USED FOR CONSTRUCTION PURPOSES.

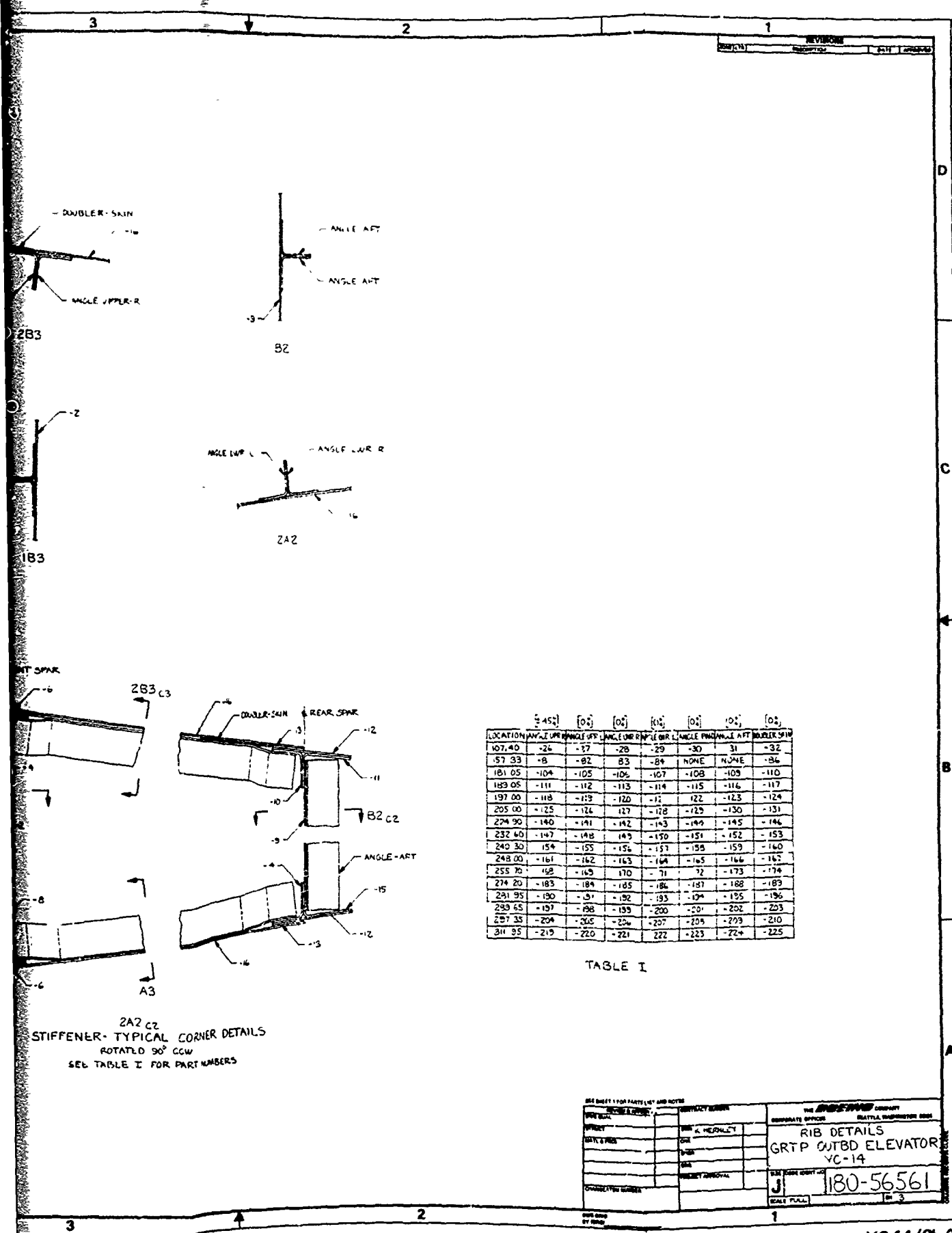
ITEM NO.	DESCRIPTION	QUANTITY	UNIT	REMARKS
1	VALVE	1	PC	
2	PIPE	1	PC	
3	PUMP	1	PC	

TABLE IV

NOTES: 1. THE ABOVE DIAGRAMS ARE FOR INFORMATION ONLY. 2. THE ABOVE DIAGRAMS ARE NOT TO BE USED FOR DESIGN PURPOSES. 3. THE ABOVE DIAGRAMS ARE NOT TO BE USED FOR CONSTRUCTION PURPOSES.

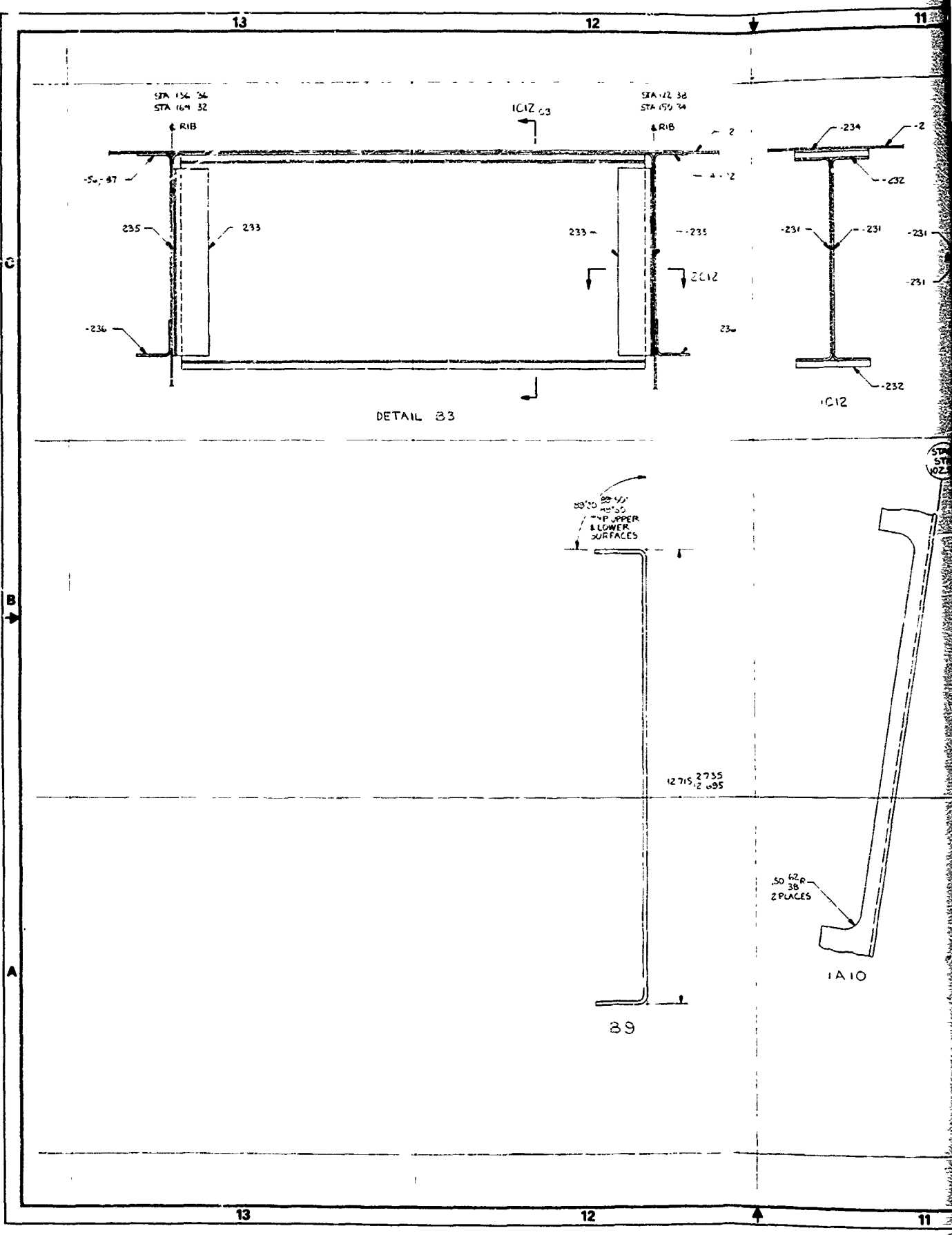
ITEM NO.	DESCRIPTION	QUANTITY	UNIT	REMARKS
1	VALVE	1	PC	
2	PIPE	1	PC	
3	PUMP	1	PC	

TABLE V



191 Figure 126. GRTP Outboard Elevator YC-14 (Sh 3)

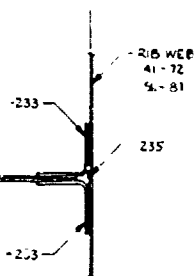
180-262614



10

9

8



2C12
TYP BOTH ENDS

STAB
STA
102.50

TRACE
& FRONT SPAR

39A12

TRACE
& REAR

17 (545)

021-18

WARP DIRECTION

1A10A11

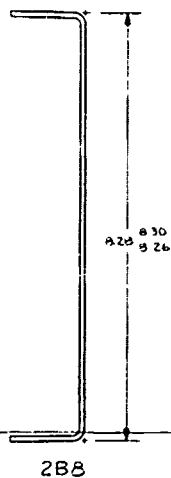
1A2
EXPOSE RIB STA 101.00
ROTATED 96 CCW

180-56561 4

10

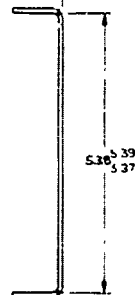
9

8

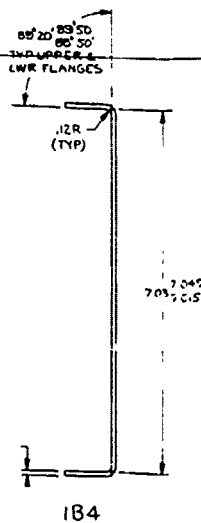


2B8

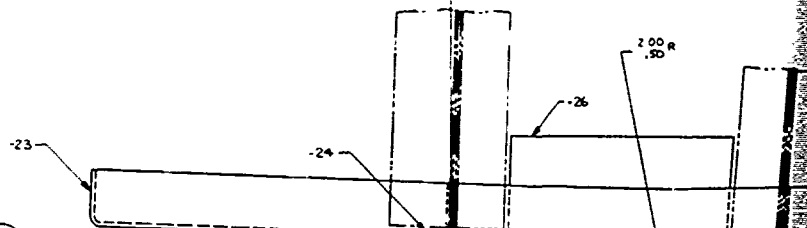
STAB
STA
329.45



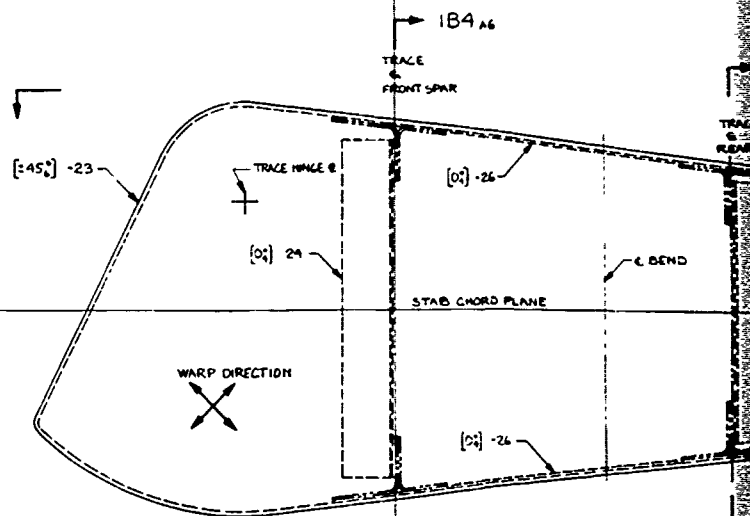
2B4



1B4



B3



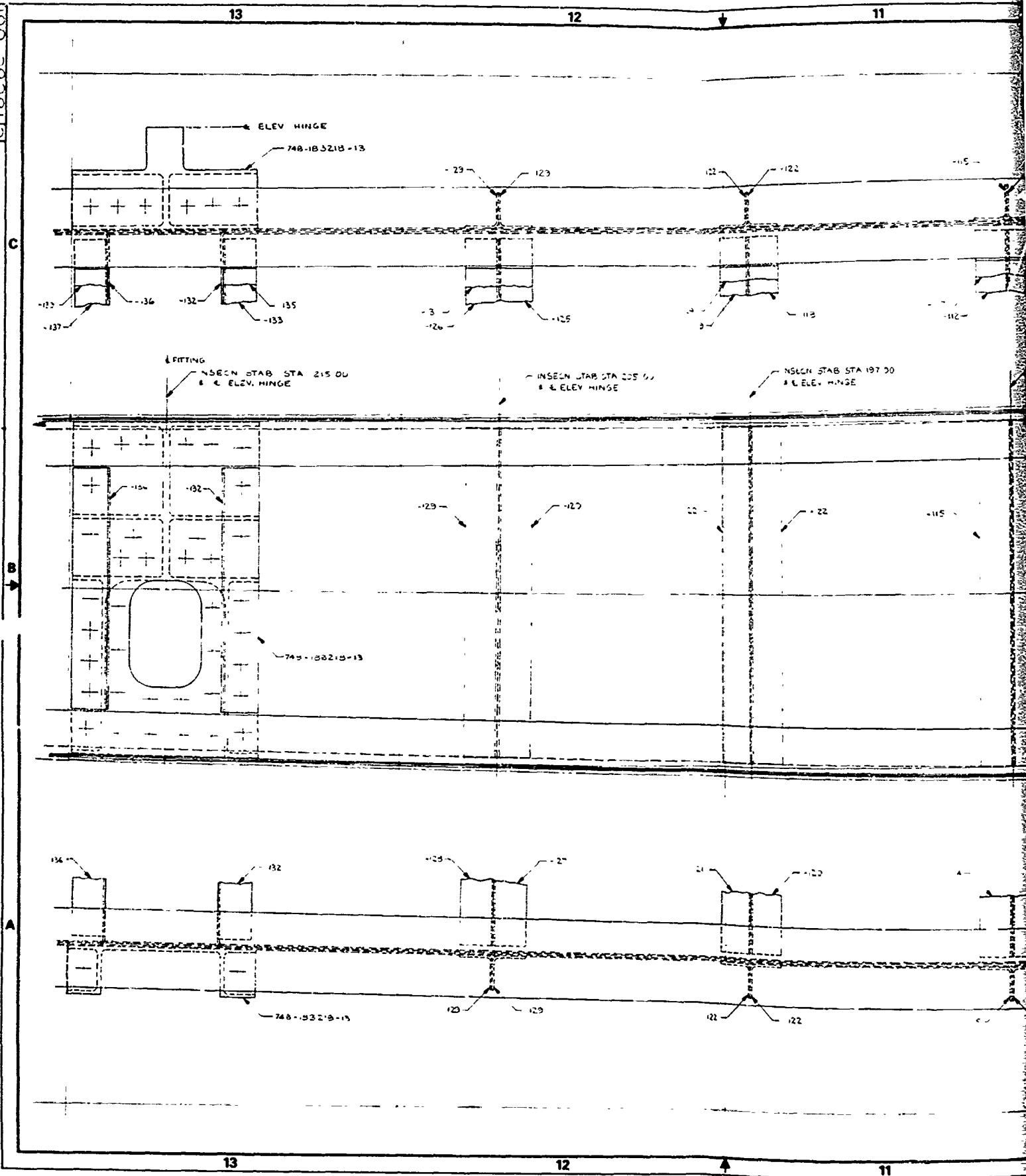
B12
CLOSURE RIB STA 329.45
ROTATED 90° CCW

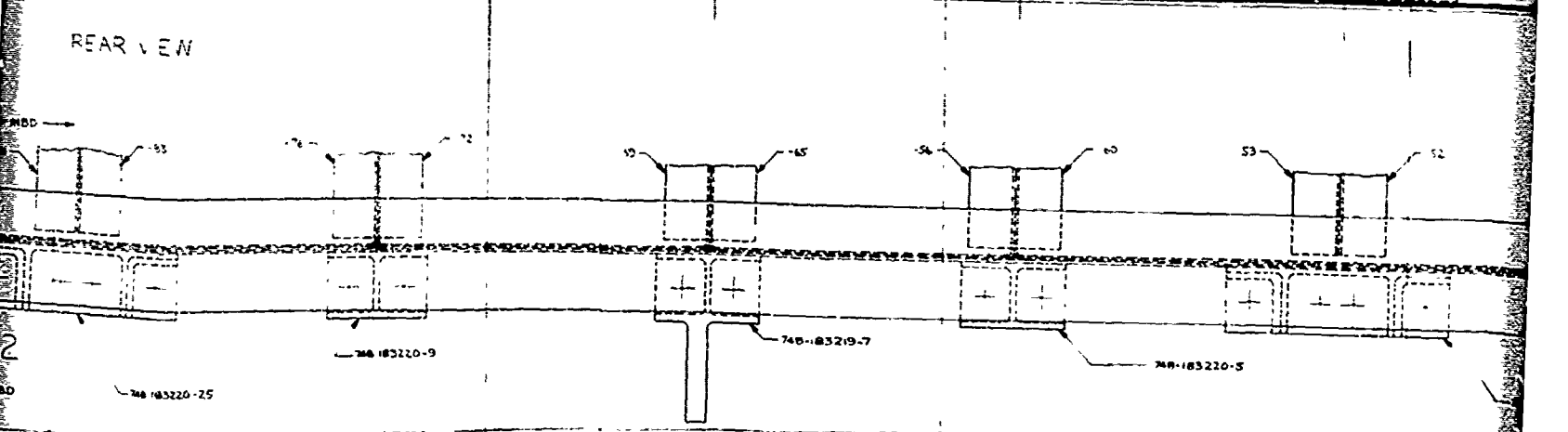
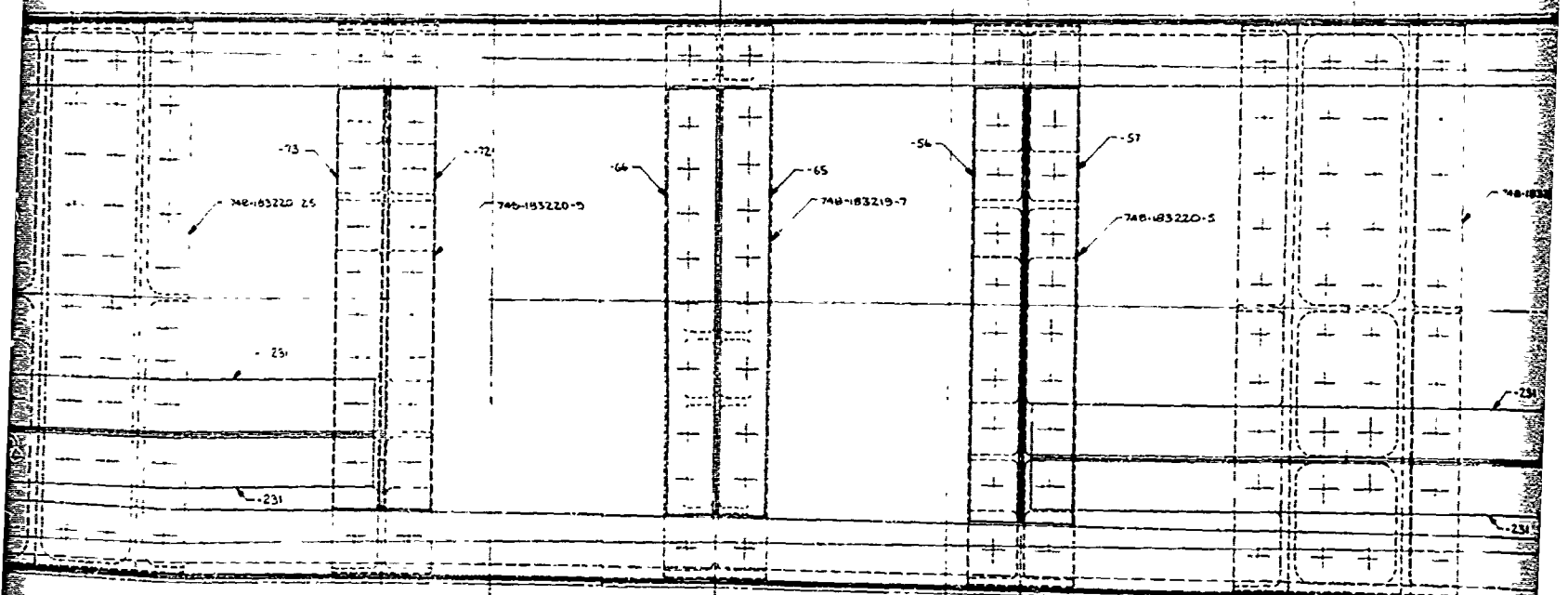
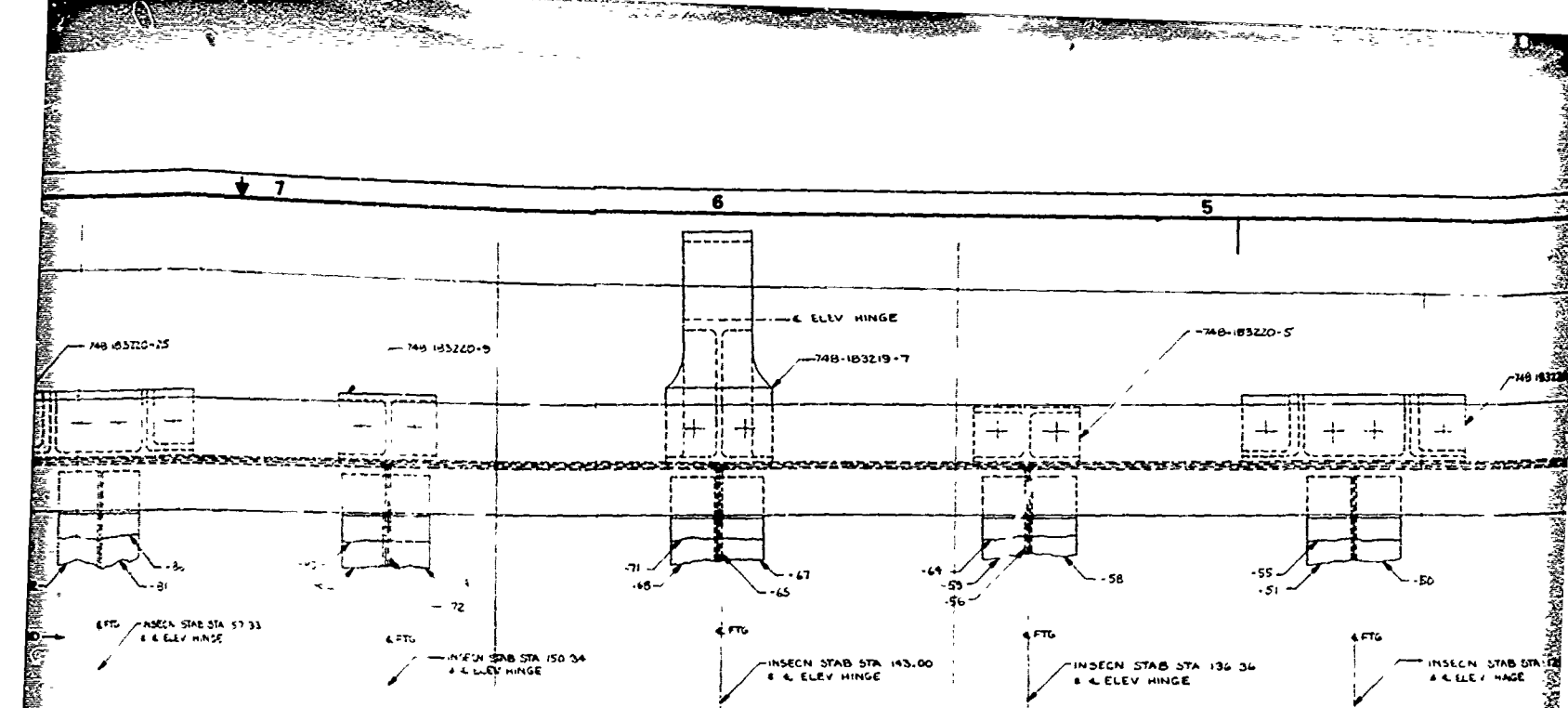
180-56561 4

180-54561 4

193 **Figure 127. GRTP Outboard Elevator YC-14 (Sh 4)**

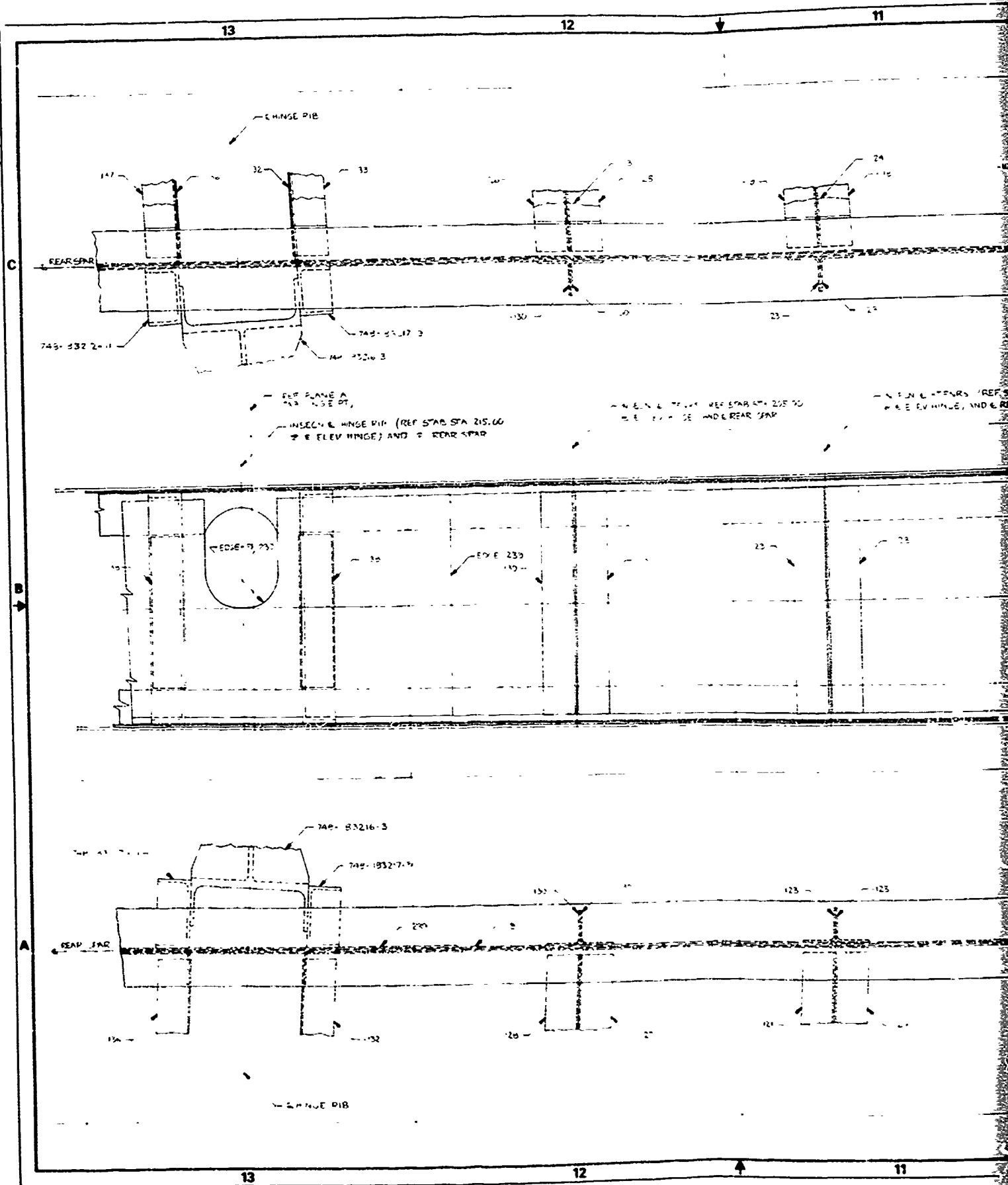
180-2020112

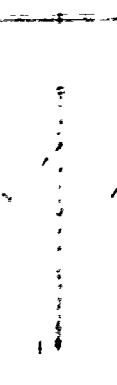
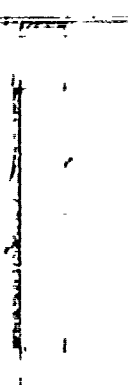
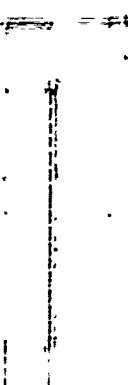
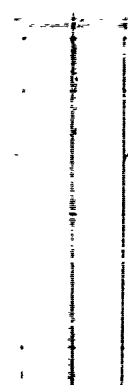
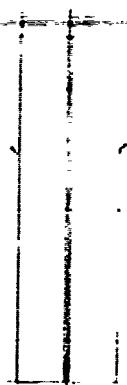
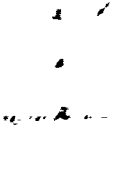
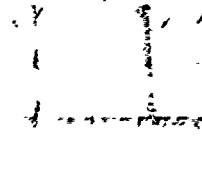
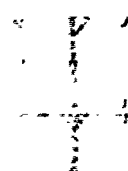
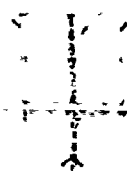


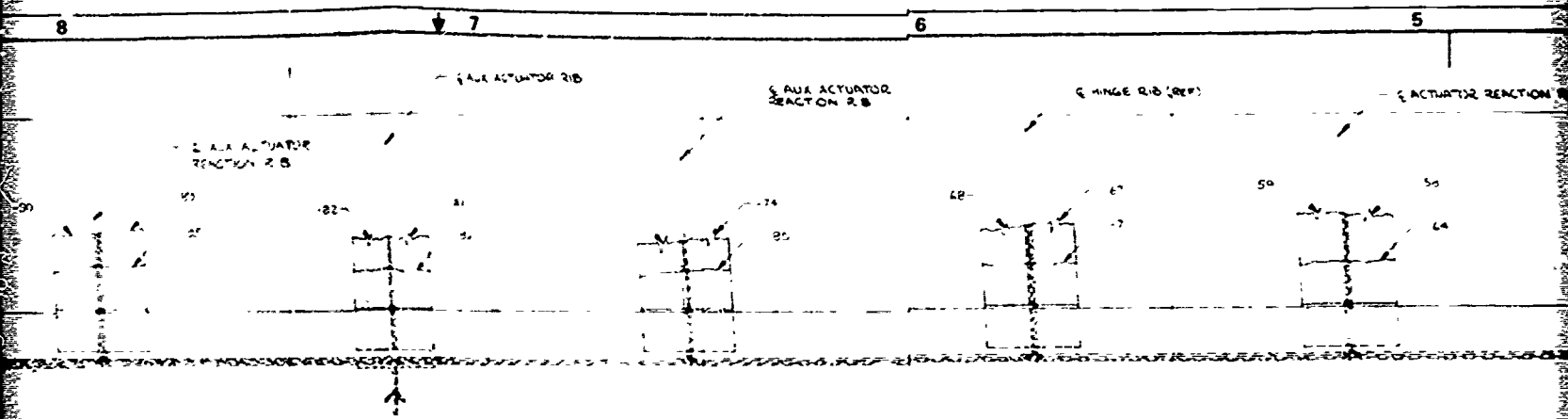


180-56561 5

180 26761 7







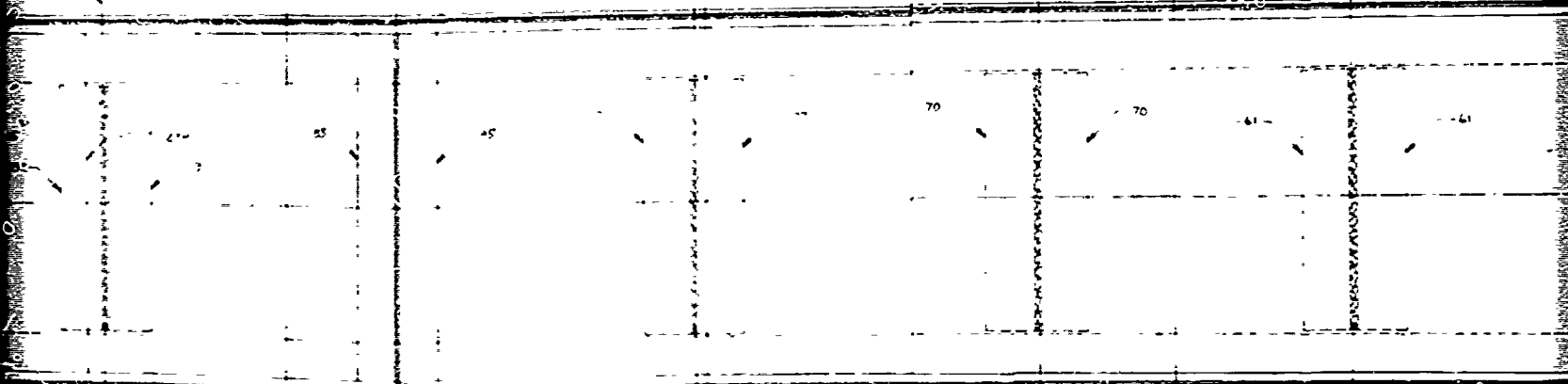
PLAN VIEW

1. AUX ACTUATOR RIB
2. AUX ACTUATOR REACTION RIB
3. HINGE RIB (REF)
4. ACTUATOR REACTION RIB

1. HINGE RIB (REF)
2. HINGE RIB (REF)
3. HINGE RIB (REF)
4. HINGE RIB (REF)

1. HINGE RIB (REF)
2. HINGE RIB (REF)
3. HINGE RIB (REF)
4. HINGE RIB (REF)

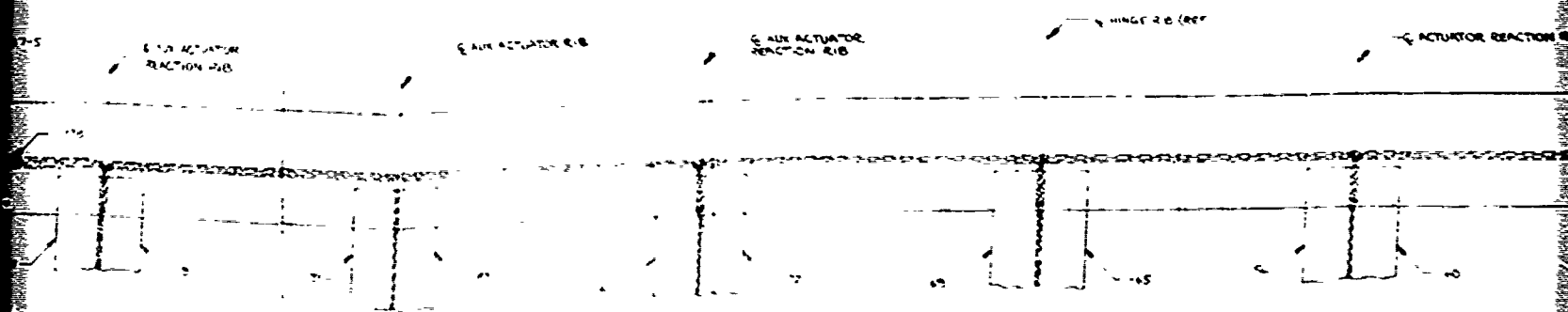
1. HINGE RIB (REF)
2. HINGE RIB (REF)
3. HINGE RIB (REF)
4. HINGE RIB (REF)



SIDE VIEW

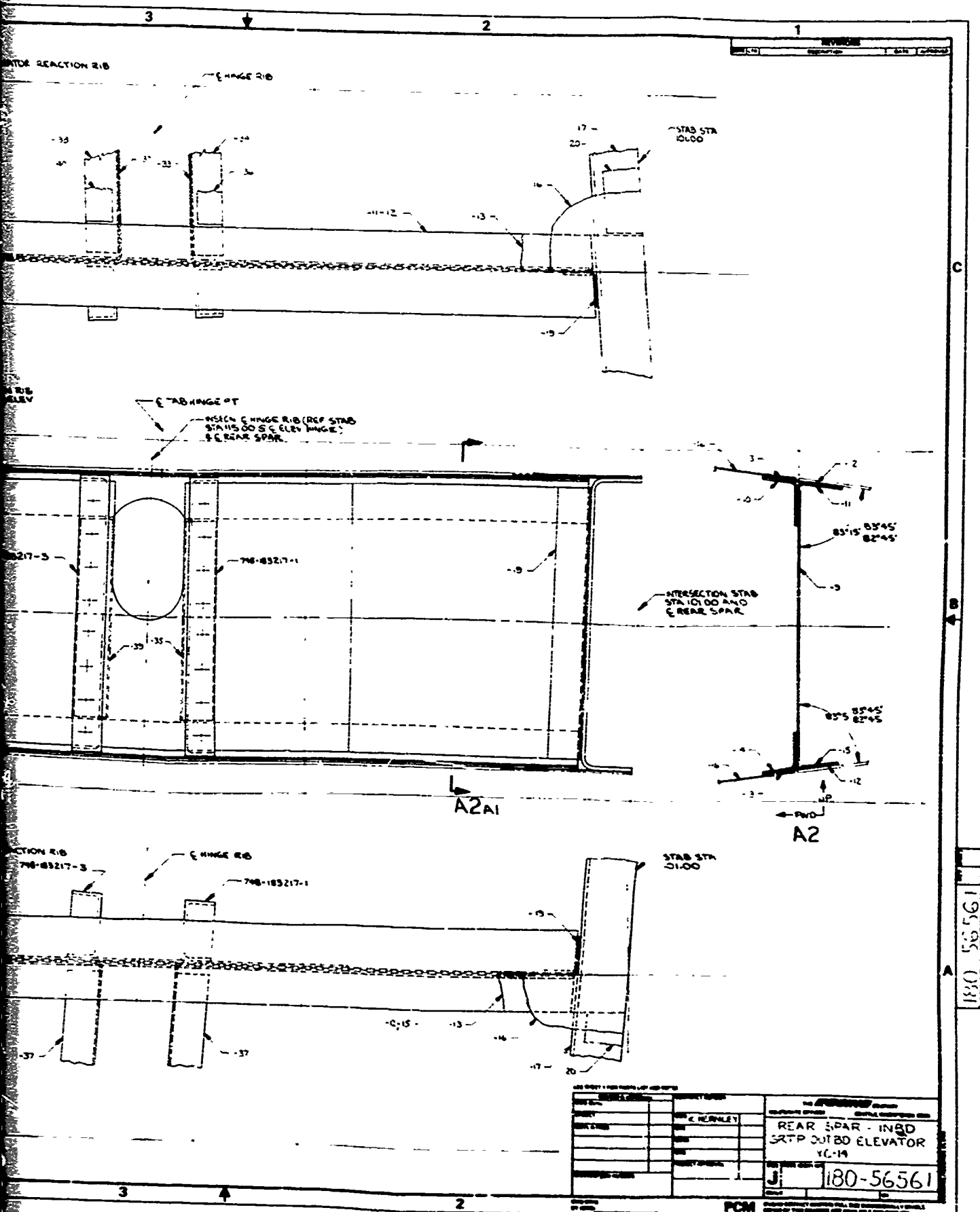
1. HINGE RIB (REF)
2. HINGE RIB (REF)
3. HINGE RIB (REF)
4. HINGE RIB (REF)

1. HINGE RIB (REF)
2. HINGE RIB (REF)
3. HINGE RIB (REF)
4. HINGE RIB (REF)

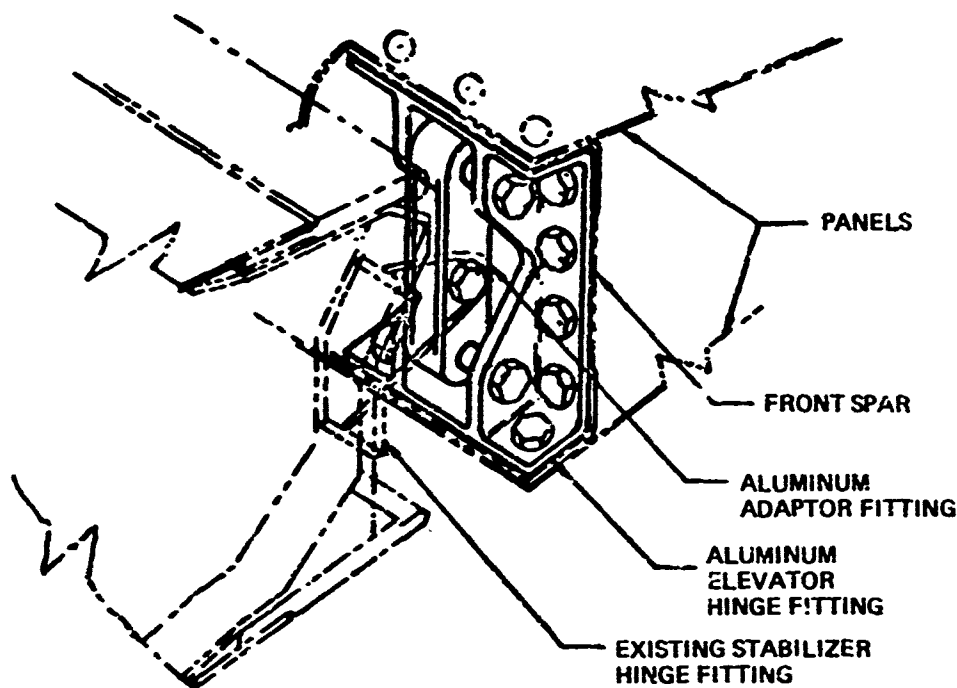


BOTTOM VIEW

180-56561



197 Figure 129. GRTP Outboard Elevator YC-14 (Sh 6)



$$\Delta T = -65^{\circ} - 160^{\circ} = 225^{\circ}\text{F}$$

$$\Delta \alpha = 13 \times 10^{-6} - 1 \times 10^{-6}$$

$$= 12 \times 10^{-6} \text{ in/in/}^{\circ}\text{F}$$

$$\text{DIFFERENTIAL GROWTH} = \Delta T \times \Delta \alpha \times L$$

$$= 225 \times 12 \times 10^{-6} \times 228.45$$

$$= 0.62''$$

Figure 130. Differential Thermal Growth

YC-14 GR/PS ELEVATOR
 3D PLOT OF ELEMENTS W/O ELEMENT NUMBERING - INPUT PLOT 1
 **PLOT DISTORTED PROJECTION (IS - 1)
 JAFR DEFINED SCALE FACTORS ACTUAL SCALE FACTOR:
 X = 1.000E-01 X = 1.000E-01 ANGLES MEASURED X AXIS IS
 Y = 1.000E-01 Y = 1.000E-01 COUNTER CLOCKWISE Y AXIS IS
 Z = 1.000E-01 Z = 1.000E-01 FROM HORIZONTAL Z AXIS IS

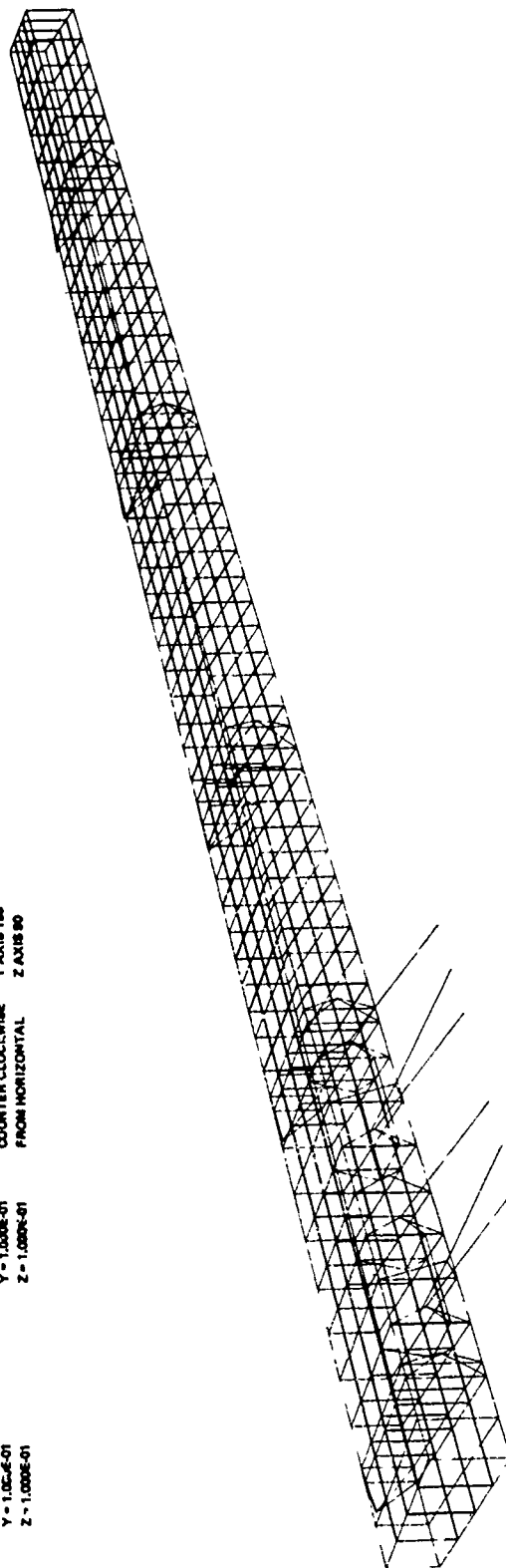


Figure 131. YC-14 GR/PS Elevator SAMECS Plot

8.0 FULL-SCALE ELEVATOR TOOLING AND FABRICATION

Three full-scale GRTP YC-14 elevators were fabricated. They were assembled in three sections to accommodate available facilities and present technology. The assembly splice locations are shown in Figure 122. The materials were initially compacted, cut and formed into details and then assembled into subassemblies. These were built into the three major assemblies as summarized in Figure 132. These were then spliced together to form the completed elevators.

8.1 ELEVATOR DETAIL FABRICATION

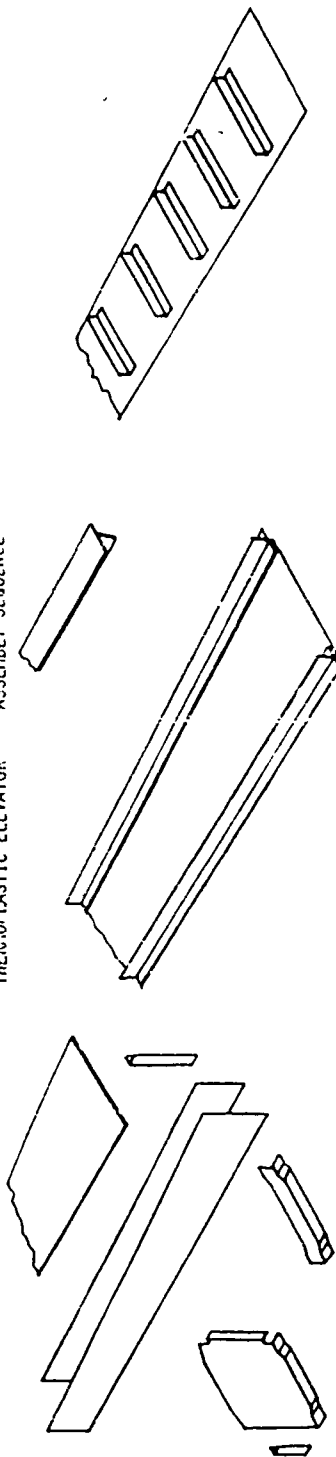
Front and rear spar stiffeners were molded using match die tooling. A four-ply pre-mold material was placed in a die which was then put in a press. This assembly was heated to 650°F and held at 200 psi for 15 minutes. The dies were then removed from the hot press and placed in a cold press until parts cooled below 250°F. Figure 133 shows molded stiffener details on the left and pre-mold layup in the die on the right.

Rib details were also molded using match die tooling. The male tool was machined from plate and the die cover was formed in a hydropress. Figure 134 shows the rib tooling and a completed rib. The rib materials, four plies of fabric at $\pm 45^\circ$; was pre-formed in a press at 600°F and 200 psi. The pre-compacted ribs were then bagged and heated in an autoclave to 600°F for 30 minutes at 200 psi to complete their fabrication.

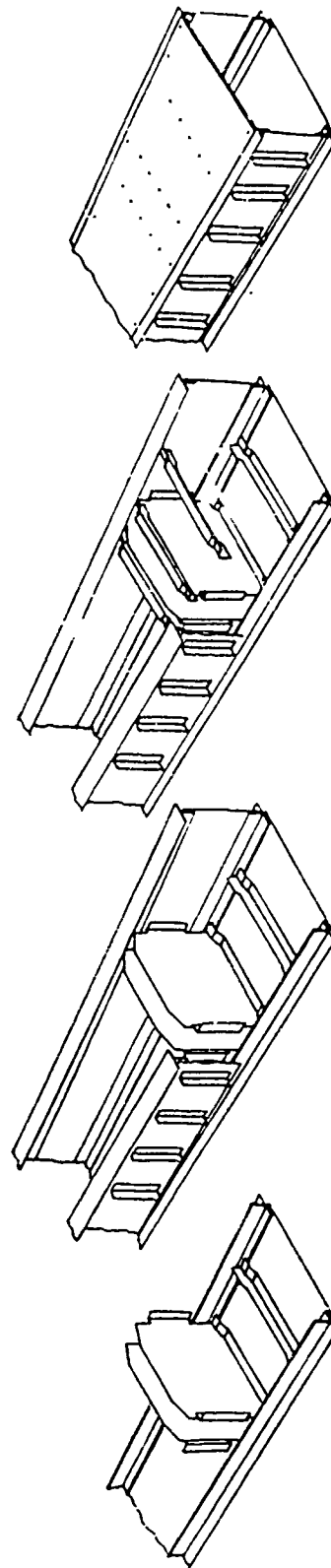
8.2 SUBASSEMBLY FABRICATION

The lower chords and skins were assembled by fusion bonding and the balance of the elevator subassemblies were assembled by adhesive bonding. The adhesive used was Hysol 9628 which was cured in an autoclave at 250°F and 50 psi. Figure 135 shows some of the rib and chord details and two of the lower skin subassemblies prior to being trimmed. Figure 136 shows some of the front and rear spar webs with their stiffeners bonded in place.

THERMOPLASTIC ELEVATOR ASSEMBLY SEQUENCE



1. FAB DETAILS
2. FUSION BOND LOWER SKIN-SPAR CHORD ASSEMBLY AND UPPER SPAR CHORDS.
3. BOND STIFFENER ANGLES TO SPAR WEBS.



4. BOND HINGE RIBS AND STIFFENER ANGLES TO LOWER SKIN-SPAR CHORD ASSEMBLY. BOND AFT ANGLES TO HINGE RIBS.
5. BOND SPAR WEB ASSEMBLIES TO LOWER SPAR CHORD-RIB ASSEMBLY. BOND UPPER SPAR CHORDS TO SPAR WEB ASSEMBLIES.
6. BOND UPPER ANGLES TO RIBS AND SPAR CHORDS.
7. MECHANICALLY FASTEN FOR SKINS.

Figure 132. Thermoplastic Elevator Assembly Sequence



Figure 133 Stiffener Match Die Tooling and Details

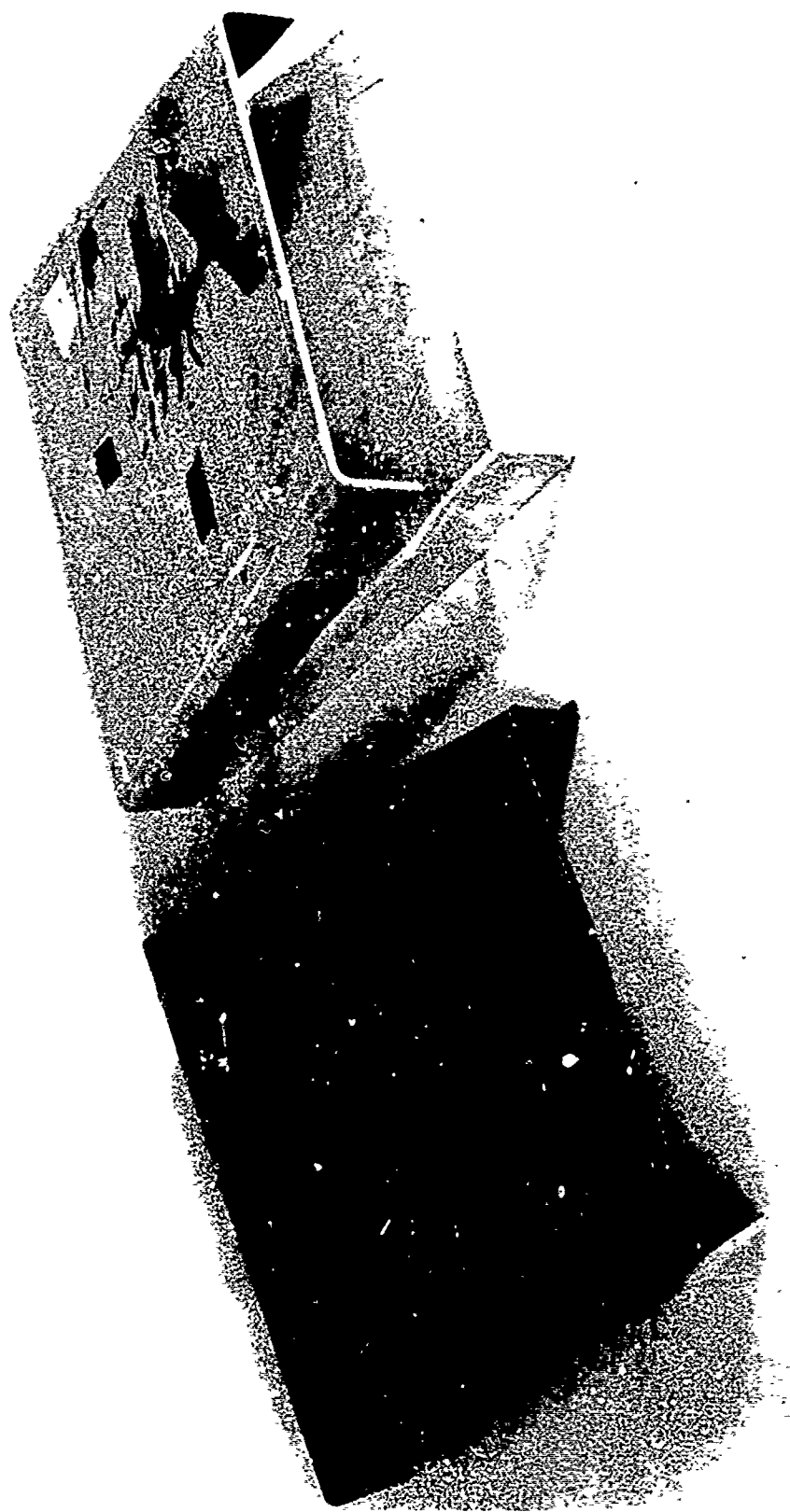


Figure 134. Matched Die Rib Tooling and Completed Rib

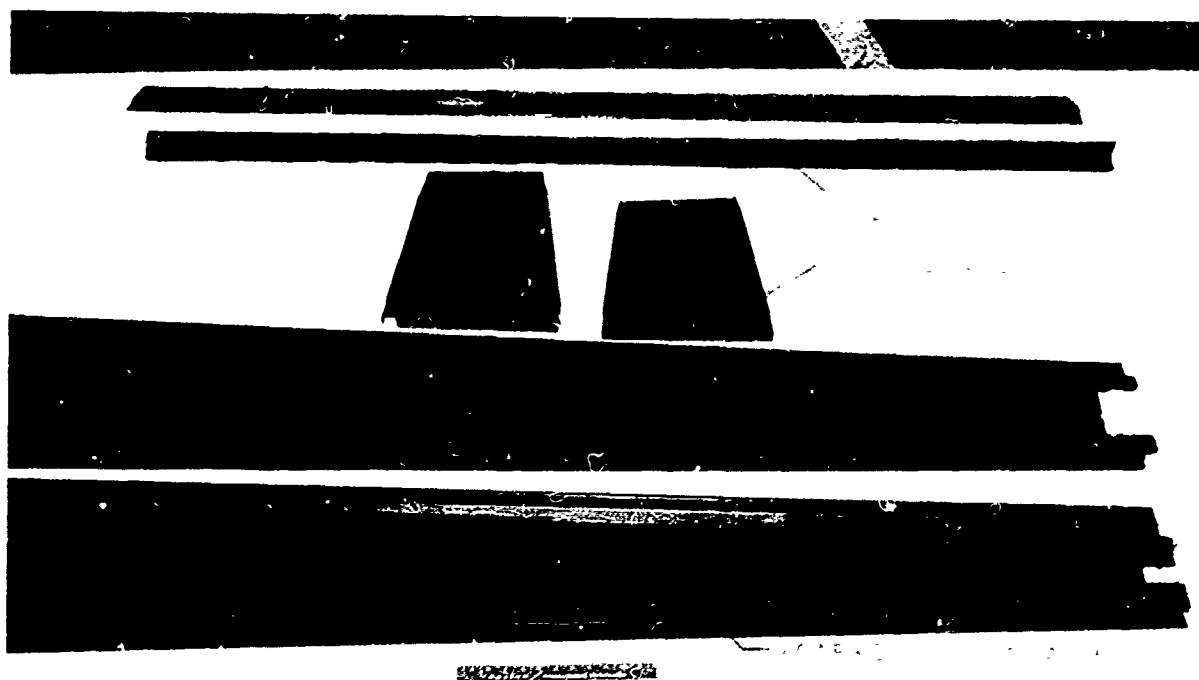


Figure 135. YC-14 Elevator Subassemblies

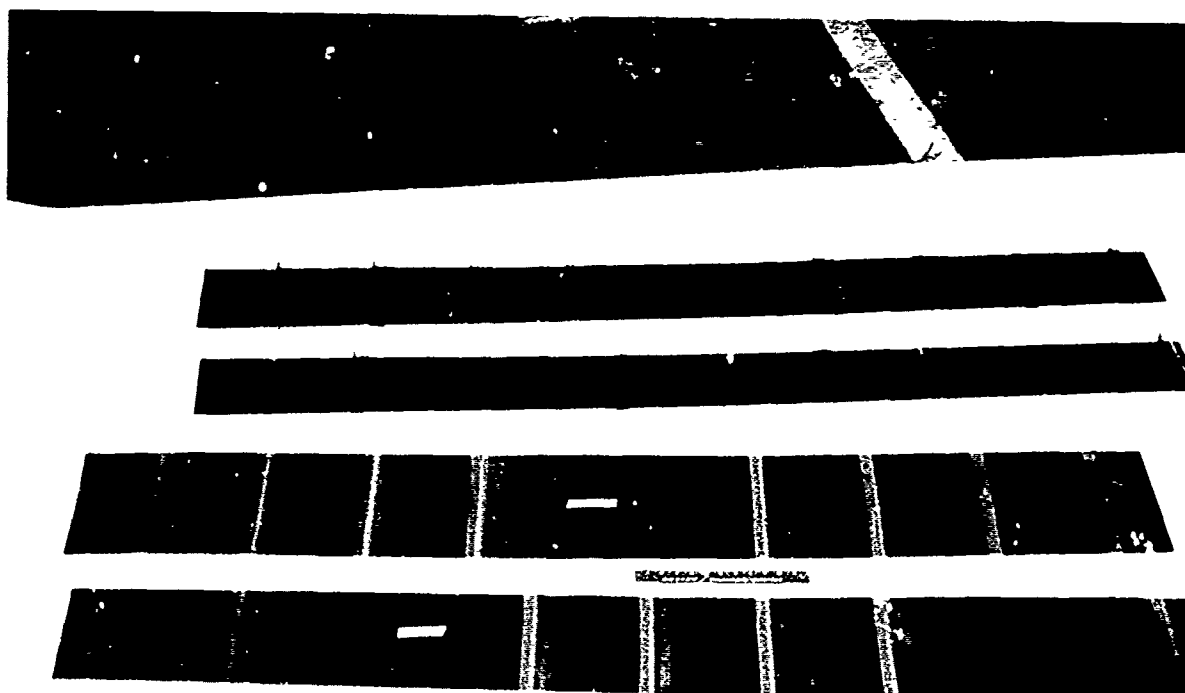


Figure 136. YC-14 Elevator Spar Web Assemblies

A fusion tool was designed to assemble the spar chords and doublers to the bottom covers by fusion bonding. This tool was made to assemble the three different size cover sections along the length of the elevator. This was accomplished by relocating one set of chord pressure bars as required to produce the various size panels.

The bottom fusion panel assemblies were made using precompacted materials and "Tee" details that were either made of pre-formed material or pre-compacted sections. The skin and doublers were cut from autoclave pre-compacted sheet stock. The initial panels used pre-formed "Tees" that were compacted during the fusion assembly cycle. The later panels incorporated pre-compacted "Tees" during assembly which produced improved components.

Prior to the fusion assembly cycle, the tools and parts were cleaned. The details were then placed in the fusion assembly tool. Figure 137 shows the details in the tool prior to the installation of the chord pressure bars. Figure 138 shows the fusion tool with the chord pressure bars in place. This assembly was then bagged, as shown in Figure 139, placed in an autoclave and processed through a fusion cycle of 30 minutes at 600°F and 200 psi. The assembly was then cooled and the assembly removed from the tool. Figure 140 shows a completed bottom panel fusion assembly.

8.3 ELEVATOR ASSEMBLY TOOLING AND FABRICATION

Two tools were fabricated to assemble the elevator sections. One tool was used for the more complex large section and the second tool was first used for the assembly of the middle section and then readjusted to hold the details for the assembly of the smaller end section of the elevator. These tools were primarily used to locate the details and provide pressure during the adhesive bonding. Figure 141 and 142 show two views of the large section tooling. Figure 143 shows a view of the middle and small section assembly. The lower cover assembly was initially located in the tool. The ribs were then locked in their proper locations after placing film adhesive at the bond interfaces (Figure 144). Rubber pads backed with metal bars were then used to distribute the bonding pressure provided by torqued set screws. This assembly was then placed in an oven and processed through the adhesive 250°F cure cycle.



Figure 137. Details Located in Fusion Assembly Tool

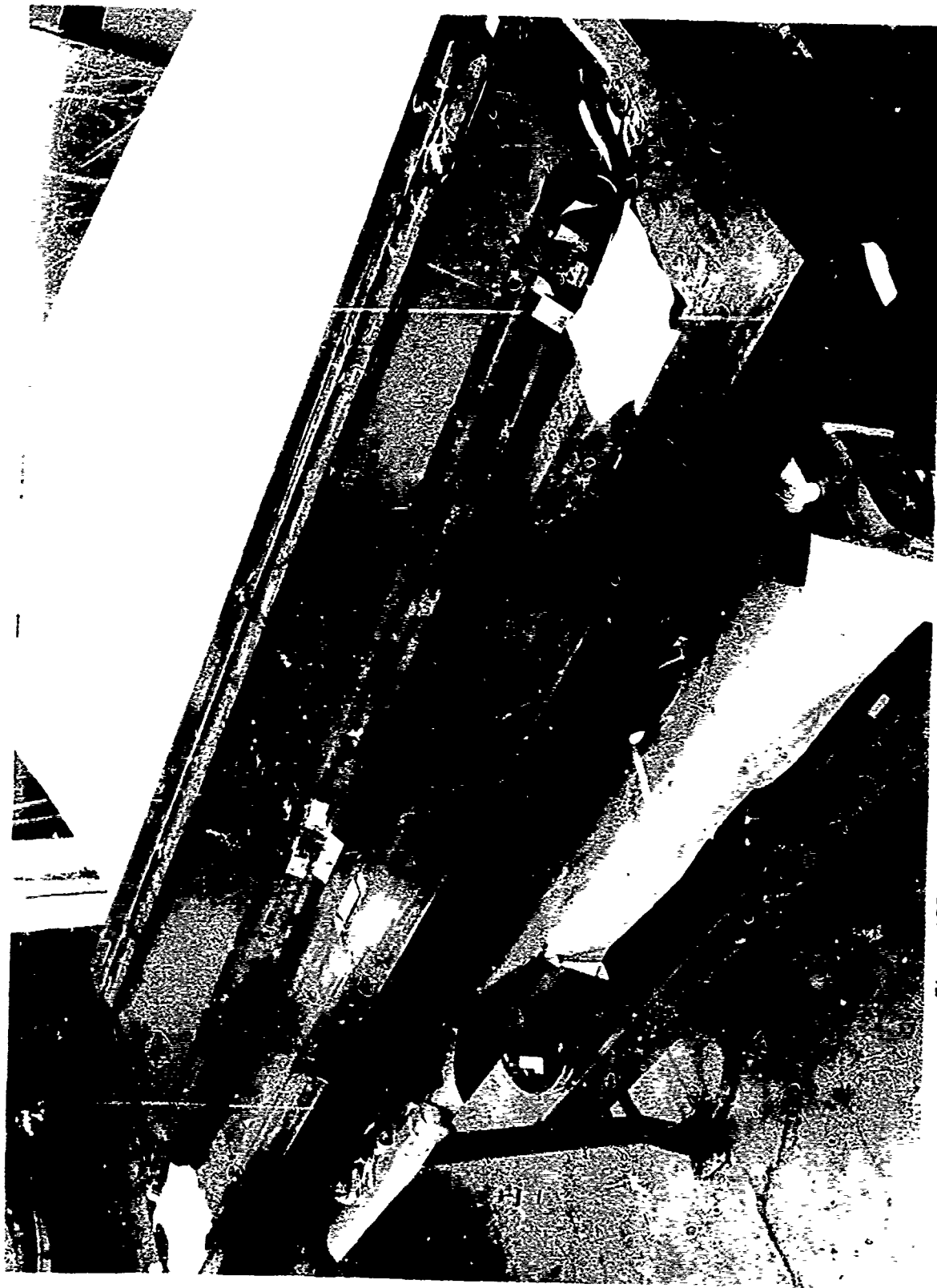


Figure 138. Details in Fusion Tool With Chord Pressure Bars in Place

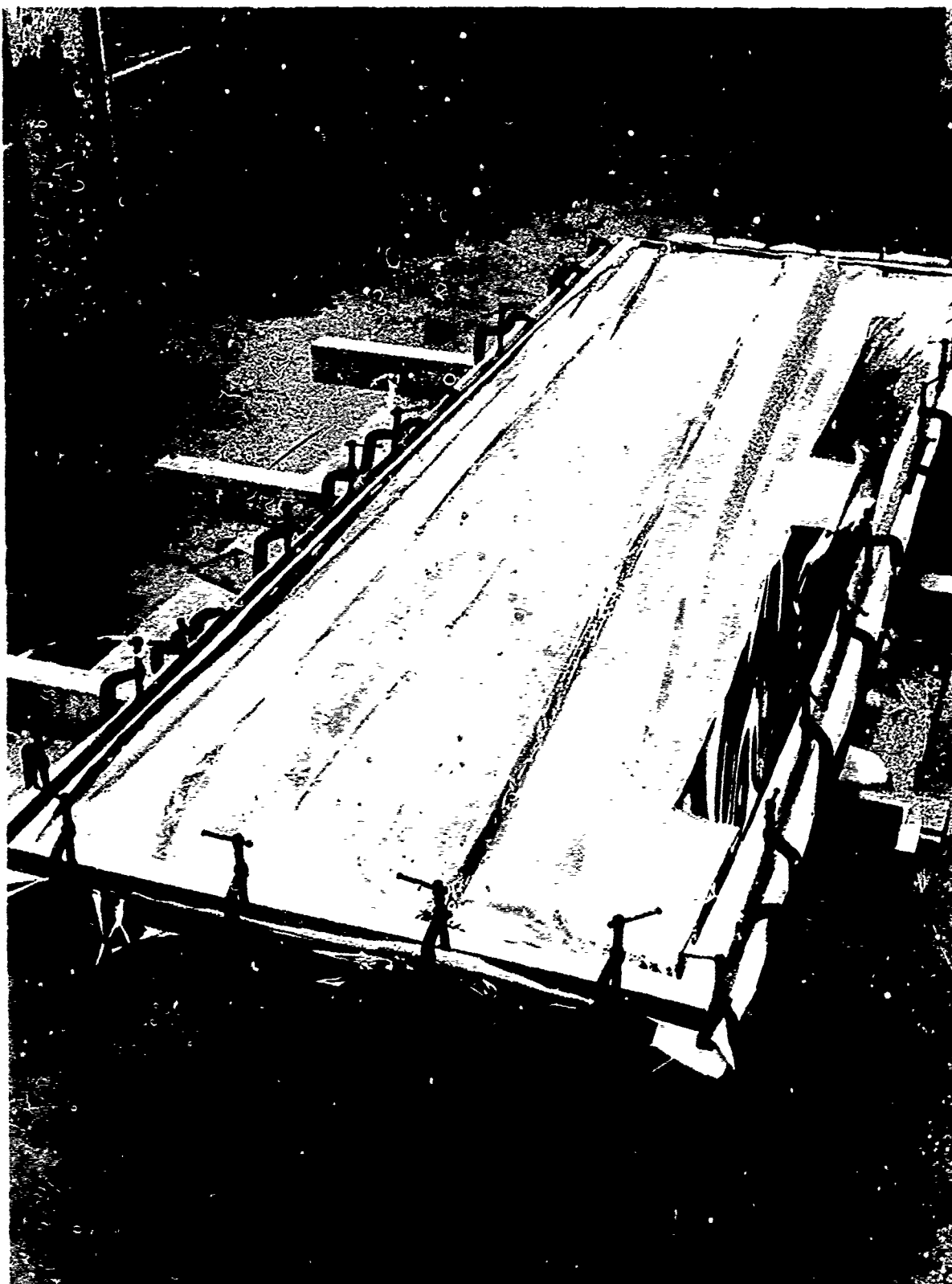


Figure 139. Fusion Tool, Loaded, Bagged and Ready for Fusion Cycle



Figure 140. Completed Side Panel Fusion Assembly – 80 Inch Length

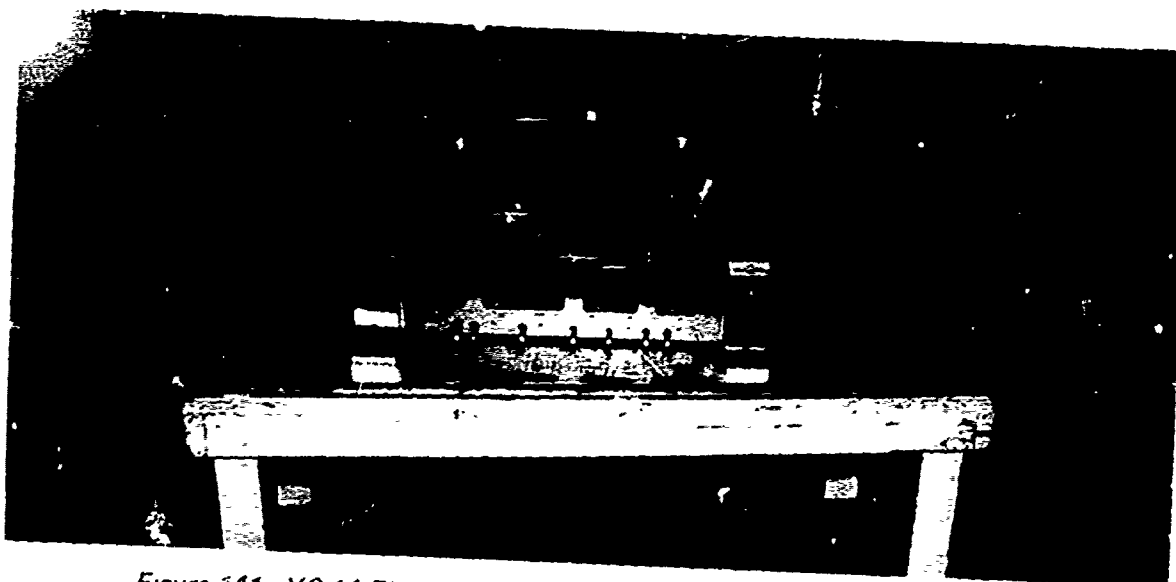


Figure 141. YC-14 Elevator Large Section Assembly Fixture – Front View

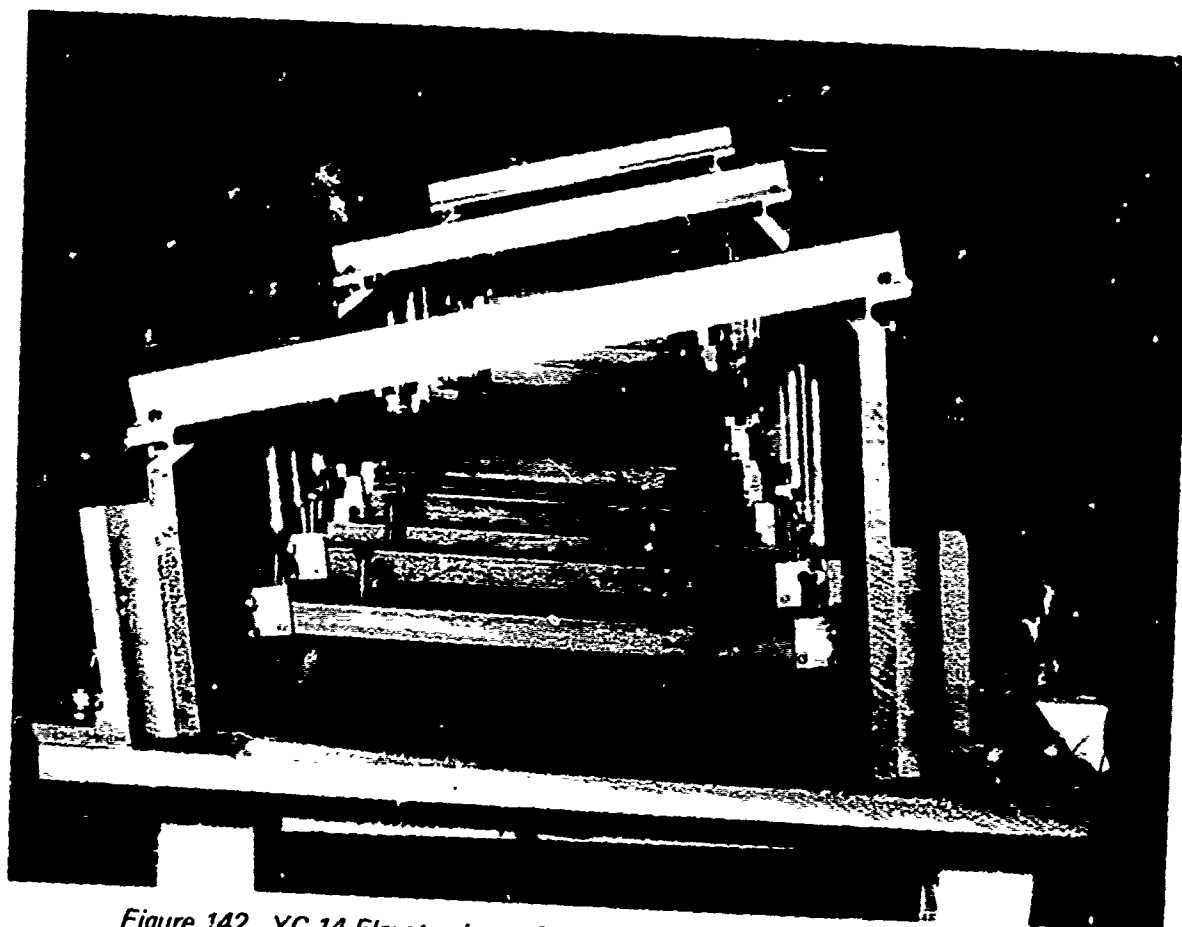


Figure 142. YC-14 Elevator Large Section Assembly Fixture – Side View

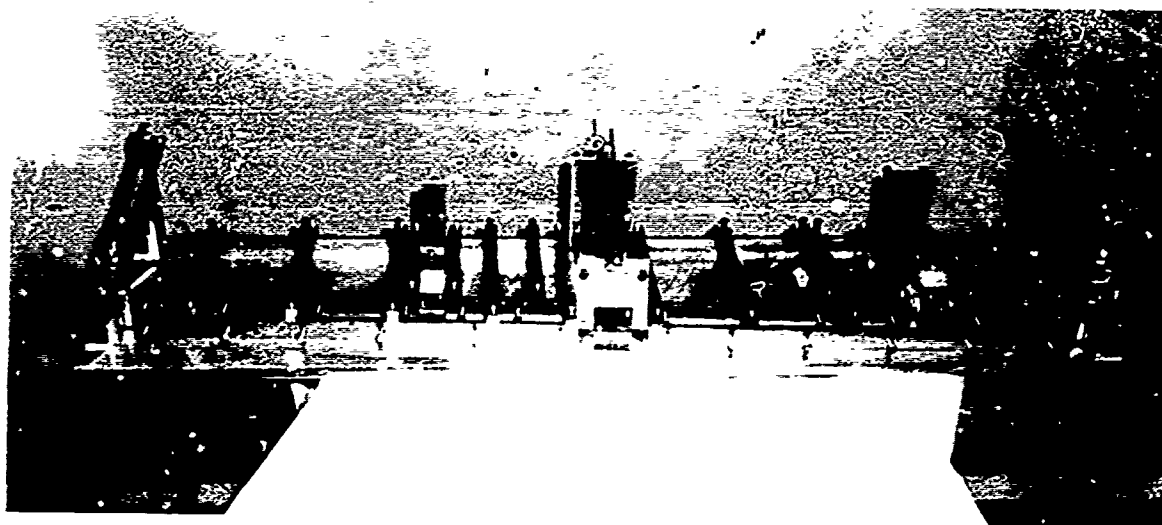


Figure 143. YC-14 Elevator: Middle and Small Section Assembly Fixture

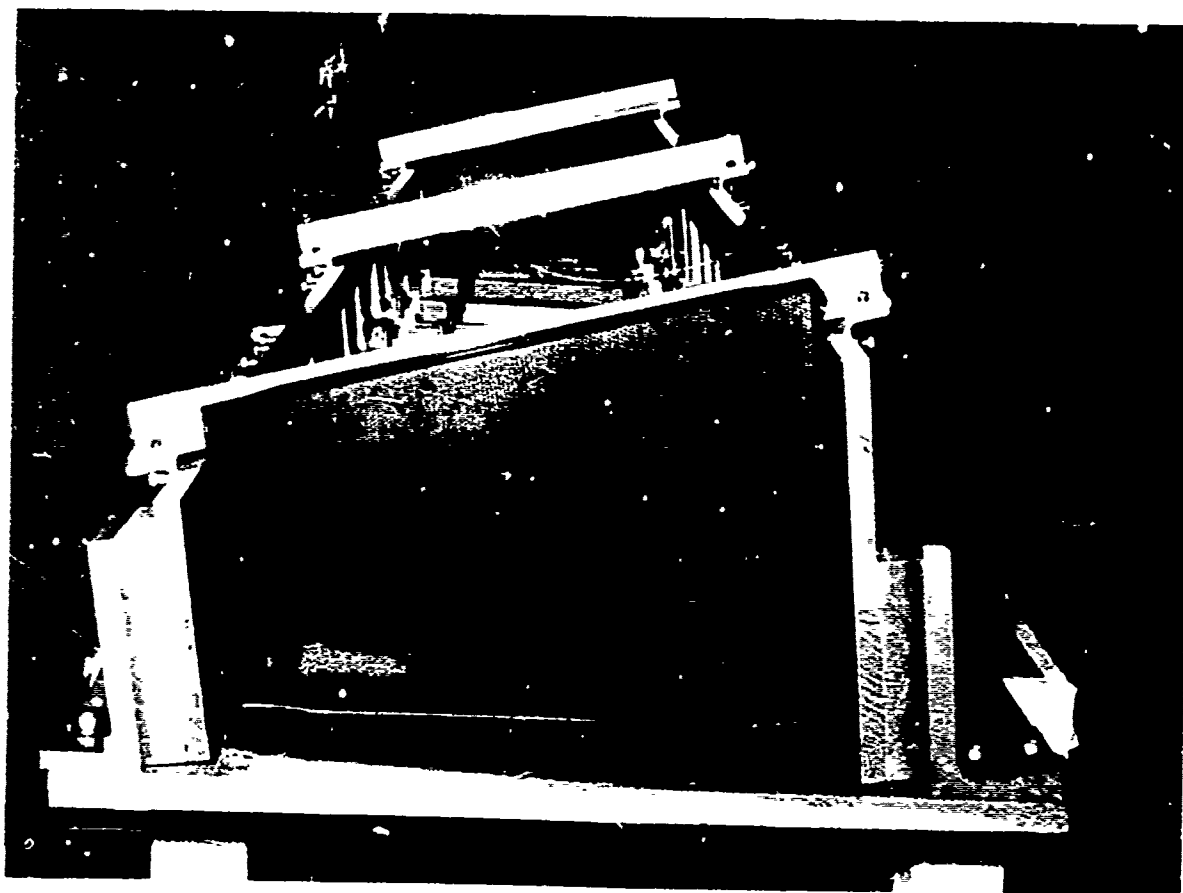


Figure 144. Details Placed in Assembly Fixture

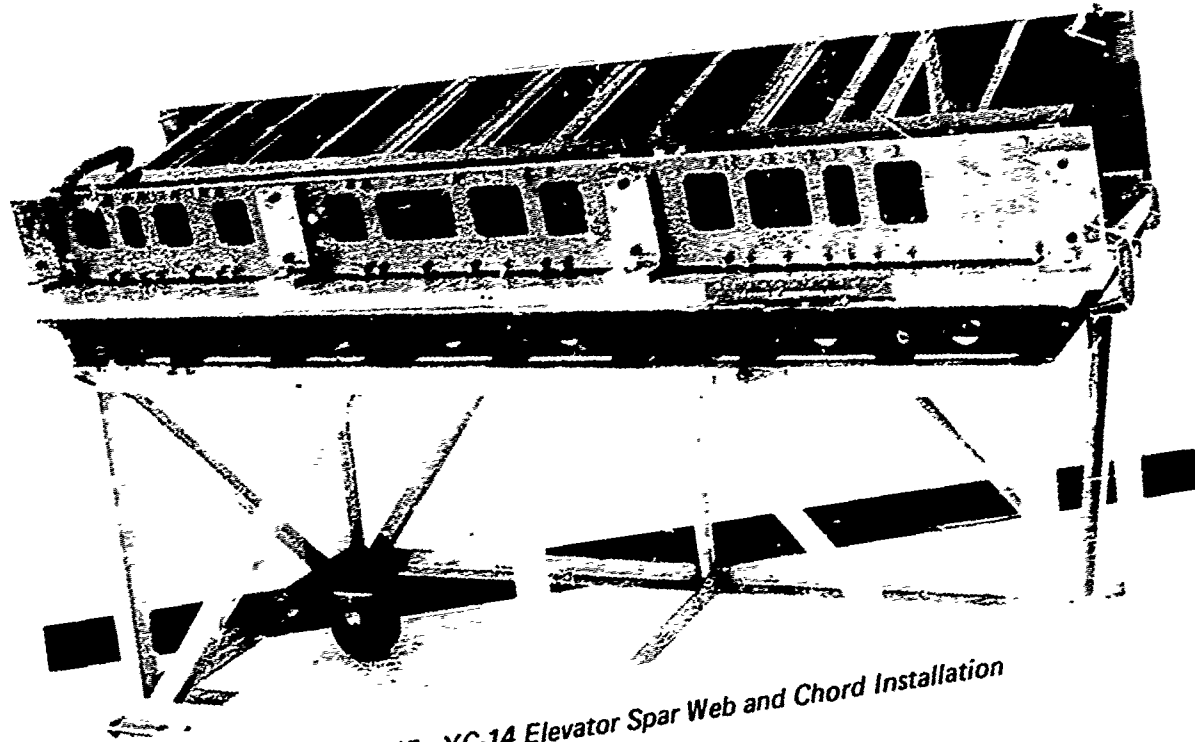


Figure 145. YC-14 Elevator Spar Web and Chord Installation



Figure 146. YC-14 Elevator Section Assembly

The spar webs were installed using pressure plates and reaction frames (Figure 145). Upper chords were then placed in their locations with adhesive (Hysol 9628) and held in place with "C" clamps and pressure bars. These assemblies were then placed in an oven and processed through the 250⁰F adhesive cure. Figure 146 shows a typical elevator section subassembly after the ribs and spar webs and chords have been bonded. The three elevator sub-sections were then assembled with mechanical attachments and Hysol 934 room temperature curing adhesive as shown in Figure 147a. The elevator covers were then installed with mechanical attachments or a room temperature curing adhesive (EA 934). The first two test elevators assembled used Visu-Lok blind fasteners for installing covers in the two smaller sections and nut plates and bolts in the larger sections. Figure 148 shows a cross-section through a typical blind fastener installation. The covers on the third elevator assembly were all installed with nut plates. Figure 147b shows a completed graphite thermoplastic YC-14 elevator assembly.

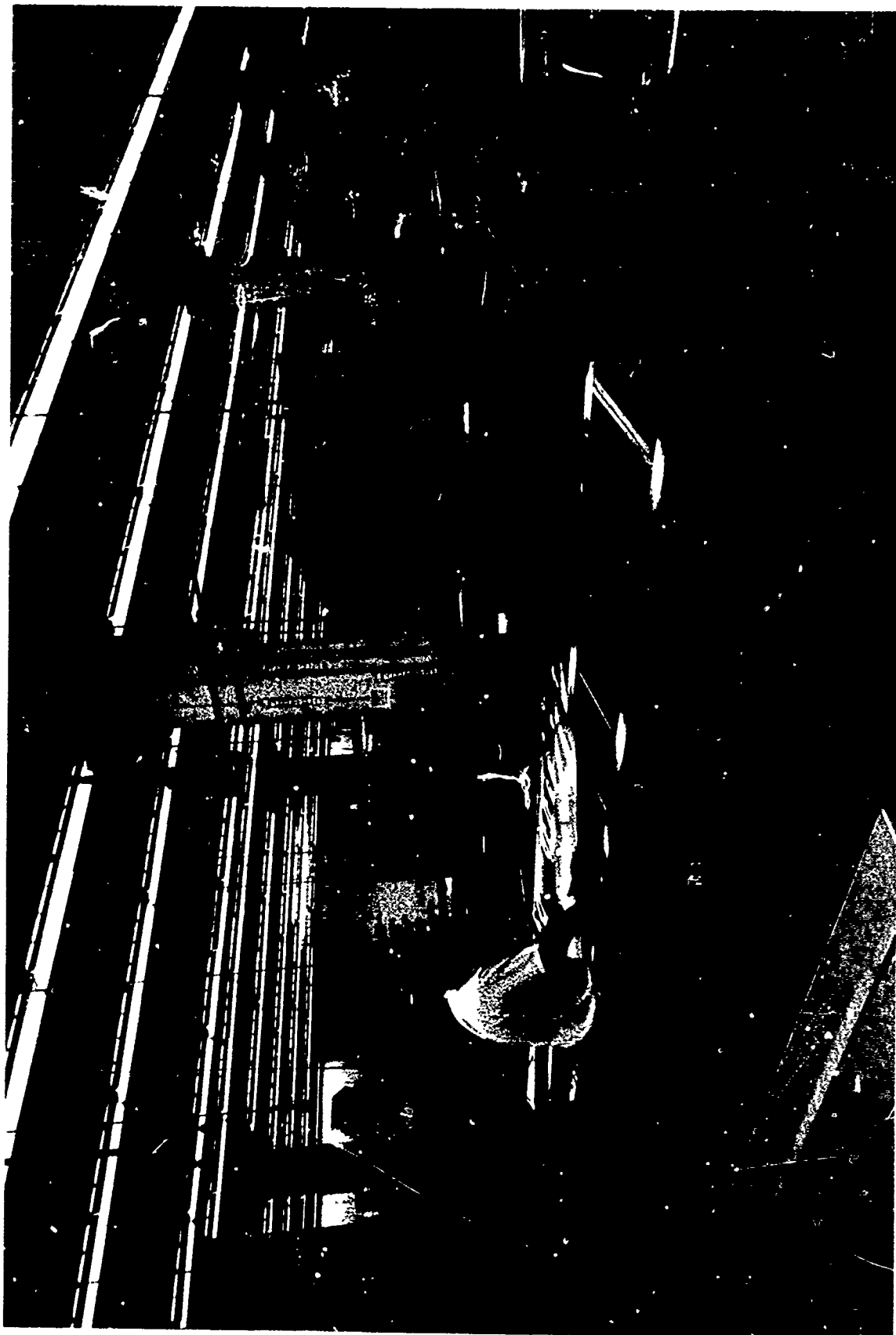


Figure 147a. YC-14 Elevator Assembly—No Covers

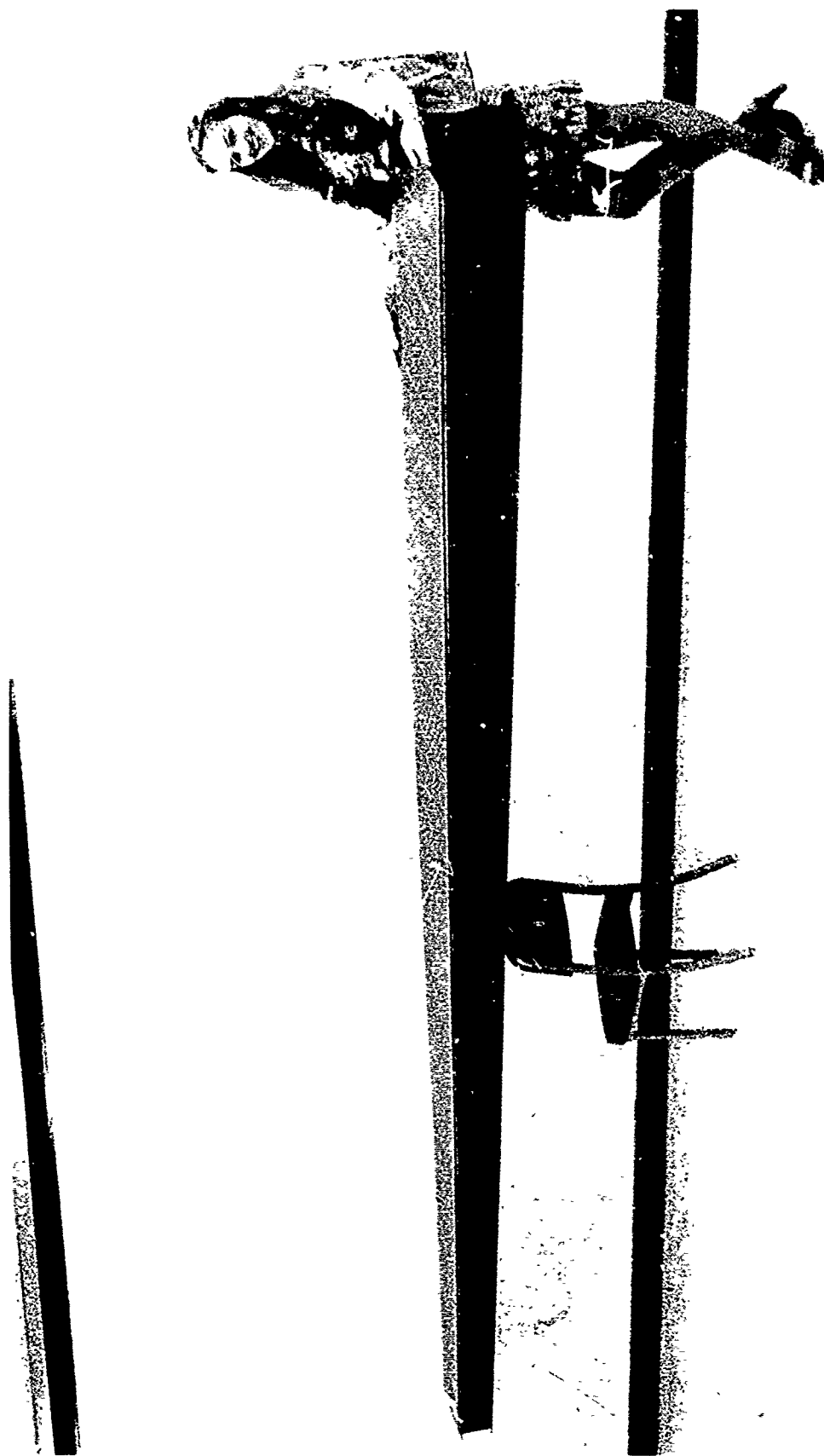


Figure 147h. YC- 4 Elevator No. 2

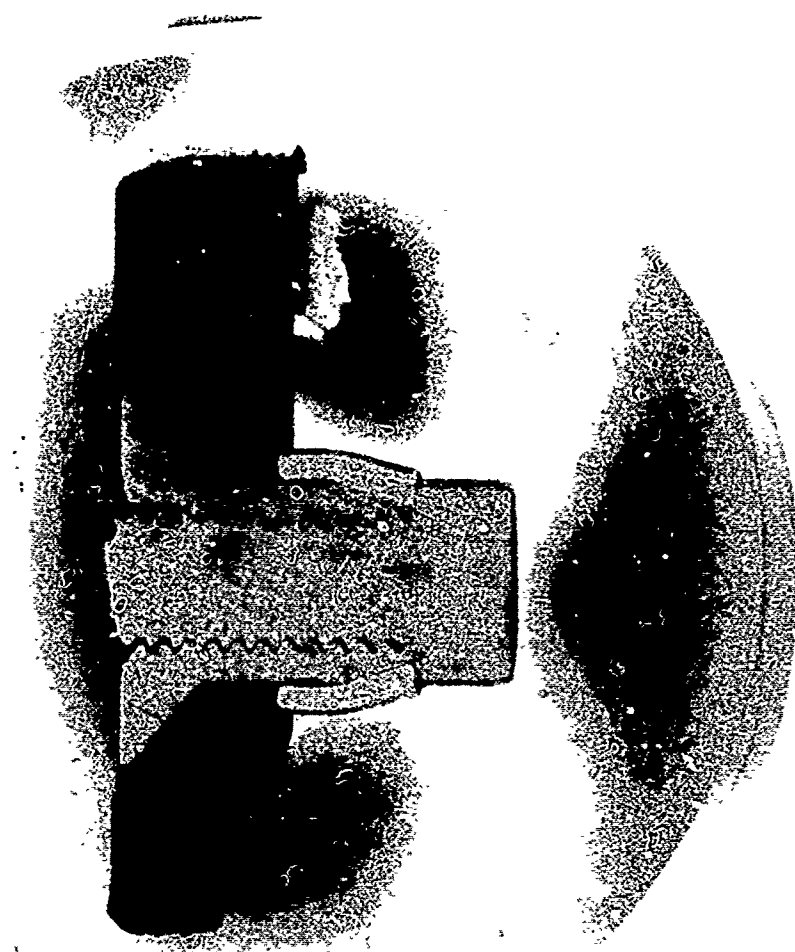


Figure 148. YC-14 Typical Viso-Lok Blind Fastener Installation

9.0 DEMONSTRATION ARTICLE TESTING

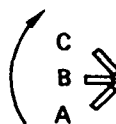
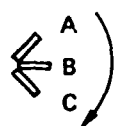
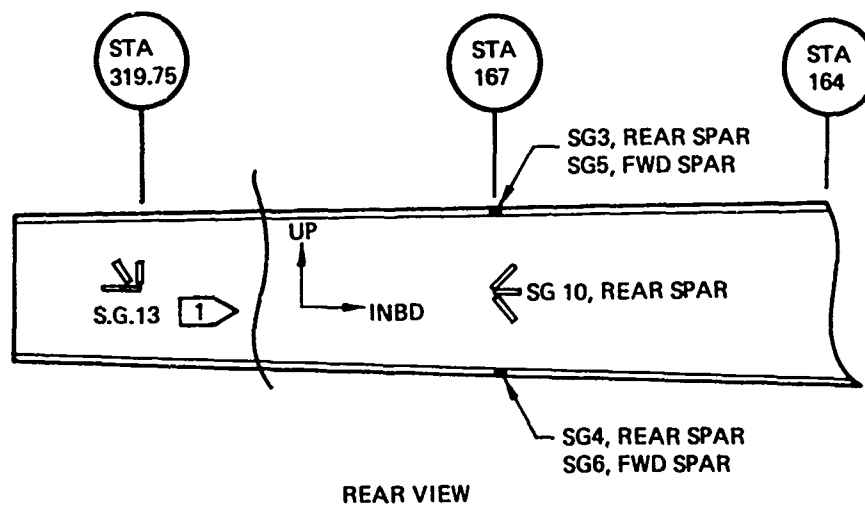
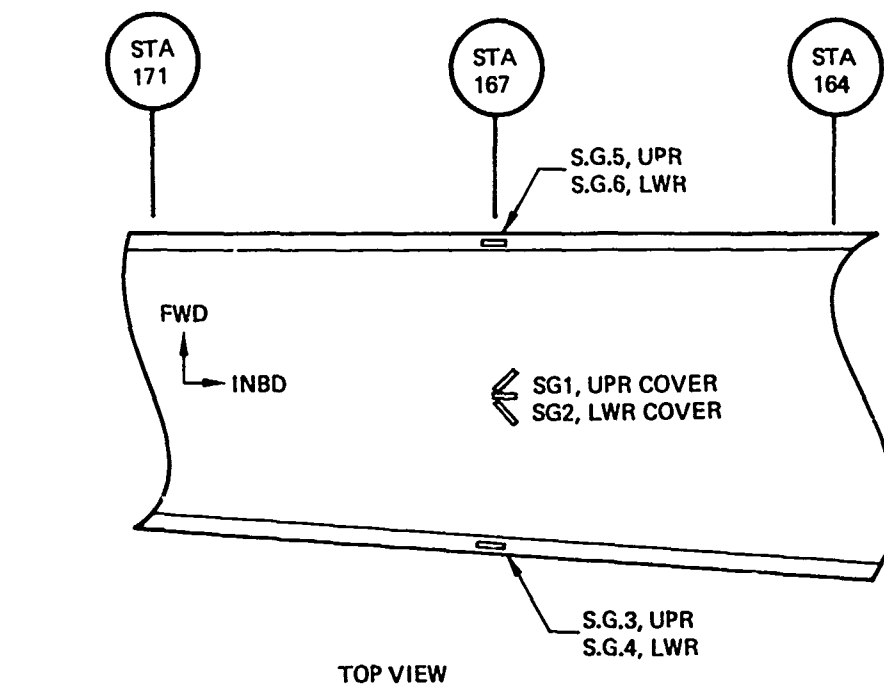
Static and fatigue load testing were completed on three graphite/thermoplastic YC-14 elevator boxes.

The first two elevator boxes were fabricated per drawing 180-56561. Following fabrication, the boxes were instrumented with strain gages as indicated in Figures 149 and 150. Rosettes #7 and #8 were not installed as originally intended because of interference with cover reinforcements. On Box #2, the interior gages were omitted because some of the cover fasteners were cemented in and could not be removed at the time of strain gage installation. The elevator boxes were also instrumented with electronic deflection indicators (EDI), and load cells to measure loads applied at 4 load points as illustrated in Figure 151.

The elevator boxes were tested in fixtures fabricated and assembled per drawing SK2-5611-0-243, and illustrated in Figure 152. Loads were applied by servo controlled hydraulic actuators at 4 loading points as noted, and reacted at two lug fittings at the outboard end and one at the centroid of the inboard end. All loading and reaction points were equipped with self aligning spherical ball bushings to allow for twisting and bending of the test article. Test loads were programmed and the hydraulic actuators controlled by the ELCADS system, which also provided signal conditioning, recording and tabular printout of strain, deflection and load data. Photos of the test system are shown in Figures 153 to 156.

The test loading conditions and sequence are tabulated in Figures 157 to 161.

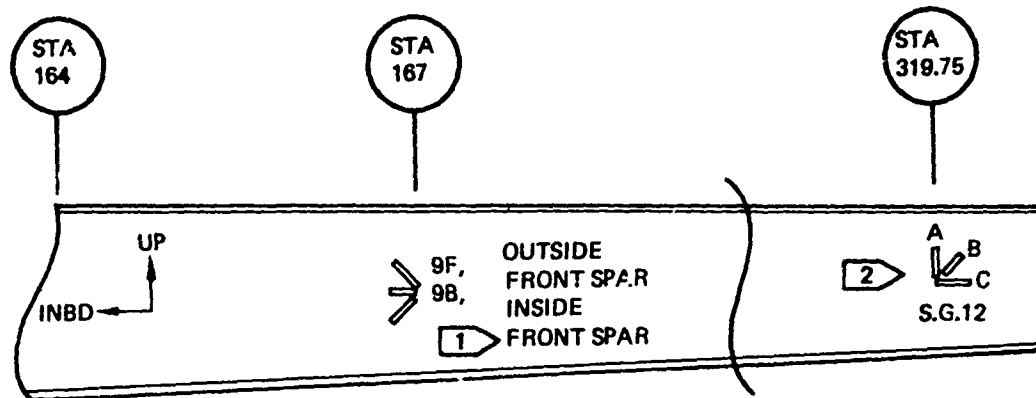
Elevator Box #1 was subjected to a bending test, with loading to 80% of D.L.L. as noted in Figure 157, followed by a torsion test to 100% D.L.L. as outlined on Figure 157. During the torsion test, stiffeners on the inner side of the lower cover at Sta. 197 and 205, were disbonded. Due to the stiffener bond failure, the test director elected to bond stiffeners on the outside of the lower cover and proceed with the fatigue test as originally intended. The



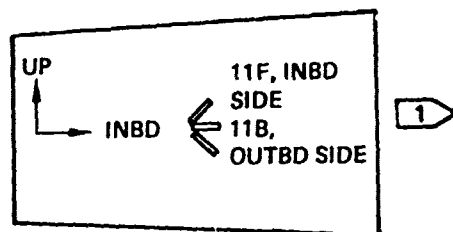
A,B,C, legs of rosettes are located
in clockwise direction when facing
the gage surface

1 TEST 2.4 ONLY

Figure 149. Strain Gage Locations



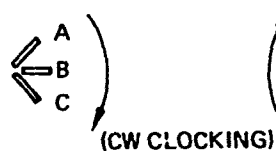
FRONT VIEW



RIB @ STA 164

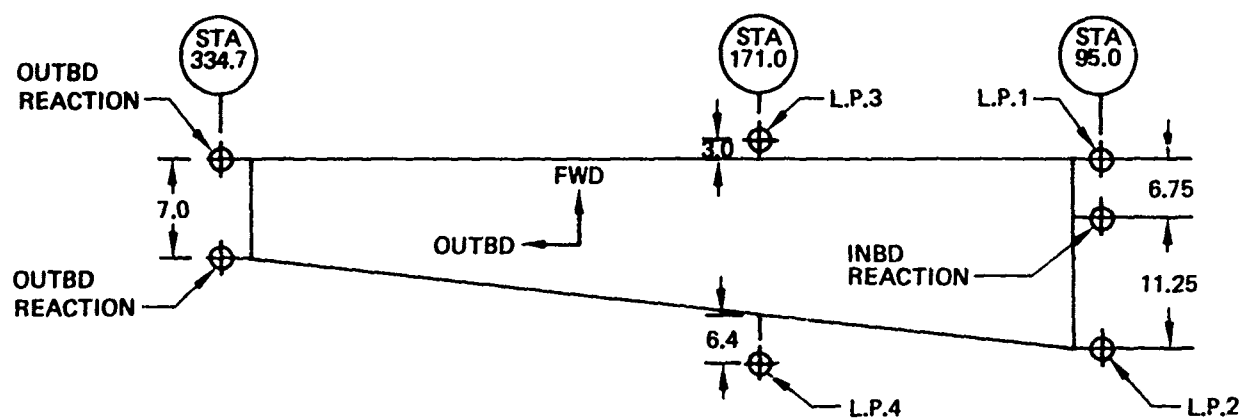
1 DELETED ON BOX NO. 2

2 TEST 2.4 ONLY

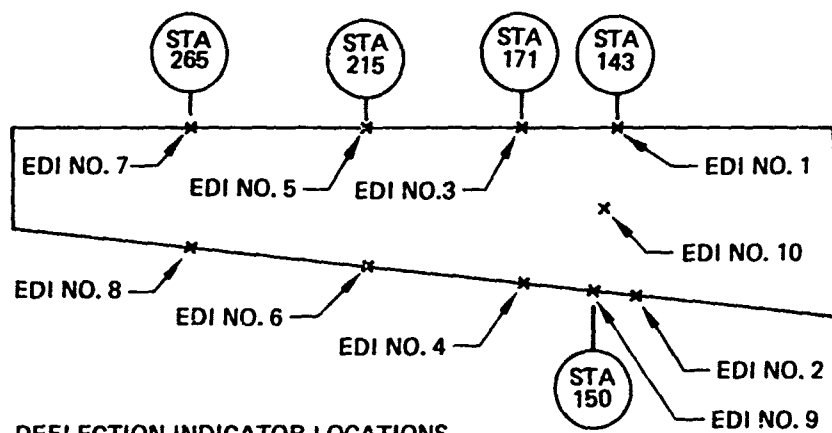


A, B, C, legs of rosettes are located in clockwise direction when facing the gage

Figure 150. Strain Gage Locations



LOAD POINT AND REACTION LOCATIONS



DEFLECTION INDICATOR LOCATIONS

Figure 151. Loading Points and Deflection Indicator Locations

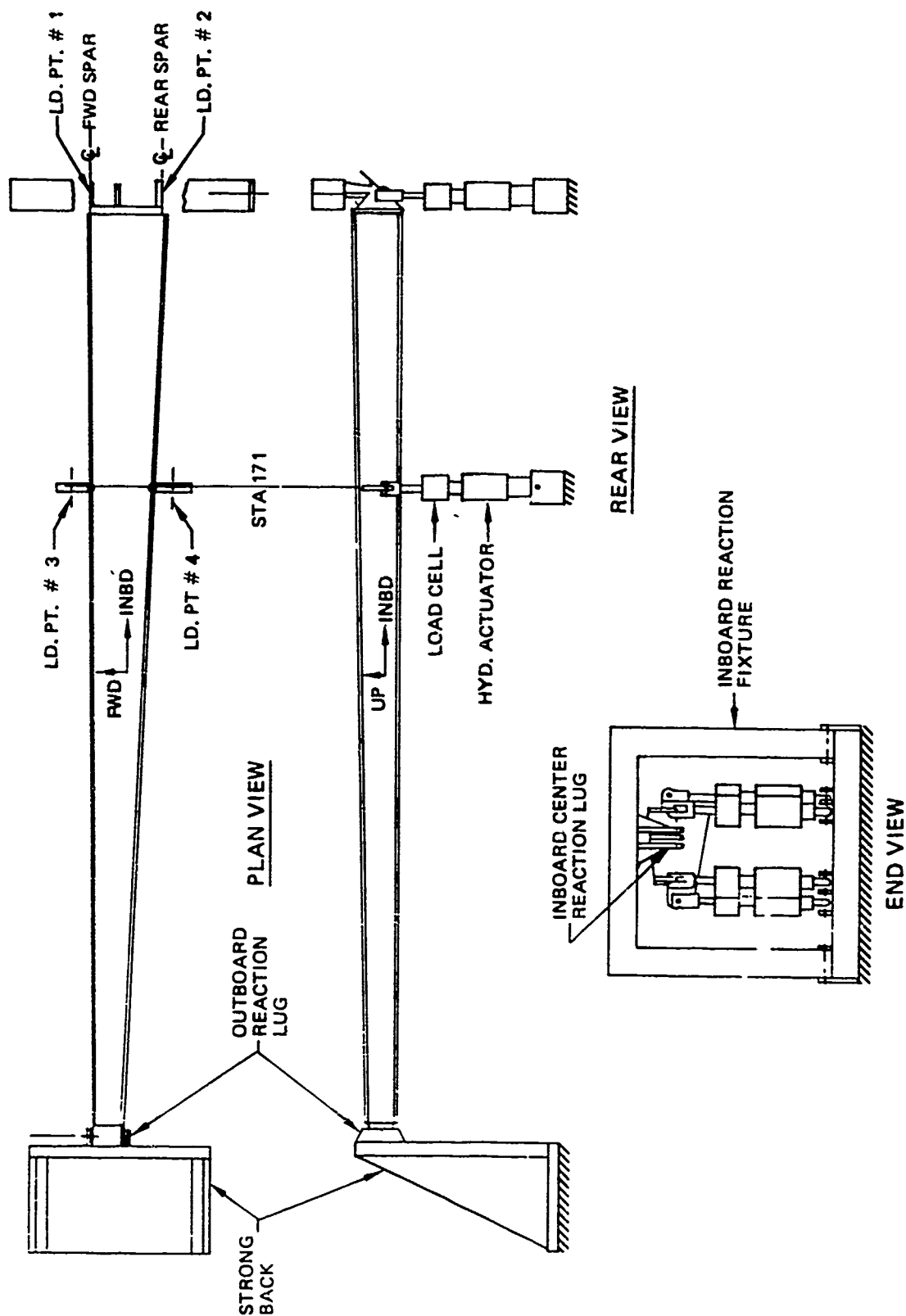


Figure 152. Elevator Test Set-Up

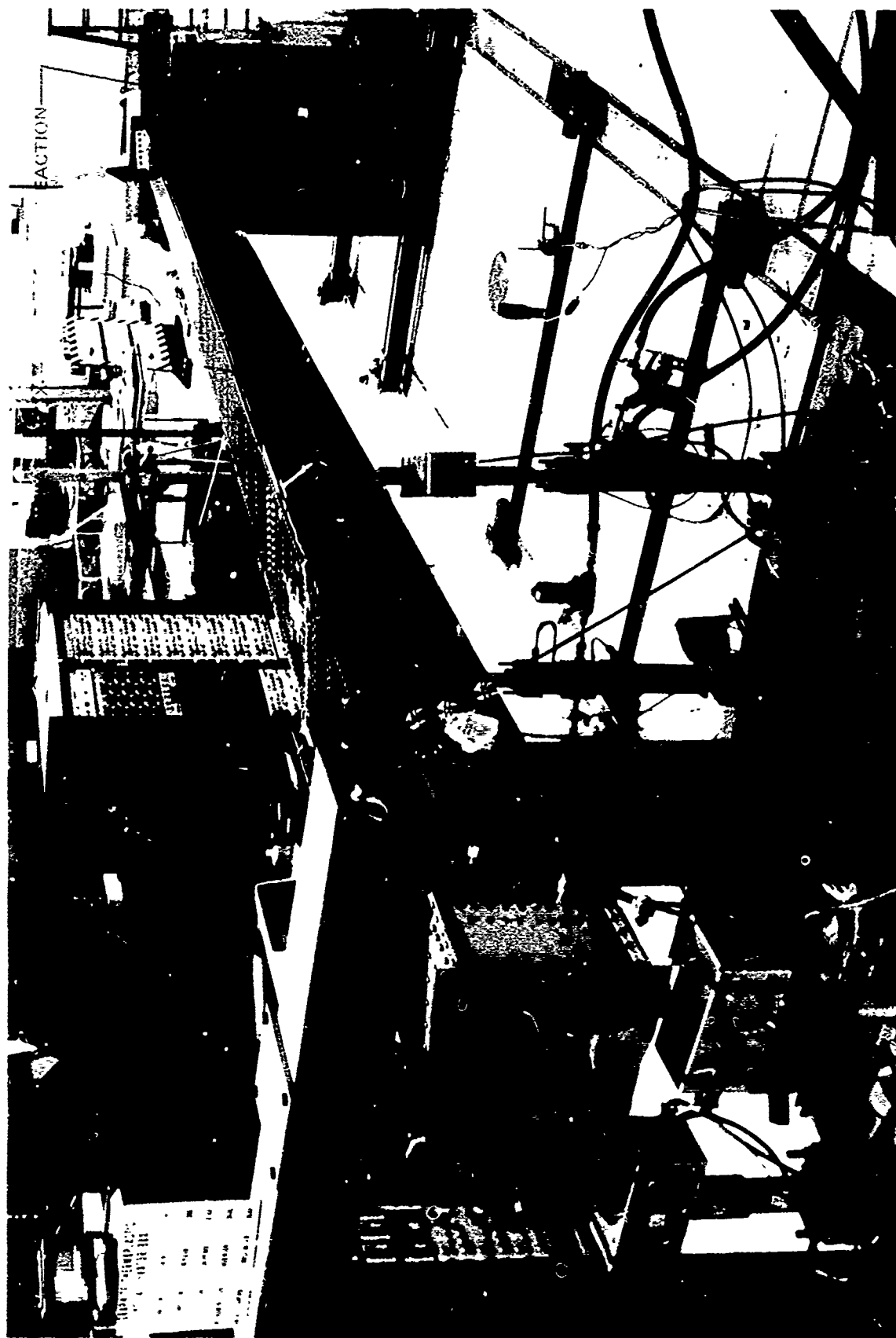


Figure 153. GR/TP YC14 Elevator Box Test -- Test Article and Fixtures

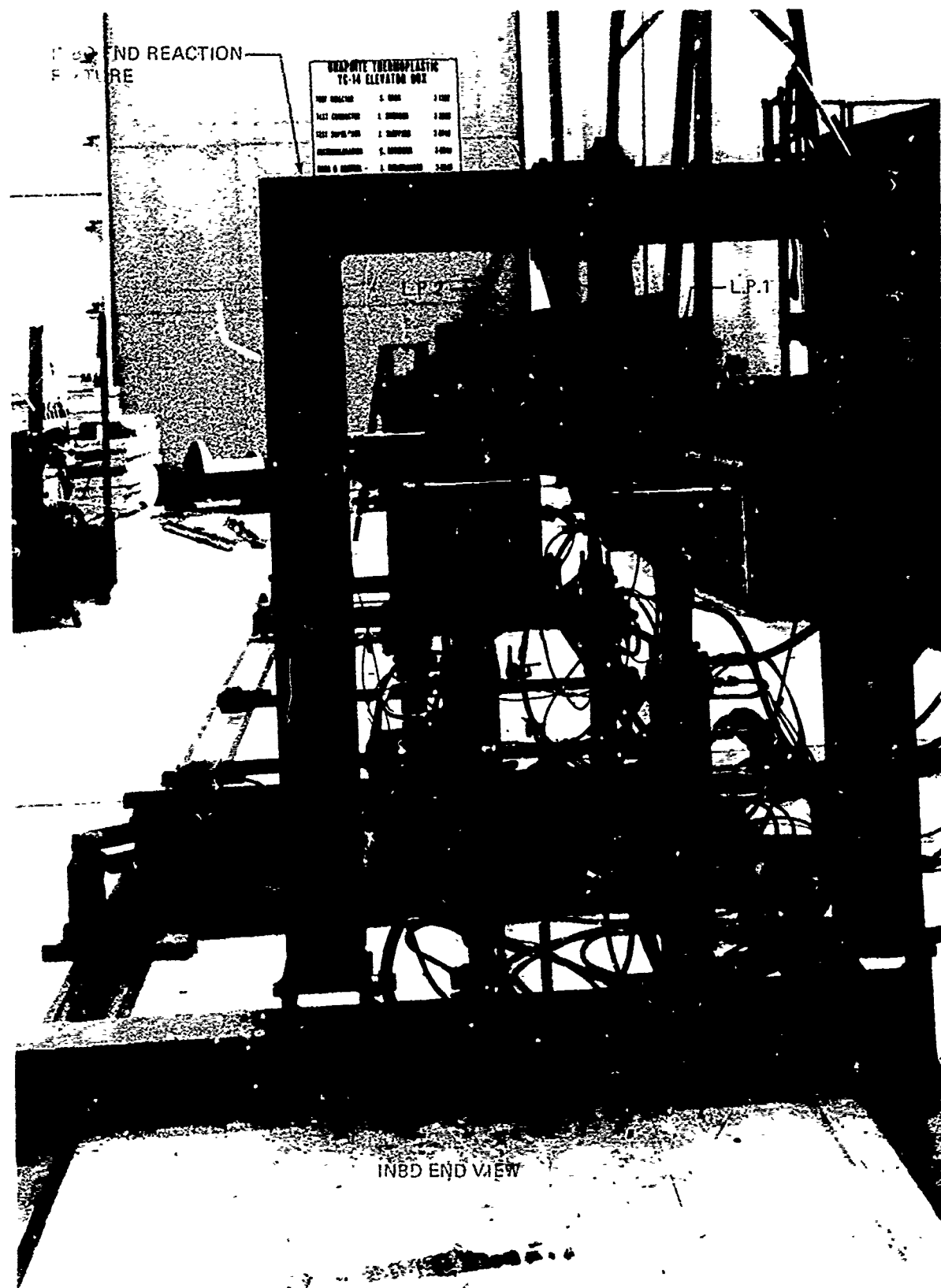


Figure 154. GR/TP YC14 Elevator Bcx Test—Test Article and Fixtures

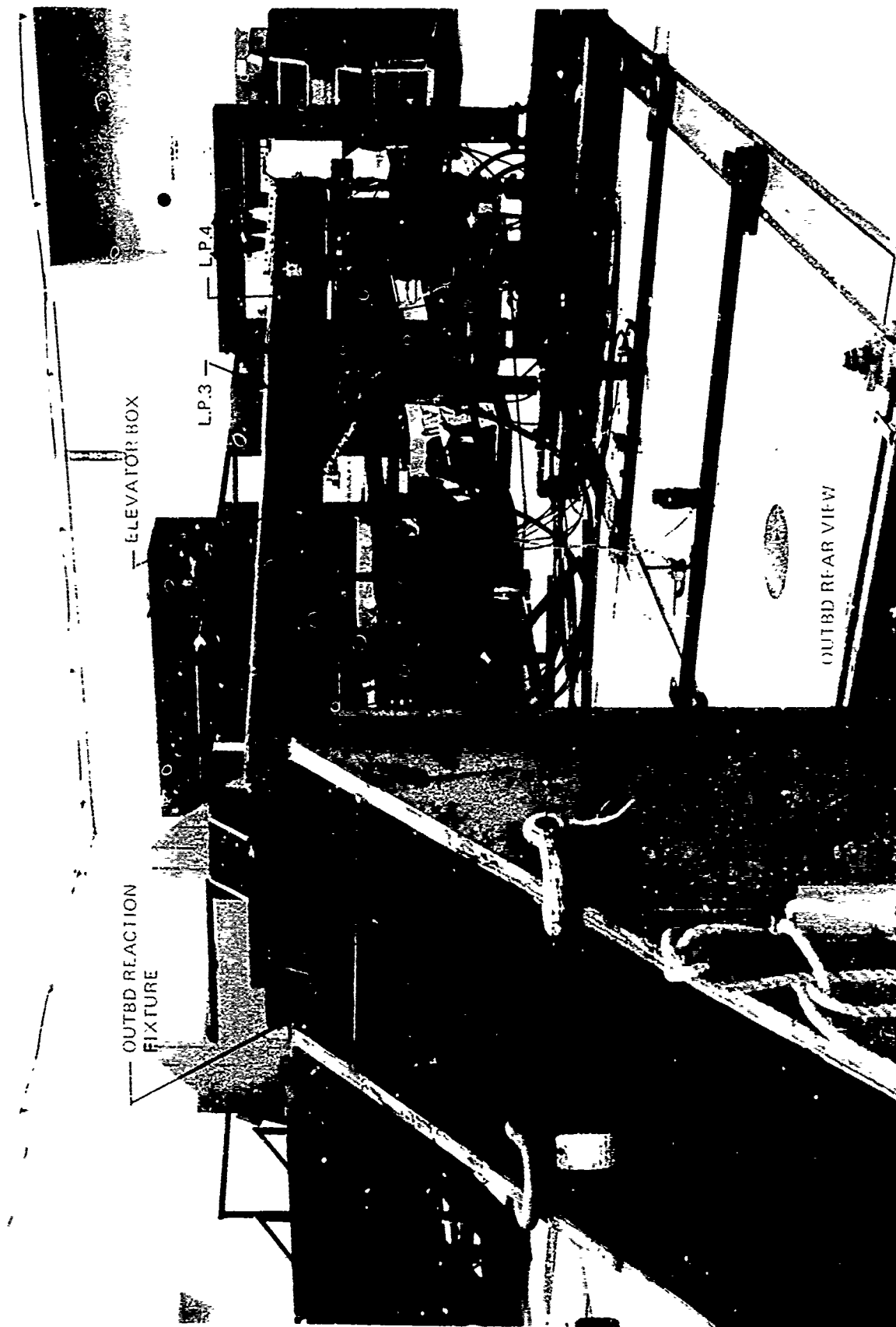


Figure 155. GWR LP Elevator Box Test Test Article and Fixtures

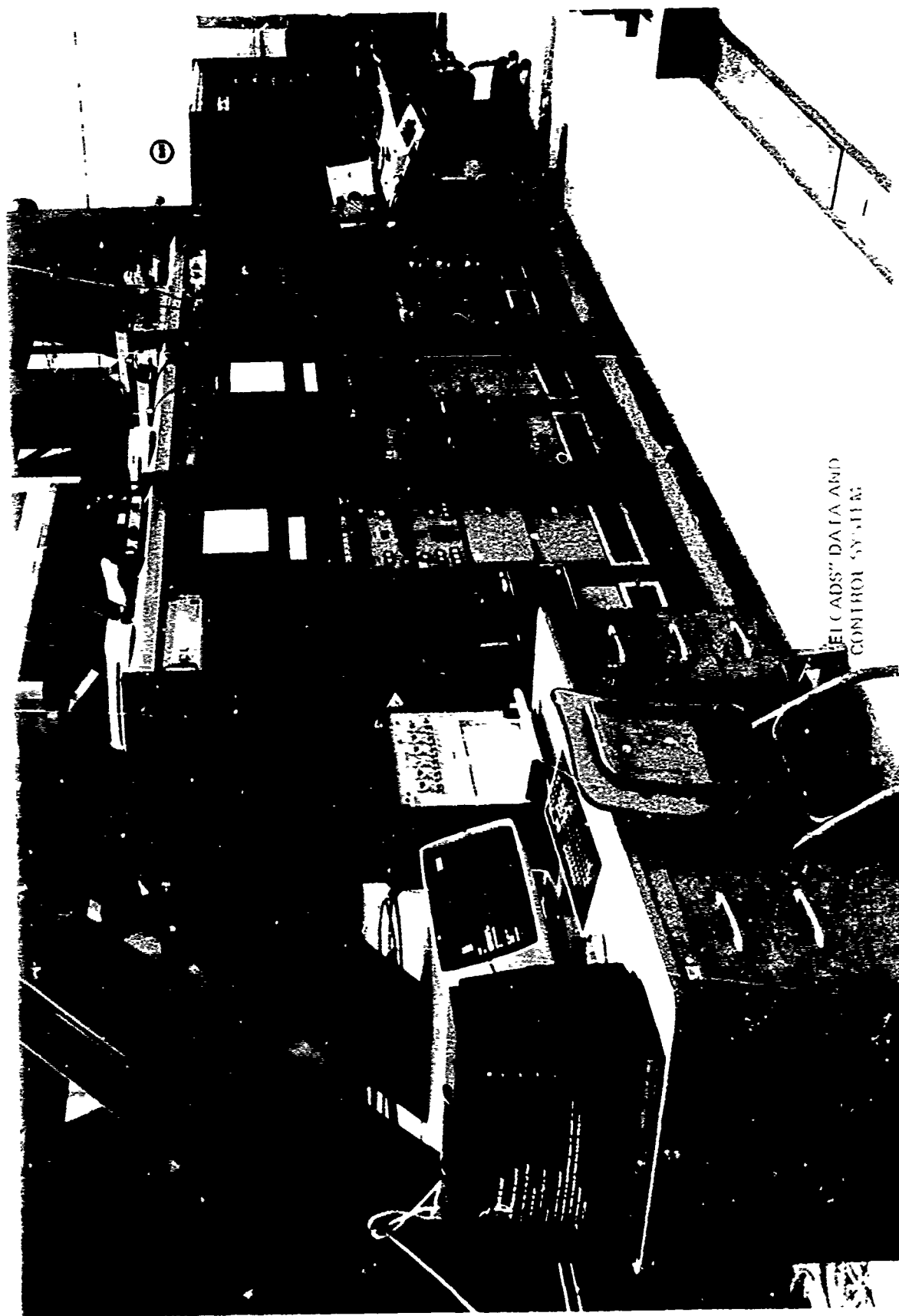


Figure 156 GR TP YC 14 Elevator Box Test Instrumentation and Control

TEST	% D.L.L.	APPLIED LOAD - POUNDS			
		LP.1	LP.2	LP.3	LP.4
Box No. 1	0	0	0	0	0
Test 1.1	20	-170	-63	1250	+93
Static Bending	40	-340	-126	+501	+186
	60	-511	-189	+752	+278
	80	-681	-252	+1003	+371
	60	-511	-189	+752	+278
	40	-340	-126	+501	+136
	20	-170	-63	+250	+93
	0	0	0	0	0
Box No. 1	0	0	0	0	0
Test 1.2A	20	+800	-800	-250	+250
Static Torsion	40	+1600	-1600	-500	+500
	60	+2400	-2400	-750	+750
	80	+3200	-3200	-1000	+1000
	0	0	0	0	0
Box No. 1	0	0	0	0	0
Test 1.2B	20	+800	-800	-250	+250
Static Torsion	40	+1600	-1600	-500	+500
	60	+2400	-2400	-750	+750
	80	+3200	-3200	-1000	+1000
	100	+4000	-4000	-1250	+1250
	80	+3200	-3200	-1000	+1000
	60	+2400	-2400	-750	+750
	40	+1600	-1600	-500	+500
	20	+800	-800	-250	+250
	0	0	0	0	0

1▶ Aborted test after 80% load due to insufficient actuator stroke @ L.P. No. 4.
Repositioned actuator and repeated as test 12.B.

Applied 4 loads simultaneously in 20% increments in 10 seconds. Held load at each increment for data recording. Tension = +, compr = -.

Figure 157. Test - Loading Schedule, Graphite Thermoplastic YC-14 Elevator Box Test

TEST	% D.L.L.	APPLIED LOAD - POUNDS			
		L.P.1	L.P.2	L.P.3	L.P.4
Box No. 1 2▶	0	0	0	0	0
Test 1.3	17	+ 662	- 662	-206	+206
Pre-Fatigue	34	+1324	-1324	-412	+412
Static Torsion	51	+1986	-1986	-618	+618
	67	+2649	-2649	-824	+824
	0	0	0	0	0
Box No. 1					
1st Lifetime Fatigue					
"A" Amplitude, MIN	3	+ 132	- 132	- 41	+ 41
cycle 1 thru 75 MAX	67	+2649	-2649	-824	+824
"B" Amplitude, MIN	2	+ 94	- 94	- 29	+ 29
cycle 76 thru 200 MAX	46	+1876	-1876	-577	+577
Repeat "A" & "B" 150 X = 1 L.T. = 30,000 cycles					
Box No. 1	0	0	0	0	0
Test 1.4	17	+ 662	- 662	-206	+206
Post Fatigue Life 1	34	+1324	-1324	-412	+412
Static Torsion	51	+1986	-1986	-618	+618
	67	+2649	-2649	-824	+824
	0	0	0	0	0
Box No. 1					
2nd Lifetime Fatigue		REPEAT AS PER 1st LIFETIME			
Box No. 1					
Test 1.5					
Post Fatigue Life 2		REPEAT AS PER TEST 1.4			
Static Torsion					
Box No. 1					
3rd Lifetime Fatigue		REPEAT AS PER 1st LIFETIME			
Box No. 1					
Test 1.6					
Post Fatigue Life 3		REPEAT AS PER TEST 1.4			
Static Torsion					

2▶ Lower cover stiffeners @ STA 197 and 205 disbonded during test 1.2B.
Exterior tee stiffeners bonded on prior to fatigue test start.

Figure 158. Test - Loading Schedule Graphite Thermoplastic YC-14 Elevator Box Test

TEST	% D.L.L.	APPLIED LOAD - POUNDS			
		L.P.1	L.P.2	L.P.3	L.P.4
Box No. 1 4th Lifetime Fatigue		REPEAT AS PER 1st LIFETIME			
Box No. 1 Test 1.7 Post Fatigue Life 4		REPEAT AS PER TEST 1.4			
Box No. 1 3 ▶	0	0	0	0	0
Test 1.8	20	+663	-850	-49	+324
Static Combined Bending and Torsion	40	+1326	-1700	-99	+648
	60	+1989	-2551	-148	+973
	80	+2652	-3402	-198	+1297
	100	+3315	-4252	-247	+1621
	110	+3646	-4677	-272	+1783
	120	+3978	-5102	-296	+1945
	130	+4310	-5527	-321	+2107
4 ▶	0	0	0	0	0
Box No. 1	0	0	0	0	0
Test 1.9	20	+663	-850	-49	+324
Static Combined Bending and Torsion - Failure	40	+1326	-1700	-99	+648
	60	+1989	-2551	-148	+973
	80	+2652	-3402	-198	+1297
	100	+3315	-4252	-247	+1621
	110	+3646	-4677	-272	+1783
	120	+3978	-5102	-296	+1945
	130	+4310	-5527	-321	+2107
	140	+4641	-5953	-346	+2269
	150	+4972	-6378	-371	+2432
Continuous to Failure		↓	↓	↓	↓

3▶ Tee stiffeners at STA 197 and 205 were poorly bonded and were replaced with aluminum angles attached with blind rivets prior to static test 1.8.

4▶ Aborted test after 130% load due to insufficient actuator stroke at L.P. No. 3. Repositioned actuator and repeated test as 1.9.

Figure 159. Test -Loading Schedule Graphite Thermoplastic YC-14 Elevator Box Test

TEST	% D.L.L.	APPLIED LOAD - POUNDS			
		L.P.1	L.P.2	L.P.3	L.P.4
Box No. 2	0	0	0	0	0
Test 2.1	20	-170	-63	+250	+93
Static Bending	40	-340	-126	+501	+186
	60	-511	-189	+752	+278
	80	-681	-252	+1003	+371
	60	-511	-189	+752	+278
	40	-340	-126	+501	+186
	20	-170	-63	+250	+93
	0	0	-0	0	0
Box No. 2	0	0	0	0	0
Test 2.2A	20	+800	-800	-250	+250
Static Torsion	40	+1600	-1600	-500	+500
	60	+2400	-2400	-750	+750
	80	+3200	-3200	-1000	+1000
	100	+4000	-4000	-1250	+1250
Box No. 2	0	0	0	0	0
Test 2.3	20	+663	-850	-49	+324
Static Combined Bend-	40	+1326	-1700	-99	+648
ing and Torsion to	60	+1989	-2551	-148	+973
failure	80	+2652	-3402	-198	+1297
	100	+3315	-4252	-247	+1621
	110	+3646	-4677	-272	+1783

5 At approximately 95% of D.L.L., the lower skin/lower front spar chord bond failed from STA 279 to 313.

6 Prior to test 2.3, the failure per 5 was repaired by bonding and installation of blind fasteners.

7 At approximately 106% of D.L.L., the front spar web/chord tee bond failed from outbd splice to the outbd end.

Figure 160. Test - Loading Schedule Graphite Thermoplastic YC-1+ Elevator Box Test

TEST	% D.L.L.	APPLIED LOAD - POUNDS			
		L.P.1	L.P.2	L.P.3	L.P.4
Box No. 2	8 ▶	0	0	0	0
Test 2.4		+663	-850	-49	+324
Static Combined Bend-		+1326	-1700	-99	+648
ing and Torsion to		+1969	-2551	-148	+973
failure		+2652	-3402	-198	+1297
		+3315	-4252	-247	+1621
		+3646	-4677	-272	+1783
	9 ▶	+3978	-5102	-296	+1945
		+4310	-5527	-321	+2107
Box No. 3		0	0	N.A.	N.A.
Test 3.1		+469	-469		
Static Torsion Test		+938	-938		
		+1407	-1407		
		+1871	-1871		
		+2345	-2345		
		+1871	-1871		
		+1407	-1407		
		+938	-938		
		+469	-469		
		0	0	N.A.	N.A.

8 ▶ Prior to test 2.4, the failure per 7 ▶ was repaired by bonding and installation of blind fasteners.

9 ▶ Failure occurred while increasing the load from 120% D.L.L. to 130%. See data for actual loads.

Figure 161. Test - Loading Schedule Graphite Thermoplastic YC-14 Elevator Box Test

fatigue test with maximum loads up to 67% of D.L.L. was conducted for the equivalent of 4 life times. After each life time of fatigue testing, strain and deflection data was recorded at static load increments of 25% of the maximum fatigue load. During the fatigue test, the stiffeners bonded to the lower cover, came loose due to poor bonds. They were replaced with aluminum angles attached with blind fasteners prior to subjecting the box to a combined bending and torsion test to failure. Loading increments for the combined test are noted on Figure 159. Box #1 was loaded to approximately 130% of D.L.L. when the actuator at L.P. 3 reached the limit of its stroke. The box was unloaded and the actuator repositioned to allow more stroke in the loading direction. The test was then repeated and the loading was incremented to approximately 185% of the D.L.L. when the box failed. Post test inspection revealed that the upper cover failed at Sta. 305 to Sta. 315 and the forward spar web/chord tee bond failed from the outboard end (approx. Sta. 330) to the outboard splice (approx. Sta. 265). Upon disassembly, it was noted that the lower skin stiffener at Sta. 318 was also disbonded. Photos of Box #1 failures are in Figures 162, 163, and 164.

Elevator Box #2 was subjected to a bending test with loading as noted in Figure 160, followed by a torsion test outlined on the same page. At approximately 95% D.L.L. of the torsion loading, the lower skin/lower front spar chord bond failed from Sta. 279 to 313. The failure was repaired by bonding and installation of blind rivets. Following the repair, Box #2 was subjected to a combined bending and torsion test loading as noted in Figure 160. At approximately 106% of D.L.L., the front spar web/chord tee bond failed from the outboard splice at Sta. 265, to the outboard end of the box. Photos of Box #2 failures are in Figures 165 and 166.

The front spar web/chord failure of Box #2 was repaired by bonding and blind rivets, as shown in the photograph on Figure 167. Following the repair, Box #2 was subjected to another static combined bending and torsion test to failure. As noted in Figure 161, failure occurred as the loading was being increased from 120% to 130% of D.L.L. Box #2 failed along the lower skin/rear spar chord bond, approximately from Sta. 305 to Sta. 256, and across the lower cover along the outboard row of fasteners at the outboard cover splice. Photos of the failed area of Box #2 are in Figures 168 and 169.

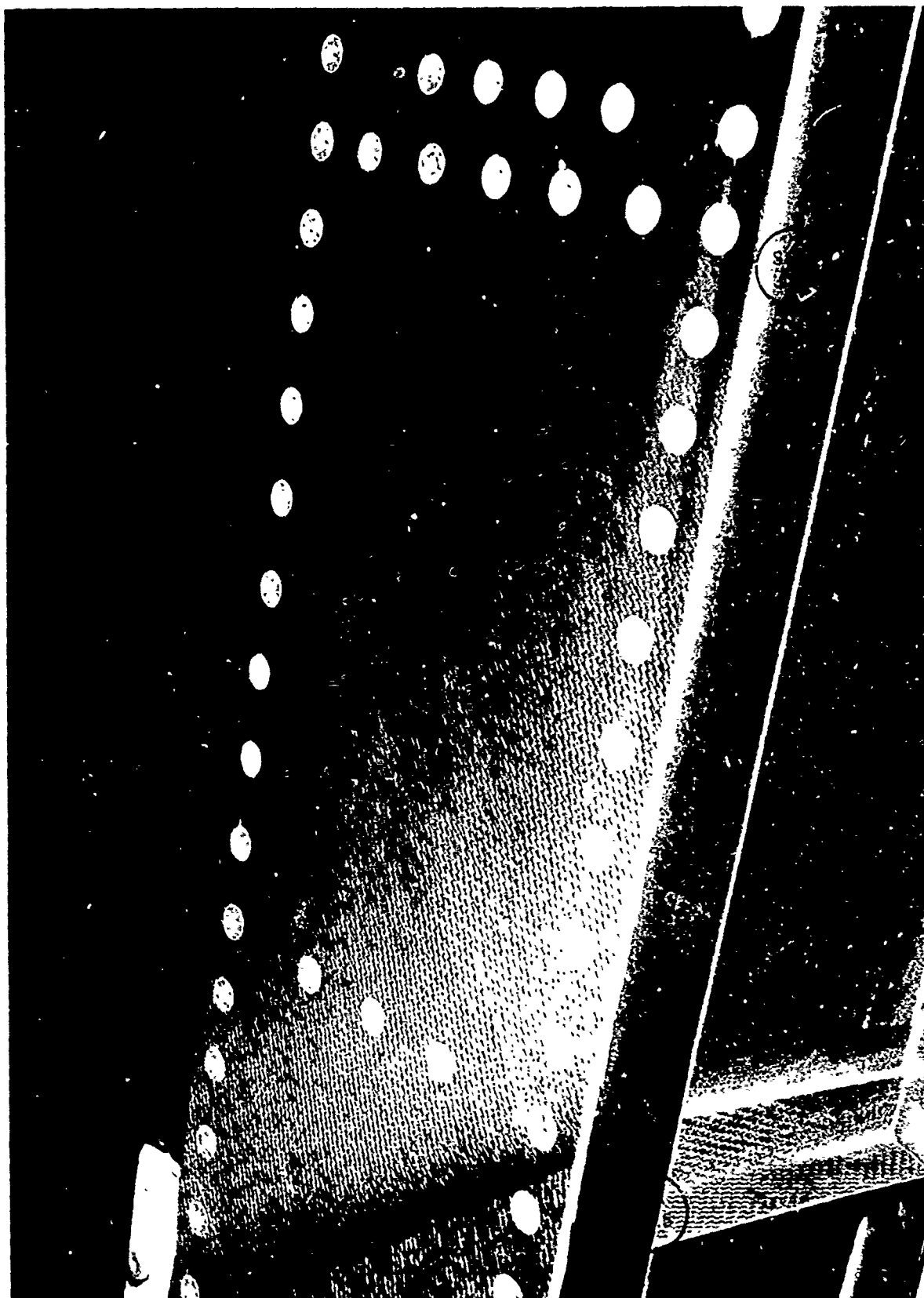


Figure 162. Upper Cover Failure—Test 1.9—Elev. Box No. 1

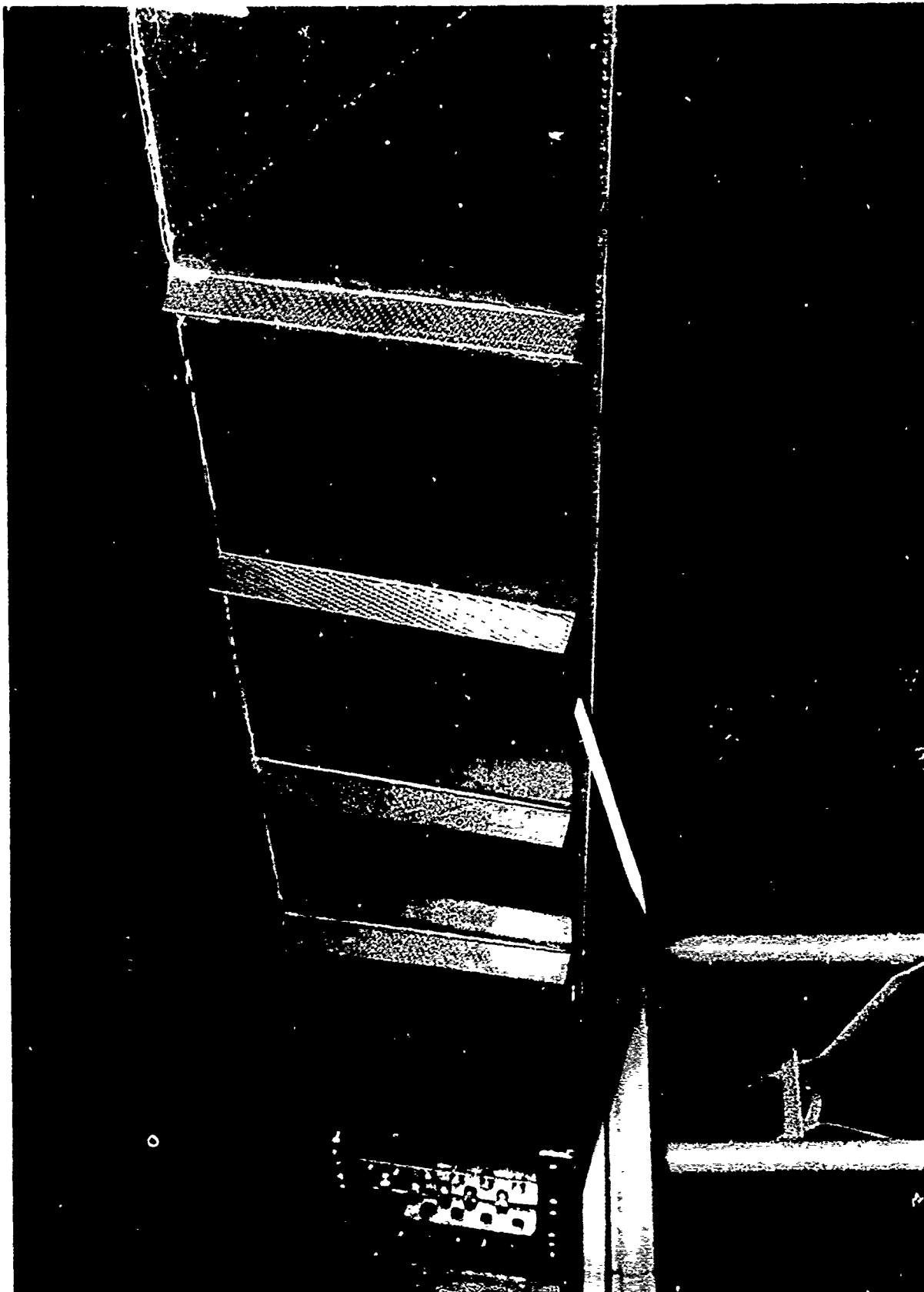


Figure 163. Front Spar: Failure- Test 1.9-Elev. Box No. 1

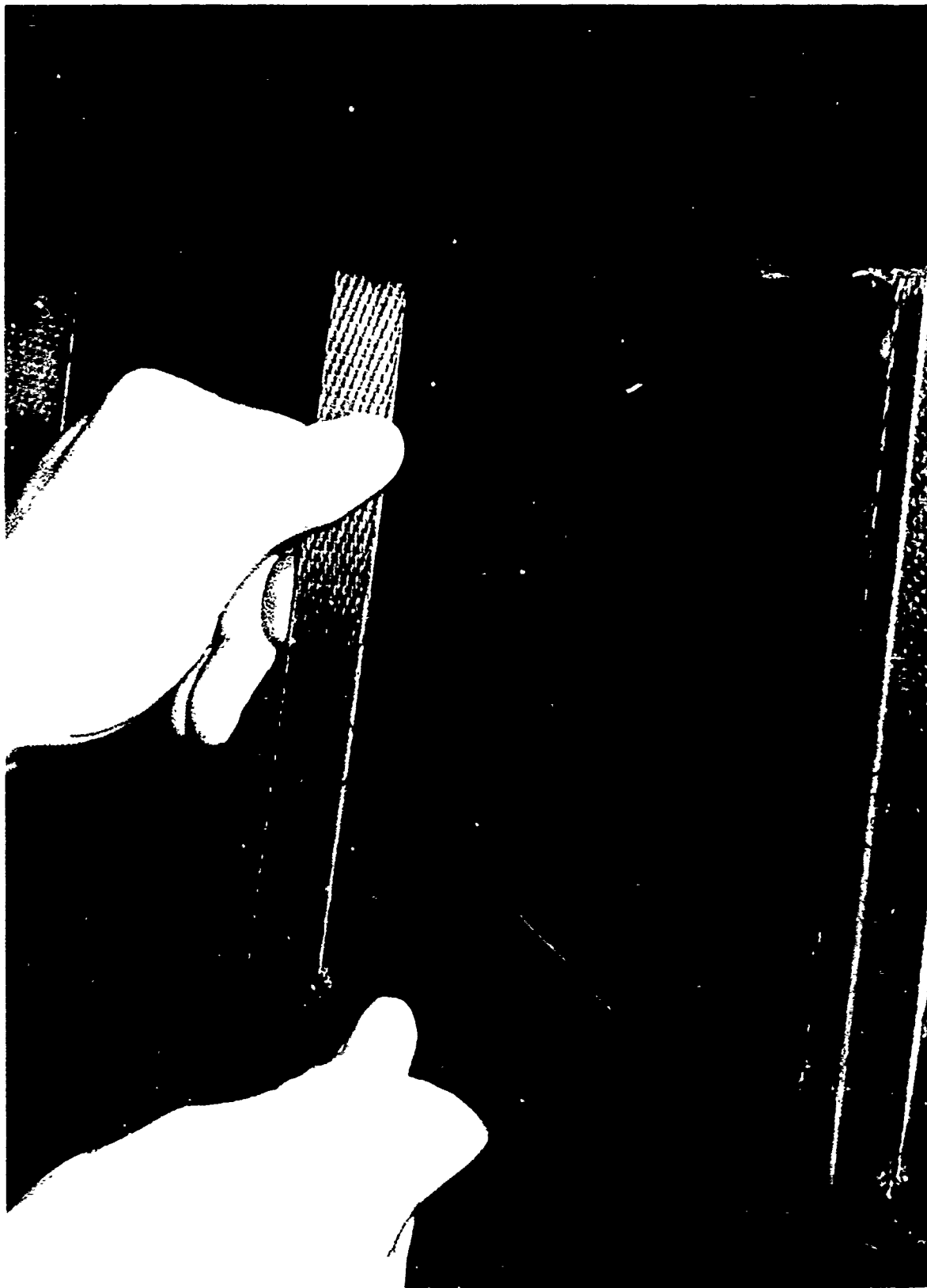


Figure 164 Front Spar Failure - 19 - Elev Box No. 1

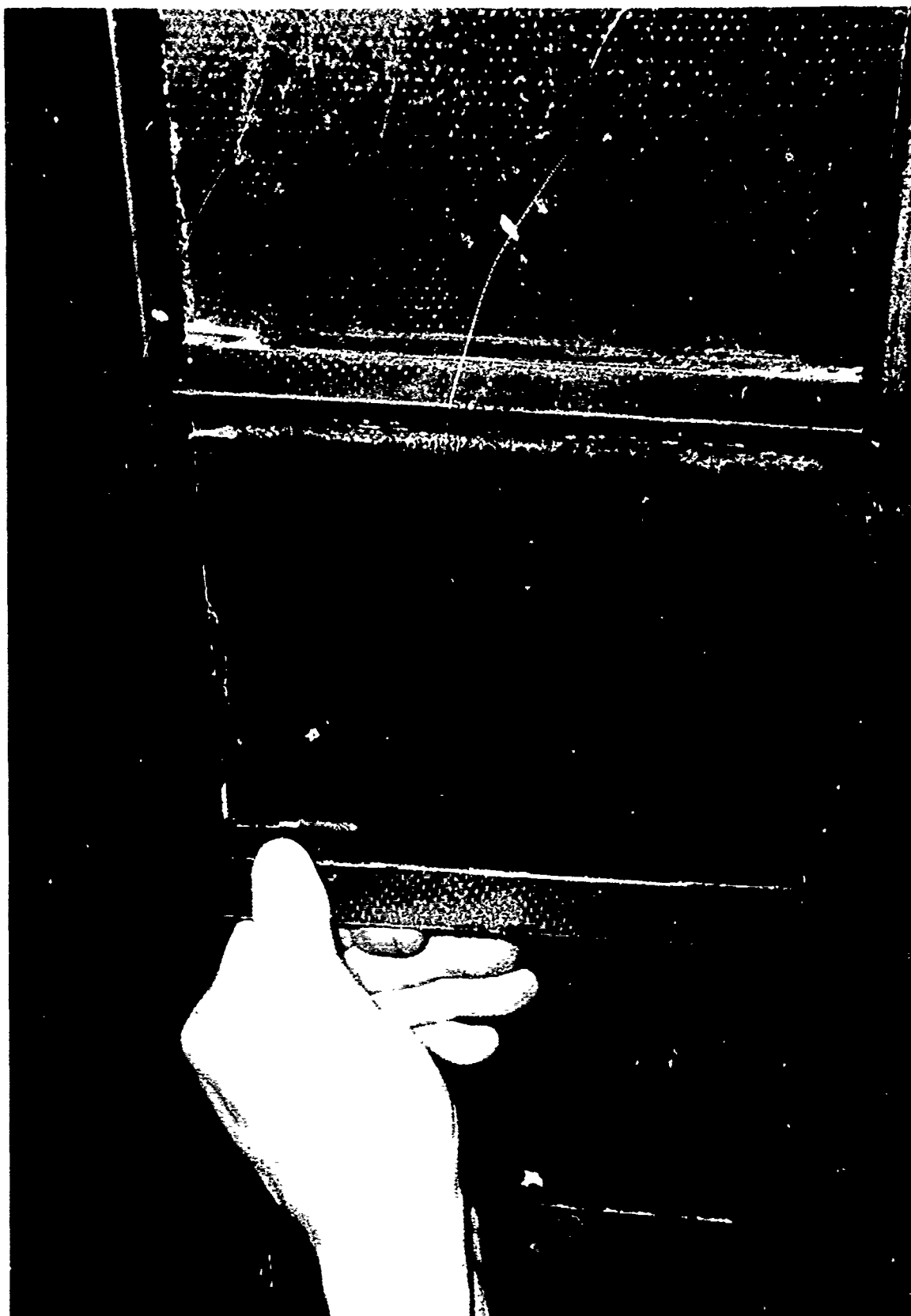


Figure 165. Front Spar Failure -- Test 2.3 -- Elev. Box No. 2

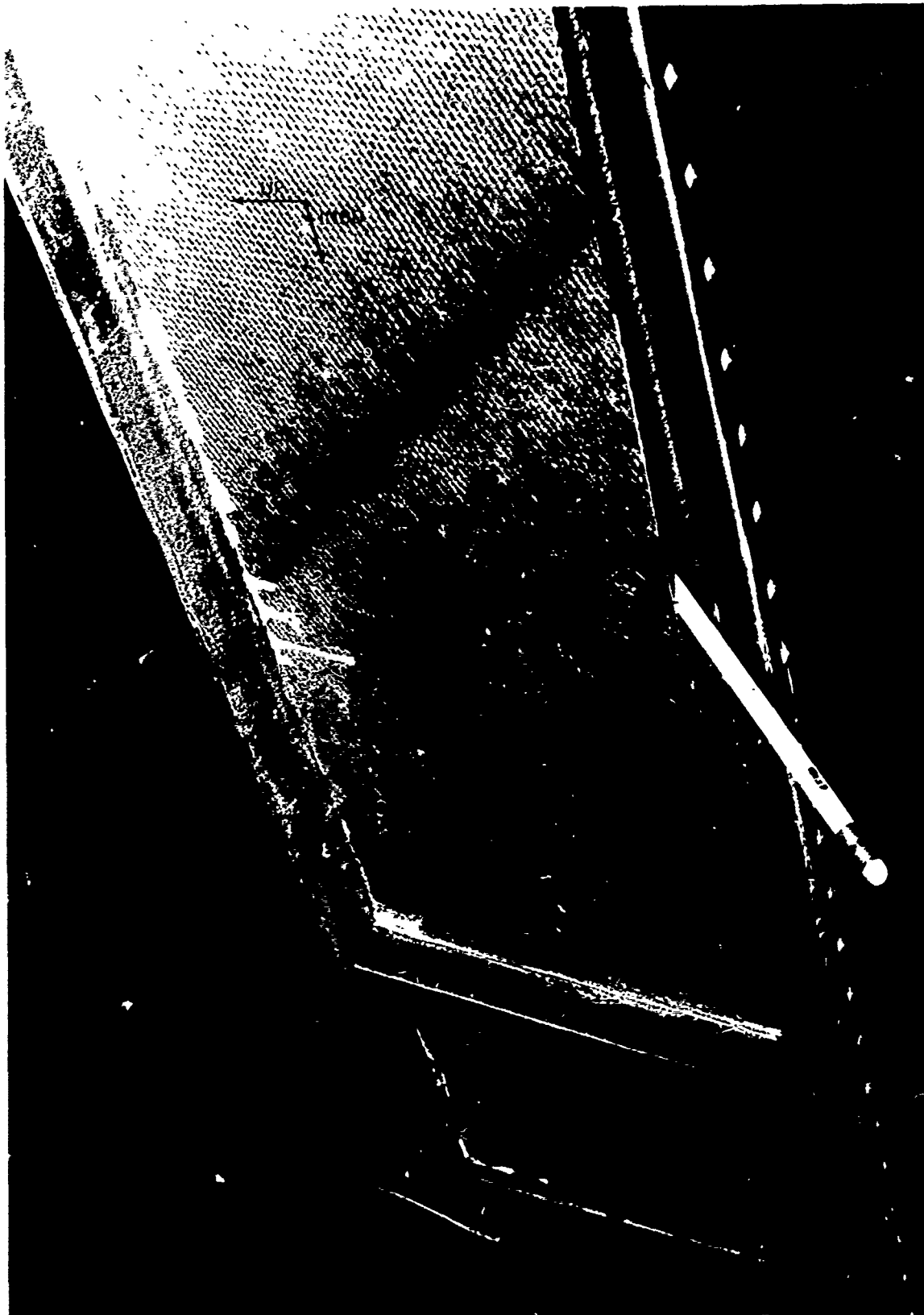


Figure 166. Front Spar Failure – Test 2.3 – Elev. Box No. 2

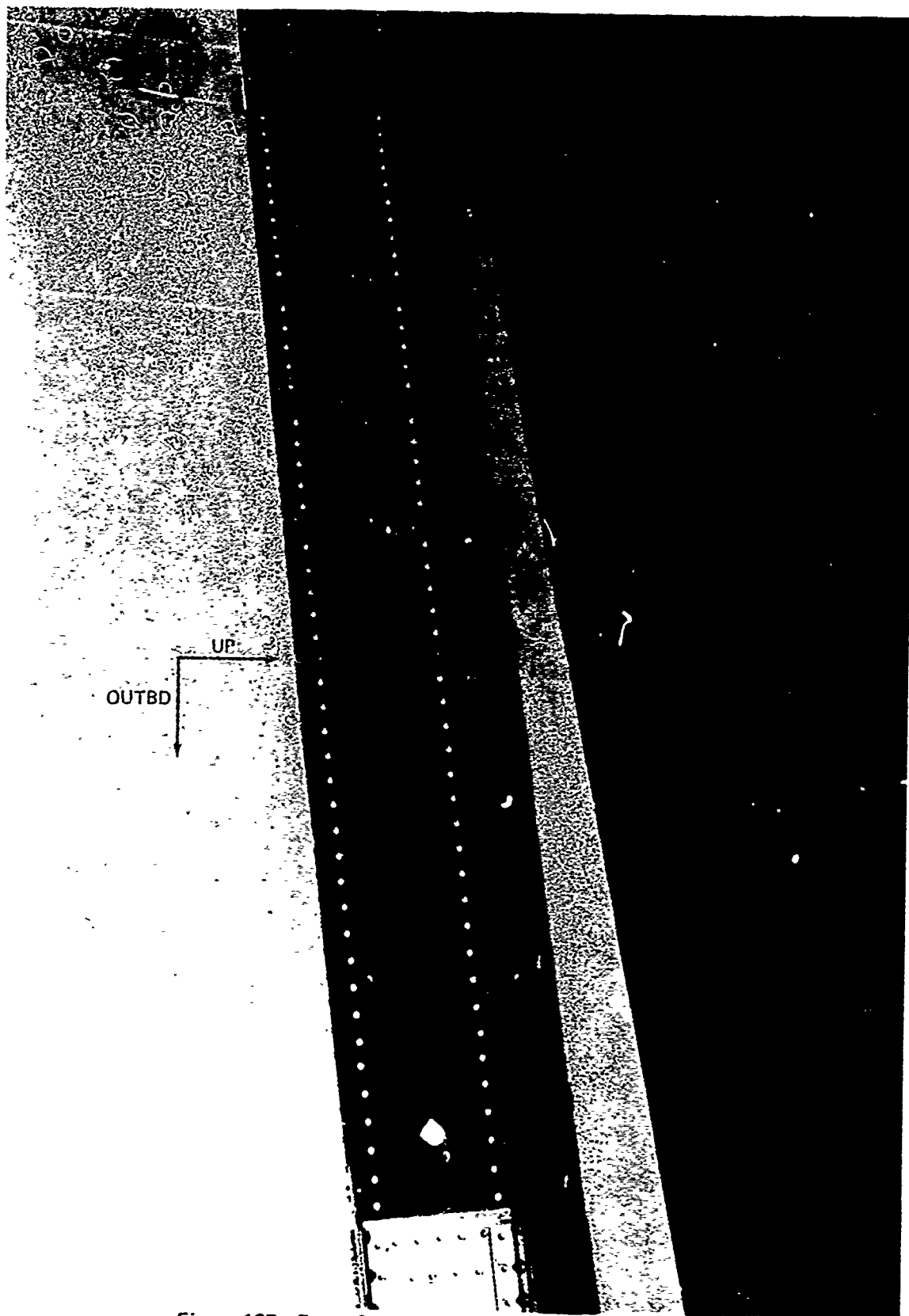


Figure 167. Front Spar Repair – Elevator Box No. 2

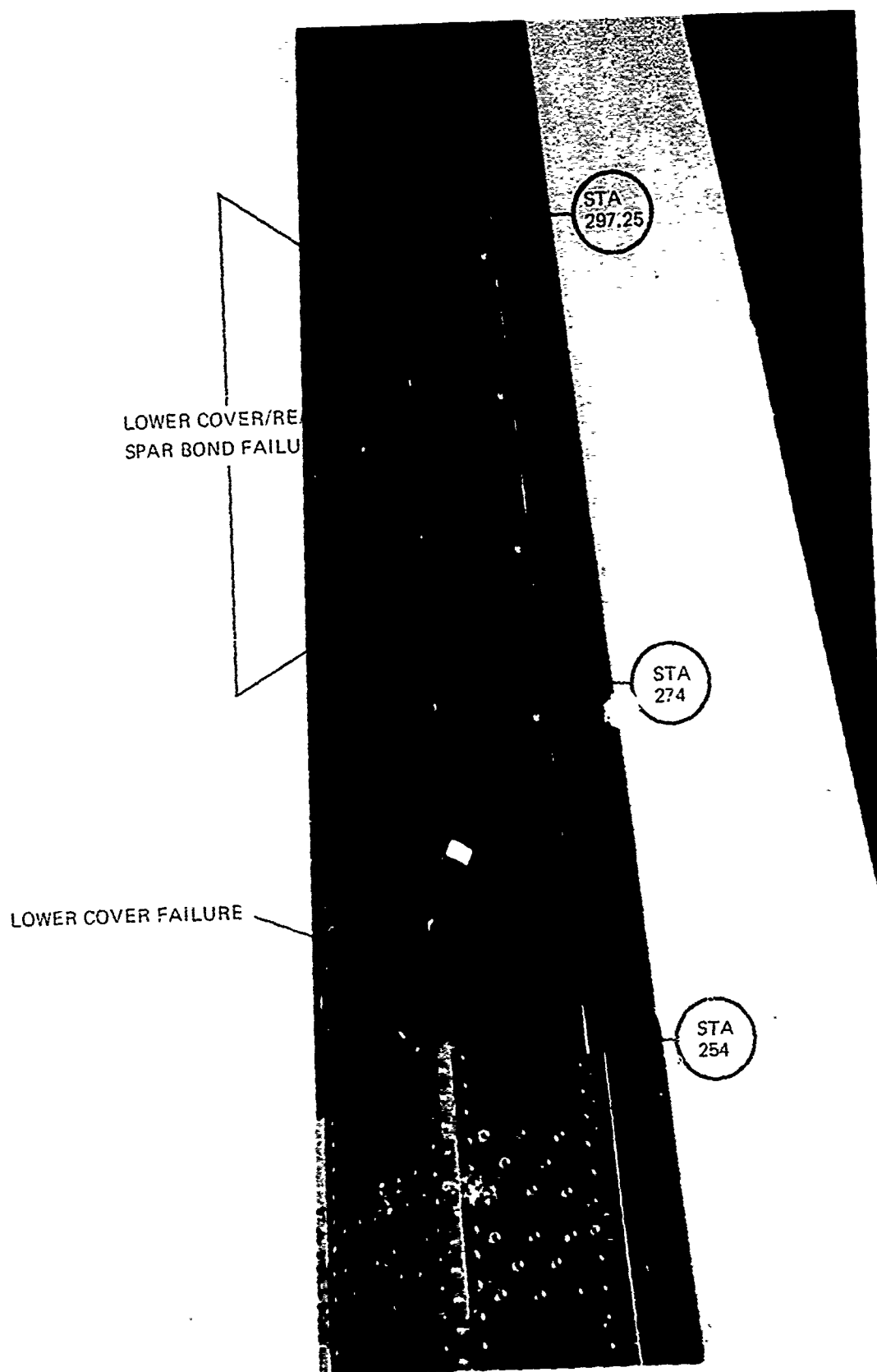


Figure 168. Lower Cover/Rear Spar Bond Failure – Test 2.4 – Elev. Box No. 2

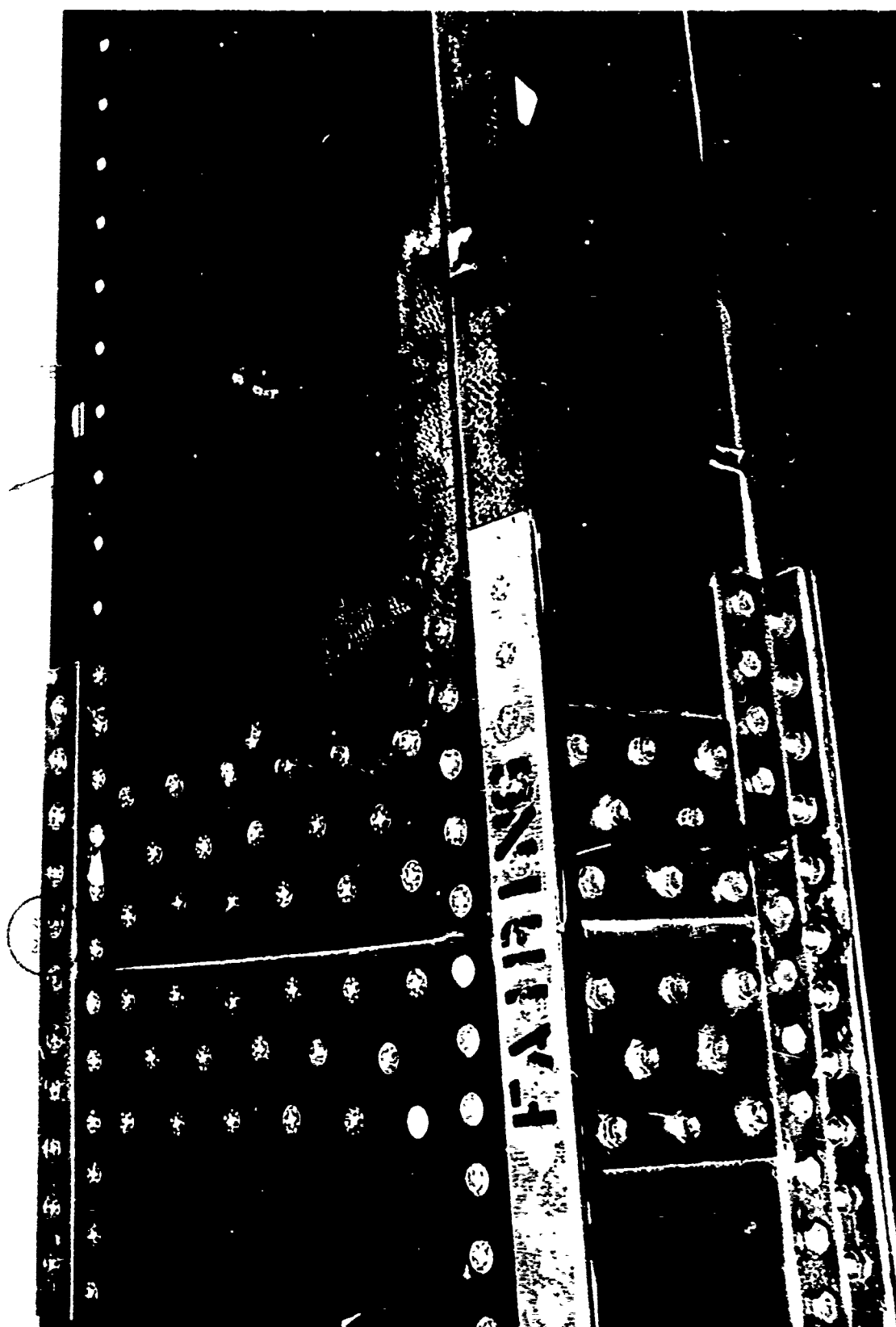


Figure 169. Lower Cover Failure – Test 2.4 – Elev. Box No. 2

Box #3 was fabricated of graphite with PKXA resin system, to the configuration of the center portion of the first two elevator boxes. The aluminum end transition sections were removed from Boxes #1 and #2 and cut down to fit Box #3. Loading and reaction point fittings were likewise installed on Box #3. The test fixtures were relocated to accommodate the shorter length of Box #3, and only two actuators at L.P. #1 and L.P. #2 were used to apply a torsional load. Four deflection indicators located as per the sketch in Figure 170 were utilized to measure torsional stiffness. Photos of Box #3 in the test fixtures are in Figures 171 and 172.

The torsional loading schedule for Box #3 is in Figure 161. The static torsional stiffness was the only test on Box #3, and no attempt was made to fail the box.

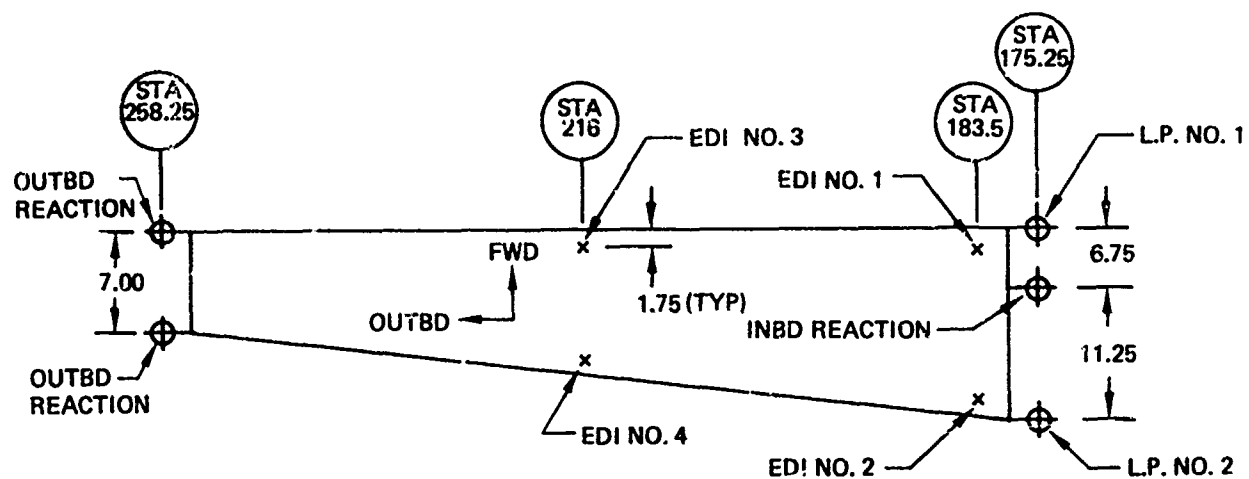


Figure 170. Load Point and EDI Locations GR/PKXA YC14 Elevator Box No. 3

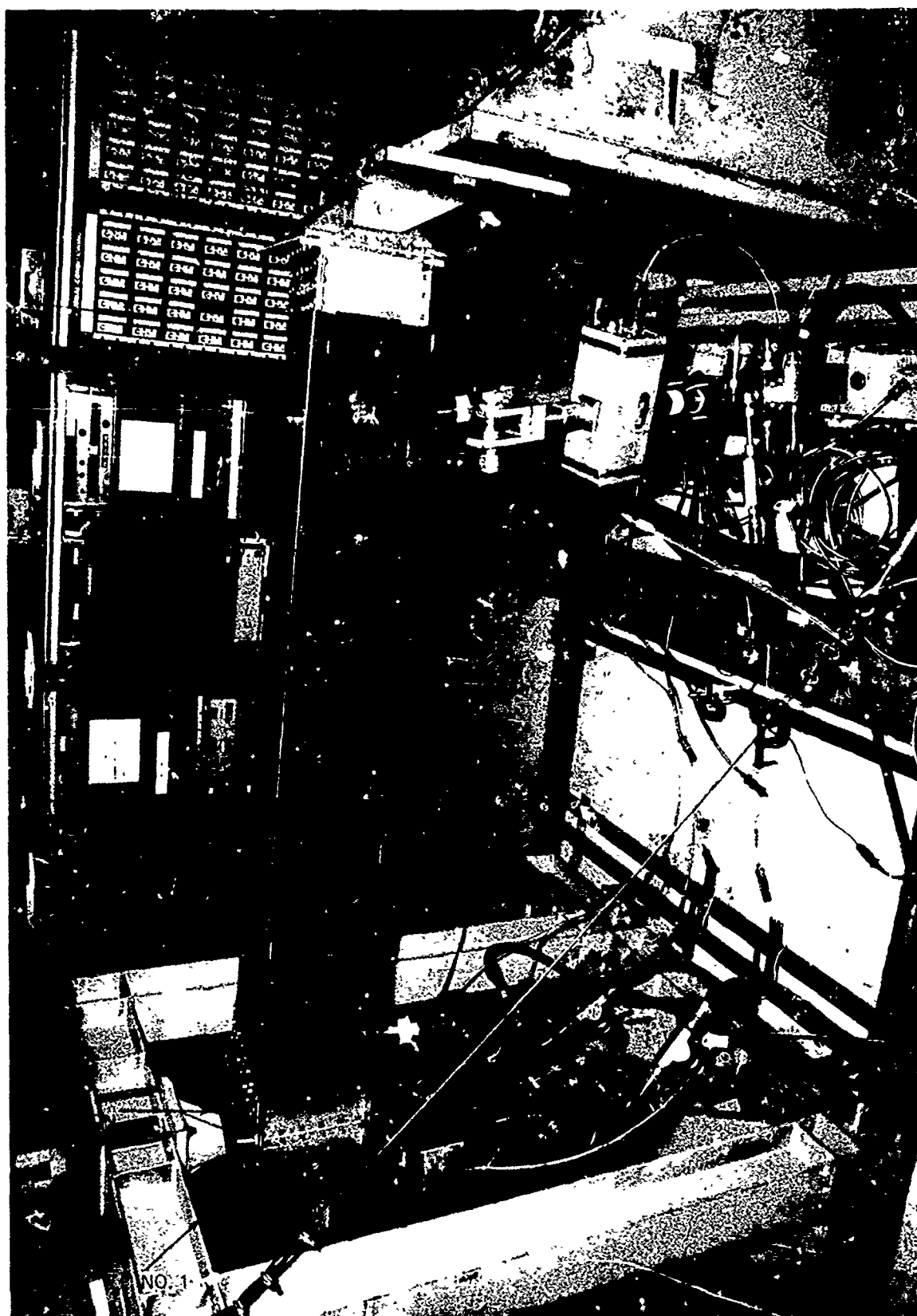


Figure 171. GR/PKXA YC-14 Elevator Box No. 3 – Test Article in Fixtures

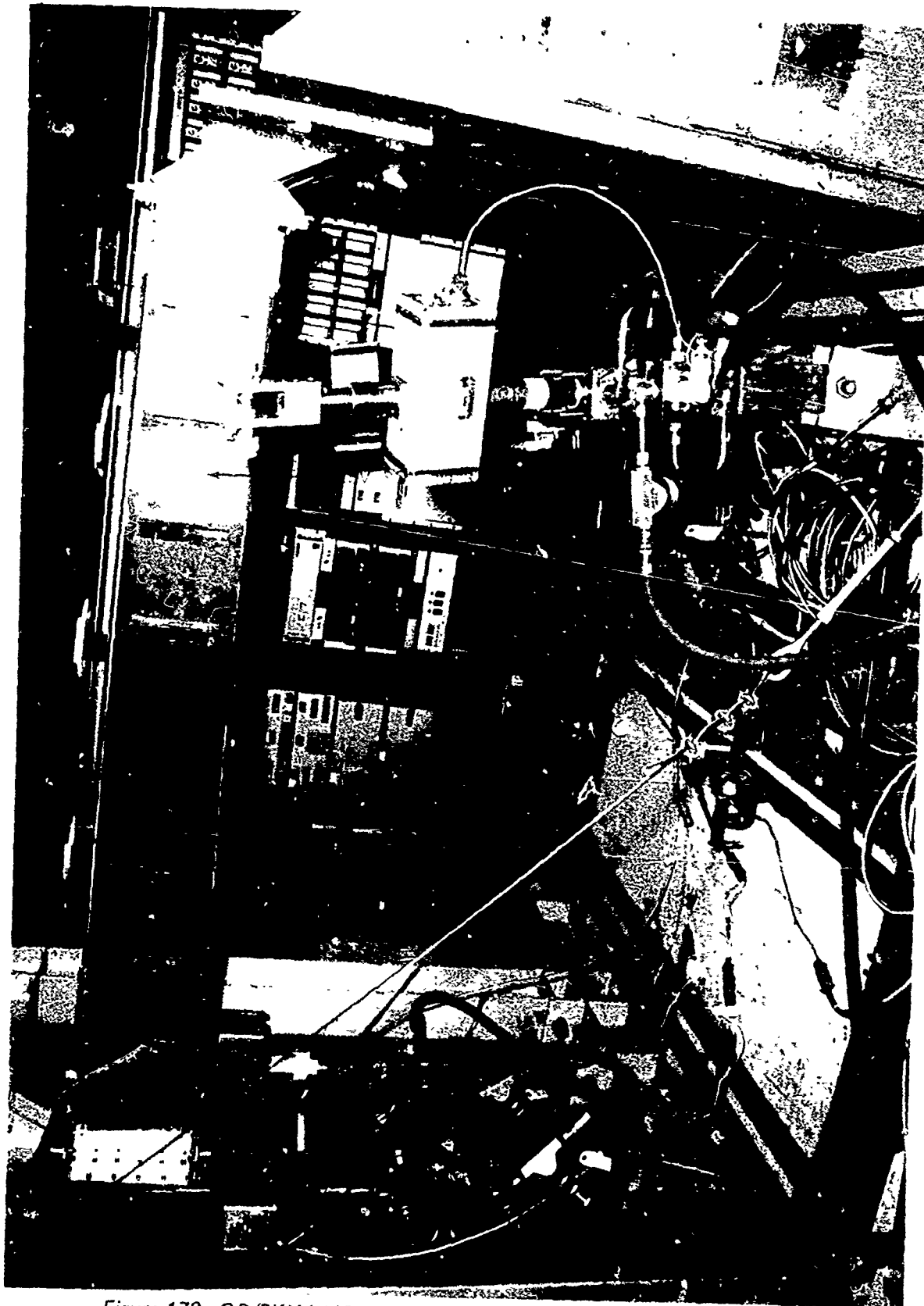


Figure 172. GR/PKXA YC-14 Elevator Box No. 3 – Test Article in Fixtures

10.0 COST AND PAYOFF ANALYSIS

Presented in this task are the cost factors associated with the various manufacturing methods and also the costs associated with the production fabrication of the YC-14 outboard elevator. Cost factors are presented in man-hours since the associated dollar factors vary between companies. Also the production times associated with thermoplastics will also fluctuate slightly depending upon facilities available since heat-up and cool-down are important considerations. Unlike thermoset materials, a slow precise heat-up rate is not required. The part must reach a temperature exceeding its softening point and the rate at which that point is reached is not particularly critical.

Table 33 shows the areas of general cost savings with reinforced thermoplastic composites. These savings apply to most methods of forming or assembly. Less labor and possibly energy savings results from not requiring a programmed cure cycle. Because thermoplastics have an infinite shelf life and no critical storage temperature requirements, savings result from less material scrappage of overaged material and eliminate the cost associated with controlled environmental storage (i.e., freezers). Since the material can be stored indefinitely, material scrap can be retained for future use or ground for molding compounds.

Thermoplastic consolidated sheet stock is rigid and tack-free enabling one man to easily handle a 4' x 8' sheet of material. This simplifies lay-up since one man can perform the lay-up of a large part that would require the efforts of 2-3 persons using a tacky thermoset prepreg system. On this program, this phenomenon proved to be a big cost saver. The individual GRTP plies are held together at the corners with a solvent solution of dissolved resin until fusing and forming.

Another big cost saver is the ability to reprocess defective parts. Standard graphite/epoxy parts have a rejection rate of about 5%. Typical rejections are delamination, resin poor areas or poorly compacted areas. An analysis of these defects revealed that the rejection rate could be reduced to 1%

Table 33. Areas of Cost Savings

	<u>Result</u>
• No fixed time, temperature, pressure profile	Less labor
• No critical storage requirements	Fewer facility requirements
• No critical shelf life	Less scrappage
• Less material cutting waste	Lower material requirements
• Ease of handling rigid sheet material	Less labor
• Reprocessing feasible	Less part scrappage
• No material bleed	Less material required
• Greater damage tolerance in fabrication	Lower labor costs

through the use of GRTP parts due to their ability to be recycled or reprocessed. This feature was used several times in the course of this program to correct defective parts. Depending on the part in question and the stage of processing at which this defect occurs, this reprocessing feature can be a big cost saver.

Another area of small savings is in the elimination of bleed ply materials. Savings occur in both material and labor through the elimination of this material. The processing of GRTP requires no resin bleed under normal conditions. One layer of vacuum bleeder material is still required however, in some processing techniques to obtain uniform pressure during forming.

Laminate Consolidation - Table 18 shows the processing times associated with press, autoclave, and pultrusion. Roll-forming as a method of consolidation was never satisfactorily demonstrated under this program and therefore no production times were generated. It is estimated, based on trial runs, that if equipment could be developed the times would be similar to those experienced for pultrusion. Processing considerations are discussed in section 4.1.

Post-Forming Methods - Table 34 shows the labor hours associated with post-forming GRTP structural elements. Times shown do not include labor associated with tool preparation, bagging or debagging. These operations vary significantly with part complexity and size.

Element Fabrication - Table 35 shows costs comparisons made between GRTP and GREP structural element fabrications. These costs studies were conducted on a production basis assuming the most cost effective method available for both epoxy and thermoplastic parts. All elements were under 4' x 8' in area and approximately 8' in length. As is evident the cost savings for small standard elements are significant. As the size approaches 32 ft², however, GRTP fabrication costs begin to significantly increase owing to the drastic increase in costs for facilities and tooling. This increase is evident in the cost change in complex shapes when the size changes for 4 ft² (70% savings) to 32 ft² (18% savings).

Table 34. Processing Times for Post-Forming

	Total Processing Time (hours)
• Press forming	2.00
• Autoclave Forming	4.00
• Pultrusion	2-6 inch/min
• Vacuum-forming	.16-20

Table 35. Element Cost Savings with Gr/T.P.

		<u>Savings*</u>
Elements	T-Stiffeners	60%
	Hat-Stiffeners	65%
	L-Channel	72%
	Honeycomb Panels	30%
	Flat Panels	42%
	(Small)	70%
	Complex Shapes (Large)	18%
Operations	Bonding	0
	Drilling	59%

*Over Gr/E (Labor)

Adhesive bonding operations show no cost savings since in using the standard epoxy system, the savings operations and procedures must be followed with GRTP as with epoxy composites. Savings do result in drilling since GRTP is more tolerant to hole misalignment and does not splinter or fray like an epoxy laminate.

YC-14 GRTP Elevator

The cost predictions made early in the program for the YC-14 elevator proved to be highly accurate during final hardware fabrication. The toolin costs however, increased over the early predictions and the revised costs are shown in Table 36. In fact the resulting tooling costs for the GRTP was 1.7 times that of the epoxy tooling; however, the GRTP elevator was still more cost effective by the 10 unit.

Summary - GRTP do show cost savings over graphite/epoxy composites for routine structural elements. The degree of cost savings is highly dependent upon the fabrication methods incorporated, available facilities, component design and production quantity. A general trend that was evident is that GRTP are not cost effective over graphite/epoxy parts at production levels under 5 units. Above 10 units, GRTP, in all trades conducted in this program, proved to be the more cost effective method of fabrication.

Table 36. YC-14 Advanced Composite Horizontal Stabilizer Cost Estimate

ADVANCED COMPOSITE MATERIAL	NO. OF UNITS	PRODUC-TION HOURS	MATERIAL DOLLARS	TOOLING HOURS	TOTAL COST DOLLARS
GRAPHITE/EPOXY	1	8,563	46,926	7,742	536,076
	10	60,936	469,260	7,742	2,529,550
	100	374,666	4,692,600	7,742	16,164,826
GRAPHITE/POLYSULFONE	1	6,050	40,015	13,147	615,925
	10	43,062	400,150	13,147	2,086,120
	100	264,712	4,001,500	13,147	12,337,270

11.0 PKXA Evaluation, Task XII

Under Navy Contract N00019-76-C-0170 and IRAD, Boeing has evaluated a new polysulfone resin system from Union Carbide Corporation, designated PKXA. This resin, when used with graphite fiber reinforcement, exhibits similar properties to P-1700 polysulfone composites. However, PKXA contains reactive end-groups on the polymer and during the processing cycle the resin cross-links into a polymer which exhibits improved solvent resistance over P-1700. The chemical structure is shown in Figure 173.

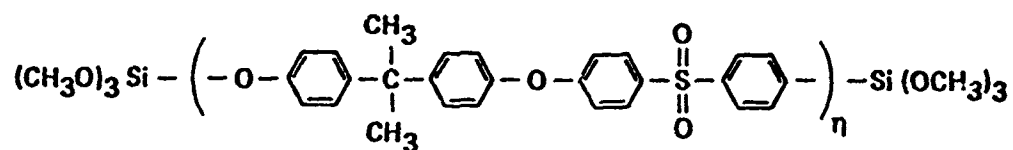
The purpose of Task XIII was to compare the structural integrity of PKXA graphite reinforced thermoplastic (GRTF) to P-1700 GRTF and consisted of the following efforts:

- (a) A design review to ensure compatibility of PKXA with the existing P-1700 design,
- (b) Element tests,
- (c) Fabrication and test of a seven foot section of the YC-14 elevator.

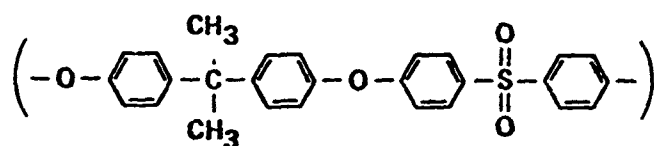
These activities are discussed in this section.

PKXA Element Tests

Static tests were conducted on rail shear, fusion bonded lap joints, mechanically attached lap joints and fracture panel specimens. Fatigue tests were also conducted on rail shear specimens to determine properties of Graphite/PKXA structural elements.



PKXA



UDEL POLYSULFONE (P-1700)

Figure 173. Chemical Formulas of PKXA and P-1700 Polysulfone

Thickness, inches	Cross section area, sq. in.	Ultimate shear stress, psi at 70°F	Shear modulus, G, 10 ⁶ psi
0.0620	0.3131	22,600	3.6
0.0623	0.3146	22,000	3.4
0.0571	0.2883	23,600	3.9

Table 36. PKXA Static Rail Shear Test Results

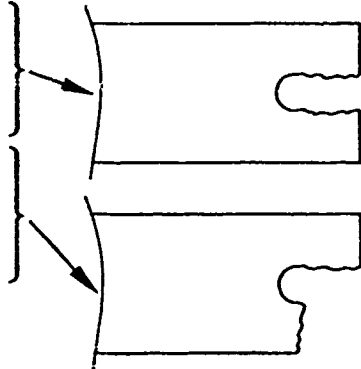
Static rail shear specimens were tested at room temperature in a 120,000 pound capacity Baldwin universal test machine. Specimens were instrumented with a single element strain gage oriented at 45° to the specimen center line, to measure shear strain. Strain and load, as measured by the test machine, were recorded on a Honeywell Model 530, X-Y plotter. The results are shown in Table 36.

Fusion bonded and mechanically fastened lap joint specimens were tested in a 120,000 pound capacity Baldwin universal test machine. Load vs. test machine crosshead displacement was recorded on the Baldwin X-Y plotter. Tests were conducted at room temperature and 160°F as noted on the data sheets. Elevated temperature tests were conducted in a resistance heated box furnace with a Thermac power controller. Specimen temperatures were sensed by Chromel-Alumel thermocouples bonded to the specimen, and indicated by a Doric digital temperature indicator. Results of the mechanically attached and fusion bonded lap shear specimens are shown in Tables 37 and 38, respectively.

Fracture panel specimens were tested in a 120,000 pound capacity Baldwin universal test machine at room temperature. Load vs. test machine crosshead displacement was recorded on the Baldwin X-Y plotter. The results are shown in Table 39.

Rail shear fatigue tests were conducted in a Sonntag SF-10U universal fatigue machine at a minimum/maximum load ratio $R = .05$. Specimens were loaded at a frequency of 30 Hz, at temperatures of 70 and 160°F . Specimens were heated by Chromalox strip heaters attached to the test fixture and surrounded by fiberglass insulation. Heater power was controlled by a Thermac power controller. Specimen temperature was sensed by Chromel-Alumel thermocouples bonded to the specimen gage section and indicated on a Doric digital temperature indicator. The number of loading cycles to failure for each specimen was recorded. These data are presented in Table 40. A comparison of these data with P-1700 data is shown in Figure 174. A general comparison of static PKXA data with static P-1700 data is shown in Table 41.

The fusion bond and mechanical attachment tests showed that the PKXA graphite composite load transfer capabilities were equivalent to the P-1700 graphite composite materials. This indicated that the load transfer details and fabrication procedures used for the P-1700 did not

Specimen axis to layup	Ultimate load, pounds	Type of failure
0-90°	730	
0-90°	688	
± 45°	1,034	
± 45°	782	

E/D = 2, fastener = BAC B30NF-4, width = 1.00
4 plies, fabric

Table 37. PKXA Mechanical Attachment, Lap Shear Test Results

Lap length, inches	Lap width, inches	Test temperature, °F	Ultimate load, pounds
0.52	1.013	70	1,849
0.52	1.013	70	1,836
0.52	1.013	70	2,068
0.52	1.017	70	2,256
0.52	1.018	180	1,775
0.52	1.018	160	2,400
0.52	1.016	180	1,328
0.52	1.016	160	2,125

4 plies, fabric, 0, 90°

Table 38. PKXA Fusion Bond, Lap Shear Test Results

Specimen axis to layup	Thickness, inches	Width, inches	Ultimate load, pounds	Gross area stress, psi
$\pm 45^\circ$	0.058	5.955	4,200	12,100
0-90°	0.055	5.995	6,460	19,500

4 plies, fabric

Table 39. PKXA Fracture Panel, Tension Test Results

Thickness, inches	Cross section area, inches	Test temperature, °F	Maximum fatigue stress, psi	Cycles to failure
0.061	0.3080	70	17,500	438,000
0.059	0.2980	70	15,000	2,566,000
0.059	0.2980	70	20,000	33,000
0.057	0.2880	160	15,000	868,000
0.058	0.2930	160	17,500	102,000

R = Minimum/maximum stress = 0.05

4 plies, T-300 fabric at $\pm 45^\circ$

7-13

Table 40. PKXA Rail Shear Fatigue Results

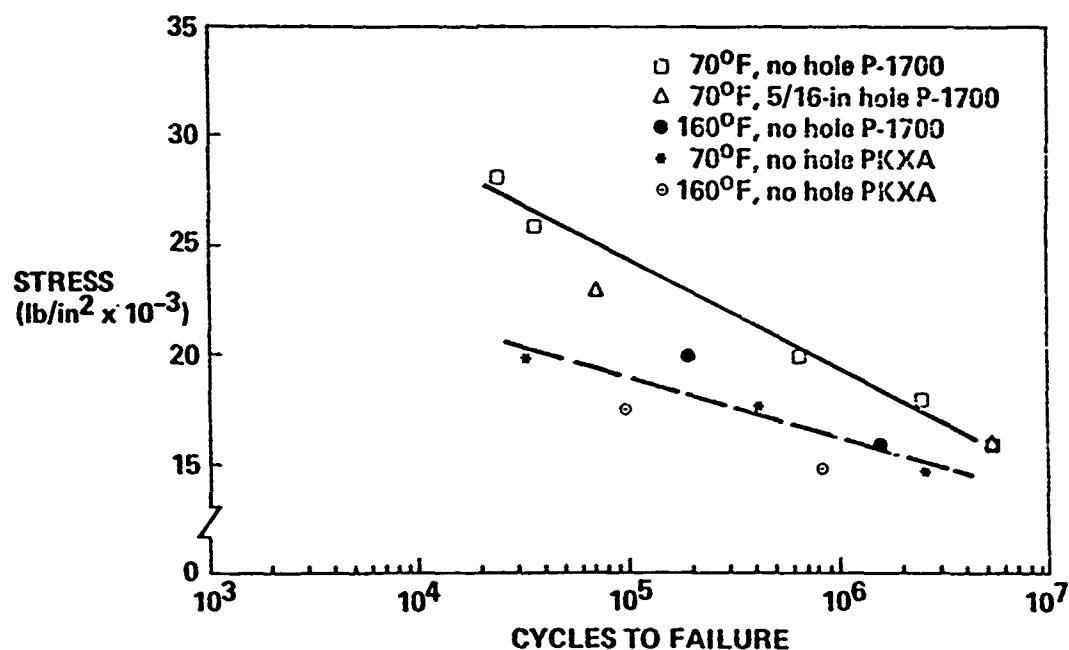


Figure 174. PKXA-P-1700 Rail Shear Fatigue Data Comparison

Element	PKXA	P-1700
Fracture panel (± 45)	4,200 lb	5,120 lb
Fracture panel (0, 90)	6,460 lb	8,140 lb
Mechanical fastener tests		
Load (E/D = 2)		
Laminate (0, 90)	730 lb	748 lb
Laminate (0, 90)	688 lb	638 lb
Laminate ± 45	1,034 lb	937 lb
Laminate ± 45	782 lb	813 lb
Fusion bond		
Laminate (0, 90) RT	4,125 psi	3,110 psi
Laminate (0, 90) RT	4,512 psi	2,990 psi
Laminate (0, 90) 160°	4,800 psi	2,500 psi
Laminate (0, 90) 160°	4,250 psi	2,540 psi
Static rail shear	22,800	30,900
	22,200	31,100
	23,800	32,500

Based on rail shear fusion bond specifications

Table 41. PKXA Polysulfone Static Element Test Data Comparison

require changes to facilitate the use of PKXA material. The fracture strength and fatigue capabilities were generally lower than the P-1700 graphite material but the modulus values are comparable. All properties were more than adequate for the proposed stiffness critical design of the YC-14 elevator. Data obtained from the ($\pm 45^{\circ}$) graphite/PKXA center notched panel shows that its gross fracture strength is below the equivalent graphite/epoxy and graphite/P-1700 but well above the design limit strain. Likewise, the PKXA composite is lower than the equivalent P-1700 in rail shear strength but with fatigue capabilities more than adequate to meet the design requirements.

PKXA - Elevator Box Section Fabrication and Test

During this task a 7' section of the YC-14 elevator box was fabricated of graphite fabric/PKXA composite construction. The PKXA resin was received in powder (fluff) form, put into solution using methylene chloride, and impregnated onto graphite fabric (24 x 24) to a nominal resin content of 35%. The prepreg was oven dried for 1/2 hour at 250°F to remove residual solvent. Then, the prepreg was consolidated into four ply sheet stock in an autoclave at 600°F for thirty minutes using 200 psi pressure.

Once the prepreg and sheet stock had been prepared, detail part fabrication and elevator assembly tooling/procedures used were the same as for the full size P-1700 polysulfone elevator boxes. The completed PKXA box section is shown in test, Figure 171.